8-7-2020

Developing models and algorithms to design a robust inland waterway transportation network under uncertainty

Farjana Nur

Developing models and algorithms to design a robust inland waterway transportation network under uncertainty

By

Farjana Nur

A Dissertation
Submitted to the Faculty of
Mississippi State University
in Partial Fulfillment of the Requirements
for the Degree of Doctor of Philosophy
in Industrial & Systems Engineering
in the Department of Industrial & Systems Engineering

Mississippi State, Mississippi

August 2020

Developing models and algorithms to design a robust inland waterway transportation network under uncertainty

By

Farjana Nur

Approved:

Mohammad Marufuzzaman
(Major Professor)

Krystel Castillo-Villar
(Committee Member)

Junfeng Ma
(Committee Member)

Jonathan Woody
(Minor Committee Member)

Linkan Bian
(Committee Member/Graduate Coordinator)

Jason M. Keith
Dean
Bagley College of Engineering

Name: Farjana Nur

Date of Degree: August 7, 2020

Institution: Mississippi State University

Major Field: Industrial & Systems Engineering

Major Professor: Mohammad Marufuzzaman

Title of Study: Developing models and algorithms to design a robust inland waterway transportation network under uncertainty

Pages of Study: 327

Candidate for Degree of Doctor of Philosophy

This dissertation develops mathematical models to efficiently manage the inland waterway port operations while minimizing the overall supply chain cost. In the first part, a capacitated, multi-commodity, multi-period mixed-integer linear programming model is proposed capturing diversified inland waterway transportation network related properties. We developed an accelerated Benders decomposition algorithm to solve this challenging NP-hard problem. The next study develops a two-stage stochastic mixed-integer nonlinear programming model to manage congestion in an inland waterway transportation network under stochastic commodity supply and water-level fluctuation scenarios. The model also jointly optimizes trip-wise towboat and barge assignment decisions and different supply chain decisions (e.g., inventory management, transportation decisions) in such a way that the overall system cost can be minimized. We develop a parallelized hybrid decomposition algorithm, combining Constraint Generation algorithm, Sam-

ple Average Approximation (SAA), and an enhanced variant of the L-shaped algorithm, to effectively solve our proposed optimization model in a timely fashion.

While the first two parts develop models from the supply chain network design viewpoint, the next two parts propose mathematical models to emphasize the port and waterway transportation related operations. Two two-stage, stochastic, mixed-integer linear programming (MILP) models are proposed under stochastic commodity supply and water level fluctuations scenarios. The last one puts the specific focus in modeling perishable inventories. To solve the third model we propose to develop a highly customized parallelized hybrid decomposition algorithm that combines SAA with an enhanced Progressive Hedging and Nested Decomposition algorithm. Similarly, to solve the last mathematical model we propose a hybrid decomposition algorithm combining the enhanced Benders decomposition algorithm and SAA to solve the large size of test instances of this complex, NP-hard problem. Both proposed approaches are highly efficient in solving the real-life test instances of the model to desired quality within a reasonable time frame.

All the four developed models are validated a real-life case study focusing on the inland waterway transportation network along the Mississippi river. A number of managerial insights are drawn for different key input parameters that impact port operations. These insights will essentially help decisions makers to effectively and efficiently manage an inland waterway-based transportation network.

Key words: Inland waterway port, Port optimization, Congestion, Perishable products, Waterlevel fluctuation, Enhanced Benders decomposition algorithm, Sample average approximation, Progressive Hedging algorithm, Hybrid nested decomposition algorithm, Parallelization.

DEDICATION

To my adorable son, my world, Arham Hossain.

ACKNOWLEDGEMENTS

I am very thankful to Almighty Allah for providing me everything I needed to complete this dissertation and strengthened me in every steps of my doctoral life.

I am thankful to my dissertation committee chair Dr. Mohammad Marufuzzaman and my committee members Dr. Krystel Castillo, Dr. Linkan Bian, Dr. Junfeng Ma, and Dr. Jonathan Woody for guiding and providing their valuable insights on this dissertation. I would like to gratefully acknowledge the funding support provided by U.S. Army Engineer Research and Development Center (ERDC) through Institute of Systems Engineering Research (ISER) Center to conduct this research. Additionally, I would like to acknowledge the funding support provided by the Bagley College of Engineering (BCoE) and the Graduate School of Mississippi State University that enabled me to showcase my research in international conferences.

I would like to extend my gratitude to Dr. Kari Babski-Reeves, Professor and Head, Department of Industrial and Systems Engineering, Associate Dean, Bagley College of Engineering, for her continuous encouragement and support throughout my doctoral studies. I am also very grateful to Dr. Reuben Burch, Assistant Professor, Department of Industrial and Systems Engineering, for his motivation and continuous support towards my career.

Special thanks to the Department of Industrial & Systems Engineering at Mississippi State University for providing me academic, financial, and all other institutional supports while needed.

I have many good friends and colleagues who helped and supported me during the past several years. I would like to thank Amin Aghalari, Dr. Mohannad Kabli, Dr. Md. Abdul Quddus, and Morteza Alizadeh for being a great research partner and co-authoring different research articles with me. I enjoyed working with them. I would also like to thank Hunter, Eboni, Ayat, Darweesh, Badr, and Milad for being great friends and classmates during my graduate school.

Moreover, I am grateful to my parents, family, colleagues, friends, who has assisted and supported me in my doctoral journey. My husband, Niamat, has been an incredible support for me. He has been a great colleague, co-researcher, classmate, best peer, and my power house during these days as always. He was there with me in every steps, despite of his business with PhD studies. Heartfelt thanks to him for his patience. Most importantly, I am extremely thankful to my little baby Arham for sharing all the work and defending the PhD Dissertation with me being in mom's womb. Thank you my little one!

TABLE OF CONTENTS

LIST OF TABLES

LIST OF FIGURES

CHAPTER 1

INTRODUCTION

1.1 Introduction

Inland waterway ports are indispensable components of the nation's waterway transportation system which greatly contributes to the overall economy of the nation. Currently, more than 60% of the United States grain exports, 22% petroleum and petroleum products, and 20% coal are transported through inland waterway ports [140]. Additionally, these ports contribute approximately 15 billion dollars to the nation's GDP (Gross Domestic Product) along with creating more than 250,000 job opportunities (both direct and indirect) annually [89]. Inland ports play a major role in the rural industrial and agricultural development for a nation [84]. Despite of their great potentiality, this segment of transportation system is frequently impacted by many factors which hurts it's productivity, including but not limited to congestion, aging infrastructure, delays caused by scheduled and unscheduled closures of locks (primarily due to maintenance activities), and many others [140]. According to the American Society of Civil Engineers (ASCE), in 2010, the United States encountered a total of $33 billions of additional annual expenditure primarily due to the delays governed by congestion and other waterway specific issues [8]. This cost will continue to increase over time and is projected to reach nearly

$49 billions by 2020 [8]. Therefore, optimizing the shipment planning is mandatory for the inland waterway ports not only to gain competitive advantage over its counterparts (e.g., rail, trucks) but also to survive in this increasingly competitive market.

Though seemingly sound similar, inland waterway ports hold some unique properties that differ them significantly from the *seaports*. For instance, these ports generally handle barge traffic drafting upto 9 feet only, located primarily near smaller bodies of water (e.g., rivers and canals), usually land intensive, and/or handle smaller counts of larger users and a large number of smaller users [84]. Additionally, the water level between the channels of two connecting inland waterway ports fluctuates heavily in different time periods of the year [139, 94, 90]. Depending on the severity of this fluctuation, these ports, including the waterway itself, often experience disruptions, such as drought and flood that may tremendously impact or even cease the port operations for an extended period of time. Another prevalent feature that distinguishes inland waterway ports over seaports is that these ports commute heavy volume of perishable agricultural products which are highly seasonal in nature. The seasonality in agricultural products coupled with time varying waterway conditions and the availability of locks and dams between two source destination ports may excessively delay the port operations which directly impacts the operational planning of the ports under consideration. With all these outstanding challenges, it is quite certain that the optimization models available in the literature for the maritime transportation may no

longer be directly applicable for the inland waterway ports. Hence, to ensure long term sustainment of the inland waterway ports, there is a critical need to develop sophisticated optimization models that best capture the unique characteristics of this cost efficient, reliable, and environmentally friendly transportation sector.

A major stream of ongoing research develop optimization models to solve diversified seaport-related problems, such as ship routing and scheduling [33, 29, 68], inventory routing [5], berth allocation and scheduling [27, 32, 141], empty container re-positioning [43], sailing speed optimization [73, 141], bunker consumption [145], emission consideration [141], disruption [43, 126], container routing [146], port delays [148], and many others. Apart from adopting mathematical approaches, few researchers develop simulation models to address similar problems (e.g., [118, 125, 121, 44]). Even though deep penetration to seaport research is observed, inland waterway ports did not receive much attention from the research community. A few considerations can be noticed for *deep draft inland ports* which are capable of handling container cargos and ships; however, almost no research has been conducted to date that puts specific considerations to model *shallow draft inland ports*[1]. These ports primarily handle shallow draft vessels (e.g., barge, towboats). Considering their outstanding contributions in the overall transportation system and economy, better understanding of shallow draft inland wa-

[1]The ports that are unable to handle barges/vessels drafting more than 9 feet are known as *shallow draft inland ports*. For the ones that can handle barges/vessels drafting more than 9 feet, are known as *deep draft inland ports*.

terway ports is imperative to successfully design and manage a sound and efficient supply chain network.

This dissertation is divided into four sections. The contribution of each section is mentioned at the corresponding chapter. The first section (CHAPTER II) investigate shallow draft inland port operations and their impacts on different supply chain decisions. We propose a multi-commodity, multi-time period Mixed-integer Linear Programming (MILP) model that optimizes short-term operational decisions such as trip-wise towboat and barge assignment with mid-term supply chain decisions (e.g., inventory management decisions) in such a way that the overall supply chain cost can be minimized. The model realistically captures a number of factors that characterize/impact the operations in a shallow draft inland port, such as towboat and barge availability, weight and volumetric capacity restriction of barges, dredging issues, commodity mix restriction, storage restrictions at ports, trip restrictions between origin-destination ports, and many others. The output of our model provides optimal towboat and barge assignment, amount of commodities stored and transported to different layers of the supply chain network so that the overall system cost can be minimized. We realize that our proposed model is an extension of the fixed charged, uncapacitated network flow problem which is already known to be an $\mathcal{NP}$-hard problem [74]. Therefore, solving large instances of this problem is a challenging task. This motivates us to develop a highly customized solution approach based on the traditional Benders decomposition algorithm. To enhance the performance of our algorithm, we create several

stronger cuts, including problem-specific valid inequalities, knapsack inequalities, pareto-optimal cuts, input ordering, and local branching. In addition to proposing the model, another important contribution of this study is to apply this model to a real world case study. We use a few states from the Southeast United States as a testing ground to visualize and validate the modeling results. The outcome of this study provides a number of managerial insights, such as impact of water level fluctuation on towboat and barge selection, demand and supply changes, and barge availability on overall system performance, which can effectively aid decision makers to design a cost-efficient shallow draft inland waterway transportation network.

In the second section (CHAPTER III) we propose a model which specifically focus in port congestion while considering shallow draft inland waterway port-related internal (e.g., barge/towboat assignments, inventory decisions, port delays) and external (e.g., waterlevel fluctuations) factors/decisions that impact the overall supply chain system performance. We propose a capacitated, multi-commodity, multi-period, two-stage stochastic mixed-integer nonlinear programming model which jointly optimizes trip-wise towboat and barge assignment decisions along with different supply chain decisions (e.g., inventory management, transportation decisions) under a congested and stochastic environment and in such a way that the overall supply chain cost can be minimized. The proposed model realistically captures a number of factors that appropriately characterize the operations of a shallow draft inland waterway port, such as towboat and barge availability,

weight and volumetric capacity restriction of barges, dredging issues, commodity mixture restrictions, storage restrictions at ports, trip restrictions between origin-destination ports, congestion issues, delays in locks and dams, and many others. We realized that our proposed mathematical model is $\mathcal{NP}$-hard. Therefore, we develop a highly customized parallelized hybrid decomposition algorithm, combining Constraint Generation algorithm, Sample Average Approximation, and an enhanced variant of the L-shaped algorithm, to effectively solve the large instances of our proposed optimization model in a reasonable amount of time. We solved a real world case study to visualize and validate our modeling results. Identical to the case study of Chapter II, inland waterway transportation network along the Mississippi river is used as a testing ground. The outcome of this study provides a number of managerial insights, such as the impact of water level fluctuations on towboat and barge selection, cost due to delay in transportation, and commodity supply fluctuations on overall system performance, which can effectively aid decision makers to design a cost-efficient shallow draft inland waterway transportation network.

The next Section (CHAPTER IV) puts more emphasize in waterway fluctuation and related issues and develops reliable optimization model that account for different factors which frequently impact the inland waterway port operations. A capacitated, multi-commodity, multi-period, two-stage stochastic mixed-integer linear programming model is proposed that jointly optimizes trip-wise barge and towboat assignment decisions along with inventory management and transporta-

tion decisions with a goal of minimizing the overall system cost under water level and commodity supply uncertainty. Since first two chapters analyze and optimize the model from a supply chain viewpoint, this chapter puts more emphasize in waterway port based transportation and resource allocation decisions removing any external tiers than the origin (the point where the waterway transportation starts) and destination ports (the point where the waterway transportation ends). To solve this $\mathcal{NP}$-hard problem and obtain solutions within a limited computational time, we develop a highly customized parallelized hybrid decomposition algorithm which combines Sample Average Approximation with an enhanced Progressive Hedging (PH) and Nested Decomposition (ND) algorithm. Several techniques are used to enhance the PH algorithm, such as penalty parameter updating, global and local heuristics, and scenario bundling techniques. On the other hand, techniques, such as problem-specific valid inequalities, strengthened Benders and Lagrangian cuts, are used to enhance the performance of the ND algorithm. To the end, two parallelization schemes are proposed to parallelize the entire hybrid decomposition algorithm. Extensive computational experiments are presented to demonstrate how the parallelized hybrid decomposition algorithm effectively and efficiently solves the proposed mathematical model. Apart from proposing the mathematical model and solution approaches, we demonstrate a real-life application by utilizing the inland waterway transportation network along the lower Mississippi River. The outcome of this study provides a number of managerial in-

sights which may effectively aid decision makers to design a cost-efficient shallow draft inland waterway transportation network.

The last section (CHAPTER V) extends the previous section (CHAPTER IV) to consider the commodity perishability issues in managing port inventories. We proposed a mathematical model that captures the prevalent inland waterway port related issues (e.g., waterlevel fluctuations, barge/towboat assignments, inventory decisions, and port delays) and combine them under the same decision making framework that magnifies their impacts on designing and managing a sound, robust inland waterway transportation network. Our proposed multi-commodity, multi-period, two-stage stochastic mixed-integer linear programming model efficiently captures all the aforementioned issues that appropriately characterizes the shallow draft inland waterway port operations. Our proposed mathematical model is $\mathcal{NP}$-hard [74]. Therefore, to cope with the computational challenge in solving this model we develop a highly customized nested decomposition algorithm. This algorithm combines enhanced Benders decomposition algorithm under Sample Average Approximation framework to effectively solve the large instances of our proposed model within a reasonable time frame. Further, we demonstrate a real life application of our proposed model considering the inland waterway transportation network along the lower Mississippi river. The outcome of this study provides a number of managerial insights, such as the impact of water level fluctuations on towboat and barge selection, and impact of commodity deterioration rate on overall system performance, which can effectively aid deci-

sion makers to design a reliable and cost-efficient shallow draft inland waterway transportation network under uncertainty.

CHAPTER 2

OPTIMIZING INLAND WATERWAY PORT MANAGEMENT DECISIONS CONSIDERING WATERLEVEL FLUCTUATIONS

2.1 Introduction

Inland waterway ports are integral components of a nation's transportation system which significantly contributes to the overall economy. Currently, more than 60% of the United States grain exports, 22% petroleum and petroleum products, and 20% coal are transported through inland waterway ports [140]. These ports contribute approximately 15 billion dollars to the country's total GDP (Gross Domestic Product) while creating more than 250,000 job opportunities (both direct and indirect) nationwide [89]. Inland waterway ports play a major role in rural industrial and agricultural development [84]. Despite their potentiality to contribute in the overall economy, this transportation system is still heavily underutilized due to a number of reasons, such as aging infrastructure, dredging issues, delays caused by scheduled and unscheduled closures of locks (primarily due to maintenance activities), and many others [140]. Therefore, optimizing the shipment planning is mandatory for the inland waterway ports not only to gain competitive advantage over its counterparts (e.g., rail, trucks) but also to survive in this increasingly competitive market.

Inland waterway ports hold some distinguishable properties that differ them from *seaports*. For instance, inland waterway ports generally cannot handle barges drafting more than 9 feet. These ports are primarily located near smaller bodies of water (e.g., rivers and canals), usually land intensive, and/or handle smaller counts of larger users and a large number of smaller users [84]. Additionally, these set of ports experience severe water level fluctuations on their channels in different time periods of a year [139, 94, 90]. Based on the severity of this fluctuation, inland waterway ports as well as the waterway may undergo disruptions such as draught and flood that may severely impact or even cease the port operations for an extended period of time. These specific characteristics indicate that the optimization models available in the literature for seaports may no longer be directly applicable for inland waterway ports. Till now a major stream of research develops optimization models to solve diversified seaport related problems, such as ship routing and scheduling [29, 68], berth allocation and scheduling [27, 32, 141], inventory routing [5], empty container repositioning [43], speed optimization [73, 141], bunker consumption [145], emission consideration [141], container routing [146], and many others. Other than optimization approaches, simulation models are also developed to solve the similar problems for the seaports (e.g., [118, 125, 121, 44]). Despite the abundance of seaport literature, inland ports did not receive much attention from the research community. Even though a few consideration is given to *deep draft inland ports* capable of handling container cargos and ships, there is

almost no research that considers *shallow draft inland ports*[1] that primarily handles shallow draft vessels (e.g., barge, towboats) only. For the remaining sections of the paper, we will refer *shallow draft inland ports* as *inland waterway ports*. Considering their novelty in the overall transportation and economy, better understanding of inland waterway ports is imperative to successfully design and manage a sound and efficient supply chain network. To fulfill this need, the current study adopts an optimization approach for showing the effects of different key managerial decisions on the overall system performance.

The aim of this study is to investigate shallow draft inland port operations and their impacts on different supply chain decisions. We propose a multi-commodity, multi-time period Mixed-integer Linear Programming (MILP) model that optimizes short-term operational decisions such as trip-wise towboat and barge assignment with mid-term supply chain decisions (e.g., inventory management decisions) in such a way that the overall supply chain cost can be minimized. The model realistically captures a number of factors that characterize/impact the operations in a shallow draft inland port, such as towboat and barge availability, weight and volumetric capacity restriction of barges, dredging issues, commodity mix restriction, storage restrictions at ports, trip restrictions between origin-destination ports, and many others. The output of our model provides optimal towboat and barge assignment, amount of commodities stored and transported to

[1]The ports that are unable to handle barges/vessels drafting more than 9 feet are known as *shallow draft inland ports*. For the ones that can handle barges/vessels drafting more than 9 feet, are known as *deep draft inland ports*.

different layers of the supply chain network so that the overall system cost can be minimized. We realize that our proposed model is an extension of the fixed charged, uncapacitated network flow problem which is already known to be an $\mathcal{NP}$-hard problem [74]. Therefore, solving large instances of this problem is a challenging task. This motivates us to develop a highly customized solution approach based on the traditional Benders decomposition algorithm. To enhance the performance of our algorithm, we create several stronger cuts, including problem-specific valid inequalities, knapsack inequalities, pareto-optimal cuts, input ordering, and local branching. In addition to proposing the model, another important contribution of this study is to apply this model to a real world case study. We use a few states from the Southeast United States as a testing ground to visualize and validate the modeling results. The outcome of this study provides a number of managerial insights, such as impact of water level fluctuation on towboat and barge selection, demand and supply changes, and barge availability on overall system performance, which can effectively aid decision makers to design a cost-efficient shallow draft inland waterway transportation network.

In summary, the key contributions of this paper are: (i) proposing a multi-commodity, multi-time period MILP model formulation that facilitates the proper management and allocation of inland waterway port operations and minimizes the overall system cost from a supply chain viewpoint; (ii) developing an accelerated Benders decomposition algorithm that provides high quality solutions for large scale problem instances in a reasonable amount of time; and (iii) presenting

a real-life case study based on the data from the Southeast region of the United States[2].

The exposition of this paper is as follows. Section 2.2 provides a review of the literature pertaining to inland waterway ports. Section 2.3 discusses the problem description and introduces the proposed mathematical model formulation. Different enhancement techniques for the standard Benders decomposition algorithm are discussed in detail in Section 2.4. Section 2.5 presents the computational performances of different variants of the Benders decomposition algorithm, conducts a real life case study, and draws a series of managerial insights. Finally, we conclude and present avenues for future research in Section 2.6.

2.2 Literature Review

In recent years few streams of ongoing research has captured different aspects of deep draft inland waterway port management and operations. These studies discuss about different issues pertaining to inland waterway transportation such as delays in locks and dams, barge and towboat routing and repositioning, berth allocation problem, port disruption, and few others. In this section, we provide a comprehensive overview of such previous researches.

To date, few studies analyze the performance of locks and dams in inland waterway transportation network. Ting and Schonfeld [129] propose an integrated tow control algorithm to minimize the delay between a series of locks. Wang

[2]This chapter has been published in Computers & Industrial Engineering [98].

and Schonfeld [147] propose a combined simulation-optimization approach to schedule investment decisions for lock reconstruction and rehabilitation. Ting and Schonfeld [130] adopt a simulation-optimization approach to decide how much capacity needs to be increased for the locks so that the costs associated with tow delays can be minimized.

Another stream of research propose mathematical models for the barge routing and empty container repositioning problem for the inland waterway transportation. Braekers et al. [20] optimizes barge routing and empty container repositioning between a sea port and few hinterland ports. The study is extended later in [19] to include vessel capacity and roundtrip service frequency. Marass [76] proposes a mixed-integer linear programming (MILP) model to optimize the transport routes of chartered container ships or tows for an inland waterway port. Alfandari et al. [6] propose a MILP model that optimizes the planning associated with liner service for a barge container shipping company. An et al. [9] formulate a mixed integer nonlinear programming (MINLP) model to solve the empty container repositioning shipping network design problem for an inland waterway transportation network. Davidovic et al. [28] propose a guided local search technique to solve a barge container ship routing problem.

Berth allocation problem, a prevalent issue experienced by inland waterway ports, received some considerations from the research community. Grubivsic et al. [50] propose an MILP model for designing a berth layout of a river port so that the overall vessel waiting time can be minimized. Depuy et al. [30] considers

fleet location capacity, total volume of barges, and average handling time to optimally allocate barge volume to different fleet locations. Guan and Cheung [51] propose two berth allocation model formulations and use tree search procedure with a composite heuristics for solving realistic size problem instances. Arango et al. [11] adopt both simulation and optimization approach to model the berth allocation problem. The authors propose a mathematical model and develop a heuristic procedure based on genetic algorithm to solve the problem.

Realizing the need that a port may fail either due to natural (e.g., hurricane, tornado) or human-induced (e.g., cyber-attack) disaster, few studies focus on identifying the resiliency of a deep draft inland waterway port. For instance, Baroud et al. [13] use stochastic resilience-based component importance measures into an optimization framework to determine the important waterway links and the precedence of link recovery in case of a disaster. MacKenzie et al. [72] analyze the economic impact of any sudden inland port closure by combining a simulation and a multi-regional input-output model. Pant et al. [103] propose a dynamic, multi-regional interdependency model to assess the effect of disruptions on the waterway networks, including both ports and waterway links. Folga et al. [42] propose a system level model to analyze the interdependency of failure followed by a disaster. Most recently, Hosseini and Barker [59] propose a Bayesian network to model the infrastructure resilience of an inland waterway port.

Some other studies related to inland waterway ports include the consideration of port-specific economic analysis [4, 87, 151, 67], optimal dredging scheduling

and investment decisions [86, 113, 18], and carbon emission [155, 71, 25]. In addition to these few recent studies (e.g., [39, 157, 45]) put specific focus on transportation from seaport to inland port to optimize different transportation related decisions. Fazi et al. (2015) consider the barge transportation from seaport to inland ports and provide a decision support system to schedule barges by modeling the problem as a vehicle routing problem [39]. Zhen et al. (2018) also consider transportation decisions from seaport to inland ports and provide a mixed-integer linear programming model to address tugboat scheduling and barge assignment problem [157]. Fu et al. (2010) illustrate the barge congestion problem and propose a simulation approach to address this issue [45].

Another stream of research considers inland waterway ports as a tier to solve different network design problems. Such considerations can be found in many application areas including biomass (e.g., [109, 79, 80]), coal (e.g., [35, 47, 62]), grain (e.g., [88, 10, 31]) supply chain design, and many others. Despite all these efforts, very few studies have captured the true characteristics of the inland waterway transportation (e.g., water level fluctuation, barge vs. towboat combination, barge availability and maintenance) while solving network designing problems. Note that the literatures included in this section are specific to deep draft inland waterway ports. Since the shallow draft inland ports hold some distinguished features over the deep draft inland waterway ports, the models used for deep draft inland waterway ports cannot be directly applied to the shallow draft inland ports. To the authors best knowledge, to date no research is available that considers shallow

draft inland ports handling shallow draft vessels. Our work extends the existing body of literature in multiple dimensions such as

- Proposing a new mathematical model which simultaneously optimizes the shallow draft inland waterway port decisions and supply chain network decisions. To date, no literature has captured the impact of shallow draft inland waterway port decisions on the overall supply chain network decisions.
- Our work effectively model different characteristics which are prevalent in the shallow draft inland waterway port system, such as barge-tow convoy considerations, barge maintenance and availability considerations, product-specific weight and volumetric restrictions, dredging impacts, and many others. Very few studies in the literature attempt to optimize the barge-towboat convoy system for container ports, but no prior attempt has been found that simultaneously captures all these waterway issues for the inland waterway transportation.

2.3 Problem Description and Model Formulation

This section presents a multi-commodity, multi-time period mixed-integer linear programming model for an inland waterway transportation network. The network considers a set of suppliers, origin and destination ports, and customers. Upon realization of demand for specific commodities, suppliers aim to supply the commodities through a combination of road and waterway transportation. The amount of product transported through the network is constrained by factors such as supplier capacities, possible connectivity to the waterway ports, storage capacities, capacity and availability of waterway transportation entities (e.g., towboat, barge), waterway capacities, and many others. The main objective of our model is to efficiently plan and manage the short-term operational decisions (e.g., trip-wise towboats, barges management at the inland ports) and mid-term supply chain decisions (e.g., inventory management, transportation decisions) in such a way that

the overall supply chain network cost can be minimized. Figure 5.1 presents a simple illustration of an inland waterway transportation network consisting of three suppliers of different commodities, two origin and three destination ports, and four markets.

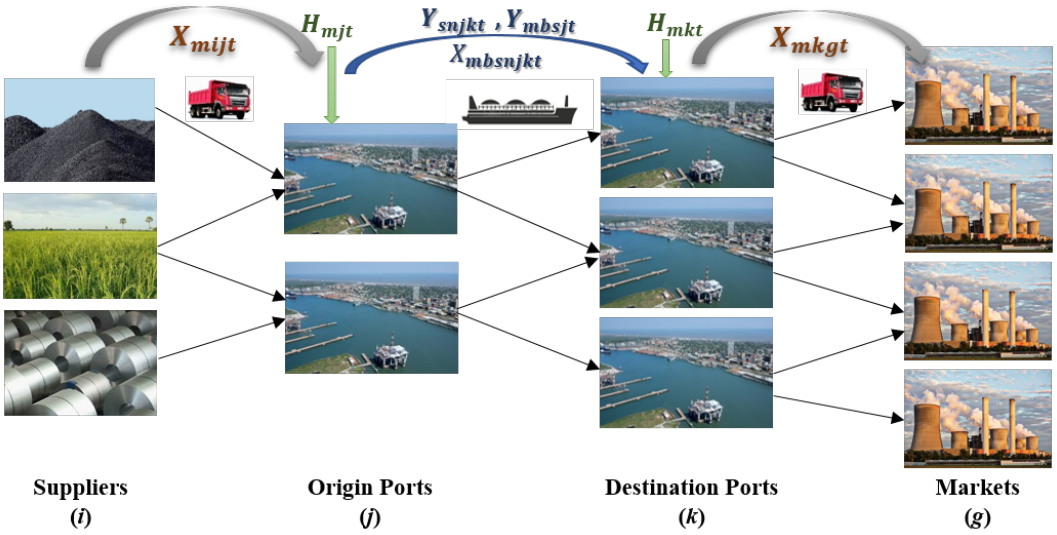

Figure 2.1

Illustration of an inland waterway transportation network

Consider a logistic network $\mathcal{L} = (\mathcal{N}, \mathcal{P})$, where $\mathcal{N}$ represents the set of nodes and $\mathcal{P}$ represents the set of arcs. Set $\mathcal{N}$ consists of the set of supply sites $\mathcal{I} = \{1, 2, 3, ..., I\}$, set of origin ports $\mathcal{J} = \{1, 2, 3, ..., J\}$, set of destination ports $\mathcal{K} = \{1, 2, 3, ..., K\}$, and a set of markets $\mathcal{G} = \{1, 2, 3, ..., G\}$ i.e., $\mathcal{N} = \mathcal{I} \bigcup \mathcal{J} \bigcup \mathcal{K} \bigcup \mathcal{G}$.

Note that $\mathcal{L}$ is not a fully connected graph i.e., not all nodes are fully connected to each other primarily due to their disperse locations. Therefore, we define two different types of subsets $\mathcal{I}_j$ and $\mathcal{J}_i$ where $\mathcal{I}_j$ represents the subset of supply sites connected to port $j \in \mathcal{J}$ and $\mathcal{J}_i$ to be the subset of origin ports that can receive commodities from supply sites $i \in \mathcal{I}$. Likewise, subsets $\mathcal{J}_k$, $\mathcal{K}_j$, $\mathcal{K}_g$, and $\mathcal{G}_k$ are used to define the appropriate interconnections between the source-destination pairs. Let $\mathcal{M} = \{1, 2, 3, ..., M\}$ be the set of commodities that need to be transported from supply site $i \in \mathcal{I}$ to market $g \in \mathcal{G}$ using origin port $j \in \mathcal{J}$ and destination port $k \in \mathcal{K}$ over a predetermined set of time periods $\mathcal{T} = \{1, 2, 3, ..., T\}$.

Let φ_{mit} be the amount of commodities of type $m \in \mathcal{M}$ available in supply site $i \in \mathcal{I}$ at time period $t \in \mathcal{T}$. Each arc $(i, j) \in (\mathcal{I}, \mathcal{J})$ carries commodities of type $m \in \mathcal{M}$ from a supply site i to origin port j and are generally located closer to each other. Therefore, trucks are preferred to carry commodities between arc $(i, j) \in (\mathcal{I}, \mathcal{J})$ by incurring an unit transportation cost of c_{mijt}. Each shipment from the supply sites are consolidated at an origin port $j \in \mathcal{J}$ before being delivered to the destination port $k \in \mathcal{K}$. We assume that a set of towboats $\mathcal{S} = \{1, 2, 3, ..., \overline{S}\}$ and barges $\mathcal{B} = \{1, 2, 3, ..., B\}$ are available to carry the commodities from the source to destination ports. Barges are flat-bottomed boats, either self-propelled or towed by towboats or tugs, can serve as a container to transport commodities between each source-destination pair. Each barge $b \in \mathcal{B}$ is restricted to a weight capacity of $\overline{w}_b$ and volume capacity of v_b. Note that the volume restriction of any barge is directly related to the density of any commodity $\{\rho_m\}_{m \in \mathcal{M}}$ carried

out by the barge. Towboats, another important component of inland waterway transportation, are also flat bottomed and can be used to push one or multiple barges in a single trip depending on their engine power capacity. We arrange set $\mathcal{S}$ in such a way that towboat 1 in set $\mathcal{S}$ to represent the least powerful towboat while $\overline{S}$ to represent the most powerful towboat. Based on their capabilities, we denote $\overline{\delta}_s$ and $\underline{\delta}_s$ to be the maximum and minimum number of barges that can be carried by any towboat $s \in \mathcal{S}$ in a single trip. Let ψ_{st} and η_{mbt} be the fixed costs associated with using a towboat $s \in \mathcal{S}$ (e.g., operator costs) and barge $b \in \mathcal{B}$ (e.g., loading and unloading costs) carrying commodity $m \in \mathcal{M}$ at time period $t \in \mathcal{T}$. Further, we define c_{mbsjkt} to be the unit cost associated with transporting commodity $m \in \mathcal{M}$ using barge $b \in \mathcal{B}$ of towboat $s \in \mathcal{S}$ along arc $(j,k) \in (\mathcal{J},\mathcal{K})$ at time period $t \in \mathcal{T}$. Finally, we assume that the commodities can be stored in any port having storage capacity $\overline{h}_j; \forall j \in \mathcal{J} \bigcup \mathcal{K}$, by incurring an unit inventory holding cost of h_{mjt} and the deterioration rate to carry the commodity of type $m \in \mathcal{M}$ from one time period to the next is denoted by α_m.

We also define a set of possible trips along arc $(j,k) \in (\mathcal{J},\mathcal{K})$ as $\mathcal{N}_{jk} = \{1,2,3,...,n_{jk}\}$. Note that due to *dredging* effects, the weight carrying capacity of a barge $\overline{w}_b$ and possible trips (τ_{jkt}) between each source-destination ports varies. The depth of navigation channel near ports or any points of the waterbody in between the source-destination ports may vary in different time periods of the year depending upon the amount of sediment, silt, or mud accumulated in the water bed. When this accumulation is very high in any portion of the waterway, it raises the height

of the waterbed. Hence, the total water depth of that particular area of the navigation channel decreases. Sometimes, this reduction in water level becomes too intense that it even resists the transportation of shallow draft water vessels through it. When this condition arises between the waterway of any origin-destination ports, barges can no longer carry commodities to their maximum design weight $\overline{w}_b$. The effective weight carrying capacity for the barge at that situation would be the minimum of the maximum weight capacity of a barge at the origin port w_{jt}, destination port w_{kt}, and the channel in between each origin-destination ports $(j,k) \in (\mathcal{J},\mathcal{K})$, denoted by w_{jkt}, i.e., $min\{w_{jt}, w_{jkt}, w_{kt}, \overline{w}_b\}$. Finally, we capture the periodic maintenance of towboats and barges at each origin port $j \in \mathcal{J}$ at time period $t \in \mathcal{T}$ through binary availability parameters a_{sjt} and a_{bjt}.

When commodities are carried by the towboats and barges to the destination ports, they are unloaded and transported to markets $g \in \mathcal{G}$ using trucks by incurring an unit transportation cost of c_{mkgt}. Each market $g \in \mathcal{G}$ demands d_{mgt} amount of commodities of type $m \in \mathcal{M}$ at time period $t \in \mathcal{T}$. The demand for the commodities are planned to satisfy through the inland waterway transportation. In case if the demand cannot be satisfied through this transportation network, we assume that another means of transport (e.g., trucks) are available to satisfy the market demand by incurring an unit penalty cost of π_{mgt}. The definitions of sets and parameters used in our proposed mathematical model are listed below.

Sets:

- $\mathcal{I}$: set of supply sites, $i \in \mathcal{I}$

- $\mathcal{J}$: set of origin ports, $j \in \mathcal{J}$
- $\mathcal{K}$: set of destination ports, $k \in \mathcal{K}$
- $\mathcal{G}$: set of markets, $g \in \mathcal{G}$
- $\mathcal{M}$: set of commodities, $m \in \mathcal{M}$
- $\mathcal{S}$: set of towboats, $s \in \mathcal{S}$
- $\mathcal{B}$: set of barges, $b \in \mathcal{B}$
- $\mathcal{N}_{jk}$: set of trips along arc $(j,k) \in (\mathcal{J},\mathcal{K})$, $n \in \mathcal{N}_{jk}$
- $\mathcal{T}$: set of time periods, $t \in \mathcal{T}$
- $\mathcal{I}_j$: set of supply sites connected to port j, $\forall j \in \mathcal{J}$
- $\mathcal{J}_i$: set of origin ports connected to supply site i, $\forall i \in \mathcal{I}$
- $\mathcal{J}_k$: set of origin ports connected to destination port k, $\forall k \in \mathcal{K}$
- $\mathcal{K}_j$: set of destination ports connected to origin port j, $\forall j \in \mathcal{J}$
- $\mathcal{K}_g$: set of destination ports connected to market g, $\forall g \in \mathcal{G}$
- $\mathcal{G}_k$: set of markets connected to destination port k, $\forall k \in \mathcal{K}$

Parameters:

- φ_{mit}: amount of product of type $m \in \mathcal{M}$ available in supply site $i \in \mathcal{I}$ at time period $t \in \mathcal{T}$
- ψ_{st}: fixed cost of using towboat $s \in \mathcal{S}$ at time period $t \in \mathcal{T}$
- η_{mbt}: fixed cost for loading and unloading commodity $m \in \mathcal{M}$ in barge $b \in \mathcal{B}$ at time period $t \in \mathcal{T}$
- c_{meft}: unit cost of transporting commodity $m \in \mathcal{M}$ along arc $(e,f) \in (\mathcal{I} \bigcup \mathcal{K}, \mathcal{J} \bigcup \mathcal{G})$ at time period $t \in \mathcal{T}$
- c_{mbsjkt}: unit cost of transporting commodity $m \in \mathcal{M}$ using barge $b \in \mathcal{B}$ of towboat $s \in \mathcal{S}$ along arc $(j,k) \in (\mathcal{J},\mathcal{K})$ at time period $t \in \mathcal{T}$
- $\overline{h}_j$: commodity storage capacity at port $j \in \mathcal{J} \bigcup \mathcal{K}$
- d_{mgt}: demand for commodity of type $m \in \mathcal{M}$ in market $g \in \mathcal{G}$ at time period $t \in \mathcal{T}$

- α_m: deterioration of commodity $m \in \mathcal{M}$
- a_{sjt}, a_{bjt}: binary availability of towboat and barge
- $\overline{\delta}_s, \underline{\delta}_s$: maximum/minimum number of barges to carry by towboat $s \in \mathcal{S}$
- w_{jt}, w_{jkt}, w_{kt}: maximum weight capacity at port $j \in \mathcal{J} \bigcup \mathcal{K}$ and the channel between port $(j,k) \in (\mathcal{J},\mathcal{K})$ at time period $t \in \mathcal{T}$. This weight depends on the depth of the waterway and should not exceed the minimal water-level between the origin-destination ports
- ρ_m: density of commodity $m \in \mathcal{M}$
- v_b: volume capacity of barge $b \in \mathcal{B}$
- $\overline{w}_b$: weight capacity of a barge $b \in \mathcal{B}$
- π_{mgt}: unit penalty cost of not satisfying demand for commodity $m \in \mathcal{M}$ in market $g \in \mathcal{G}$ at time period $t \in \mathcal{T}$
- h_{mjt}: unit inventory holding cost for commodity $m \in \mathcal{M}$ in port $j \in \mathcal{J} \bigcup \mathcal{K}$ at time period $t \in \mathcal{T}$
- θ_{jt}: total number of barges available in port $j \in \mathcal{J}$ at time period $t \in \mathcal{T}$
- τ_{jkt}: maximum number of trips that can be made along arc $(j,k) \in (\mathcal{J},\mathcal{K})$ at time period t

Decision Variables:

- Y^1_{snjkt}: 1 if a towboat $s \in \mathcal{S}$ is used in arc $(j,k) \in (\mathcal{J},\mathcal{K})$ for trip $n \in \mathcal{N}_{jk}$ at time period $t \in \mathcal{T}$; 0 otherwise
- Y^2_{mbsjt}: 1 if commodity $m \in \mathcal{M}$ is carried on barge $b \in \mathcal{B}$ of towboat $s \in \mathcal{S}$ from port $j \in \mathcal{J}$ at time period $t \in \mathcal{T}$; 0 otherwise
- X_{meft}: amount of commodities of type $m \in \mathcal{M}$ transported along arc $(e,f) \in (\mathcal{I} \bigcup \mathcal{K}, \mathcal{J} \bigcup \mathcal{G})$ at time period $t \in \mathcal{T}$
- $X_{mbsnjkt}$: amount of commodities of type $m \in \mathcal{M}$ transported using barge $b \in \mathcal{B}$ of towboat $s \in \mathcal{S}$ of trip $n \in \mathcal{N}_{jk}$ along arc $(j,k) \in (\mathcal{J},\mathcal{K})$ at time period $t \in \mathcal{T}$
- H_{mjt}: amount of commodities of type $m \in \mathcal{M}$ stored in port $j \in \mathcal{J} \bigcup \mathcal{K}$ at time period $t \in \mathcal{T}$

- U_{mgt}: amount of commodities of type $m \in \mathcal{M}$ shortage in market $g \in \mathcal{G}$ at time period $t \in \mathcal{T}$

We now introduce the following decision variables for our proposed mathematical model formulation. The first set of decision variables $\mathbf{Y}^1 := \{Y^1_{snjkt} | \forall s \in \mathcal{S}, n \in \mathcal{N}_{jk}, j \in \mathcal{J}, k \in \mathcal{K}_j, t \in \mathcal{T}\}$ and $\mathbf{Y}^2 := \{Y^2_{mbsjt} | \forall m \in \mathcal{M}, b \in \mathcal{B}, s \in \mathcal{S}, j \in \mathcal{J}, t \in \mathcal{T}\}$ determine which towboat to use between any origin-destination pair in a given time period and which barge to use for carrying any particular product at any given origin port, respectively, i.e.,

$$Y^1_{snjkt} = \begin{cases} 1 & \text{if a towboat } s \text{ is used in arc } (j,k) \in (\mathcal{J},\mathcal{K}) \text{ for trip } n \text{ at time period } t \\ 0 & \text{otherwise;} \end{cases}$$

$$Y^2_{mbsjt} = \begin{cases} 1 & \text{if barge } b \text{ connected to towboat } s \text{ is used to carry commodity } m \\ & \text{at port } j \text{ in time period } t \\ 0 & \text{otherwise;} \end{cases}$$

For notation simplicity, we define $\mathbf{Y}$ as $\mathbf{Y} := \mathbf{Y}^1 \bigcup \mathbf{Y}^2$. Additionally, we introduce $\mathbf{X}^1 := \{X_{meft} | \forall m \in \mathcal{M}, (e,f) \in (\mathcal{I} \bigcup \mathcal{K}, \mathcal{J} \bigcup \mathcal{G}), t \in \mathcal{T}\}$ to denote the amount of commodities of type $m \in \mathcal{M}$ transported along arc $(e,f) \in (\mathcal{I} \bigcup \mathcal{K}, \mathcal{J} \bigcup \mathcal{G})$ at time period $t \in \mathcal{T}$ and $\mathbf{X}^2 := \{X_{mbsnjkt} | \forall m \in \mathcal{M}, b \in \mathcal{B}, s \in \mathcal{S}, n \in \mathcal{N}_{jk}, (j,k) \in (\mathcal{J},\mathcal{K}), t \in \mathcal{T}\}$ to denote the amount of commodities of type $m \in \mathcal{M}$ transported using barge $b \in \mathcal{B}$ of towboat $s \in \mathcal{S}$ of trip $n \in \mathcal{N}_{jk}$ along arc $(j,k) \in (\mathcal{J},\mathcal{K})$ at time period $t \in \mathcal{T}$ and $\mathbf{X} := \mathbf{X}^1 \bigcup \mathbf{X}^2$. We also introduce decision variables

$\mathbf{H} := \{H_{mjt} | \forall m \in \mathcal{M}, j \in \mathcal{J} \bigcup \mathcal{K}, t \in \mathcal{T}\}$ to identify the amount of commodities of type $m \in \mathcal{M}$ disjointly stored in both origin and destination port $j \in \mathcal{J} \bigcup \mathcal{K}$ at time period $t \in \mathcal{T}$. The amount of unsatisfied demand of any commodity $m \in \mathcal{M}$ in market $g \in \mathcal{G}$ at any given time period $t \in \mathcal{T}$ is determined by variables $\mathbf{U} := \{U_{mgt} | \forall m \in \mathcal{M}, g \in \mathcal{G}, t \in \mathcal{T}\}$. With these variables, we now introduce the *inland waterway port management optimization problem* **[IMP]** as follows,

$$\textbf{[IMP]} \quad \underset{\mathbf{Y,X,H,U}}{Minimize} \sum_{t\in\mathcal{T}} \Bigg(\sum_{s\in\mathcal{S}} \sum_{n\in\mathcal{N}_{jk}} \sum_{j\in\mathcal{J}} \sum_{k\in\mathcal{K}_j} \psi_{st} Y^1_{snjkt} + \sum_{m\in\mathcal{M}} \Bigg(\sum_{b\in\mathcal{B}} \sum_{s\in\mathcal{S}} \sum_{j\in\mathcal{J}} \eta_{mbt} Y^2_{mbsjt} + \sum_{(e,f)\in(\mathcal{I}\bigcup\mathcal{K},\mathcal{J}\bigcup\mathcal{G})} c_{meft} X_{meft} + \sum_{b\in\mathcal{B}} \sum_{s\in\mathcal{S}} \sum_{n\in\mathcal{N}_{jk}} \sum_{(j,k)\in(\mathcal{J},\mathcal{K})} c_{mbsjkt} X_{mbsnjkt} + \sum_{j\in\mathcal{J}\bigcup\mathcal{K}} h_{mjt} H_{mjt} + \sum_{g\in\mathcal{G}} \pi_{mgt} U_{mgt} \Bigg) \Bigg) \tag{2.1}$$

subject to

$$\sum_{j\in\mathcal{J}_i} X_{mijt} \leq \varphi_{mit} \forall m \in \mathcal{M}, i \in \mathcal{I}, t \in \mathcal{T} \tag{2.2}$$

$$\sum_{i\in\mathcal{I}_j} X_{mijt} + (1-\alpha_m) H_{mj,t-1} = \sum_{b\in\mathcal{B}} \sum_{s\in\mathcal{S}} \sum_{n\in\mathcal{N}_{jk}} \sum_{k\in\mathcal{K}_j} X_{mbsnjkt} + H_{mjt} \quad \forall m \in \mathcal{M}, j \in \mathcal{J}, t \in \mathcal{T} \tag{2.3}$$

$$\sum_{b\in\mathcal{B}} \sum_{s\in\mathcal{S}} \sum_{n\in\mathcal{N}_{jk}} \sum_{j\in\mathcal{J}_k} X_{mbsnjkt} + (1-\alpha_m) H_{mk,t-1} = \sum_{g\in\mathcal{G}_k} X_{mkgt} + H_{mkt} \quad \forall m \in \mathcal{M}, k \in \mathcal{K}, t \in \mathcal{T} \tag{2.4}$$

$$\sum_{k\in\mathcal{K}_g} X_{mkgt} + U_{mgt} = d_{mgt} \forall m \in \mathcal{M}, g \in \mathcal{G}, t \in \mathcal{T} \tag{2.5}$$

$$\sum_{m\in\mathcal{M}} H_{mjt} \leq \overline{h}_j \forall j \in \mathcal{J} \bigcup \mathcal{K}, t \in \mathcal{T} \tag{2.6}$$

$$\sum_{m\in\mathcal{M}} Y^2_{mbsjt} \leq 1 \forall b \in \mathcal{B}, s \in \mathcal{S}, j \in \mathcal{J}, t \in \mathcal{T} \quad (2.7)$$

$$\sum_{s\in\mathcal{S}} Y^1_{snjkt} \leq 1 \forall n \in \mathcal{N}_{jk}, j \in \mathcal{J}, k \in \mathcal{K}_j, t \in \mathcal{T} \quad (2.8)$$

$$\sum_{n\in\mathcal{N}_{jk}} \sum_{k\in\mathcal{K}_j} \underline{\delta}_s Y^1_{snjkt} \leq \sum_{m\in\mathcal{M}} \sum_{b\in\mathcal{B}} Y^2_{mbsjt} \leq \sum_{n\in\mathcal{N}_{jk}} \sum_{k\in\mathcal{K}_j} \overline{\delta}_s Y^1_{snjkt} \quad \forall s \in \mathcal{S}, j \in \mathcal{J}, t \in \mathcal{T} \quad (2.9)$$

$$\sum_{n\in\mathcal{N}_{jk}} X_{mbsnjkt} \leq min\{w_{jt}, w_{jkt}, w_{kt}, \overline{w}_b\} Y^2_{mbsjt} \quad \forall m \in \mathcal{M}, b \in \mathcal{B}, s \in \mathcal{S}, j \in \mathcal{J}, k \in \mathcal{K}_j, t \in \mathcal{T} \quad (2.10)$$

$$\sum_{n\in\mathcal{N}_{jk}} \sum_{k\in\mathcal{K}_j} \left(\frac{X_{mbsnjkt}}{\rho_m}\right) \leq v_b Y^2_{mbsjt} \forall m \in \mathcal{M}, b \in \mathcal{B}, s \in \mathcal{S}, j \in \mathcal{J}, t \in \mathcal{T} \quad (2.11)$$

$$\sum_{s\in\mathcal{S}} \sum_{n\in\mathcal{N}_{jk}} Y^1_{snjkt} \leq \tau_{jkt} \forall j \in \mathcal{J}, k \in \mathcal{K}_j, t \in \mathcal{T} \quad (2.12)$$

$$\sum_{m\in\mathcal{M}} \sum_{b\in\mathcal{B}} \sum_{s\in\mathcal{S}} Y^2_{mbsjt} \leq \theta_{jt} \forall j \in \mathcal{J}, t \in \mathcal{T} \quad (2.13)$$

$$\sum_{n\in\mathcal{N}_{jk}} \sum_{k\in\mathcal{K}_j} Y^1_{snjkt} \leq a_{sjt} \forall s \in \mathcal{S}, j \in \mathcal{J}, t \in \mathcal{T} \quad (2.14)$$

$$\sum_{m\in\mathcal{M}} \sum_{s\in\mathcal{S}} Y^2_{mbsjt} \leq a_{bjt} \forall b \in \mathcal{B}, j \in \mathcal{J}, t \in \mathcal{T} \quad (2.15)$$

$$Y^2_{mbsjt} \in \{0,1\} \forall m \in \mathcal{M}, b \in \mathcal{B}, s \in \mathcal{S}, j \in \mathcal{J}, t \in \mathcal{T} \quad (2.16)$$

$$Y^1_{snjkt} \in \{0,1\} \forall s \in \mathcal{S}, n \in \mathcal{N}_{jk}, j \in \mathcal{J}, k \in \mathcal{K}_j, t \in \mathcal{T} \quad (2.17)$$

$$X_{mijt}, X_{mjkbsnt}, X_{mkgt}, H_{mjt}, H_{mkt}, U_{mgt} \in \mathbb{R}^+ \quad (2.18)$$

In **[IMP]**, the objective function minimizes the overall logistics cost for the inland waterway transportation network. The objective function consists of six terms: the first and second term represent, respectively, the fixed costs associated with using towboats, and loading and unloading commodities into the barges. The third term in the objective function represents the total transportation cost

associated with transporting any commodity to and from any origin-destination port using trucks. The costs incurred due to transporting commodities between each origin-destination ports are captured by the fourth term in the objective function. The last two terms in the objective function specify the total storage cost and penalty cost due to unsatisfied demand.

Constraints (2.2) indicate that the amount of commodity of type $m \in \mathcal{M}$ transported from a supply site $i \in \mathcal{I}$ at any given time period $t \in \mathcal{T}$ is restricted by the supply capacity φ_{mit}. Constraints (2.3) and (2.4) are the flow balance constraints which ensure that at any given time period $t \in \mathcal{T}$ the amount of commodity of type $m \in \mathcal{M}$ can be either shipped or stored in a source or destination port $j \in \mathcal{J} \bigcup \mathcal{K}$. Constraints (2.5) indicate that the demand for commodity $m \in \mathcal{M}$ in market $g \in \mathcal{G}$ at any given time $t \in \mathcal{T}$ can be either completely or partially satisfied through the inland waterway transportation network. If partially satisfied, we assume that the balance commodities can be satisfied though external sources via a higher penalty cost π_{mgt}. Constraints (2.6) restrict the storage quantity of a given commodity $m \in \mathcal{M}$ at port $j \in \mathcal{J} \bigcup \mathcal{K}$ to its maximum storage capacity $\overline{h}_j$. The commodity mix restriction is handled by constraints (2.7) which indicate that only one commodity of type $m \in \mathcal{M}$ can be loaded in any barge $b \in \mathcal{B}$ of a given towboat $s \in \mathcal{S}$. Constraints (2.8) indicate that only one towboat $s \in \mathcal{S}$ can be used in trip $n \in \mathcal{N}_{jk}$ between each source-destination pair at a given time period $t \in \mathcal{T}$. Constraints (2.9) set restrictions on the maximum ($\overline{\delta}_s$) and minimum ($\underline{\delta}_s$) number of barges that can be connected with any particular towboat $s \in \mathcal{S}$ in

port $j \in \mathcal{J}$ at time period $t \in \mathcal{T}$. The dredging issues are captured in constraints (2.10). These constraints indicate that at any given time period $t \in \mathcal{T}$ a barge $b \in \mathcal{B}$ can only carry the minimum of $\{w_{jt}, w_{jkt}, w_{kt}, \overline{w}_b\}$ amount of commodity between each origin-destination port. The volumetric capacity restriction of a barge $b \in \mathcal{B}$ is handled by constraints (2.11). Constraints (2.12) restrict the maximum number of possible trips (τ_{jkt}) between each origin-destination port. Constraints (2.13) indicate the maximum availability of barges (θ_{jt}) in port $j \in \mathcal{J}$ at time period $t \in \mathcal{T}$. Barges and towboats can go for periodic maintenance. These are handled in constraints (2.14) and (2.15) via binary availability parameters a_{sjt} and a_{bjt}, respectively. Finally, constraints (2.16) and (2.17) are the integrality constraints and (2.18) are the standard non-negativity constraints, respectively.

2.4 Solution Approach

By setting $|\mathcal{M}| = 1$, $|\mathcal{S}| = 1$, $|\mathcal{B}| = 1$, $|\mathcal{N}_{jk}| = 1$, $|\mathcal{T}| = 1$ i.e., a single commodity, a single towboat, a single barge, a single trip, and a single time-period, problem **[IMP]** can be simplified to a special case of a fixed-charge network flow problem which is already known to be an $\mathcal{NP}$-hard problem [74]. Therefore, commercial solvers, such as CPLEX/GUROBI, can only able to solve small scale problem instances of such problems. Our problem **[IMP]** involves solving a mixed-integer linear programming model which can be considered very challenging from solution standpoint depending on the size of sets $|\mathcal{M}|$, $|\mathcal{I}|$, $|\mathcal{J}|$, $|\mathcal{K}|$, $|\mathcal{G}|$, $|\mathcal{B}|$, $|\mathcal{S}|$, $|\mathcal{N}_{jk}|$, and $|\mathcal{T}|$. To alleviate this problem, in this section, we first employ a well-

known partitioning method, commonly referred to as *Benders decomposition* algorithm [15, 83], to solve our proposed optimization model **[IMP]**. Later in this section, we demonstrate multiple enhancement techniques to accelerate the performance of the basic Benders decomposition algorithm and to solve problem **[IMP]** efficiently. The techniques used to enhance the Benders decomposition algorithm include problem-specific valid-inequalities, input ordering, pareto-optimal cut, knapsack inequalities, and local branching procedure. The aim is to produce high-quality feasible solutions for solving realistic-size instances of problem **[IMP]** in a reasonable amount of time.

2.4.1 Benders Decomposition Algorithm

In Benders decomposition, the original problem can be decomposed into two subproblems: an integer *master problem* and a linear *subproblem*. Before introducing the subproblems, let us first present the underlying Benders reformulation for model **[IMP]** as follows:

$$\begin{aligned} \textit{Minimize} \quad & \Big\{ \sum_{t\in\mathcal{T}} \Big(\sum_{s\in\mathcal{S}} \sum_{n\in\mathcal{N}_{jk}} \sum_{j\in\mathcal{J}} \sum_{k\in\mathcal{K}_j} \psi_{st} Y^1_{snjkt} + \sum_{m\in\mathcal{M}} \sum_{b\in\mathcal{B}} \sum_{s\in\mathcal{S}} \sum_{j\in\mathcal{J}} \eta_{mbt} Y^2_{mbsjt} \Big) + \\ & [\mathbf{SP}](\mathbf{X},\mathbf{H},\mathbf{U} \,|\hat{\mathbf{Y}}^1, \hat{\mathbf{Y}}^2) \Big\} \end{aligned} \tag{2.19}$$

subject to (2.2)-(2.18). We represent $[\mathbf{SP}](\mathbf{X},\mathbf{H},\mathbf{U}|\hat{\mathbf{Y}}^1, \hat{\mathbf{Y}}^2)$ as Benders subproblem, which is presented below. For given values of $\hat{\mathbf{Y}}^1 := \{Y^1_{snjkt} | s \in \mathcal{S}, n \in \mathcal{N}_{jk}, j \in \mathcal{J}, k \in \mathcal{K}, t \in \mathcal{T}\}$ and $\hat{\mathbf{Y}}^2 := \{Y^2_{mbsjt} | m \in \mathcal{M}, b \in \mathcal{B}, s \in \mathcal{S}, j \in \mathcal{J}, t \in \mathcal{T}\}$ which satisfy integrality restrictions (2.16) and (2.17), problem **[IMP]** can be deduced to

the following *primal subproblem* involving only continuous variables **X, H, U** as follows:

$$\textbf{[SP]}\ (\mathbf{X,H,U}|\hat{\mathbf{Y}}^1,\hat{\mathbf{Y}}^2)\ \underset{\mathbf{X,H,U}}{Minimize} \sum_{t\in\mathcal{T}}\sum_{m\in\mathcal{M}}\Bigg(\sum_{j\in\mathcal{J}\cup\mathcal{K}} h_{mjt}H_{mjt} + \sum_{(e,f)\in(\mathcal{I}\cup\mathcal{K},\mathcal{J}\cup\mathcal{G})} c_{meft}X_{meft} + \sum_{b\in\mathcal{B}}\sum_{s\in\mathcal{S}}\sum_{n\in\mathcal{N}_{jk}}\sum_{(j,k)\in(\mathcal{J},\mathcal{K})} c_{mbsjkt}X_{mbsnjkt} + \sum_{g\in\mathcal{G}}\pi_{mgt}U_{mgt}\Bigg) \tag{2.20}$$

subject to constraints (2.2)-(2.6), (2.10)-(2.11), and (2.18). We let $\boldsymbol{\mu} = \{\mu_{mit} \geq 0 | \forall m \in \mathcal{M}, i \in \mathcal{I}, t \in \mathcal{T}\}$, $\boldsymbol{\vartheta} = \{\vartheta_{mjt} | \forall m \in \mathcal{M}, j \in \mathcal{J}, t \in \mathcal{T}\}$, and $\boldsymbol{\zeta} = \{\zeta_{mkt} | \forall m \in \mathcal{M}, k \in \mathcal{K}, t \in \mathcal{T}\}$ be the vector of the dual variables associated with constraints (2.2)-(2.4); $\boldsymbol{\varepsilon} = \{\varepsilon_{mgt} | \forall m \in \mathcal{M}, g \in \mathcal{G}, t \in \mathcal{T}\}$ be the dual variables for constraints (2.5); $\boldsymbol{\kappa} = \{\kappa_{jt} \geq 0 | \forall j \in \mathcal{J}, t \in \mathcal{T}\}$ and $\boldsymbol{\iota} = \{\iota_{kt} \geq 0 | \forall k \in \mathcal{K}, t \in \mathcal{T}\}$ be the dual variables for constraints (2.6); and $\boldsymbol{\xi} = \{\xi_{mbsjkt} \geq 0 | \forall m \in \mathcal{M}, b \in \mathcal{B}, s \in \mathcal{S}, j \in \mathcal{J}, k \in \mathcal{K}, t \in \mathcal{T}\}$ and $\boldsymbol{\chi} = \{\chi_{mbsjt} \geq 0 | \forall m \in \mathcal{M}, b \in \mathcal{B}, s \in \mathcal{S}, j \in \mathcal{J}, t \in \mathcal{T}\}$ be the vector of the dual variables associated with constraints (2.10)-(2.11). We present the dual of the primal subproblem **[SP]**, referred to as **[DP]**, as follows:

$$\begin{aligned}\textbf{[DP]}\quad & Maximize \sum_{t\in\mathcal{T}}\Bigg(\sum_{m\in\mathcal{M}}\Bigg(\sum_{g\in\mathcal{G}} d_{mgt}\varepsilon_{mgt} - \sum_{i\in\mathcal{I}}\varphi_{mit}\mu_{mit} - \sum_{b\in\mathcal{B}}\sum_{s\in\mathcal{S}}\sum_{j\in\mathcal{J}}\Bigg(\sum_{k\in\mathcal{K}} \\ & min\{w_{jt}, w_{jkt}, w_{kt}, \overline{w}_b\}\hat{Y}^2_{mbsjt}\xi_{mbsjkt} + v_b\hat{Y}^2_{mbsjt}\chi_{mbsjt}\Bigg)\Bigg) - \sum_{j\in\mathcal{J}}\overline{h}_j\kappa_{jt} \\ & - \sum_{k\in\mathcal{K}}\overline{h}_k\iota_{kt}\Bigg)\end{aligned} \tag{2.21}$$

subject to

$$-\mu_{mit} + \vartheta_{mjt} \leq c_{mijt} \quad \forall m \in \mathcal{M}, i \in \mathcal{I}, j \in \mathcal{J}, t \in \mathcal{T} \quad (2.22)$$

$$-\vartheta_{mjt} + \zeta_{mkt} - \xi_{mbsjkt} - \frac{\chi_{mbsjt}}{\rho_m} \leq c_{mbsjkt} \; \forall m \in \mathcal{M}, b \in \mathcal{B}, s \in \mathcal{S}, j \in \mathcal{J}, k \in \mathcal{K}_j, t \in \mathcal{T} \quad (2.23)$$

$$(1-\alpha_m)\vartheta_{mj,t+1} - \vartheta_{mjt} - \kappa_{jt} \leq h_{mjt} \quad \forall m \in \mathcal{M}, j \in \mathcal{J}, t \in \mathcal{T} \quad (2.24)$$

$$(1-\alpha_m)\zeta_{mk,t+1} - \zeta_{mkt} - \iota_{kt} \leq h_{mkt} \quad \forall m \in \mathcal{M}, k \in \mathcal{K}, t \in \mathcal{T} \quad (2.25)$$

$$-\zeta_{mkt} + \varepsilon_{mgt} \leq c_{mkgt} \quad \forall m \in \mathcal{M}, k \in \mathcal{K}, g \in \mathcal{G}, t \in \mathcal{T} \quad (2.26)$$

$$\varepsilon_{mgt} \leq \pi_{mgt} \quad \forall m \in \mathcal{M}, g \in \mathcal{G}, t \in \mathcal{T} \quad (2.27)$$

$$\mu_{mit}, \kappa_{jt}, \iota_{kt}, \xi_{mbsjkt}, \chi_{mbsjt} \in \mathbb{R}^+ \quad (2.28)$$

$$\vartheta_{mjt}, \zeta_{mkt}, \varepsilon_{mgt} \in \mathbb{R} \quad (2.29)$$

Now, in the underlying Benders reformulation, we can introduce an additional free variable θ and define the following Benders *Master problem* **[MP]**:

$$\textbf{[MP]} \quad \underset{\mathbf{Y},\boldsymbol{\theta}}{Minimize} \sum_{t\in\mathcal{T}} \Bigg(\sum_{s\in\mathcal{S}} \sum_{n\in\mathcal{N}_{jk}} \sum_{j\in\mathcal{J}} \sum_{k\in\mathcal{K}_j} \psi_{st} Y^1_{snjkt} + \sum_{m\in\mathcal{M}} \sum_{b\in\mathcal{B}} \sum_{s\in\mathcal{S}} \sum_{j\in\mathcal{J}} \eta_{mbt} Y^2_{mbsjt} \Bigg) + \theta \quad (2.30)$$

subject to constraints (2.7)-(2.9), (2.12)-(2.17), and

$$\theta \geq \sum_{t\in\mathcal{T}} \Bigg(\sum_{m\in\mathcal{M}} \Bigg(\sum_{g\in\mathcal{G}} d_{mgt}\varepsilon_{mgt} - \sum_{i\in\mathcal{I}} \varphi_{mit}\mu_{mit} - \sum_{b\in\mathcal{B}} \sum_{s\in\mathcal{S}} \sum_{j\in\mathcal{J}} \Bigg(v_b Y^2_{mbsjt}\chi_{mbsjt} + \sum_{k\in\mathcal{K}} min\{w_{jt}, w_{jkt}, w_{kt}, \overline{w}_b\} Y^2_{mbsjt}\xi_{mbsjkt} \Bigg) \Bigg) - \sum_{j\in\mathcal{J}} \overline{h}_j\kappa_{jt} - \sum_{k\in\mathcal{K}} \overline{h}_k\iota_{kt} \Bigg)$$
$$\forall (\mu, \varepsilon, \chi, \xi, \kappa, \iota) \in \mathcal{P}_D \quad (2.31)$$

Constraints (2.31) are referred to as *optimality cut* constraints where $\mathcal{P}_D$ is the set of extreme points in the feasible region of **[DP]**. The objective function value of **[DP]** bounds the variable θ from above i.e.,

$$\theta \geq \sum_{t\in\mathcal{T}}\Bigg(\sum_{m\in\mathcal{M}}\Bigg(\sum_{g\in\mathcal{G}} d_{mgt}\varepsilon_{mgt} - \sum_{i\in\mathcal{I}}\varphi_{mit}\mu_{mit} - \sum_{b\in\mathcal{B}}\sum_{s\in\mathcal{S}}\sum_{j\in\mathcal{J}}\Bigg(v_b Y^2_{mbsjt}\chi_{mbsjt} + \sum_{k\in\mathcal{K}} min\{w_{jt}, w_{jkt}, w_{kt}, \overline{w}_b\} Y^2_{mbsjt}\xi_{mbsjkt}\Bigg)\Bigg) - \sum_{j\in\mathcal{J}}\overline{h}_j\kappa_{jt} - \sum_{k\in\mathcal{K}}\overline{h}_k\iota_{kt}\Bigg) \quad \forall(\mu,\varepsilon,\chi,\xi,\kappa,\iota)\in\mathcal{P}_D$$

Note that, no *feasibility cut* is added in **[MP]** since for any feasible solutions of **Y**, constraints (2.5) ensure that primal subproblem $[\mathbf{SP}](\mathbf{X,H,U}|\hat{\mathbf{Y}}^1,\hat{\mathbf{Y}}^2)$ will always remain feasible. Moreover, since parameters c_{mijt}, c_{mbsjkt}, h_{mjt}, h_{mkt}, c_{mkgt}, and π_{mgt} are finite, any feasible solution of $[\mathbf{SP}](\mathbf{X,H,U}|\hat{\mathbf{Y}}^1,\hat{\mathbf{Y}}^2)$ must be bounded. By strong duality theory, we can state that the dual subproblem **[DP]** will also remain feasible and bounded.

The overall Benders decomposition algorithm is outlined below. Let UB^r and LB^r be an upper and lower bound for the original problem **[IMP]** which are obtained during the Benders decomposition algorithm at each iteration r. We also define z^r_{MAS} as follows:

$$z^r_{MAS} = \sum_{t\in\mathcal{T}}\Bigg(\sum_{s\in\mathcal{S}}\sum_{n\in\mathcal{N}_{jk}}\sum_{j\in\mathcal{J}}\sum_{k\in\mathcal{K}_j}\psi_{st}\hat{Y}^{1r}_{snjkt} + \sum_{m\in\mathcal{M}}\sum_{b\in\mathcal{B}}\sum_{s\in\mathcal{S}}\sum_{j\in\mathcal{J}}\eta_{mbt}\hat{Y}^{2r}_{mbsjt}\Bigg) \tag{2.32}$$

In Benders decomposition algorithm, we iteratively solve master problem **[MP]** to obtain the solutions $\{\hat{Y}^{1r}_{snjkt}\}_{s\in\mathcal{S},n\in\mathcal{N}_{jk},j\in\mathcal{J},k\in\mathcal{K},t\in\mathcal{T}}$ and $\{\hat{Y}^{2r}_{mbsjt}\}_{m\in\mathcal{M},b\in\mathcal{B},s\in\mathcal{S},j\in\mathcal{J},t\in\mathcal{T}}$. The objective function value obtained from solving **[MP]** provides a valid lower bound for the original problem **[IMP]**, which is denoted by z^r_{MP}. We then fix the values of $\{\hat{Y}^{1r}_{snjkt}\}$ and $\{\hat{Y}^{2r}_{mbsjt}\}$ to solve the dual subproblem **[DP]**. In each iteration r of the Benders decomposition algorithm, the summation of z^r_{MAS} (obtained from the master problem) and z^r_{SUB} (obtained from the subproblem) provides a valid upper bound for the original problem **[IMP]**. The overall Benders decomposition algorithm is terminated when the gap between the upper and lower bound falls below a pre-specified threshold limit ϵ; otherwise, the optimality cut (2.31) is updated and added to the master problem **[MP]**. Note that the Benders reformulation contains an exponential number of constraints that can been handled through a cutting plane approach. Let $\mathcal{P}^r_D$ be the restricted set of extreme points of D at iteration r. Thus, the relaxed master problem **[MP]** is solved containing a small subset of the constraints in (2.31) i.e., $\mathcal{P}^r_D \subset \mathcal{P}_D$ and gradually add them until the gap between the upper and lower bound falls below the threshold limit ϵ. The pseudo-code for the basic Benders decomposition algorithm is provided in **Algorithm 1**.

2.4.2 Enhancement of Benders Decomposition Algorithm

2.4.2.1 Valid inequalities

By utilizing the special structure of our problem **[IMP]**, we generate a number of valid inequalities that can be used to accelerate the performance of the over-

all Benders decomposition algorithm. The following set of valid inequalities are added in each iteration of the *Benders master problem* **[MP]**:

- The following *surrogate constraints* (2.33) are added in each iteration of the Benders master problem **[MP]** which provide a lower bound on the number of barges required to satisfy commodity demand $m \in \mathcal{M}$ at time period $t \in \mathcal{T}$. Here, we can initialize the value of σ between 0.0 to 1.0. When $\sigma = 1.0$, constraints (2.33) ensure that all the demand is required to be satisfied from the inland waterway port network.

$$\sum_{b\in\mathcal{B}}\sum_{s\in\mathcal{S}}\sum_{j\in\mathcal{J}} Y^2_{mbsjt}\overline{w}_b \;\geq\; \sum_{g\in\mathcal{G}} \sigma d_{mgt} \qquad \forall m \in \mathcal{M}, t \in \mathcal{T} \qquad (2.33)$$

- Symmetries may result during the selection of the barges since all the barges are of similar capacities. To alleviate this problem, the following *lexicographic ordering constraints* [122, 63] ((2.34) and (2.35)) are added in each iteration of the Benders master problem **[MP]** that set priorities by which the solver can select the barges. It is expected that such priorities will break the duplications caused by the barge selection symmetry and accelerate the performance of the branch-and-bound process.

$$Y^2_{1,b-1,sjt} \;\geq\; Y^2_{1bsjt} \qquad \forall b \in \mathcal{B}\setminus\{1\}, s \in \mathcal{S}, j \in \mathcal{J}, t \in \mathcal{T} \qquad (2.34)$$

$$\sum_{p=1}^{m} 2^{(m-p)} Y^2_{p,b-1,sjt} \;\geq\; \sum_{p=1}^{m} 2^{(m-p)} Y^2_{pbsjt} \quad \forall m \in \mathcal{M}, b \in \mathcal{B}\setminus\{1\}, s \in \mathcal{S}, j \in \mathcal{J}, t \in \mathcal{T} \qquad (2.35)$$

- In addition to handling symmetries that can arise while selecting barges, we also handle the possible symmetries that may arise between same type of towboats. Let $\mathcal{S}^{'}_e$ be the subset of towboats belongs to the same type i.e., $\mathcal{S}^{'}_e \subset \mathcal{S}$ and $s^{'}_e \in \mathcal{S}^{'}_e$, where $s^{'}_e$ represents a set of non-decreasing order of the members belongs to $\mathcal{S}^{'}_e$. The following lexicographical ordering constraints ((2.36) and (2.37)) are applied for each $\mathcal{S}^{'}_e$ to determine the priority of utilizing towboats of the same type.

$$Y^1_{s^{'}_e-1,njkt} \;\geq\; Y^1_{s^{'}_e njkt} \qquad \forall s^{'}_e \in \mathcal{S}^{'}_e\setminus\{1\}, n \in \mathcal{N}_{jk}, j \in \mathcal{J}, k \in \mathcal{K}, t \in \mathcal{T} \qquad (2.36)$$

$$\psi_{s^{'}_e-1,t} Y^1_{s^{'}_e-1,njkt} \;\geq\; \psi_{s^{'}_e t} Y^1_{s^{'}_e njkt} \forall s^{'}_e \in \mathcal{S}^{'}_e\setminus\{1\}, n \in \mathcal{N}_{jk}, j \in \mathcal{J}, k \in \mathcal{K}, t \in \mathcal{T} \qquad (2.37)$$

- The following set of constraints, (2.38) and (2.39), set a lower bound on the number of barges that are required to satisfy the demand between time interval $[t_1, t_2]$ where $t_2 \geq t_1$. These constraints indicate that if the sum of the

demands over period $[t_1, t_2]$ is greater than or equal to the maximum possible inventory held ($\overline{h}_k$) or initial inventory (H_{mk0}), then there has to be at least a certain number of barges used in that time interval:

$$\sum_{b\in\mathcal{B}}\sum_{s\in\mathcal{S}}\sum_{j\in\mathcal{J}}\sum_{t=t_1}^{t_2} Y^2_{mbsjt} \geq \left\lceil \frac{\sum_{g\in\mathcal{G}}\sum_{t=t_1}^{t_2}\sigma d_{mgt} - \sum_{k\in\mathcal{K}}\overline{h}_k}{\overline{w}_b} \right\rceil \quad \forall m\in\mathcal{M}, (t_1,t_2)\in\mathcal{T}, t_2\geq t_1 \tag{2.38}$$

$$\sum_{b\in\mathcal{B}}\sum_{s\in\mathcal{S}}\sum_{j\in\mathcal{J}}\sum_{t=t_1}^{t_2} Y^2_{mbsjt} \geq \left\lceil \frac{\sum_{g\in\mathcal{G}}\sum_{t=t_1}^{t_2}\sigma d_{mgt} - \sum_{k\in\mathcal{K}} H_{mk0}}{\overline{w}_b} \right\rceil \quad \forall m\in\mathcal{M}, (t_1,t_2)\in\mathcal{T}, t_2\geq t_1 \tag{2.39}$$

- Likewise, constraints (2.40) and (2.41) set lower bounds on the number of towboats to be used between any time interval $[t_1, t_2]$ where $t_2 \geq t_1$. Here, $\overline{\delta}_{\overline{s}}$ represents the capacity of the most powerful towboat $\overline{S}$.

$$\sum_{s\in\mathcal{S}}\sum_{n\in\mathcal{N}}\sum_{j\in\mathcal{J}}\sum_{k\in\mathcal{K}}\sum_{t=t_1}^{t_2} Y^1_{snjkt} \geq \left\lceil \frac{\sum_{m\in\mathcal{M}}\sum_{g\in\mathcal{G}}\sum_{t=t_1}^{t_2}\sigma d_{mgt} - \sum_{k\in\mathcal{K}}\overline{h}_k}{\overline{w}_b\overline{\delta}_{\overline{s}}} \right\rceil \quad \forall (t_1,t_2)\in\mathcal{T}, t_2\geq t_1 \tag{2.40}$$

$$\sum_{s\in\mathcal{S}}\sum_{n\in\mathcal{N}}\sum_{j\in\mathcal{J}}\sum_{k\in\mathcal{K}}\sum_{t=t_1}^{t_2} Y^1_{snjkt} \geq \left\lceil \frac{\sum_{m\in\mathcal{M}}\left(\sum_{g\in\mathcal{G}}\sum_{t=t_1}^{t_2}\sigma d_{mgt} - \sum_{k\in\mathcal{K}} H_{mk0}\right)}{\overline{w}_b\overline{\delta}_{\overline{s}}} \right\rceil \quad \forall (t_1,t_2)\in\mathcal{T}, t_2\geq t_1 \tag{2.41}$$

2.4.2.2 Knapsack inequalities

Santoso et al. [119] show that, if the Benders decomposition algorithm generates a good upper bound, adding a knapsack inequality of the following form along with the optimality cut constraint (2.31) can significantly impact the solution quality obtained from the Benders master problem. Further, the state-of-the-art

solvers, such as CPLEX, GUROBI, can derive a variety of valid inequalities from the knapsack inequality [119]. These derived inequalities may help to expedite the convergence of the overall Benders decomposition algorithm. Let UB^r denote the *best known upper bound* obtained during the first r iterations of the Benders decomposition algorithm. The following knapsack inequality can be added to **[MP]** in iteration $r+1$:

$$\begin{aligned} UB^r \geq & \sum_{t\in\mathcal{T}}\Bigg(\sum_{m\in\mathcal{M}}\Bigg(\sum_{g\in\mathcal{G}} d_{mgt}\varepsilon_{mgt} - \sum_{i\in\mathcal{I}}\varphi_{mit}\mu_{mit} - \sum_{b\in\mathcal{B}}\sum_{s\in\mathcal{S}}\sum_{j\in\mathcal{J}}\Bigg(v_b Y^2_{mbsjt}\chi_{mbsjt} \\ & + \sum_{k\in\mathcal{K}} min\{w_{jt}, w_{jkt}, w_{kt}, \overline{w}_b\} Y^2_{mbsjt}\xi_{mbsjkt}\Bigg)\Bigg) - \sum_{j\in\mathcal{J}}\overline{h}_j\kappa_{jt} - \sum_{k\in\mathcal{K}}\overline{h}_k\iota_{kt} \\ & + \sum_{s\in\mathcal{S}}\sum_{n\in\mathcal{N}_{jk}}\sum_{j\in\mathcal{J}}\sum_{k\in\mathcal{K}_j}\psi_{st}Y^1_{snjkt} + \sum_{m\in\mathcal{M}}\sum_{b\in\mathcal{B}}\sum_{s\in\mathcal{S}}\sum_{j\in\mathcal{J}}\eta_{mbt}Y^2_{mbsjt}\Bigg) \end{aligned} \tag{2.42}$$

Likewise, let LB^r denote the *best known lower bound* obtained till iteration r of the Benders decomposition algorithm. To speed up the branch-and-bound procedure of the solver, the following inequality can be added in each iteration of the Benders master problem **[MP]** starting from iteration $r+1$:

$$LB^r \leq \sum_{t\in\mathcal{T}}\Bigg(\sum_{s\in\mathcal{S}}\sum_{n\in\mathcal{N}_{jk}}\sum_{j\in\mathcal{J}}\sum_{k\in\mathcal{K}_j}\psi_{st}Y^1_{snjkt} + \sum_{m\in\mathcal{M}}\sum_{b\in\mathcal{B}}\sum_{s\in\mathcal{S}}\sum_{j\in\mathcal{J}}\eta_{mbt}Y^2_{mbsjt}\Bigg) + \theta \tag{2.43}$$

2.4.2.3 Pareto-optimal cuts

Pareto-optimal cuts, first introduced by Magnanti and Wong [74], are added to the master problem to improve the convergence of the Benders decomposition algorithm. In each iteration of the Benders decomposition algorithm, these cuts are

generated in such a way that they will be stronger and non-dominated over the cuts generated previously. However, this technique heavily relied on the solution obtained from the dual subproblem. To overcome this problem, Papadakos [104] proposed an approach that generates *subproblem independent pareto-optimal cuts*, commonly known as the *modified Magnanti-Wong (MMW) pareto-optimal cut*. In this research, we have used this subproblem independent pareto-optimal cut as proposed by Papadakos [104]. We refer to this subproblem as **[DP(MMW)]**.

Let $\mathbf{Y}^{LP}$ be the polyhedron defined by (2.7)-(2.9)and (2.12)-(2.15), $0 \leq \{Y^2_{mbsjt}\}_{m\in\mathcal{M},\, b\in\mathcal{B},s\in\mathcal{S},j\in\mathcal{J},t\in\mathcal{T}} \leq 1$ and $0 \leq \{Y^1_{snjkt}\}_{s\in\mathcal{S},n\in\mathcal{N}_{jk},j\in\mathcal{J},k\in\mathcal{K},t\in\mathcal{T}} \leq 1$. Let $ri(\mathbf{Y}^{LP})$ denote the relative interior of $\mathbf{Y}^{LP}$. A Pareto-optimal cut can be obtained by solving the following subproblem where $Y^{2(core)}_{mbsjt} \in ri(\mathbf{Y}^{LP}); \forall m \in \mathcal{M}, b \in \mathcal{B}, s \in \mathcal{S}, j \in \mathcal{J}, t \in \mathcal{T}$.

[DP(MMW)]

$$\begin{aligned} Maximize \sum_{t\in\mathcal{T}}\Bigg(\sum_{m\in\mathcal{M}}\Bigg(\sum_{g\in\mathcal{G}} d_{mgt}\varepsilon_{mgt} - \sum_{i\in\mathcal{I}}\varphi_{mit}\mu_{mit} - \sum_{b\in\mathcal{B}}\sum_{s\in\mathcal{S}}\sum_{j\in\mathcal{J}} \\ \Bigg(\sum_{k\in\mathcal{K}} min\{w_{jt}, w_{jkt}, w_{kt}, \overline{w}_b\} Y^{2(core)}_{mbsjt}\xi_{mbsjkt} + v_b Y^{2(core)}_{mbsjt}\chi_{mbsjt}\Bigg)\Bigg) \\ - \sum_{j\in\mathcal{J}}\overline{h}_j\kappa_{jt} - \sum_{k\in\mathcal{K}}\overline{h}_k\iota_{kt}\Bigg) \end{aligned} \tag{2.44}$$

subject to

$$-\mu_{mit} + \vartheta_{mjt} \leq c_{mijt} \quad \forall m \in \mathcal{M}, i \in \mathcal{I}, j \in \mathcal{J}, t \in \mathcal{T} \quad (2.45)$$

$$-\vartheta_{mjt} + \zeta_{mkt} - \xi_{mbsjkt} - \frac{\chi_{mbsjt}}{\rho_m} \leq c_{mbsjkt} \forall m \in \mathcal{M}, b \in \mathcal{B}, s \in \mathcal{S}, j \in \mathcal{J}, k \in \mathcal{K}_j, t \in \mathcal{T} \quad (2.46)$$

$$(1-\alpha_m)\vartheta_{mj,t+1} - \vartheta_{mjt} - \kappa_{jt} \leq h_{mjt} \quad \forall m \in \mathcal{M}, j \in \mathcal{J}, t \in \mathcal{T} \quad (2.47)$$

$$(1-\alpha_m)\zeta_{mk,t+1} - \zeta_{mkt} - \iota_{kt} \leq h_{mkt} \quad \forall m \in \mathcal{M}, k \in \mathcal{K}, t \in \mathcal{T} \quad (2.48)$$

$$-\zeta_{mkt} + \varepsilon_{mgt} \leq c_{mkgt} \quad \forall m \in \mathcal{M}, k \in \mathcal{K}, g \in \mathcal{G}, t \in \mathcal{T} \quad (2.49)$$

$$\varepsilon_{mgt} \leq \pi_{mgt} \quad \forall m \in \mathcal{M}, g \in \mathcal{G}, t \in \mathcal{T} \quad (2.50)$$

$$\mu_{mit}, \kappa_{jt}, \iota_{kt}, \xi_{mbsjkt}, \chi_{mbsjt} \in \mathbb{R}^+ \quad (2.51)$$

$$\vartheta_{mjt}, \zeta_{mkt}, \varepsilon_{mgt} \in \mathbb{R} \quad (2.52)$$

In **[DP(MMW)]**, $\{Y^{2(core)}_{mbsjt}\}_{m\in\mathcal{M},b\in\mathcal{B},s\in\mathcal{S},j\in\mathcal{J},t\in\mathcal{T}}$ denote the core points which we initialized as $Y^{2(core)}_{mbsjt} \leftarrow 1; \forall m \in \mathcal{M}, b \in \mathcal{B}, s \in \mathcal{S}, j \in \mathcal{J}, t \in \mathcal{T}$[104, 105]. Later, in each iteration of the Benders decomposition algorithm, we update the core points as follows: $Y^{2(core)}_{mbsjt} = \tau Y^{2(core)}_{mbsjt} + (1-\tau)\hat{Y}^2_{mbsjt}; \forall m \in \mathcal{M}, b \in \mathcal{B}, s \in \mathcal{S}, j \in \mathcal{J}, t \in \mathcal{T}$. Here, $\hat{Y}^2_{mbsjt}$ refers to the solution obtained from solving the Benders master problem. Depending on the results of multiple experimentation, authors suggest to set $\tau = 0.5$ which provides the best empirical results for **[IMP]**. The generation of pareto-optimal cuts require solving two linear subproblems in one iteration, i.e., use $\{\hat{Y}^2_{mbsjt}\}_{m\in\mathcal{M},b\in\mathcal{B},s\in\mathcal{S},j\in\mathcal{J},t\in\mathcal{T}}$ to solve **[DP]** and then use $\{Y^{2(core)}_{mbsjt}\}_{m\in\mathcal{M},b\in\mathcal{B},s\in\mathcal{S},j\in\mathcal{J},t\in\mathcal{T}}$ to solve **[DP(MMW)]**. Papadakos [104] claimed that this *modified Magnanti-Wong pareto-optimal cut* is independent from the solutions

of the dual subproblem **[DP]** which results the Benders master problem to be one step closer to the optimal solution from the very first iteration.

2.4.2.4 Input ordering

Jans and Desrosiers [64] showed that the order at which the input data are loaded into a model can have a major impact on the Linear Programming (LP) relaxation, node exploration, and ultimately to the solution time of the overall problem. In this research, we use this concept to rank the *destination ports* based on their potentiality to serve customer demands throughout the entire planning horizon. Essentially, the ports with high potential for customer demands are ranked first in the input file in an attempt to quickly obtain a lower bound for the Benders master problem **[MP]**. Since the demand for different commodities d_{mgt} are set on the markets $g \in \mathcal{G}$ rather than the destination ports, we made a demand projection at each destination port $k \in \mathcal{K}$ based on the arcs connecting them to the markets ($\mathcal{G}_k$). Figure 2.2 is used to provide a numerical illustration of this projection which is consisting of four destination ports (k_1-k_4) and twelve markets (g_1-g_{12}). The arrow head represents all possible arcs between each source to destination pairs. Based on Figure 2.2, the potential demand for each destination port $k \in \mathcal{K}$ can be calculated by summing the demand for all commodities in the markets connected to them during the entire planning horizon. For instance, a demand projection for port k_2 can be made as follows: $\sum_{m \in \mathcal{M}} \sum_{g=g_4}^{g_7} \sum_{t \in \mathcal{T}} d_{mgt} = 12,000$ tons. We use this approach to project the demand for the remaining ports. Based on this projected

demand, we sort all destination ports $k \in \mathcal{K}$ in a descending order and place them accordingly in the input file.

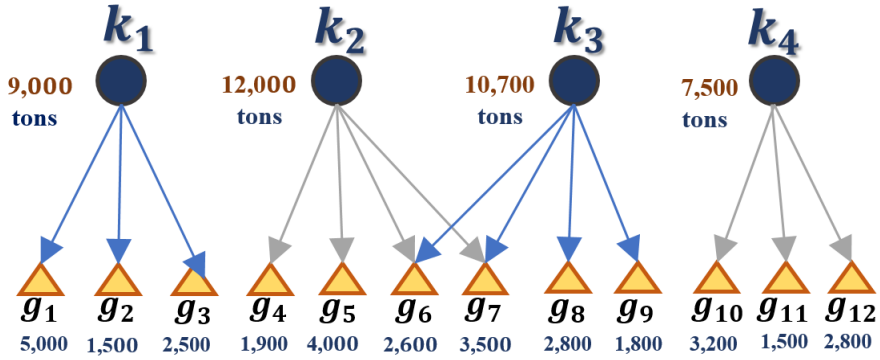

Figure 2.2

Customer demand sorting

2.4.2.5 Local Branching

The earlier iterations of the Benders decomposition algorithm suffers from slow convergence i.e., the gap between the upper and lower bound drops slowly even after the incorporation of pareto-optimality cuts. To alleviate this problem, we utilize *local branching procedure*, initially proposed by Fischetti and Lodi [41] and later utilized by Rei et al. (2009) [116] under the classical Benders framework, in an attempt to accelerate the performance of the Benders master problem [MP]. The core concept lies in local branching is to divide the entire feasible region into a series

of smaller subproblems which can be solved by any generic solver (e.g., GUROBI, CPLEX) within an acceptable time limit. Below we provide a brief discussion of the local branching procedure.

The local branching procedure begins with a feasible solution $\mathbf{Y}$ of **[MP]** and a positive integer parameter k_v. This feasible solution serves as a reference point to create *local branching subproblems*. Let $\bar{\mathbf{Y}}^1$ be an optimal solution of the master problem **[MP]**. We can divide the feasible region of **[MP]** into the following two reduced subproblems.

$$\Delta(\mathbf{Y}, \bar{\mathbf{Y}}^1) \leq k_v \quad \vee \quad \Delta(\mathbf{Y}, \bar{\mathbf{Y}}^1) \geq k_v + 1 \tag{2.53}$$

We use GUROBI to solve the reduced subproblem of **[MP]** which is created by adding the *left branching constraint* presented in the first part of constraint (2.53). This reduced subproblem is referred to as *left branching subproblem*. The succinct representation of constraint (2.53) can be expanded as follows:

$$\begin{aligned}\Delta(\mathbf{Y}, \bar{\mathbf{Y}}^1) := & \sum_{(s,n,j,k,t)\notin y_s^l} Y^1_{snjkt} + \sum_{(s,n,j,k,t)\in y_s^l} (1 - Y^1_{snjkt}) + \\ & \sum_{(m,b,s,j,t)\notin y_m^l} Y^2_{mbsjt} + \sum_{(m,b,s,j,t)\in y_m^l} (1 - Y^2_{mbsjt}) \leq k_v\end{aligned} \tag{2.54}$$

where y_s^l and y_m^l are defined as follows: $y_s^l = \{\hat{Y}^1_{snjkt} = 1 | \forall s \in \mathcal{S}, n \in \mathcal{N}_{jk}, j \in \mathcal{J}, k \in \mathcal{K}, t \in \mathcal{T}\}$ and $y_m^l = \{\hat{Y}^2_{mbsjt} = 1 | \forall m \in \mathcal{M}, b \in \mathcal{B}, s \in \mathcal{S}, j \in \mathcal{J}, t \in \mathcal{T}\}$. The solutions of $\hat{Y}^1_{snjkt}$ and $\hat{Y}^2_{mbsjt}$ obtained by solving **[MP]** at iteration l, are used to construct constraint (2.54), which are then applied to iteration $l+1$. Let,$\bar{\mathbf{Y}}^2$ be a solution of the local branching subproblem which can be obtained by setting a time

limit TL and optimality gap ϵ_k. Typically, the value of k_v is set to a small number which will allow local branching to quickly explore different feasible regions of **[MP]**. After solving the local branching subproblem, depending on the status of the optimizer one of the following cases might arise.

- **Case 1:** If an optimal solution is found for the current local branching subproblem within a predefined timelimit TL and optimality gap ϵ_k, the left branching constraint should be replaced by the right branching constraint i.e., $\Delta(\mathbf{Y}, \bar{\mathbf{Y}}^1) \geq k_v + 1$. At this point, we will update the reference point $\bar{\mathbf{Y}}^1$ to $\bar{\mathbf{Y}}^2$ and apply the branching condition based on this new reference point. Therefore, the new left branching condition would be $\Delta(\mathbf{Y}, \bar{\mathbf{Y}}^2) \leq k_v$.
- **Case 2:** The second case arises when the current subproblem is proven infeasible. In this case, we replace the left branching constraint with the right branching constraint i.e., $\Delta(\mathbf{Y}, \bar{\mathbf{Y}}^1) \geq k_v + 1$. In this situation, we apply a diversification procedure (d_v) through increasing the size of the feasible solution region by $\lceil k_v/2 \rceil$ i.e., $(k_v + \lceil k_v/2 \rceil)$. The local branching procedure is then continued with this new extended solution space.
- **Case 3:** If the feasible solution of the current subproblem is improved, but not optimal, at the end of the time limit TL, the left branching constraint will be eliminated without adding the right branching constraint. Moreover, a *tabu* constraint $\Delta(\mathbf{Y}, \bar{\mathbf{Y}}^2) \geq 1$ will be added to remove $\bar{\mathbf{Y}}^2$ from the current subproblem. Next, we create a new subproblem by adding the left branching constraint with the new reference point $\Delta(\mathbf{Y}, \bar{\mathbf{Y}}^2) \leq k_v$ and the process continues.
- **Case 4:** In this case, we check if the subproblem exceeds the predefined time limit TL without improving the objective function value. If yes, the right hand size of the left branching constraint will be decreased by one, i.e., $k_v - 1$, and the tabu cut will be added to ensure that $\bar{\mathbf{Y}}^2$ will not be considered in further. We then solve the current subproblem in an attempt to find a better solution. If no improved solution is found, we re-operate the diversification procedure that will enlarge the size of the feasible region.

Note that at the beginning of the local branching procedure, we add the tabu constraint $\Delta(\mathbf{Y}, \bar{\mathbf{Y}}^1) \geq 1$ in **[MP]** to ensure that the previously explored solutions are not repeated in the current iteration. Let N_{div} and $iter_{max}$ be the maximum

number of diversification and iteration, respectively, for the local branching procedure. We further denote $\bar{\mathbf{Y}}_h$ to store the h^{th} feasible solution obtained during any iteration of the local branching procedure. At the end of the local branching procedure, we update the lower bound of the Benders decomposition algorithm by evaluating **[MP]**'s objective function using the feasible solutions $\bar{\mathbf{Y}}_h$ obtained through the local branching procedure. The pseudo-code of the overall local branching algorithm is presented in **Algorithm 2**.

2.5 Experimental Results

This section conducts a computational study on model **[IMP]** to test the performance of the proposed Benders decomposition algorithm and to draw managerial insights. The proposed mathematical model and the solution algorithms are coded in python 2.7 on a desktop with Intel Core i7 3.6 GHz processor and 16.0 GB RAM. The optimization solver used is Gurobi Optimizer 6.5[3]. The following subsection present the performance of the accelerated Benders decomposition algorithm for realistic test instances. Additionally, in subsection 2.5.2 we demonstrate a real life case study considering four states in the Southeast region of the United States, namely, Arkansas (AR), Louisiana (LA), Mississippi (MS), and Tennessee (TN) to visualize and validate the modeling results. The input parameters used in this case study are discussed in subsection 2.5.2.1. All costs are calculated based on

[3]Available from: `http://www.gurobi.com/`

2018 dollars value. To the end subsection 2.5.2.2 reports the managerial insights drawn from our experimental study.

2.5.1 Analyzing the Performance of the Solution Algorithms

This section presents our computational experience in solving model **[IMP]** using the algorithms proposed in Section 2.4. We assess the performances of different accelerated techniques within the standard Benders decomposition algorithm and compare their computational efficiency with Gurobi. Table 2.1 summarizes the problem instances considered for analyzing the performance of the solution algorithms. We vary set $|\mathcal{I}|$, $|\mathcal{J}|$, $|\mathcal{K}|$, $|\mathcal{G}|$, $|\mathcal{S}|$, $|\mathcal{N}_{jk}|$, and $|\mathcal{T}|$ to obtain 20 different problem instances. The following criterion are set to terminate the algorithms: (i) the optimality gap (i.e., $\epsilon = |UB - LB|/UB$) falls below a threshold value (e.g., $\epsilon = 0.01$); or (ii) the maximum time limit (t_{max}) is reached (e.g., $t_{max} = 10{,}800$ CPU seconds); or (iii) the maximum iteration limit (r_{max}) is reached (e.g., $r_{max} = 500$). To help the readers follow our approaches, we have used the following notations to represent the algorithms:

- **Benders+VI**: Benders decomposition algorithm + valid inequalities
- **Benders+VI+KI**: Benders decomposition algorithm + valid inequalities + knapsack inequalities
- **Benders+VI+KI+PO**: Benders decomposition algorithm + valid inequalities + knapsack inequalities + pareto-optimal cuts
- **All cuts**: Benders decomposition algorithm + valid inequalities + knapsack inequalities + pareto-optimal cuts + input ordering + local branching

Table 2.2 summarizes the computational performances between different enhancements of the Benders decomposition algorithm with Gurobi using the test instances presented in Table 2.1. The column headings $t(s)$, $t_{MP}(s)$, $\epsilon(\%)$, and r represent running time of the algorithm, running time of the master problem, optimality gap, and number of iteration for each respective algorithm. Note that, in reporting the computational performance of the algorithms, we highlighted the algorithm/Gurobi which is solved in less than the stopping criteria ϵ while simultaneously producing the smallest running time (represented by $t(s)$ in Tables 2.2 and 2.3) for a given test instance. Otherwise, if such a quality solution is not found within the maximum time or iteration limit, the algorithm/Gurobi with the smallest optimality gap (represented by $\epsilon(\%)$ in Tables 2.2 and 2.3) is highlighted. In the following, we summarize our observations for combined Tables 2.2 and 2.3):

- Clearly, Gurobi outperforms all variants of the Benders decomposition algorithm to solve small/medium scale problem instances (e.g., Case 1-7, 11-13, 16, 17) by obeying the pre-specified termination criterion. For those instances, the solver generates solutions with an average optimality gap of 0.82% and solution time of 491 CPU *seconds*, which are significantly lower than different variants of the Benders decomposition algorithm. However, for larger instances (e.g., Case 8-10, 14, 15, 18-20), the solver was unable to produce any results due to getting *out of memory* in solving model **[IMP]**.
- Introduction of *knapsack inequalities* (**Benders+VI+KI**) slightly improves the performance of the **Benders+VI** algorithm in solving smaller test instances (e.g., Case 1-7) for problem **[IMP]**; however, both **Benders+VI** and **Benders+VI+KI** algorithms are unable to produce any satisfactory results for relatively medium to large sized problem instances. Note that we did not report any computational results for standard Benders decomposition algorithm since the algorithm is unable to solve any problem instances reported in Table 2.1.

- We observe significant improvement in computational performances over **Benders +VI** and **Benders+VI+KI** algorithms when *pareto-optimal* cut is introduced in **Benders+VI+ KI+PO**. Results in Tables 2.2 and 2.3) show that algorithm **Benders+VI+KI+PO** is now capable of solving 17/20 problem instances, over 7/20 instances solved by both **Benders+VI** and **Benders+VI+ KI** algorithms, within the prespecified termination criterion. On average, algorithm **Benders+VI+ KI+PO** drops the running time of **Benders+VI+KI** algorithm by 37.1 % with an average optimality gap of 1.16%. Finally, we note that algorithm **Benders+VI+KI+PO** is capable of solving 8/20 problem instances within an acceptable optimality gap for which Gurobi gets *out of memory*.

- Results in Tables 2.2 and 2.3) indicate that the introduction of *input ordering* and *local branching* in **All cuts** algorithm consistently produces high quality solutions over different variants of the Benders decomposition algorithm. On average, algorithm **All cuts** is 24.23% faster than algorithm **Benders+VI+ KI+PO** while producing an average optimality gap of 0.55%. Further, the algorithm provides superior computational performances in solving large-scale problem instances when Gurobi gets *out of memory*. Note that the introduction of *input ordering* itself slightly improves the performance of the **All cuts** algorithm. Therefore, we did not show a separate column to demonstrate the computational performance of this variant of the Benders decomposition algorithm. This implies that majority of the improvements in **All cuts** algorithm is mainly contributing by the *local branching* technique. Moreover, as implied by columns $t_{MP}(s)$ in Tables 2.2 and 2.3), different variants of the Benders decomposition algorithm utilize on average 80.0-95.2% of its running time to solve only the Benders master problem.

To summarize, algorithm **All cuts** seems to offer high quality solutions consistently in solving **[IMP]** within the experimental range. Since, the performance improvement using algorithm **All cuts** is due to the inclusion of *local branching*, in Tables 2.4 and 2.5 we detail the comparisons between few settings of this local branching technique. We pick instance 3 and 18 from Table 2.1 as a representative of *small instance* and *large instance*, respectively. From Table 2.4 it is clearly visible that with the larger value of k_v and N_{div}, the performance of this algorithm drops i.e., the selected instance needs more time to solve. On the other hand, Table 2.5

shows the benefit of having a higher k_v and N_{div} while solving the large instance. In both tables we highlight the setting with the lowest solution time. While conducting experimentation for large instance we noticed that higher k_v and N_{div} provide quicker solution time, therefore, we increased the k_v to one more step $k_v = 4$ that was not necessary for the small instance. Finally, in running the experiments reported in Tables 2.2 and 2.3) we used the understanding obtained from Tables 2.4 and 2.5 and selected different values of k_v and N_{div} as appropriate. To be specific we used k_v value ranging from 2 to 6 in applying algorithm **All cuts**.

Our experimental results in Tables 2.2 and 2.3) can be easily validated by following the studies of Fischetti and Lodi [41], Rei et al. [116], and Gonzalez et al. [49]. Fischetti and Lodi [41] conducted a comprehensive experimentation that demonstrates the performance of Local Branching as an exact metaheuristic approach. Authors solved multiple MIP test instances and showed the performance of Local branching in solving them. Gonzalez et al. [49] applies Local branching techniques for multiple random test instances and perform statistical analysis to observe the statistical significance of this technique. To observe the statistical significance of our experimental results obtained in Table 2, we perform paired Wilcoxon signed rank test between Enhanced Benders decomposition algorithm variant with local branching (algorithm **All cuts**) and without local branching (algorithm **Benders+VIQ+KI+PO**). The test verifies whether the optimality gap and the mean solution time obtained by the **Benders+VIQ+KI+PO** and **All cuts** shown in Table 2 are same or significantly different. We are interested in administering

two tests, one for the optimality gap (Test 1) and another one for the mean solution time (Test 2). The null hypothesis, alternative hypothesis, and obtained p-values for these two tests can be seen in Table 2.6. Note that before applying the Wilcoxon signed ranked test, we verified all assumptions of this test. The first and second test shows the p-value of 0.000293 and 0.0001974, respectively which confirms the superiority of the proposed local branching strategy (algorithm All cuts) in terms of both solution quality and time under our current settings.

Algorithm 1: Benders Decomposition Algorithm

Initialize, $r \leftarrow 1$, ϵ, $UB^r \leftarrow +\infty$, $LB^r \leftarrow -\infty$, $\mathcal{P}_D^r \leftarrow 0$

$terminate \leftarrow false$

while $terminate =$ ***false*** **do**

Solve **[MP]** to obtain the values of $\{Y_{snjkt}^{1r}\}_{s\in\mathcal{S},n\in\mathcal{N}_{jk},j\in\mathcal{J},k\in\mathcal{K},t\in\mathcal{T}}$,

$\{Y_{mbsjt}^{2r}\}_{m\in\mathcal{M},b\in\mathcal{B},s\in\mathcal{S},j\in\mathcal{J},t\in\mathcal{T}}$, z_{MP}^r, and z_{MAS}^r ;

if $z_{MP}^r > LB^r$ **then**

$LB^r \leftarrow z_{MP}^r$

end

For fixed $\{\hat{Y}_{snjkt}^{1r}\}_{s\in\mathcal{S},n\in\mathcal{N}_{jk},j\in\mathcal{J},k\in\mathcal{K},t\in\mathcal{T}}$ and $\{\hat{Y}_{mbsjt}^{2r}\}_{m\in\mathcal{M},b\in\mathcal{B},s\in\mathcal{S},j\in\mathcal{J},t\in\mathcal{T}}$

solve **[DP]** to obtain $(\mu_{mit}, \kappa_{jt}, \iota_{kt}, \xi_{mbsjkt}, \chi_{mbsjt}, \vartheta_{mjt}, \zeta_{mkt}, \varepsilon_{mgt}) \in \mathcal{P}_D^r$

and z_{SUB}^r

if $z_{SUB}^r + z_{MAS}^r < UB^r$ **then**

$UB^r \leftarrow z_{SUB}^r + z_{MAS}^r$;

end

if $\frac{(UB^r - LB^r)}{UB^r} \leq \epsilon$ **then**

$terminate \leftarrow$ **true**

else

$\mathcal{P}_D^{r+1} = \mathcal{P}_D^r \bigcup \{(\mu_{mit}, \kappa_{jt}, \iota_{kt}, \xi_{mbsjkt}, \chi_{mbsjt}, \vartheta_{mjt}, \zeta_{mkt}, \varepsilon_{mgt})\}$

end

$r \leftarrow r + 1$

end

Algorithm 2: Local Branching Algorithm

Initialize, $rhs \leftarrow k_v$, $iter \leftarrow 1$, $d_v \leftarrow 1$, $diversify \leftarrow false$, $h \leftarrow 1$, $\bar{\mathbf{Y}}_h \leftarrow \emptyset$, TL, ϵ_k

Add $\Delta(\mathbf{Y}, \bar{\mathbf{Y}}^1) \geq 1$

while $(iter \leq iter_{max}) \vee (d_v \leq N_{div})$ **do**

Add $\Delta(\mathbf{Y}, \bar{\mathbf{Y}}^1) \leq rhs$

Solve the local branching subproblem and obtain $\bar{\mathbf{Y}}^2$

if ***Case 1:*** *optimal solution is found within defined TL and gap* ϵ_k **then**

Reverse the last local branching constraint as $\Delta(\mathbf{Y}, \bar{\mathbf{Y}}^1) \geq k_v + 1$

$\bar{\mathbf{Y}}^1 \leftarrow \bar{\mathbf{Y}}^2$, $diversify \leftarrow false$, $rhs \leftarrow k_v$, $\bar{\mathbf{Y}}_h \leftarrow \bar{\mathbf{Y}}^2$, $h \leftarrow h + 1$, $iter \leftarrow iter + 1$

end

if ***Case 2:*** *subproblem is infeasible* **then**

Reverse the last local branching constraint into $\Delta(\mathbf{Y}, \bar{\mathbf{Y}}^1) \geq k_v + 1$

$rhs \leftarrow k_v + \left\lceil \frac{k_v}{2} \right\rceil$, $d_v \leftarrow d_v + 1$

end

if ***Case 3:*** *solution is suboptimal* **then**

Remove the last local branching constraint $\Delta(\mathbf{Y}, \bar{\mathbf{Y}}^1) \leq k_v$

Add $\Delta(\mathbf{Y}, \bar{\mathbf{Y}}^1) \geq 1$ to the current problem

$\bar{\mathbf{Y}}^1 \leftarrow \bar{\mathbf{Y}}^2$, $diversify \leftarrow false$, $rhs \leftarrow k_v$, $\bar{\mathbf{Y}}_h \leftarrow \bar{\mathbf{Y}}^2$, $h \leftarrow h + 1$, $iter \leftarrow iter + 1$

end

if ***Case 4:*** *subproblem reached timelimit TL without improvement* **then**

Remove the last local branching constraint $\Delta(\mathbf{Y}, \bar{\mathbf{Y}}^1) \leq k_v$

Add $\Delta(\mathbf{Y}, \bar{\mathbf{Y}}^1) \geq 1$ to the current problem

if *diversify* **then**

$d_v \leftarrow d_v + 1$, $rhs \leftarrow k_v + 1$

else

$rhs \leftarrow k_v - 1$

end

$diversify \leftarrow$ **true**

end

end

Table 2.1

Problem size and test cases

Case	$\|\mathcal{I}\|$	$\|\mathcal{J}\|$	$\|\mathcal{K}\|$	$\|\mathcal{G}\|$	$\|\mathcal{S}\|$	$\|\mathcal{N}_{jk}\|$	$\|\mathcal{T}\|$	Binary variables	Continuous variables	Total variables	No. of constraints
1	40	5	5	40	15	15	4	135,000	4,507,200	4,642,200	379,700
2	40	5	5	40	15	15	8	270,000	9,014,400	9,284,400	759,400
3	40	5	5	40	15	15	12	405,000	13,521,600	13,926,600	1,139,100
4	40	5	5	40	15	15	16	540,000	18,028,800	18,568,800	1,518,800
5	40	5	5	40	15	15	20	675,000	22,536,000	23,211,000	1,898,500
6	40	8	8	40	15	15	4	288,000	11,531,136	11,819,136	896,288
7	40	8	8	40	15	15	8	576,000	23,062,272	23,638,272	1,792,576
8	40	8	8	40	15	15	12	864,000	34,593,408	35,457,408	2,688,864
9	40	8	8	40	15	15	16	1,152,000	46,124,544	47,276,544	3,585,152
10	40	8	8	40	15	15	20	1,440,000	57,655,680	59,095,680	4,481,440
11	83	13	8	43	10	10	4	312,000	8,343,792	8,655,792	972,704
12	83	13	8	43	10	10	8	624,000	16,687,584	17,311,584	1,945,408
13	83	13	8	43	10	10	12	936,000	25,031,376	25,967,376	2,918,112
14	83	13	8	43	10	10	16	1,248,000	33,375,168	34,623,168	3,890,816
15	83	13	8	43	10	10	20	1,560,000	41,718,960	43,278,960	4,863,520
16	83	13	13	43	10	10	4	442,000	13,547,312	13,989,312	1,495,664
17	83	13	13	43	10	10	8	884,000	27,094,624	27,978,624	2,991,328
18*	83	13	13	43	10	10	12	1,326,000	40,641,936	41,967,936	4,486,992
19	83	13	13	43	10	10	16	1,768,000	54,189,248	55,957,248	5,982,656
20	83	13	13	43	10	10	20	2,210,000	67,736,560	69,946,560	7,478,320

*Representative problem size for the real life case study.

Table 2.2

Comparison of different solution approaches

Case	Gurobi		Benders				Benders+VIQ				Benders+VIQ+KI				Benders+VIQ+KI+PO				All cuts			
	$t(s)$	$\epsilon(\%)$	$t(s)$	$t_{MP}(s)$	$\epsilon(\%)$	r	$t(s)$	$t_{MP}(s)$	$\epsilon(\%)$	r	$t(s)$	$t_{MP}(s)$	$\epsilon(\%)$	r	$t(s)$	$t_{MP}(s)$	$\epsilon(\%)$	r	$t(s)$	$t_{MP}(s)$	$\epsilon(\%)$	r
1	**76**	0.88	10,800	9,678	76.91	296	590	499	0.68	24	497	410	0.34	23	230	185	0.99	12	353	292	0.99	16
2	**172**	0.98	10,800	9,183	77.15	169	1,396	1,118	0.43	29	1,296	1,037	0.22	27	699	584	0.53	12	876	742	0.46	14
3	**277**	0.97	10,800	9,696	81.59	111	3,289	2,901	0.62	39	3,105	2,767	0.31	34	998	888	0.36	11	1,389	1,260	0.18	13
4	**398**	0.78	10,800	9,681	88.61	92	5,028	4,517	0.4	42	4,869	4,407	0.2	38	1,680	1,546	0.39	11	2,079	1,945	0.18	11
5	**680**	0.6	10,800	10,026	89.99	86	5,717	5,321	0.57	44	5,517	5,148	0.34	41	1,851	1,761	0.53	10	2,109	2,028	0.17	9
6	**207**	0.66	10,800	8,974	91.61	117	3,477	2,899	0.78	37	3,126	2,642	0.15	31	2,124	1,687	0.40	28	1,104	901	0.18	13
7	**538**	0.56	10,800	9,095	97.99	67	8,986	7,586	0.99	55	8,238	6,991	0.91	49	3,524	2,989	0.98	21	2,612	2,281	0.20	13
8	-[a]	-	10,800	9,643	99.99	40	10,800	9,672	99.98	39	10,800	9,817	99.96	34	4,679	4,245	0.86	15	**4,118**	3,742	0.21	13
9	-	-	10,800	9,982	99.99	31	10,800	9,982	99.99	31	10,800	10,114	99.98	26	6,123	5,727	0.97	15	**5,723**	5,380	0.85	13
10	-	-	10,800	9,985	99.99	26	10,800	10,016	99.99	25	10,800	10,142	99.99	21	8,700	8,261	0.90	14	**6,521**	6,176	0.87	10

[a]Out of Memory

Table 2.3

Comparison of different solution approaches (cont'd)

Case	Gurobi		Benders				Benders+VIQ				Benders+VIQ+KI				Benders+VIQ+KI+PO				All cuts			
	$t(s)$	$\epsilon(\%)$	$t(s)$	$t_{MP}(s)$	$\epsilon(\%)$	r	$t(s)$	$t_{MP}(s)$	$\epsilon(\%)$	r	$t(s)$	$t_{MP}(s)$	$\epsilon(\%)$	r	$t(s)$	$t_{MP}(s)$	$\epsilon(\%)$	r	$t(s)$	$t_{MP}(s)$	$\epsilon(\%)$	r
11	**301**	0.99	10,800	9,542	99.97	89	10,800	9,612	99.63	84	10,800	9,683	99.52	79	2,524	2,001	0.96	37	1,260	1,048	0.47	15
12	**459**	0.8	10,800	9,278	99.98	50	10,800	9,369	99.72	47	10,800	9,491	99.52	43	4,038	3,490	0.90	18	3,746	3,380	0.67	12
13	**1,037**	0.67	10,800	8,480	99.99	37	10,800	8,731	99.95	33	10,800	8,982	99.95	29	6,131	5,191	0.74	15	5,297	4,608	0.74	11
14	-	-	10,800	9,566	99.99	26	10,800	9,708	99.98	23	10,800	9,898	99.96	19	9,821	9,251	0.99	12	**6,359**	5,975	0.75	9
15	-	-	10,800	9,779	99.99	18	10,800	9,892	99.99	16	10,800	10,063	99.98	13	10,800	10,176	4.34	11	**6,880**	6,370	0.92	9
16	**680**	0.99	10,800	8,908	99.99	76	10,800	8,983	99.46	73	10,800	9,132	99.35	67	4,203	3,331	0.64	35	1,915	1,542	0.01	15
17	**1,072**	0.98	10,800	8,679	99.99	53	10,800	8,749	99.69	50	10,800	8,995	99.65	44	5,439	4,701	0.16	18	4,231	3,780	0.36	11
18	-	-	10,800	8,279	99.99	25	10,800	8,254	99.96	25	10,800	8,865	99.95	19	9,959	8,432	0.96	15	**6,429**	5,513	0.90	9
19	-	-	10,800	9,652	99.99	22	10,800	9,704	99.98	21	10,800	10,017	99.98	15	10,800	10,174	4.71	12	**7,761**	7,291	0.99	9
20	-	-	10,800	9,670	99.99	16	10,800	9,638	99.99	16	10,800	10,074	99.99	10	10,800	10,219	1.97	8	**8,956**	8,593	0.99	5
Avg*	491	0.82	10,800	9,389	95.18	72	8,444	7,358	65.14	38	8,352	7,434	65.01	33	5,256	4,742	1.16	17	3,986	3,642	0.55	12

*Combined average for Tables 2.2 and 2.3

Table 2.4

Comparison between different settings of local branching (for small instance)

Instance	k_v	N_{div}	$t(s)$	$\epsilon(\%)$
Small Instance	**2**	2	1,408	0.16
		3	**1,389**	0.18
		4	1,376	0.18
	3	2	1,498	0.33
		3	1,750	0.35
		4	1,810	0.39

Table 2.5

Comparison between different settings of local branching (for large instance)

Instance	k_v	N_{div}	$t(s)$	$\epsilon(\%)$
		2	8,420	0.96
	2	3	8,398	0.89
		4	8,480	0.95
		2	7,620	0.87
Large Instance	3	3	7,457	0.86
		4	7,680	0.90
		2	7,180	0.98
	4	**3**	**6,429**	0.90
		4	6,490	0.91

Table 2.6

Results of Wilcoxon signed rank test

	Test 1	Test 2
Null Hypothesis (H0)	There is no significant difference between the quality of the solution found with algorithm **Benders+VIQ+KI+PO** and algorithm **All cuts**	There is no significant difference between the solution time required to solve [IMP] using algorithm **Benders+VIQ+KI+PO** and algorithm **All cuts**
Alternative Hypothesis (H1)	The solution quality obtained with algorithm **All cuts** are significantly better than that found by algorithm **Benders+VIQ+KI+PO**	The solution time required to solve [IMP] using algorithm **All cuts** is significantly faster than that needed by algorithm **Benders+VIQ+KI+PO**
p-value	0.000293	0.0001974
Confidence level	99%	99%
Significance level	0.01	0.01

2.5.2 Case Study

This subsection demonstrates a real life case study considering four Southeast U.S. states, Arkansas (AR), Louisiana (LA), Mississippi (MS), and Tennessee (TN). In our case study, we considered thirteen waterway ports along Mississippi river as origin ports ($|\mathcal{J}| = 13$) and destination ports ($|\mathcal{K}| = 13$). The set sizes related to this case study is reported in Table 2.1 (case 18)[4]. In the next few subsections we introduce the case study region and the network parameters used in this case study. Note that, in order to solve this case study and perform sensitivity analysis, we used the algorithm that performs best in solving case 18 following Table 2.2, i.e., **All cuts**.

[4]A sample dataset can be downloaded from `https://www.farjananur.net/publications`

2.5.2.1 Data Description

***Inland Waterway Port Location*:** This study considers a total of thirteen inland waterway ports along the Mississippi River. Figure 5.2 shows the geographical locations of the ports considered in this study. Among them five ports, namely, the Port of Rosedale, Port of Greenville, Port of Vicksburg, Port of Natchez, and Port of Yazoo County, are located in Mississippi. Note that the first four ports are located alongside the Mississippi River, whereas the Port of Yazoo County is situated along a stream flowing from the Mississippi River. We exclude the Port of Claiborne County from further consideration since the facility is currently unavailable for operation [85]. Besides these ports, we consider the Port of Geismar Louisiana, Port of Greater Baton Rouge, Port of South Louisiana, and Port of Gramercy from Louisiana, Port of Little Rock from Arkansas, and Port of Memphis, Pemiscot County Port, and New Madrid County Port from Tennessee. All the ports are directly connected with each other via the Mississippi River.

***Supply Data*:** Four commodities, namely, rice, corn, woodchips, and fertilizer are selected to transport them from their supply sites to demand locations via the inland waterway transportation network. Figure 4.6 shows the supply distribution (in 1,000 tons) of these four commodities in the test region. Only the suppliers that are located within a radius of 60 miles from the ports are considered for the study. Among the four commodities, rice and corn are highly seasonal in nature

Figure 2.3

Existing inland waterway port locations along the Mississippi River

and are not available throughout the year. Rice is available only between August and October of each year whereas corn is harvested only between mid-July and early December of each year [133]. Similarly, it is observed that woodchips remain available year-round except three months during the winter (December to February) [133]. However, availability of fertilizer is uniform throughout the year. The test region produces 6.3 and 113.8 million tons of rice and corn per year from 42 and 59 different counties, respectively [135]. On the other hand, the region produces 8.3 and 0.4 million tons of woodchips and fertilizer per year from 31 and 22 different counties, respectively [136, 137].

***Demand Data*:** This study considers a total of 43 industries in Mississippi as demand points for the commodities. These facilities are located nearby the inland waterway ports. The annual demand for the commodities are set to be 3.8, 68.3, 8.3, and 0.37 million tons of rice, corn, woodchips, and fertilizer, respectively [135, 137]. Figure 2.5 shows the location and distribution of demand points for all the four commodities in Mississippi.

***Transportation Costs*:** This study considers two modes of transportation to transport commodities from their sources to destinations: trucks and barges. Transportation distances between supply sites $i \in \mathcal{I}$ and origin ports $j \in \mathcal{J}$, and destination ports $k \in \mathcal{K}$ to markets $g \in \mathcal{G}$ are short. Therefore, trucks are preferred to carry the commodities between them. A semi truck having 25 tons of load

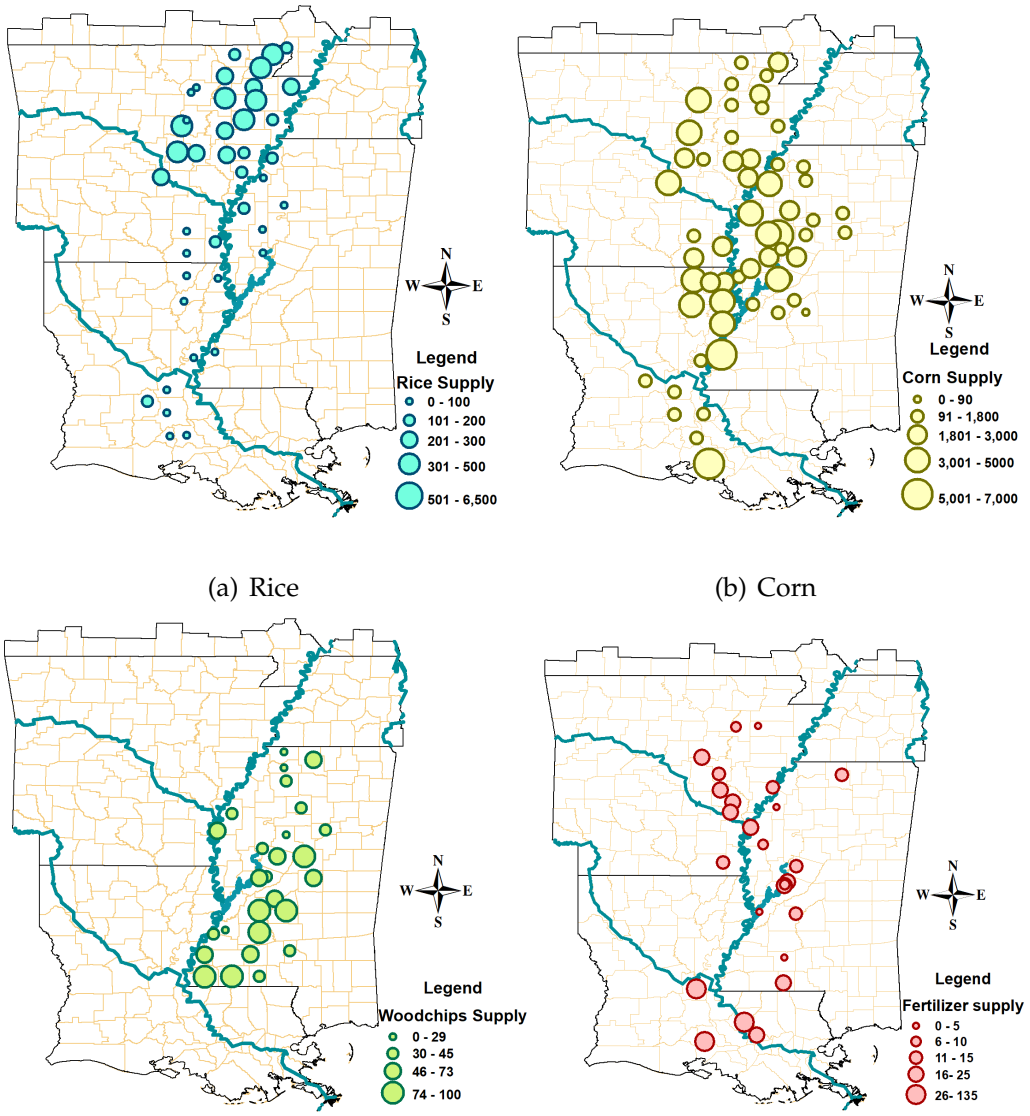

(a) Rice (b) Corn

(c) Woodchips (d) Fertilizer

Figure 2.4

Supply availability for (a) rice, (b) corn, (c) fertilizer, and (d) woodchips in the test region (in 1,000 tons)

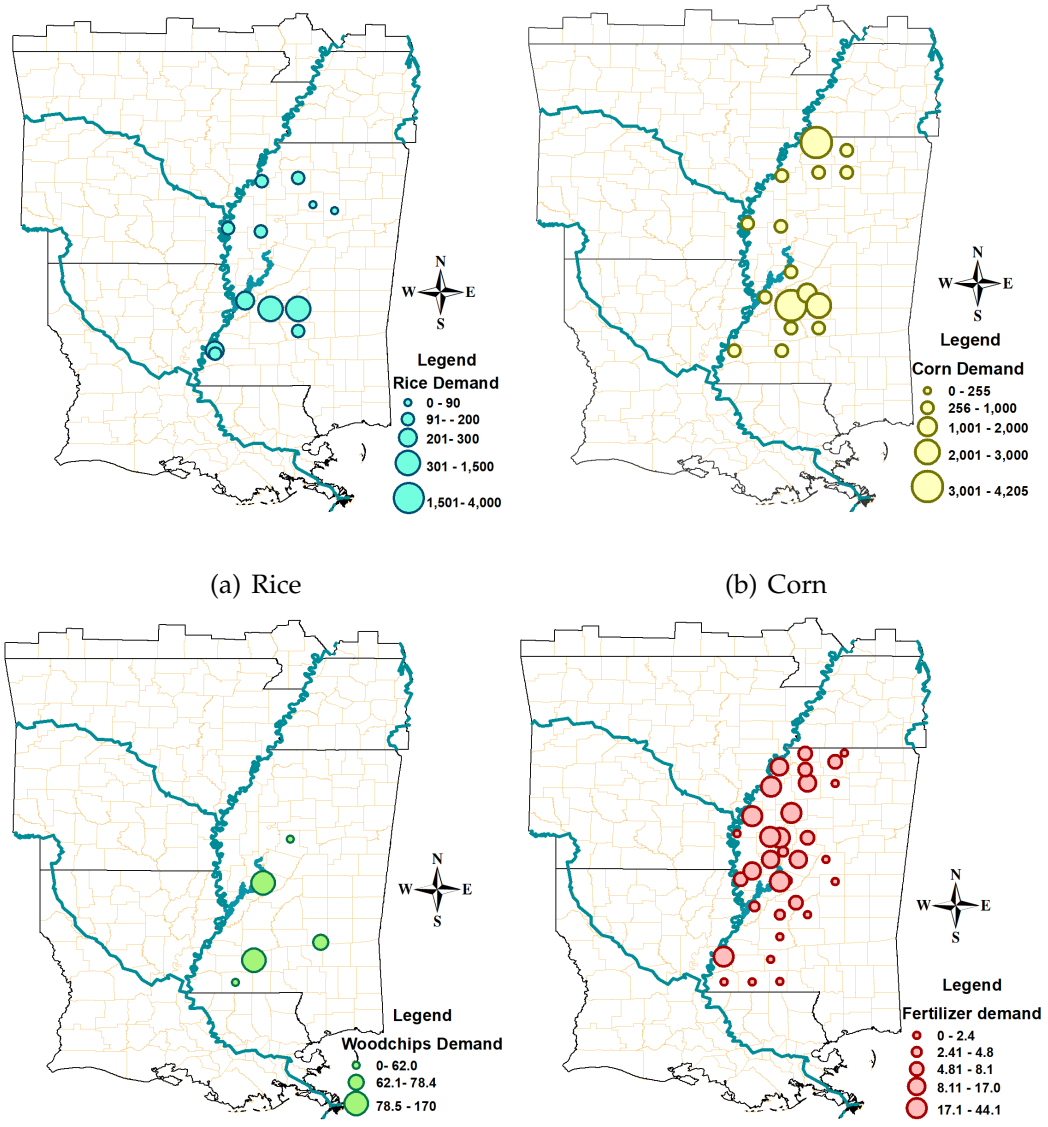

(a) Rice

(b) Corn

(c) Woodchips

(d) Fertilizer

Figure 2.5

Demand for (a) rice, (b) corn, (c) fertilizer, and (d) woodchips in the test region (in 1,000 tons)

capacity can be used to serve this purpose. The fixed cost (e.g., loading and unloading cost) and variable cost (e.g., fuel cost) for such a truck can be \$5/ton and \$1.20/mile/truckload, respectively [36]. On the other hand, waterway transportation is primarily conducted between origin ports $j \in \mathcal{J}$ and destination ports $k \in \mathcal{K}$ by the association of barges and towboats. Using a towboat that can carry a maximum of eight barges, incurs a fixed loading and unloading cost of \$244.38 [138]. Considering the waterway depth in the Mississippi River, towboat capacity is restricted to a maximum of 15 barges having a maximum capacity of 1,500 tons each [138]. Barge rate is set as \$0.017/mile/ton that is adopted from a study of Gonzales et al. [48].

***Water-level Fluctuations*:** Water level fluctuation is one of the notable issues that significantly impacts the Inland waterway transportation system. Different waterbodies all over the world face this unavoidable phenomenon in different time period of the year such as Yangtze River at China [94], Rhine River at Europe [94], Tagliamento River at Europe [131] and many others. The Mississippi River also experiences water level fluctuations in different locations and time periods of a year that significantly impacts the inland waterway port operations. For instance, lower Mississippi River has better flow compared to the upper Mississippi River; therefore, the load carrying capacity of this segment of river is better and more reliable compared to the upper Mississippi River. On the other hand, it is evident from the historical records that the water level of this portion of river experiences

significant variations over the year that impacts the barge traffic flowing through this waterway. This fluctuation often becomes significant even in different weeks of the same month. Figure 5.5 provides an example demonstrating the water level fluctuations between Port of Rosedale and Port of Greenville from July, 2016 to June, 2017 [139]. Each data point in this figure shows the weekly *water stage*[5] variation (e.g., minimum, maximum, and average water level) as reported by the US Army Corps of Engineers [139]. It is observed that the water level drops primarily between the middle of August and end of December of a calender year where the drop becomes maximum during the first three weeks of October (week 14-16 in Figure 5.5). Note that, other than this time period, the water stage generally remains above the desired level of 14.2 feet, except in May when the level reaches to 42 feet, which is greater than the flood level (37 feet) [139].

2.5.2.2 Experimental Results

Impact of water level fluctuation on towboat and barge selection:

Our first set of experiments examine the impact of water level fluctuation on overall system performance. To run these experiments, we create three different scenarios which are summarized in Table 2.7. These scenarios are created based on our observations in Figure 5.5. Note that the difference between scenario 3 with 2 is to consider water fluctuation up to flooding level which typically occurs during the month of May in the test region [132]. Figure 2.7 illustrates how the selection of

[5]A popular measure for water level in a river stream with respect to a reference height

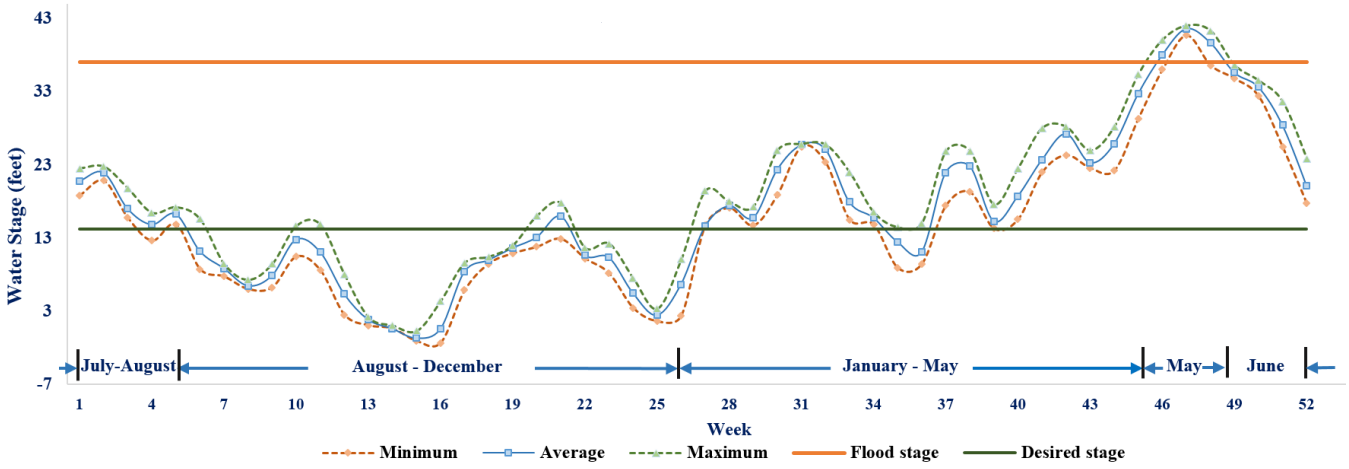

Figure 2.6

Example demonstrating water level fluctuations between Port of Rosedale and Port of Greenville from July, 2016 to June, 2017 [139]

barges (Y^2_{mbsjt}) and barge to towboat ratio[6] (Y^2_{mbsjt}/Y^1_{snjkt}) are impacted under three different scenarios as described in Table 2.7. Clearly, Y^2_{mbsjt} as well as Y^2_{mbsjt}/Y^1_{snjkt} decisions are significantly impacted if water level fluctuations are taken into consideration. It is observed that the test region is required to use an additional 81.5% and 39.7% of Y^2_{mbsjt} and Y^1_{snjkt}, respectively, if the water level fluctuation is appropriately measured and taken into consideration in model **[IMP]**. These decisions increase Y^2_{mbsjt}/Y^1_{snjkt} by approximately 16.1% since on average more barges are now required to connect with a single towboat to satisfy the market demand for the commodities. Note that both Y^2_{mbsjt} and Y^2_{mbsjt}/Y^1_{snjkt} are highly sensitive to

[6]The ratio indicates on average how many barges are connected with a towboat in a single trip

peak supply seasons (e.g., July-November) and has little to no impact during the off supply/demand seasons (e.g., February-June) (shown in Figure 2.7). Finally, we observe that, if flood level is taken into consideration (scenario 3), then model **[IMP]** forces no inland waterway transportation for the month of May, which results in a 6.9% increase in U_{mgt} and 7.1% increase in overall system cost for the test region.

Table 2.7

Description of scenarios

Scenario	Description
1	Water level fluctuation is ignored
2	Water level fluctuation is considered but flooding level is ignored
3	Water level fluctuation is considered with flooding level

Impact of supply (φ_{mit}) changes on overall system performance:

This set of experiments analyze the impact of supply changes on overall system performance. To run the experiments, we change the base supply (φ_{mit}) by $\pm$15% and $\pm$30% and observe its impact on towboat (Y^1_{snjkt}) and barge selection (Y^2_{mbsjt}), unsatisfied demand (U_{mgt}), and storage level (H_{mjt}) of the commodities. Figure 2.8 illustrates the impact of supply changes on overall system performance. Note that in Figure 2.8, $t = 1$ represents a representative week of month *July*. Further, to run

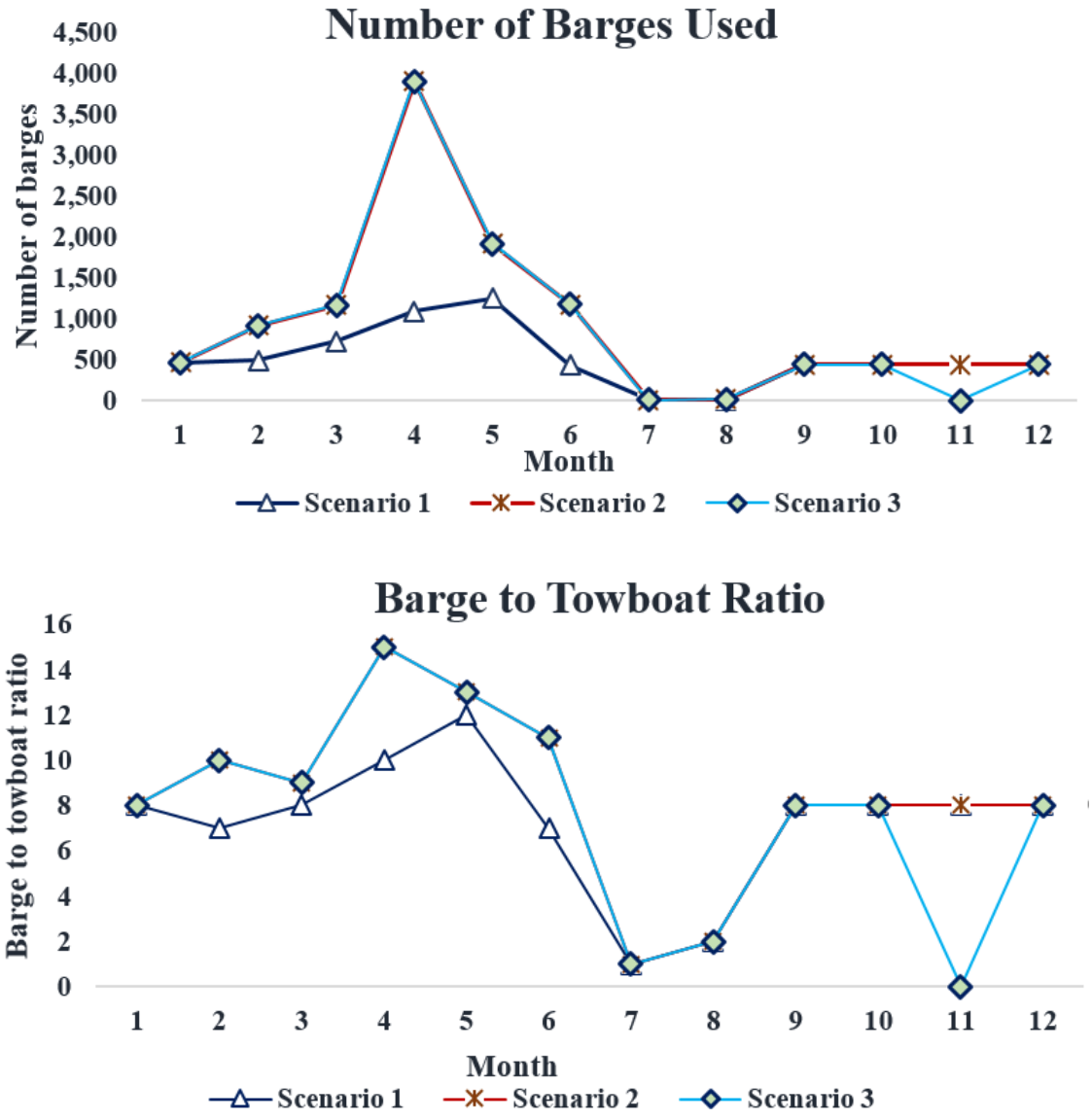

Figure 2.7

Selection of Y^2_{mbsjt} and Y^2_{mbsjt}/Y^1_{snjkt} under different water level scenarios

the experiments, we kept the demand d_{mgt} fixed under all scenarios. Experimental results indicate that if φ_{mit} changes by $\pm 30\%$, selection of Y^1_{snjkt} and Y^2_{mbsjt} changes by 14.1%/-15.8% and 12%/-49%, respectively. Observe that the reduction in φ_{mit} significantly increases the unsatisfied demand quantity U_{mgt}, primarily in the time period between August ($t = 2$) to November ($t = 5$) of the planning horizon. Note that this is the *peak* supply and demand period of the year when all four commodities are available, including rice and corn. This, in turn, also impacts the inventory management decisions H_{mjt} of the ports. For instance, if φ_{mit} changes by $\pm 30\%$, H_{mjt} is changed by 50%/-78% posing some serious challenges for the inland port managers to manage inventories during those peak supply seasons.

Impact of demand (d_{mgt}) changes on overall system performance:

This set of experiments provide a similar analysis as in Section 2.5.2.2, but changing the demand by $\pm 15\%$ and $\pm 30\%$ from the base demand d_{mgt} in order to observe their impacts on overall system performance. Figure 2.9 illustrates the impact of changes in d_{mgt} on towboat (Y^1_{snjkt}) and barge selection (Y^2_{mbsjt}), unsatisfied demand (U_{mgt}), and storage level (H_{mjt}) of the commodities. Experimental results indicate that the selection of Y^1_{snjkt} and Y^2_{mbsjt} is highly sensitive to the changes in d_{mgt} on the overall planning horizon, but in particular to months from July to November, when the supply and demand peaks for the commodities. For instance, if d_{mgt} changes by $\pm 30\%$, selection of Y^1_{snjkt} and Y^2_{mbsjt} changes by 14.3%/-52.1% and 25.4%/-32.2%, respectively. We further observe the changes in d_{mgt} on U_{mgt} and H_{mjt} decisions. For instance, H_{mjt} utilization is only realized between

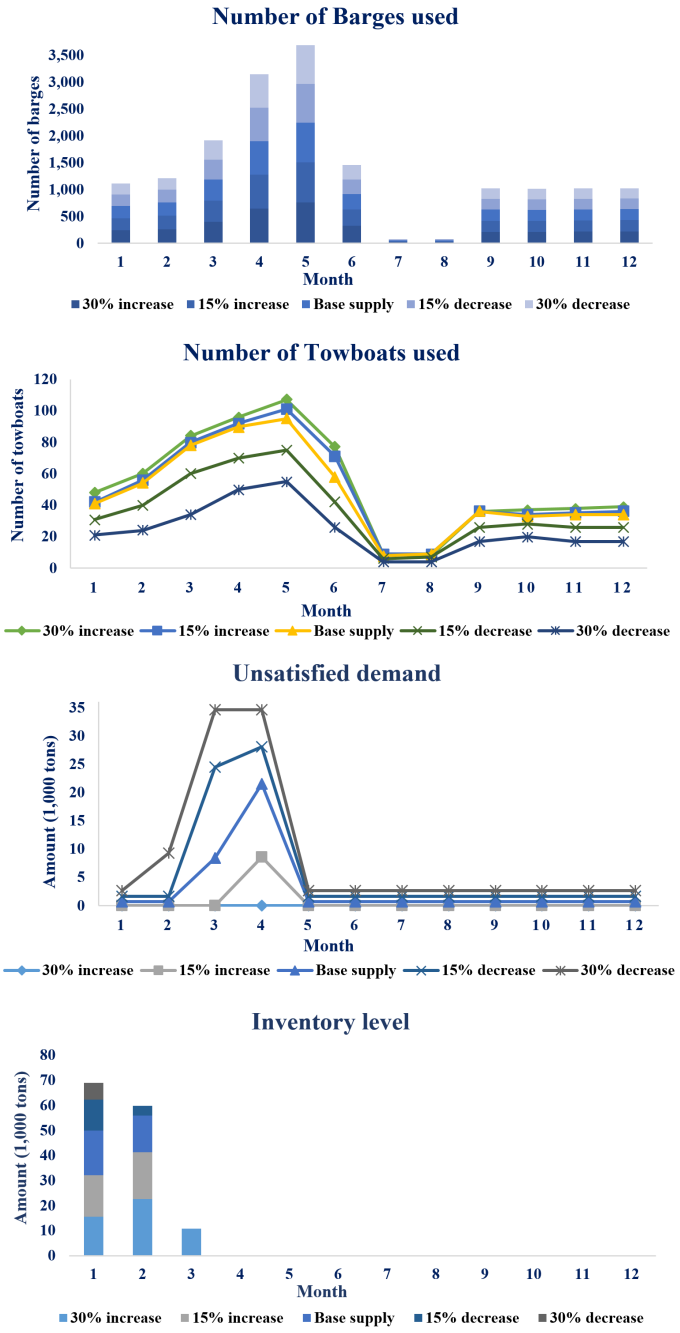

Figure 2.8

Impact of supply changes on system performances

months from July to September in a planning horizon when the supply season peaks. However, H_{mjt} drops by 34% and 62.8% when d_{mgt} is increased by 15% and 30%, respectively. This is understandable since the model finds it economical to transport more commodities to satisfy market demands rather than storing them in the inventories.

Impact of Barge availability on system performance:

Barges are the key elements of the inland waterway transportation. Depending on the products handled, three types of barges are commonly used along the Mississippi River: (i) *covered barges* to carry grains and agricultural products (e.g., corn), (ii) *tank barges* to carry liquid products (e.g., petroleum), and (iii) *open barges* to carry dry products (e.g., coal) [134]. According to the American Waterways Operators, more than 22% of the existing barges are expected to become obsolete by the end of 2018, primarily due to exceeding their useful service life [134]. This not only will significantly impact the barge availabilities a_{bjt}, but also will raise concerns for waterway transportation like the Mississippi River that contributes approximately 80% of the country's overall inland waterway transportation [128]. Note that, with fewer barges, the overall inland waterway transportation will be largely impacted, especially during the peak demand season (September to November) in the Southeast region of the United States. Therefore, we conduct sensitivity analysis by dropping the overall barge availability $\bar{a}_t = \sum_{b\in\mathcal{B},j\in\mathcal{J}} a_{bjt}; \forall t \in \mathcal{T}$ by 30%, 45%, and 60%, respectively from the base case scenario and analyzing its impact on the overall system performance. Note

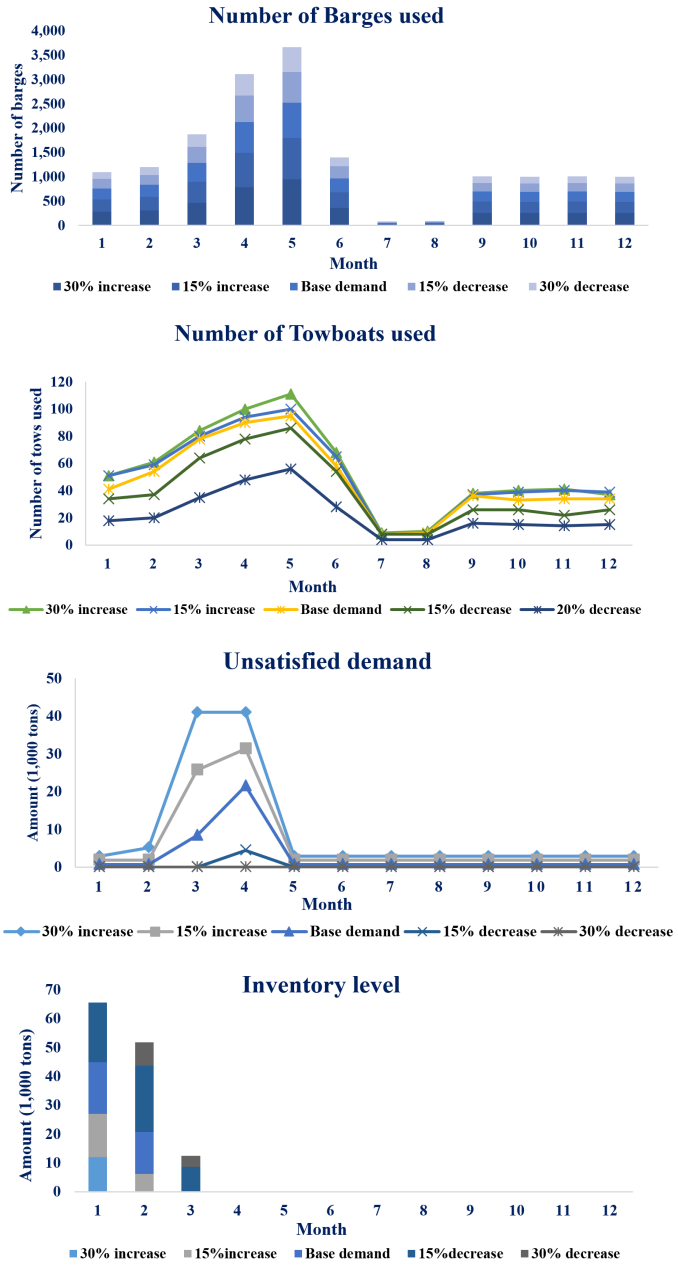

Figure 2.9

Impact of demand changes on system performances

that towboats have better rebuild and repair rates [128]; hence, their availabilities (a_{sjt}) remain fixed for this set of experiments. Results in Figure 2.10 clearly indicate that $\bar{a}_t$ significantly impacts the number of barges handled by the Mississippi River ($|Y^2_{mbsjt}|$) and it's consequence to overall demand satisfaction (U_{mgt}) during the high production seasons for this region. For instance, a 30%/60% drop in $\bar{a}_t$ decreases $|Y^2_{mbsjt}|$ and U_{mgt} by 13%/34.2% and 11%/29.3%, respectively and the significance is more prominent for the time period between September to November, when both the supply and demand for all four commodities are high. We end of our discussion by highlighting that $\bar{a}_t$ has marginal to no impact on the off-peak production seasons as evidenced from the results in Figure 2.10.

2.6 Conclusion

This paper proposes a mathematical model formulation which minimizes the short-term operational decisions (e.g., trip-wise towboat and barge assignment) and mid-term supply chain decisions (e..g., inventory management, transportation decisions) for an inland waterway transportation network in such a way that the overall supply chain cost can be minimized. We present an enhanced Benders decomposition algorithm to efficiently solve our proposed optimization model in a timely manner. We then use few Southeast US States as a test bed to visualize and validate the modeling results. A number of managerial insights are drawn, such as how the water level fluctuation, supply and demand variation, and barge availability impact the inland waterway transportation.

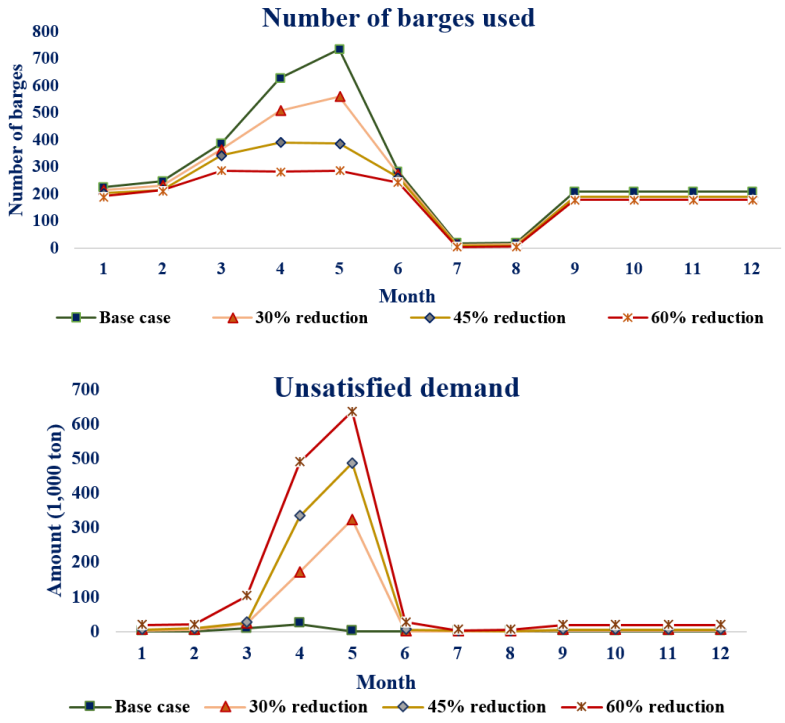

Figure 2.10

Impact of barge availability on system performances

To summarize, the major contributions of this study include: (i) proposing a multi-commodity, multi-time period mathematical model that optimizes inland waterway port operations and minimizes the overall system cost from a supply chain viewpoint; (ii) testing an efficient variant of the Benders decomposition algorithm (more specifically, local branching procedure with pareto-optimal cut, knapsack, and valid inequalities) to solve realistic-size network design problems; and (iii) drawing managerial insights from a real-life case study. We believe the proposed methodologies and managerial insights obtained from this study will help decision makers to design an efficient supply chain including inland waterway ports.

This research can be extended in several directions. First, it would be interesting to see how the stochasticity associated with commodity supply and demand impact the inland waterway transportation. The model can also be extended to incorporate barge and tow routing, scheduling, and re-positioning issues. Next, our study assumes that the inland waterway ports will never be impacted by any disruption. However, in practice both natural (e.g., hurricane, tornado) or human-induced (e.g., cyber attack) disruption can significantly impact the port operations. These issues will be examined in future studies. Further, we used an enhanced variant of the Benders decomposition algorithm that includes different cut generation techniques and heuristics such as valid inequalities, knapsack inequalities, pareto-optimal cuts, input ordering, and local branching techniques. However, further enhancement of Benders decomposition algorithm is possible by applying

MP size management techniques, generating alternative formulations, using additional heuristics, adding covering cuts, or using few Benders-type heuristics as proposed by Rahmaniani et al. [111]. Our future studies will examine the applicability and performance of these techniques to solve different inland waterway transportation based logistic network design problems.

CHAPTER 3

A PARALLELIZED HYBRID DECOMPOSITION ALGORITHM TO SOLVE A CONGESTED INLAND WATERWAY PORT MANAGEMENT PROBLEM UNDER UNCERTAINTY

3.1 Introduction

Inland waterway ports are indispensable components of the nation's waterway transportation system which greatly contributes to the overall economy of the nation. In the United States, these ports contribute approximately 15 billion dollars to the nation's GDP (Gross Domestic Product) along with creating more than 250,000 job opportunities (both direct and indirect) annually [89]. Additionally, these ports play a major role in the rural industrial and agricultural development for a nation [84]. Despite of their great potentiality, this segment of transportation system is frequently impacted by many factors which hurts it's productivity, including but not limited to congestion, aging infrastructure, delays caused by scheduled and unscheduled closures of locks (primarily due to maintenance activities), and many others [140]. According to the American Society of Civil Engineers (ASCE), in 2010, the United States encountered a total of $33 billions of additional annual expenditure primarily due to the delays governed by congestion and other waterway specific issues [8]. This cost will continue to increase

over time and is projected to reach nearly $49 billions by 2020 [8]. Therefore, it now becomes imperative to alleviate congestion from the inland waterway ports, primarily via optimal resource utilization/allocation and efficient transportation planning. Doing such will not only attract potential investors to utilize inland waterway transportation over freight transportation but also continue to support retaining the national GDP and employment in this sector while reducing the unexpected monetary investment due to congestion and other port related issues.

Though seemingly sound similar, inland waterway ports hold some unique properties that differ them significantly from the *seaports*. For instance, these ports generally handle barge traffic drafting upto 9 feet only, located primarily near smaller bodies of water (e.g., rivers and canals), usually land intensive, and/or handle smaller counts of larger users and a large number of smaller users [84]. Additionally, the water level between the channels of two connecting inland waterway ports fluctuates heavily in different time periods of the year [139, 94, 90]. Depending on the severity of this fluctuation, these ports, including the waterway itself, often experience disruptions, such as drought and flood that may tremendously impact or even cease the port operations for an extended period of time. Another prevalent feature that distinguishes inland waterway ports over seaports is that these ports commute heavy volume of perishable agricultural products which are highly seasonal in nature. The seasonality in agricultural products coupled with time varying waterway conditions and the availability of locks and dams between two source destination ports may excessively delay the port op-

erations which directly impacts the operational planning of the ports under consideration. With all these outstanding challenges, it is quite certain that the optimization models available in the literature for the maritime transportation may no longer be directly applicable for the inland waterway ports. Hence, to ensure long term sustainment of the inland waterway ports, there is a critical need to develop sophisticated optimization models that best capture the unique characteristics of this cost efficient, reliable, and environmentally friendly transportation sector.

A major stream of ongoing research develop optimization models to solve diversified seaport-related problems, such as ship routing and scheduling [29, 68], inventory routing [5], berth allocation and scheduling [27, 32, 141], empty container re-positioning [43], sailing speed optimization [73, 141], bunker consumption [145], emission consideration [141], disruption [43, 126], container routing [146], port delays [148], and many others. Apart from adopting mathematical approaches, few researchers develop simulation models to address similar problems (e.g., [118, 125, 121, 44]). Even though deep penetration to seaport research is observed, inland waterway ports did not receive much attention from the research community. A few considerations can be noticed for *deep draft inland ports* which are capable of handling container cargos and ships; however, almost no research has been conducted to date that puts specific considerations to model *shallow draft inland ports*[1]. These ports primarily handle shallow draft vessels (e.g.,

[1]The ports that are unable to handle barges/vessels drafting more than 9 feet are known as *shallow draft inland ports*. For the ones that can handle barges/vessels drafting more than 9 feet, are known as *deep draft inland ports*.

barge, towboats). Considering their outstanding contributions in the overall transportation system and economy, better understanding of shallow draft inland waterway ports is imperative to successfully design and manage a sound and efficient supply chain network.

To address this need, this study proposes a model which magnifies how different shallow draft inland waterway port-related internal (e.g., barge/towboat assignments, inventory decisions, port delays) and external (e.g., waterlevel fluctuations) factors/decisions impact the overall supply chain system performance. More specifically, we propose a capacitated, multi-commodity, multi-period, two-stage stochastic mixed-integer nonlinear programming model which jointly optimizes trip-wise towboat and barge assignment decisions along with different supply chain decisions (e.g., inventory management, transportation decisions) under a congested and stochastic environment and in such a way that the overall supply chain cost can be minimized. The proposed model realistically captures a number of factors that appropriately characterize the operations of a shallow draft inland waterway port, such as towboat and barge availability, weight and volumetric capacity restriction of barges, dredging issues, commodity mixture restrictions, storage restrictions at ports, trip restrictions between origin-destination ports, congestion issues, delays in locks and dams, and many others. We realized that our proposed mathematical model is an extension of the fixed charged, uncapacitated network flow problem which is already known to be an $\mathcal{NP}$-hard problem [74]. Therefore, we develop a highly customized parallelized hybrid decomposition al-

gorithm, combining Constraint Generation algorithm, Sample Average Approximation, and an enhanced variant of the L-shaped algorithm, to effectively solve the large instances of our proposed optimization model in a reasonable amount of time.

Apart from proposing the mathematical model and solution approaches, another important contribution of this study is the application of this model to a real world case study. We use the inland waterway transportation network along the Mississippi river as a testing ground to visualize and validate the modeling results. The outcome of this study provides a number of managerial insights, such as the impact of water level fluctuations on towboat and barge selection, cost due to delay in transportation, and commodity supply fluctuations on overall system performance, which can effectively aid decision makers to design a cost-efficient shallow draft inland waterway transportation network.

This paper is organized as follows. Section 3.2 reviews the related works. Section 3.3 describes the problem statement and introduces the proposed mathematical model formulation. Section 3.4 introduces different algorithms to solve our proposed mathematical model including the parallelized hybrid nested decomposition algorithms. Section 3.5 presents a real life case study, draw several managerial insights from the case study, and summarizes the computational performances of the proposed algorithms. Finally, we conclude our study and discuss several future research avenues in Section 3.6.

3.2 Literature Review

Different realistic aspects of deep draft inland waterway ports have attracted the research community for many years, including specific problems in optimizing barge and towboat routing and repositioning, berth allocation, port disruption, delays in locks and dams, and a few others. This section provides a comprehensive literature overview on these specific research problems.

Berth allocation problem is a common problem that typically experiences by both seaports and inland waterway ports. To date, few researchers have attempted to solve this problem for the deep draft inland waterway ports. For instance, Grubivsic et al. [50] solve a berth layout design problem to minimize the overall vessel waiting time. Depuy et al. [30] consider several factors, such as fleet location capacity, total volume of barges, and average handling time, to optimally allocate barge volume to different fleet locations. Arango et al. [11] adopt a combined simulation-optimization approach to solve a berth allocation problem. Guan and Cheung [51] propose two berth allocation model formulations while adopting a tree search solution procedure to solve the problems in realistic size test instances.

In addition to this research challenge, another stream of research study how the performances of locks and dams impact the deep draft inland waterway transportation network. For instance, Ting and Schonfeld [130] utilize a simulation-optimization framework to decide how much capacity increment is required for the locks so that the costs associated with tow delays can be minimized. Wang and Schonfeld [147] also adopt a combined simulation-optimization approach to

schedule the investment decisions for lock reconstruction and rehabilitation. Ting and Schonfeld [129] introduce an integrated tow control algorithm in order to reduce the delays between a series of locks. Most recently, Tan et al. [127] propose an optimization model that jointly optimizes ship schedule and sailing speed for the deep draft inland shipping services under uncertain dam transit time.

Another stream of research focus on optimizing the barge routing and empty container repositioning problem for the deep draft inland waterway ports. One such study is conducted by Braekers et al. [20] where the authors optimize barge routing and empty container repositioning between a sea port and few hinterland ports. The extension of this work [19] includes vessel capacity and round trip service frequency to the barge routing and empty container repositioning problem. Marass [76] proposes a mixed-integer linear programming (MILP) model to optimize the transport routes of chartered container ships or tows for an inland waterway port. Another MILP model is proposed by Alfandari et al. [6] to provide an optimal planning associated with liner service for a barge container shipping company. Davidovic et al. [28] study a barge container ship routing problem and propose a guided local search technique to solve this problem. Most recently, An et al. [9] formulate a MINLP model to solve an empty container repositioning shipping network design problem.

Realizing the need that a port may fail either due to natural (e.g., hurricane, tornado) or human-induced (e.g., cyber-attack) disaster, few studies focus on identifying the resiliency of a deep draft inland waterway port. For instance, Baroud et

al. [13] convert different stochastic resilience-based component importance measures into an optimization framework to determine the important waterway links and the precedence of link recovery in case of a disaster. Oztanriseven and Nachtman [102] develop a simulation-based approach to estimate the potential economic impacts of inland waterways disruption response. The authors utilize McClellan-Kerr Arkansas River navigation system as a testbed to visualize and validate the simulation results. MacKenzie et al. [72] analyze the economic impact of any sudden inland port closure by combining a simulation and a multi-regional input-output model. Pant et al. [103] propose a dynamic, multi-regional interdependency model to assess the effect of disruptions on the waterway networks, including both ports and waterway links. Folga et al. [42] propose a system level model to analyze the interdependency of failure followed by a disaster. Hosseini and Barker [59] propose a Bayesian network to model the infrastructure resilience of an inland waterway port. Other studies related to inland waterway ports include the consideration of port-specific economic analysis [4, 87, 151, 67], optimal dredging scheduling and investment decisions [86, 113, 18], the efficiency of inland waterway container terminals [152], tug scheduling between seaport to inland ports [39, 45, 157], and carbon emission [155, 71, 25].

Different from the studies discussed above, our study captures different realistic shallow draft inland waterway port-related features (e.g., waterlevel fluctuation, delay in locks and dams, port congestion, towboat and barge assignment decisions, barge availability and maintenance) and magnifies their impact

on the overall supply chain system performance. Note that till now a number of existing studies in the literature consider inland waterway ports as a medium of transportation while designing a supply chain network, examples include but not limited to biomass supply chain (e.g., [109, 79, 80]), coal supply chain (e.g., [35, 47, 62]), grain supply chain (e.g., [88, 10, 31]), and many other application areas. However, very few studies have captured the true characteristics of the inland waterway transportation (e.g., water level fluctuation, barge/towboat assignment decisions, barge availability and maintenance) while solving a network designing problem. Another important feature of our model is the consideration of congestion caused by the seasonality of the supplies (primarily, agricultural products as handled most by the inland waterway ports), waterlevel fluctuation, unavailability of resources (primarily, caused by barge availability and frequent maintenance needs), delay in locks and dams, limited service capacity in the ports, and many others. Though a rich stream of research available in the literature to efficiently manage congestion in diversified fields, including traffic networks [149, 101], telecommunication networks [143], service networks [3], and biomass supply chain networks [78, 106], and more specific to maritime ports [156, 38], waterways [154], and river ports [123], none of the studies manage congestion for a shallow draft inland waterway port and its possible impact to the overall supply chain system performance.

3.3 Problem Description and Model Formulation

This section presents a two-stage stochastic programming model formulation for the design and management of an shallow draft inland waterway transportation-based logistics network while stochastic nature of commodity supply and water-level fluctuations are taken into consideration. Further, the model attempts to minimize the sudden congestion that may possibly arise due to water-level and commodity supply fluctuations. The main objective of our model is to jointly optimize tripwise towboat and barge assignment decisions and different supply chain decisions (e.g., inventory, transportation decisions) in such a way that the overall system cost can be minimized. Figure 3.1 illustrates a simplified logistics network consisting of three supply sites, two origin and three destination ports, and four markets. For simplicity in the remaining sections of this paper, we shall refer *shallow draft inland ports* as *inland waterway ports*.

Consider a logistics network consisting of a set of supply sites $\mathcal{I} = \{1, 2, 3, ..., I\}$, set of origin ports $\mathcal{J} = \{1, 2, 3, ..., J\}$, set of destination ports $\mathcal{K} = \{1, 2, 3, ..., K\}$, and a set of markets $\mathcal{G} = \{1, 2, 3, ..., G\}$. Let $\mathcal{M} = \{1, 2, 3, ..., M\}$ be the set of commodities that need to be transported along this logistics network over a predetermined set of time periods $\mathcal{T} = \{1, 2, 3, ..., T\}$. Note that to handle the appropriate interconnections between the source and destination pairs, we introduce a number of subsets (e.g., $\mathcal{I}_j$, $\mathcal{I}_g$, $\mathcal{J}_i$, $\mathcal{J}_k$, $\mathcal{K}_j$, $\mathcal{K}_g$, $\mathcal{G}_k$, and $\mathcal{G}_i$) in our model. For instance,

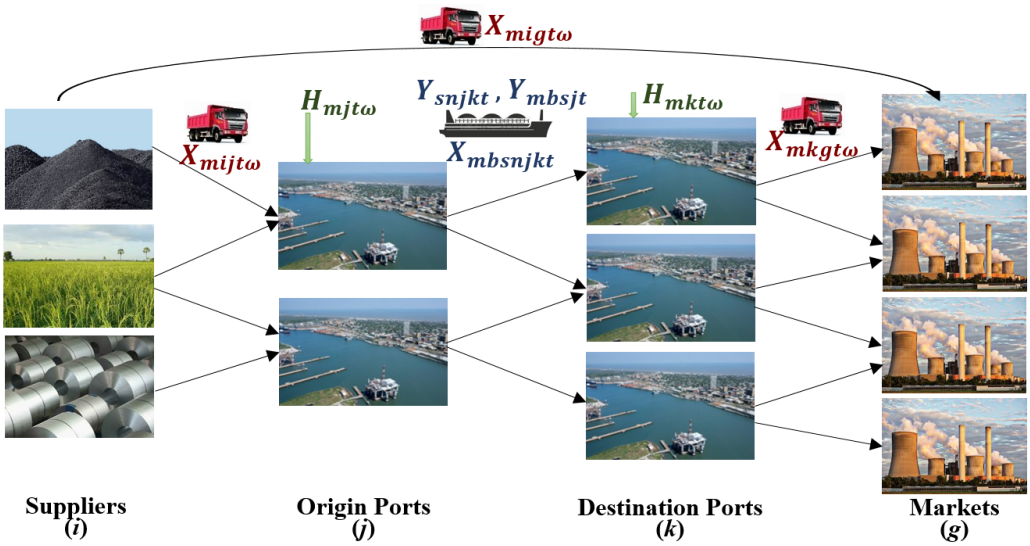

Figure 3.1

Illustration of an inland waterway transportation network

set $\mathcal{I}_j$ represents the subset of supply sites connected to port $j \in \mathcal{J}$. We use the similar convention to define other subsets. To account for different scenarios of water-level and commodity supply fluctuations, we introduce scenario set $\omega \in \Omega$ where ρ_ω defines probability of a given realization and $\sum_{\omega \in \Omega} \rho_\omega = 1$.

Each supply site $i \in \mathcal{I}$ produces a stochastic amount of commodity $\varphi_{mit\omega}$ of type $m \in \mathcal{M}$ at time period $t \in \mathcal{T}$ under scenario $\omega \in \Omega$. Suppliers have the option to send the commodities directly from a supply site $i \in \mathcal{I}$ or via an inland waterway transportation network, primarily through origin and destination ports $\mathcal{J}$ and $\mathcal{K}$, to a market $g \in \mathcal{G}$. The transportation distance between a supplier $i \in \mathcal{I}$ and an origin port $j \in \mathcal{J}$ is usually short. Therefore, truck is preferred to carry

commodities between these arcs $(i,j) \in (\mathcal{I},\mathcal{J})$ by incurring an unit transportation cost of c_{mijt}. Each shipment from the supply sites are consolidated in any origin port $j \in \mathcal{J}$ before being delivered to a destination port $k \in \mathcal{K}$. We assume that a set of towboats $\mathcal{S} = \{1,2,3,...,\overline{S}\}$ and barges $\mathcal{B} = \{1,2,3,...,B\}$ are available to carry commodities from any pair $(j,k) \in (\mathcal{J},\mathcal{K})$ of the origin-destination ports. Note that we sort set $\mathcal{S}$ based on the capabilities of the towboats (e.g., towboat 1 in set $\mathcal{S}$ is the least powerful towboat while $\overline{S}$ to represent the most powerful towboat). Based on the capabilities, we denote $\overline{\delta}_s$ and $\underline{\delta}_s$ to be the maximum and minimum number of barges that can be carried out by a towboat $s \in \mathcal{S}$ in a single trip. Let ψ_{st} and η_{mbt} be the fixed cost associated with using a towboat $s \in \mathcal{S}$ and loading and unloading commodity $m \in \mathcal{M}$ in barge $b \in \mathcal{B}$ at time period $t \in \mathcal{T}$. Each barge $b \in \mathcal{B}$ is restricted to a weight and volume carrying capacity of $\overline{w}_b$ and v_b, respectively. We further denote c_{mbsjkt} to be the unit cost of transporting commodity $m \in \mathcal{M}$ using barge $b \in \mathcal{B}$ connected with a towboat $s \in \mathcal{S}$ along arc $(j,k) \in (\mathcal{J},\mathcal{K})$ at time period $t \in \mathcal{T}$. Both the barges and towboats need to undergo periodic maintenance. This is captured via introducing binary availability parameters a_{bjt} and a_{sjt}, respectively. Finally, we define c_{mbsjkt} to be the unit cost of transporting commodity $m \in \mathcal{M}$ using barge $b \in \mathcal{B}$ connected with a towboat $s \in \mathcal{S}$ along arc $(j,k) \in (\mathcal{J},\mathcal{K})$ at time period $t \in \mathcal{T}$.

Each port $j \in \mathcal{J} \bigcup \mathcal{K}$, is restricted to a maximum of commodity processing capacity of $\overline{c}_{jt}$ and storage capacity of $\overline{h}_j$. Let h_{mjt} be the unit inventory holding cost for commodity $m \in \mathcal{M}$ in port $j \in \mathcal{J} \bigcup \mathcal{K}$ at time period $t \in \mathcal{T}$. We further de-

fine α_m to capture the deterioration rate of carrying commodity $m \in \mathcal{M}$ between two consecutive time periods. We also introduce a set $\mathcal{N}_{jk} = \{1, 2, 3, ..., n_{jk}\}$ to capture the possible trips that can be made by a towboat between each origin-destination port $(j,k) \in (\mathcal{J}, \mathcal{K})$. Note that due to *dredging* effect, the weight carrying capacity of a barge $\overline{w}_b$ as well as the possible number of trips between each origin-destination port, denoted by parameter τ_{jkt}, at time period $t \in \mathcal{T}$ may vary. We now first define three parameters $w_{jt\omega}$, $w_{kt\omega}$, and $w_{jkt\omega}$ to denote the maximum weight carrying capacity at port $j \in \mathcal{J} \bigcup \mathcal{K}$ and $w_{jkt\omega}$ the allowable weight that can be carried between the channel $(j,k) \in (\mathcal{J}, \mathcal{K})$ at time period $t \in \mathcal{T}$ under scenario $\omega \in \Omega$. It is observed that the depth of navigation channel near ports or the waterbody that connects a source-destination port may vary in different time period of the year depending upon the amount of sediment, silt, or mud accumulated in the waterbed. When this accumulation is high in any portion of the waterway (e.g., near ports or between two connecting ports), it raises the height of the waterbed and results a decrease in the water depth. Unfortunately, when the reduction of this water level becomes too intense, it seriously impacts the transportation of shallow draft water vessels through the channel. Resultantly, the barges are now restricted to carry commodities below to their designed weight carrying capacity of $\overline{w}_b$. In practice, the *maximum effective weight* that a barge $b \in \mathcal{B}$ can carry under this restriction would be the *minimum* weight between the weight capacity near origin and destination ports, namely, $w_{jt\omega}$ and $w_{kt\omega}$, and the channel between each origin-destination ports $(j,k) \in (\mathcal{J}, \mathcal{K})$, namely, $w_{jkt\omega}$, i.e., $min\{\overline{w}_{jkt\omega}, \overline{w}_b\}$

where $\overline{w}_{jkt\omega} := min\{w_{jt\omega}, w_{jkt\omega}, w_{kt\omega}\}$. Further, due to the unpredictability to accurately estimate this restriction, we consider $\overline{w}_{jkt\omega}$ to be a stochastic parameter in our proposed model formulation. Finally, in addition to carrying the commodities through the inland waterway transportation, we also assume that the demand for commodities at the markets, denoted by d_{mgt}, can be satisfied either via direct shipments from the supplier sites (primarily via trucks) or via an external source by paying a unit penalty cost of π_{mgt}. We now summarize the following notations for our proposed mathematical model formulation.

Sets:

- $\mathcal{I}$: set of supply sites, $i \in \mathcal{I}$
- $\mathcal{J}$: set of origin ports, $j \in \mathcal{J}$
- $\mathcal{K}$: set of destination ports, $k \in \mathcal{K}$
- $\mathcal{G}$: set of markets, $g \in \mathcal{G}$
- $\mathcal{M}$: set of commodities, $m \in \mathcal{M}$
- $\mathcal{S}$: set of towboats, $s \in \mathcal{S}$
- $\mathcal{B}$: set of barges, $b \in \mathcal{B}$
- $\mathcal{N}_{jk}$: set of trips along arc $(j,k) \in (\mathcal{J},\mathcal{K})$, $n \in \mathcal{N}_{jk}$
- $\mathcal{T}$: set of time periods, $t \in \mathcal{T}$
- $\mathcal{I}_j$: set of supply sites connected to port j, $\forall j \in \mathcal{J}$
- $\mathcal{I}_g$: set of supply sites connected to market g, $\forall g \in \mathcal{G}$
- $\mathcal{J}_i$: set of origin ports connected to supply site i, $\forall i \in \mathcal{I}$
- $\mathcal{J}_k$: set of origin ports connected to destination port k, $\forall k \in \mathcal{K}$
- $\mathcal{K}_j$: set of destination ports connected to origin port j, $\forall j \in \mathcal{J}$
- $\mathcal{K}_g$: set of destination ports connected to market g, $\forall g \in \mathcal{G}$
- $\mathcal{G}_k$: set of markets connected to destination port k, $\forall k \in \mathcal{K}$

- $\mathcal{G}_i$: set of markets connected to destination port i, $\forall i \in \mathcal{I}$
- Ω: set of possible scenarios ω, $\forall \omega \in \Omega$

Parameters:

- $\varphi_{mit\omega}$: amount of product of type $m \in \mathcal{M}$ available in supply site $i \in \mathcal{I}$ at time period $t \in \mathcal{T}$ under scenario $\omega \in \Omega$
- ψ_{st}: fixed cost of using towboat $s \in \mathcal{S}$ at time period $t \in \mathcal{T}$
- η_{mbt}: fixed cost for loading and unloading commodity $m \in \mathcal{M}$ in barge $b \in \mathcal{B}$ at time period $t \in \mathcal{T}$
- c_{migt}: unit cost of transporting commodity $m \in \mathcal{M}$ along arc $(i,g) \in (\mathcal{I},\mathcal{G})$ at time period $t \in \mathcal{T}$
- c_{meft}: unit cost of transporting commodity $m \in \mathcal{M}$ along arc $(e,f) \in (\mathcal{I} \bigcup \mathcal{K}, \mathcal{J} \bigcup \mathcal{G})$ at time period $t \in \mathcal{T}$
- c_{mbsjkt}: unit cost of transporting commodity $m \in \mathcal{M}$ using barge $b \in \mathcal{B}$ of towboat $s \in \mathcal{S}$ along arc $(j,k) \in (\mathcal{J},\mathcal{K})$ at time period $t \in \mathcal{T}$
- c^o_{jt}/c^o_{kt}: congestion cost in port $j \in \mathcal{J} \bigcup \mathcal{K}$ at time $t \in \mathcal{T}$
- $\overline{h}_j$: commodity storage capacity at port $j \in \mathcal{J} \bigcup \mathcal{K}$
- d_{mgt}: demand for commodity of type $m \in \mathcal{M}$ in market $g \in \mathcal{G}$ at time period $t \in \mathcal{T}$
- α_m: deterioration rate of commodity $m \in \mathcal{M}$
- a_{sjt}, a_{bjt}: binary availability of towboat and barge
- $\overline{\delta}_s$, $\underline{\delta}_s$: maximum/minimum number of barges to carry by towboat $s \in \mathcal{S}$
- $\overline{w}_{jkt\omega}$: the minimum of $\{w_{jt\omega}, w_{jkt\omega}, w_{kt\omega}\}$ where $w_{jt\omega}$ and $w_{kt\omega}$ indicate the maximum weight carrying capacity at port $j \in \mathcal{J} \bigcup \mathcal{K}$ and $w_{jkt\omega}$ the allowable weight that can be carried between the channel $(j,k) \in (\mathcal{J},\mathcal{K})$ at time period $t \in \mathcal{T}$ under scenario $\omega \in \Omega$. The last weight ($w_{jkt\omega}$) depends on the depth of the waterway and should not exceed the minimal water-level between the origin-destination ports
- ρ_m: density of commodity $m \in \mathcal{M}$
- v_b: volume capacity of barge $b \in \mathcal{B}$

- $\overline{w}_b$: weight capacity of a barge $b \in \mathcal{B}$
- π_{mgt}: unit penalty cost of not satisfying demand for commodity $m \in \mathcal{M}$ in market $g \in \mathcal{G}$ at time period $t \in \mathcal{T}$
- h_{mjt}: unit inventory holding cost for commodity $m \in \mathcal{M}$ in port $j \in \mathcal{J} \bigcup \mathcal{K}$ at time period $t \in \mathcal{T}$
- θ_{jt}: total number of barges available in port $j \in \mathcal{J}$ at time period $t \in \mathcal{T}$
- τ_{jkt}: maximum number of trips that can be made along arc $(j,k) \in (\mathcal{J},\mathcal{K})$ at time period t
- $\overline{c}_{jt}, \overline{c}_{kt}$: commodity processing capacity of port $j \in \mathcal{J} \bigcup \mathcal{K}$ at time period $t \in \mathcal{T}$
- t_l, t_u: average loading and unloading time of a barge
- Δ: average delay in locks
- l_{jk}: number of locks between origin port $j \in \mathcal{J}$ and destination port $k \in \mathcal{K}$
- d_{jk}: distance between origin port $j \in \mathcal{J}$ and destination port $k \in \mathcal{K}$
- $\bar{v}_{st}$: average speed of towboat $s \in \mathcal{S}$ at time period $t \in \mathcal{T}$
- $\bar{t}_{jk}$: allowable transport time limit between each origin port $j \in \mathcal{J}$ to destination port $k \in \mathcal{K}$
- ρ_ω: probability of scenario $\omega \in \Omega$

First Stage Decision Variables:

- Y_{snjkt}: 1 if a towboat $s \in \mathcal{S}$ is used in arc $(j,k) \in (\mathcal{J},\mathcal{K})$ for trip $n \in \mathcal{N}_{jk}$ at time period $t \in \mathcal{T}$; 0 otherwise
- Y_{mbsjt}: 1 if commodity $m \in \mathcal{M}$ is carried on barge $b \in \mathcal{B}$ of towboat $s \in \mathcal{S}$ from port $j \in \mathcal{J}$ at time period $t \in \mathcal{T}$; 0 otherwise

Second Stage Decision Variables:

- $X_{migt\omega}$: amount of commodities of type $m \in \mathcal{M}$ transported along arc $(i,g) \in (\mathcal{I} \bigcup \mathcal{G})$ at time period $t \in \mathcal{T}$ under scenario $\omega \in \Omega$
- $X_{meft\omega}$: amount of commodities of type $m \in \mathcal{M}$ transported along arc $(e,f) \in (\mathcal{I} \bigcup \mathcal{K}, \mathcal{J} \bigcup \mathcal{G})$ at time period $t \in \mathcal{T}$ under scenario $\omega \in \Omega$

- $X_{mbsnjkt\omega}$: amount of commodities of type $m \in \mathcal{M}$ transported using barge $b \in \mathcal{B}$ of towboat $s \in \mathcal{S}$ of trip $n \in \mathcal{N}_{jk}$ along arc $(j,k) \in (\mathcal{J},\mathcal{K})$ at time period $t \in \mathcal{T}$ under scenario $\omega \in \Omega$
- $H_{mjt\omega}$: amount of commodities of type $m \in \mathcal{M}$ stored in port $j \in \mathcal{J} \bigcup \mathcal{K}$ at time period $t \in \mathcal{T}$ under scenario $\omega \in \Omega$
- $U_{mgt\omega}$: amount of commodities of type $m \in \mathcal{M}$ shortage in market $g \in \mathcal{G}$ at time period $t \in \mathcal{T}$ under scenario $\omega \in \Omega$

We now introduce the following first and second-stage decision variables for our proposed two-stage stochastic programming model formulation. The first-stage decision variables $\mathbf{Y}^1 := \{Y_{snjkt} | \forall s \in \mathcal{S}, n \in \mathcal{N}_{jk}, j \in \mathcal{J}, k \in \mathcal{K}_j, t \in \mathcal{T}\}$ and $\mathbf{Y}^2 := \{Y_{mbsjt} | \forall m \in \mathcal{M}, b \in \mathcal{B}, s \in \mathcal{S}, j \in \mathcal{J}, t \in \mathcal{T}\}$ determine which towboat to use between any origin-destination pair in a given time period and which barge to use for carrying any particular product at any given origin port, respectively, i.e.,

$$Y_{snjkt} = \begin{cases} 1 & \text{if a towboat } s \text{ is used in arc } (j,k) \in (\mathcal{J},\mathcal{K}) \text{ for trip } n \text{ at time period } t \\ 0 & \text{otherwise;} \end{cases}$$

$$Y_{mbsjt} = \begin{cases} 1 & \text{if barge } b \text{ connected to towboat } s \text{ is used to carry commodity } m \\ & \text{at port } j \text{ in time period } t \\ 0 & \text{otherwise;} \end{cases}$$

The second-stage decision variables $\mathbf{X}^1 := \{X_{migt\omega} | \forall m \in \mathcal{M}, (i,g) \in (\mathcal{I} \bigcup \mathcal{G}), t \in \mathcal{T}, \omega \in \Omega\}$ determine the amount of commodities of type $m \in \mathcal{M}$ transported along arc $(i,g) \in (\mathcal{I} \bigcup \mathcal{G})$ at time period $t \in \mathcal{T}$ under scenario $\omega \in \Omega$; $\mathbf{X}^2 := \{X_{meft\omega} | \forall m \in \mathcal{M}, (e,f) \in (\mathcal{I} \bigcup \mathcal{K}, \mathcal{J} \bigcup \mathcal{G}), t \in \mathcal{T}, \omega \in \Omega\}$ to denote the amount of commodities of type $m \in \mathcal{M}$ transported along arc $(e,f) \in (\mathcal{I} \bigcup \mathcal{K}, \mathcal{J} \bigcup \mathcal{G})$ at

time period $t \in \mathcal{T}$ under scenario $\omega \in \Omega$; $\mathbf{X}^3 := \{X_{mbsnjkt\omega} | \forall m \in \mathcal{M}, b \in \mathcal{B}, s \in \mathcal{S}, n \in \mathcal{N}_{jk}, (j,k) \in (\mathcal{J},\mathcal{K}), t \in \mathcal{T}, \omega \in \Omega\}$ to denote the amount of commodities of type $m \in \mathcal{M}$ transported using barge $b \in \mathcal{B}$ of towboat $s \in \mathcal{S}$ of trip $n \in \mathcal{N}_{jk}$ along arc $(j,k) \in (\mathcal{J},\mathcal{K})$ at time period $t \in \mathcal{T}$ under scenario $\omega \in \Omega$; $\mathbf{H} := \{H_{mjt\omega} | \forall m \in \mathcal{M}, j \in \mathcal{J} \bigcup \mathcal{K}, t \in \mathcal{T}, \omega \in \Omega\}$ to denote the amount of commodities of type $m \in \mathcal{M}$ stored in port $j \in \mathcal{J} \bigcup \mathcal{K}$ at time period $t \in \mathcal{T}$ under scenario $\omega \in \Omega$; and $\mathbf{U} := \{U_{mgt\omega}\}$ to denote the amount of commodities of type $m \in \mathcal{M}$ shortage in market $g \in \mathcal{G}$ at time period $t \in \mathcal{T}$ under scenario $\omega \in \Omega$. For notation simplicity, we define $\mathbf{Y}$ as $\mathbf{Y} := \mathbf{Y}^1 \bigcup \mathbf{Y}^2$ and $\mathbf{X}$ as $\mathbf{X} := \mathbf{X}^1 \bigcup \mathbf{X}^2 \bigcup \mathbf{X}^3$.

Inland waterway ports handle a number of agricultural products (e.g., corn, rice, woodchips) which are highly seasonal in nature. For instance, rice is available only between August to October in a given calendar year. Likewise, corn is harvested between mid-July to late November of each year [133]. Such seasonality coupled with stochastic availability of the commodities can create a unique challenge for port managers from the managing and handling viewpoint. The most predominant impact would be the waiting time for the trucks to be serviced in a given port during peak harvesting seasons. This results *congestion* in the ports which eventually impairs the shipment delivery time and hence increase the overall transportation cost. To realistically capture this effect, we borrow the *congestion function* proposed by Elhedhli and Wu [34] to add in the objective function of our proposed model formulation and to evaluate the performance of the inland waterway transportation network under this critical consideration. Es-

sentially, it can be stated that the average waiting time for the commodities increases as the total commodity flow approaches *very close* to the capacities $(\overline{c}_{jt}, \overline{c}_{kt})$ of a given port $j \in \mathcal{J} \bigcup \mathcal{K}$. Mathematically, this term can be represented as: $\left(\frac{\sum_{m \in \mathcal{M}} \sum_{b \in \mathcal{B}} \sum_{s \in \mathcal{S}} \sum_{n \in \mathcal{N}_{jk}} \sum_{k \in \mathcal{K}} X_{mbsnjkt\omega}}{\overline{c}_{jt} - \sum_{m \in \mathcal{M}} \sum_{b \in \mathcal{B}} \sum_{s \in \mathcal{S}} \sum_{n \in \mathcal{N}_{jk}} \sum_{k \in \mathcal{K}} X_{mbsnjkt\omega}} \right)$ for port $j \in \mathcal{J}$ at time period $t \in \mathcal{T}$ and under scenario $\omega \in \Omega$. Note that we represent $\overline{c}_{jt} = \tilde{c}_{jt} + \overline{\Delta}$ where $\tilde{c}_{jt}$ is the *actual processing capacity* for port $j \in \mathcal{J}$ in time $t \in \mathcal{T}$ and $\overline{\Delta}$ is a small number. Clearly, if the total commodity flow $X_{mbsnjkt\omega}$ exceeds $\tilde{c}_{jt}$ i.e., approaching very close to $\overline{c}_{jt}$, ratio of the equation will increase exponentially and thus will realistically address the impact of congestion to a given port. Likewise, congestion function for port $k \in \mathcal{K}$ at time $t \in \mathcal{T}$ under scenario $\omega \in \Omega$ can be represented as: $\left(\frac{\sum_{m \in \mathcal{M}} \sum_{g \in \mathcal{G}} X_{mkgt\omega}}{\overline{c}_{kt} - \sum_{m \in \mathcal{M}} \sum_{g \in \mathcal{G}} X_{mkgt\omega}} \right)$. Let c^o_{jt} and c^o_{kt} be the congestion cost in port $j \in \mathcal{J} \bigcup \mathcal{K}$ at time period $t \in \mathcal{T}$. Therefore, for each $t \in \mathcal{T}$ and $\omega \in \Omega$, the overall system-wide congestion cost can be represented as follows:

$$\sum_{j \in \mathcal{J}} c^o_{jt} \left(\frac{\sum_{m \in \mathcal{M}} \sum_{b \in \mathcal{B}} \sum_{s \in \mathcal{S}} \sum_{n \in \mathcal{N}_{jk}} \sum_{k \in \mathcal{K}} X_{mbsnjkt\omega}}{\overline{c}_{jt} - \sum_{m \in \mathcal{M}} \sum_{b \in \mathcal{B}} \sum_{s \in \mathcal{S}} \sum_{n \in \mathcal{N}_{jk}} \sum_{k \in \mathcal{K}} X_{mbsnjkt\omega}} \right)$$
$$+ \sum_{k \in \mathcal{K}} c^o_{kt} \left(\frac{\sum_{m \in \mathcal{M}} \sum_{g \in \mathcal{G}} X_{mkgt\omega}}{\overline{c}_{kt} - \sum_{m \in \mathcal{M}} \sum_{g \in \mathcal{G}} X_{mkgt\omega}} \right)$$

We note that in addition to capturing congestion in the ports during peak supply seasons, towboats may also experience congestion in the locks between two connecting ports. However, to simplify the modeling process, in this study we ignore the congestion caused by the locks between two connecting ports. Meanwhile, total travel time for a towboat between each source-destination pair is ap-

proximated and a feasible time limit is provided. Let Δ, l_{jk}, and d_{jk} be the average delay in locks, the number of locks between each origin-destination port, and the traveling distance between each pair of ports $(j,k) \in (\mathcal{J},\mathcal{K})$. We further denote $\bar{v}_{st}$ to be the average speed of towboat $s \in \mathcal{S}$ at time period $t \in \mathcal{T}$ and t_l and t_u to be the average loading and unloading time for a barge. We can then approximate the total travel time for a towboat $s \in \mathcal{S}$ in trip $n \in \mathcal{N}_{jk}$ between each origin destination port $(j,k) \in (\mathcal{J},\mathcal{K})$ at time $t \in \mathcal{T}$ as: $\left\{ \sum_{m\in\mathcal{M}} \sum_{b\in\mathcal{B}} (t_l + t_u) Y_{mbsjt} + (\frac{d_{jk}}{\bar{v}_{st}} + \Delta l_{jk}) Y_{snjkt} \right\}$, and we assume that this travel time should be restricted by a feasible time limit $\bar{t}_{jk}$.

We are now ready to introduce the objective function of our proposed two-stage stochastic programming mathematical formulation, referred to as **[IPM]**. The model introduces two uncertain parameters, supply availability ($\phi_{mit\omega}$), and allowable weight limit in waterway connecting ports ($\overline{w}_{jkt\omega}$). To capture the interaction between the stochastic parameters we define ζ as the vector of these uncertain parameters, i.e., $\zeta = (\phi, \overline{w})$, and ζ^ω is a given realization of the uncertain parameters, $\zeta^\omega \in \zeta$. The decisions about towboat and barge selection (**Y**) are made prior to a realization of any stochastic event. However, after the stochasticity is revealed, the second-stage decisions such as the transportation (**X**), storage (**H**), and

shortage (**U**) decisions are made. The proposed mathematical model is now given below.

$$\textbf{[IPM]} \quad \underset{\mathbf{Y}}{Minimize} \sum_{s\in\mathcal{S}}\sum_{j\in\mathcal{J}}\sum_{t\in\mathcal{T}}\left(\sum_{n\in\mathcal{N}_{jk}}\sum_{k\in\mathcal{K}_j}\psi_{st}Y_{snjkt}+\sum_{m\in\mathcal{M}}\sum_{b\in\mathcal{B}}\eta_{mbt}Y_{mbsjt}\right) \tag{3.1}$$
$$+\sum_{\omega\in\Omega}\rho_\omega \mathbb{Q}(\mathbf{Y},\zeta^\omega)$$

subject to

$$\sum_{m\in\mathcal{M}} Y_{mbsjt} \leq 1 \qquad \forall b\in\mathcal{B}, s\in\mathcal{S}, j\in\mathcal{J}, t\in\mathcal{T} \tag{3.2}$$

$$\sum_{s\in\mathcal{S}} Y_{snjkt} \leq 1 \qquad \forall n\in\mathcal{N}_{jk}, j\in\mathcal{J}, k\in\mathcal{K}_j, t\in\mathcal{T} \tag{3.3}$$

$$\sum_{n\in\mathcal{N}_{jk}}\sum_{k\in\mathcal{K}_j}\underline{\delta}_s Y_{snjkt} \leq \sum_{m\in\mathcal{M}}\sum_{b\in\mathcal{B}} Y_{mbsjt} \leq \sum_{n\in\mathcal{N}_{jk}}\sum_{k\in\mathcal{K}_j}\bar{\delta}_s Y_{snjkt} \;\forall s\in\mathcal{S}, \; j\in\mathcal{J}, t\in\mathcal{T} \tag{3.4}$$

$$\sum_{s\in\mathcal{S}}\sum_{n\in\mathcal{N}_{jk}} Y_{snjkt} \leq \tau_{jkt} \qquad \forall j\in\mathcal{J}, k\in\mathcal{K}_j, t\in\mathcal{T} \tag{3.5}$$

$$\sum_{m\in\mathcal{M}}\sum_{b\in\mathcal{B}}\sum_{s\in\mathcal{S}} Y_{mbsjt} \leq \theta_{jt} \qquad \forall j\in\mathcal{J}, t\in\mathcal{T} \tag{3.6}$$

$$\sum_{n\in\mathcal{N}_{jk}}\sum_{k\in\mathcal{K}_j} Y_{snjkt} \leq a_{sjt} \qquad \forall s\in\mathcal{S}, j\in\mathcal{J}, t\in\mathcal{T} \tag{3.7}$$

$$\sum_{m\in\mathcal{M}}\sum_{s\in\mathcal{S}} Y_{mbsjt} \leq a_{bjt} \qquad \forall b\in\mathcal{B}, j\in\mathcal{J}, t\in\mathcal{T} \tag{3.8}$$

$$\sum_{m\in\mathcal{M}}\sum_{b\in\mathcal{B}}(t_l+t_u)Y_{mbsjt} \leq \bar{t}_{jk}-(\frac{d_{jk}}{\bar{v}_{st}}+\Delta l_{jk})Y_{snjkt} \;\forall s\in\mathcal{S}, n\in\mathcal{N}_{jk}, \; j\in\mathcal{J}, k\in\mathcal{K}_j, t\in\mathcal{T} \tag{3.9}$$

$$Y_{mbsjt} \in \{0,1\} \quad \forall m\in\mathcal{M}, b\in\mathcal{B}, s\in\mathcal{S}, j\in\mathcal{J}, t\in\mathcal{T} \tag{3.10}$$

$$Y_{snjkt} \in \{0,1\} \quad \forall s\in\mathcal{S}, n\in\mathcal{N}_{jk}, j\in\mathcal{J}, k\in\mathcal{K}_j, t\in\mathcal{T} \tag{3.11}$$

with $\mathbb{Q}(\mathbf{Y},\zeta^\omega)$ being the solution of the following second-stage problem:

$$\mathbb{Q}(\mathbf{Y},\zeta^{\omega}) = \underset{\mathbf{X,H,U}}{Minimize} \sum_{t\in\mathcal{T}}\Bigg(\sum_{(e,f)\in(\mathcal{I}\bigcup\mathcal{K},\mathcal{J}\bigcup\mathcal{G})} c_{meft}X_{meft\omega} + \sum_{(i,g)\in(\mathcal{I},\mathcal{G})} c_{migt}X_{migt\omega}$$
$$+ \sum_{b\in\mathcal{B}}\sum_{s\in\mathcal{S}}\sum_{n\in\mathcal{N}_{jk}}\sum_{(j,k)\in(\mathcal{J},\mathcal{K})} c_{mbsjkt}X_{mbsnjkt\omega} + \sum_{j\in\mathcal{J}\bigcup\mathcal{K}} h_{mjt}H_{mjt\omega}$$
$$+ \sum_{j\in\mathcal{J}} c^{o}_{jt}\left(\frac{\sum_{m\in\mathcal{M}}\sum_{b\in\mathcal{B}}\sum_{s\in\mathcal{S}}\sum_{n\in\mathcal{N}_{jk}}\sum_{k\in\mathcal{K}} X_{mbsnjkt\omega}}{\overline{c}_{jt} - \sum_{m\in\mathcal{M}}\sum_{b\in\mathcal{B}}\sum_{s\in\mathcal{S}}\sum_{n\in\mathcal{N}_{jk}}\sum_{k\in\mathcal{K}} X_{mbsnjkt\omega}}\right) +$$
$$\sum_{k\in\mathcal{K}} c^{o}_{kt}\left(\frac{\sum_{m\in\mathcal{M}}\sum_{g\in\mathcal{G}} X_{mkgt\omega}}{\overline{c}_{kt} - \sum_{m\in\mathcal{M}}\sum_{g\in\mathcal{G}} X_{mkgt\omega}}\right) + \sum_{g\in\mathcal{G}} \pi_{mgt}U_{mgt\omega}\Bigg) \quad (3.12)$$

subject to

$$\sum_{j\in\mathcal{J}_i} X_{mijt\omega} + \sum_{g\in\mathcal{G}_i} X_{migt\omega} \leq \varphi_{mit\omega}\forall m\in\mathcal{M}, i\in\mathcal{I}, t\in\mathcal{T}, \omega\in\Omega \quad (3.13)$$

$$\sum_{i\in\mathcal{I}_j} X_{mijt\omega} + (1-\alpha_m)H_{mj,t-1,\omega} = \sum_{b\in\mathcal{B}}\sum_{s\in\mathcal{S}}\sum_{n\in\mathcal{N}_{jk}}\sum_{k\in\mathcal{K}_j} X_{mbsnjkt\omega} + H_{mjt\omega}$$
$$\forall m\in\mathcal{M}, j\in\mathcal{J}, t\in\mathcal{T}, \omega\in\Omega \quad (3.14)$$

$$\sum_{b\in\mathcal{B}}\sum_{s\in\mathcal{S}}\sum_{n\in\mathcal{N}_{jk}}\sum_{j\in\mathcal{J}_k} X_{mbsnjkt\omega} = \sum_{g\in\mathcal{G}_k} X_{mkgt\omega} + H_{mkt\omega} - (1-\alpha_m)H_{mk,t-1,\omega}$$
$$\forall m\in\mathcal{M}, k\in\mathcal{K}, t\in\mathcal{T}, \omega\in\Omega \quad (3.15)$$

$$\sum_{i\in\mathcal{I}_g} X_{migt\omega} + \sum_{k\in\mathcal{K}_g} X_{mkgt\omega} + U_{mgt\omega} = d_{mgt}\forall m\in\mathcal{M}, g\in\mathcal{G}, t\in\mathcal{T}, \omega\in\Omega \quad (3.16)$$

$$\sum_{m\in\mathcal{M}} H_{mjt\omega} \leq \overline{h}_j\forall j\in\mathcal{J}\bigcup\mathcal{K}, t\in\mathcal{T}, \omega\in\Omega \quad (3.17)$$

$$\sum_{n\in\mathcal{N}_{jk}} X_{mbsnjkt\omega} \leq min\{\overline{w}_{jkt\omega}, \overline{w}_b\}Y_{mbsjt}\forall m\in\mathcal{M}, b\in\mathcal{B},$$
$$s\in\mathcal{S}, j\in\mathcal{J}, k\in\mathcal{K}_j, t\in\mathcal{T}, \omega\in\Omega \quad (3.18)$$

$$\sum_{n\in\mathcal{N}_{jk}}\sum_{k\in\mathcal{K}_j}\left(\frac{X_{mbsnjkt\omega}}{\rho_m}\right) \leq v_bY_{mbsjt}\forall m\in\mathcal{M}, b\in\mathcal{B}, s\in\mathcal{S},$$
$$j\in\mathcal{J}, t\in\mathcal{T}, \omega\in\Omega \quad (3.19)$$

$$\sum_{m\in\mathcal{M}}\sum_{b\in\mathcal{B}}\sum_{s\in\mathcal{S}}\sum_{n\in\mathcal{N}_{jk}}\sum_{k\in\mathcal{K}_j} X_{mbsnjkt\omega} \leq \overline{c}_{jt} \forall j \in \mathcal{J}, t \in \mathcal{T}, \omega \in \Omega \quad (3.20)$$

$$\sum_{m\in\mathcal{M}}\sum_{g\in\mathcal{G}_k} X_{mkgt\omega} \leq \overline{c}_{kt} \forall k \in \mathcal{K}, t \in \mathcal{T}, \omega \in \Omega \quad (3.21)$$

$$X_{migt\omega}, X_{mjkbsnt\omega}, X_{mkgt\omega}, H_{mjt\omega}, H_{mkt\omega}, U_{mgt\omega} \in \mathbb{R}^{+} \quad (3.22)$$

The objective function (3.1) is the sum of the first-stage costs and the expected second-stage costs. The first-stage costs represent the fixed costs associated with using towboats and loading and unloading commodities into the barges. Constraints (3.2) ensure that only one commodity of type $m \in \mathcal{M}$ can be loaded to a given barge $b \in \mathcal{B}$ in time period $t \in \mathcal{T}$. Constraints (3.3) restrict the usage of only one towboat of type $s \in \mathcal{S}$ in a given trip $n \in \mathcal{N}_{jk}$ between each origin-destination pair at time period $t \in \mathcal{T}$. Constraints (3.4) set restriction on the minimum ($\underline{\delta}_s$) and maximum ($\overline{\delta}_s$) number of barges that can be connected with a given towboat $s \in \mathcal{S}$. Constraints (3.5) restrict the maximum number of possible trips (τ_{jkt}) between each origin-destination port $(j,k) \in (\mathcal{J},\mathcal{K})$ in a given time period $t \in \mathcal{T}$. Constraints (3.6) indicate the maximum availability of barges (θ_{jt}) in a given port $j \in \mathcal{J}$ at time period $t \in \mathcal{T}$. The unavailability of towboat and barge, primarily due to periodic maintenance activities, are captured by binary parameters a_{sjt} and a_{bjt} in constraints (3.7) and (3.8). Constraints (3.9) restrict the maximum time availability ($\bar{t}_{jk}$) for a towboat $s \in \mathcal{S}$ to travel between each origin-destination port $(j,k) \in (\mathcal{J},\mathcal{K})$ in a given time period $t \in \mathcal{T}$. Finally, constraints (3.10) and (3.11) set the integrality constraints.

The objective function of the second-stage costs consists of seven terms: the first three terms represent the transportation costs of flowing commodities across the entire network; the fourth and fifth terms represent respectively the cost associated with storing commodities at the source and destination ports and commodity shortage costs at the markets; finally, the last two terms in the objective function capture the congestion cost at the source and destination ports. Constraints (3.13) restrict the availability ($\varphi_{mit\omega}$) of commodity $m \in \mathcal{M}$ at a supply site $i \in \mathcal{I}$ in time period $t \in \mathcal{T}$ under scenario $\omega \in \Omega$. Constraints (3.14) and (3.15) are the flow balance constraints which ensure that at a given time $t \in \mathcal{T}$, commodity $m \in \mathcal{M}$ can be either stored or transported in a source or a destination port $j \in \mathcal{J} \bigcup \mathcal{K}$. Constraints (3.16) ensure that at a given time period $t \in \mathcal{T}$, the demand (d_{mgt}) for commodity $m \in \mathcal{M}$ can be satisfied either through the inland waterway transportation network or through an external supply source via paying a higher penalty cost of π_{mgt}. Constraints (3.17) set the storage capacity of a port $j \in \mathcal{J} \bigcup \mathcal{K}$ to $\overline{h}_j$. Constraints (3.18) and (3.19) handle the weight and volumetric capacity restriction for a barge $b \in \mathcal{B}$. Note that the dredging impact is captured via constraints (3.18) where it is shown that at each time period $t \in \mathcal{T}$, a barge $b \in \mathcal{B}$ is restricted to carry the minimum of $\{\overline{w}_{jkt\omega}, \overline{w}_b\}$ amount of commodity between each source-destination pair. Constraints (3.20) and (3.21) set commodity processing capacity of port $j \in \mathcal{J} \bigcup \mathcal{K}$ at time period $t \in \mathcal{T}$. Finally, constraints (3.22) are the standard non-negativity constraints.

3.3.1 Linear Reformulation

The presence of congestion terms in the objective function (3.12) makes the model **[IPM]** nonlinear. To linearize these nonlinear congestion terms, we adopt the linearization technique introduced by Elhedhli and Wu [34]. This subsection illustrates the step by step linearization process of the first congestion term in (3.12). Let us first introduce a non-negative auxiliary variable $\mathbf{R} := \{R_{jt\omega}\}_{j\in\mathcal{J},t\in\mathcal{T},\omega\in\Omega}$ such that:

$$R_{jt\omega} = \left(\frac{\sum_{m\in\mathcal{M}} \sum_{b\in\mathcal{B}} \sum_{s\in\mathcal{S}} \sum_{n\in\mathcal{N}_{jk}} \sum_{k\in\mathcal{K}} X_{mbsnjkt\omega}}{\bar{c}_{jt} - \sum_{m\in\mathcal{M}} \sum_{b\in\mathcal{B}} \sum_{s\in\mathcal{S}} \sum_{n\in\mathcal{N}_{jk}} \sum_{k\in\mathcal{K}} X_{mbsnjkt\omega}} \right) \forall j \in \mathcal{J}, t \in \mathcal{T}, \omega \in \Omega \quad (3.23)$$

The terms in constraints (3.23) can be rearranged as follows:

$$\sum_{m\in\mathcal{M}} \sum_{b\in\mathcal{B}} \sum_{s\in\mathcal{S}} \sum_{n\in\mathcal{N}_{jk}} \sum_{k\in\mathcal{K}} X_{mbsnjkt\omega} = \left(\frac{R_{jt\omega}}{1 + R_{jt\omega}} \right) \bar{c}_{jt} \forall j \in \mathcal{J}, t \in \mathcal{T}, \omega \in \Omega \quad (3.24)$$

Lemma 1 *The function* $f(R_{jt\omega}) := \left(\frac{R_{jt\omega}}{1 + R_{jt\omega}} \right)$ *is concave in* $R_{jt\omega} \in [0, \infty)$.

Proof: Differentiating function $f(R_{jt\omega})$ with respect to $\{R_{jt\omega}\}_{j\in\mathcal{J},t\in\mathcal{T},\omega\in\Omega}$, we obtain the following first and second derivatives:

$$f'(R_{jt\omega}) = \frac{\delta}{\delta R_{jt\omega}} \left(\frac{R_{jt\omega}}{1 + R_{jt\omega}} \right) = \frac{1}{(1 + R_{jt\omega})^2} \geq 0$$

$$f''(R_{jt\omega}) = \frac{\delta^2}{\delta R_{jt\omega}^2} \left(\frac{R_{jt\omega}}{1 + R_{jt\omega}} \right) = \frac{-2}{(1 + R_{jt\omega})^3} \leq 0$$

Since the first derivative is positive and the second one is negative, we can conclude that the function $f(R_{jt\omega})$ is concave in $R_{jt\omega} \in [0, \infty]$ ∎

Lemma 1 proves that the function $f(R_{jt\omega})$ is concave. Note that this function can be outer approximated by a set of tangent cutting planes, denoted by set $\mathcal{P}^1$. For

a given set of points $p_1 \in \mathcal{P}^1$, we outer approximate the function $f(R_{jt\omega})$ using Taylor series approximation and by a set of piecewise linear functions that are tangent to $f(R_{jt\omega})$ at points $\{R^{p_1}_{jt\omega}\}_{p_1 \in \mathcal{H}^1}$ as follows:

$$\begin{aligned} f(R_{jt\omega}) &\approx f(R^{p_1}_{jt\omega}) + f'(R^{p_1}_{jt\omega})(R_{jt\omega} - R^{p_1}_{jt\omega}) \\ &\approx \frac{R_{jt\omega}}{(1+R^{p_1}_{jt\omega})^2} + \frac{(R^{p_1}_{jt\omega})^2}{(1+R^{p_1}_{jt\omega})^2} \end{aligned}$$

since $f(R_{jt\omega})$ is concave in $R_{jt\omega} \in [0, \infty]$, the function can be expressed as follows:

$$\frac{R_{jt\omega}}{(1+R_{jt\omega})} = \min_{p_1 \in \mathcal{P}^1} \left\{ \frac{R_{jt\omega}}{(1+R^{p_1}_{jt\omega})^2} + \frac{(R^{p_1}_{jt\omega})^2}{(1+R^{p_1}_{jt\omega})^2} \right\}$$

This is equivalent to the following set of constraints :

$$\frac{R_{jt\omega}}{(1+R_{jt\omega})} \leq \frac{R_{jt\omega}}{(1+R^{p_1}_{jt\omega})^2} + \frac{(R^{p_1}_{jt\omega})^2}{(1+R^{p_1}_{jt\omega})^2} \tag{3.25}$$

where $\{R^{p_1}_{jt\omega}\}_{j \in \mathcal{J}, t \in \mathcal{T}, \omega \in \Omega}$ are the set of points used for approximating (3.25). We now derive constraints (3.26) from constraints (3.24) and (3.25) which are added to model **[IPM]** for linearizing the first congestion function in objective (3.12).

$$\sum_{m \in \mathcal{M}} \sum_{b \in \mathcal{B}} \sum_{s \in \mathcal{S}} \sum_{n \in \mathcal{N}_{jk}} \sum_{k \in \mathcal{K}} X_{mbsnjkt\omega} \leq \left(\frac{R_{jt\omega}}{(1+R^{p_1}_{jt\omega})^2} \right) \bar{c}_{jt} + \left(\frac{R^{p_1}_{jt\omega}}{1+R^{p_1}_{jt\omega}} \right)^2 \bar{c}_{jt} \tag{3.26}$$

$$\forall j \in \mathcal{J}, t \in \mathcal{T}, \omega \in \Omega, p_1 \in \mathcal{P}^1$$

$$R_{jt\omega} \in \mathbb{R}^+ \quad \forall j \in \mathcal{J}, t \in \mathcal{T}, \omega \in \Omega \tag{3.27}$$

Following the same approach, we can introduce another non-negative auxiliary variable $\mathbf{W} := \{W_{kt\omega}\}_{k \in \mathcal{K}, t \in \mathcal{T}, \omega \in \Omega}$ for the second congestion term in objective (3.12). Likewise, constraints (3.28) and (3.29) are added to model **[IPM]** for lin-

earizing the second congestion term in objective (3.12) where $\{W^{p_2}_{kt\omega}\}_{k\in\mathcal{K},t\in\mathcal{T},\omega\in\Omega,p_2\in\mathcal{P}^2}$ are the set of points used for approximating (3.28).

$$\sum_{m\in\mathcal{M}}\sum_{g\in\mathcal{G}} X_{mkgt\omega} \leq \left(\frac{W_{kt\omega}}{(1+W^{p_2}_{kt\omega})^2}\right)\bar{c}_{kt} + \left(\frac{W^{p_2}_{kt\omega}}{1+W^{p_2}_{kt\omega}}\right)^2 \bar{c}_{kt} \quad \forall k\in\mathcal{K}, t\in\mathcal{T}, \omega\in\Omega, p_2\in\mathcal{P}^2 \tag{3.28}$$

$$W_{kt\omega} \in \mathbb{R}^+ \forall k\in\mathcal{K}, t\in\mathcal{T}, \omega\in\Omega \tag{3.29}$$

Model **[IPM]** can now be linearized as follows, referred to as **[LIPM]**:

$$\textbf{[LIPM]} \quad \underset{\mathbf{Y}}{Minimize} \sum_{s\in\mathcal{S}}\sum_{j\in\mathcal{J}}\sum_{t\in\mathcal{T}}\left(\sum_{n\in\mathcal{N}_{jk}}\sum_{k\in\mathcal{K}_j}\psi_{st}Y_{snjkt} + \sum_{m\in\mathcal{M}}\sum_{b\in\mathcal{B}}\eta_{mbt}Y_{mbsjt}\right) + \sum_{\omega\in\Omega}\rho_\omega \mathbb{Q}(\mathbf{Y},\zeta^\omega)$$

subject to (3.2)- (3.11) and with $\mathbb{Q}(\mathbf{Y},\zeta^\omega)$ being the solution of the following linearized second-stage problem:

$$\begin{aligned}\mathbb{Q}(\mathbf{Y},\zeta^\omega) = \quad & \underset{\mathbf{X,H,U}}{Minimize} \sum_{t\in\mathcal{T}}\Bigg(\sum_{(e,f)\in(\mathcal{I}\bigcup\mathcal{K},\mathcal{J}\bigcup\mathcal{G})} c_{meft}X_{meft\omega} + \sum_{(i,g)\in(\mathcal{I},\mathcal{G})} c_{migt}X_{migt\omega} \\ & + \sum_{b\in\mathcal{B}}\sum_{s\in\mathcal{S}}\sum_{n\in\mathcal{N}_{jk}}\sum_{(j,k)\in(\mathcal{J},\mathcal{K})} c_{mbsjkt}X_{mbsnjkt\omega} + \sum_{j\in\mathcal{J}\bigcup\mathcal{K}} h_{mjt}H_{mjt\omega} \\ & + \sum_{g\in\mathcal{G}}\pi_{mgt}U_{mgt\omega} + \sum_{j\in\mathcal{J}} c^o_{jt}R_{jt\omega} + \sum_{k\in\mathcal{K}} c^o_{kt}W_{kt\omega}\Bigg)\end{aligned} \tag{3.30}$$

subject to (3.13)-(3.22) and (3.26)-(3.29). We further denote **[LIPM]** as **[LIPM]**$(\mathcal{P}^1,\mathcal{P}^2)$ where it can be shown below in **Proposition 1** that there exist at least one $p^1\in\mathcal{P}^1$ and one $p^2\in\mathcal{P}^2$ for which constraints (3.26) and (3.28) can be solved at equality.

Proposition 1: *There exists at least one constraint in* (3.26) *and one in* (3.28) *for which model* ***[LIPM]***$(\mathcal{P}^1,\mathcal{P}^2)$ *will be binding at optimality.*

Proof: We first prove that $\exists p_1 \in \mathcal{P}^1$ in (3.26) for which **[LIPM]**$(\mathcal{P}^1, \mathcal{P}^2)$ will be binding at optimality. Likewise, one can similarly prove that $\exists p_2 \in \mathcal{P}^2$ in (3.28) for which **[LIPM]**$(\mathcal{P}^1, \mathcal{P}^2)$ will also be binding at optimality. After rearranging the terms, constraints (3.26) can be rewritten as follows:

$$R_{jt\omega} \geq (1 + R_{jt\omega}^{p_1})^2 \left(\frac{\sum_{m \in \mathcal{M}} \sum_{b \in \mathcal{B}} \sum_{s \in \mathcal{S}} \sum_{n \in \mathcal{N}_{jk}} \sum_{k \in \mathcal{K}} X_{mjkbsnt\omega}}{\overline{c}_{jt}} \right) - (R_{jt\omega}^{p_1})^2$$
$$\forall j \in \mathcal{J}, t \in \mathcal{T}, \omega \in \Omega, p_1 \in \mathcal{P}^1 \quad (3.31)$$

Since $\{R_{jt\omega}\}_{j \in \mathcal{J}, t \in \mathcal{T}, \omega \in \Omega}$ holds positive coefficient in the objective function (3.30), **[LIPM]**$(\mathcal{P}^1, \mathcal{P}^2)$ only reaches to an optimum value when $R_{jt\omega}$ is minimized. This indicates that $\forall j \in \mathcal{J}, t \in \mathcal{T}, \omega \in \Omega, \exists p_1 \in \mathcal{P}^1$ for which (3.31) holds with equality if $(1 + R_{jt\omega}^{p_1})^2 \left(\frac{\sum_{m \in \mathcal{M}} \sum_{b \in \mathcal{B}} \sum_{s \in \mathcal{S}} \sum_{n \in \mathcal{N}_{jk}} \sum_{k \in \mathcal{K}} X_{mjkbsnt\omega}}{\overline{c}_{jt}} \right) - (R_{jt\omega}^{p_1})^2 \geq 0$, else $R_{jt\omega} = 0$. Let $\varrho_{jt\omega}$ be the average utilization of port $j \in \mathcal{J}$ which can be defined as follows:

$$\varrho_{jt\omega} := \left(\frac{\sum_{m \in \mathcal{M}} \sum_{b \in \mathcal{B}} \sum_{s \in \mathcal{S}} \sum_{n \in \mathcal{N}_{jk}} \sum_{k \in \mathcal{K}} X_{mjkbsnt\omega}}{\overline{c}_{jt}} \right)$$

The above inequalities can be expanded in further as follows:

$$\begin{aligned} 0 &\leq (1 + R_{jt\omega}^{p_1})^2 \left(\frac{\sum_{m \in \mathcal{M}} \sum_{b \in \mathcal{B}} \sum_{s \in \mathcal{S}} \sum_{n \in \mathcal{N}_{jk}} \sum_{k \in \mathcal{K}} X_{mjkbsnt\omega}}{\overline{c}_{jt}} \right) - (R_{jt\omega}^{p_1})^2 \\ &= (1 + R_{jt\omega}^{p_1})^2 \varrho_{jt\omega} - (R_{jt\omega}^{p_1})^2 \\ &= (\varrho_{jt\omega} - 1)(R_{jt\omega}^{p_1})^2 + 2\varrho_{jt\omega} R_{jt\omega}^{p_1} - \varrho_{jt\omega} \end{aligned}$$

Applying quadratic equation rule, we see that $R^{p_1}_{jt\omega}$ can be bounded as follows:

$R^{p_1}_{jt\omega} \in$
$\left[\frac{-\varrho_{jt\omega} - \sqrt{\varrho_{jt\omega}}}{1-\varrho_{jt\omega}}, \frac{\varrho_{jt\omega} + \sqrt{\varrho_{jt\omega}}}{1-\varrho_{jt\omega}}\right] \forall p_1 \in \mathcal{P}^1.$

For $0 < \varrho_{jt\omega} < 1$, the term $\left(\frac{-\varrho_{jt\omega} - \sqrt{\varrho_{jt\omega}}}{1-\varrho_{jt\omega}}\right)$ will yield a negative value; hence, the model will turn out to be *infeasible*. Therefore, without any loss of generality, we can then write $R^{p_1}_{jt\omega} \in \left[0, \frac{\varrho_{jt\omega} + \sqrt{\varrho_{jt\omega}}}{1-\varrho_{jt\omega}}\right]; \forall p_1 \in \mathcal{P}^1$. Further, to prove that $\exists p_1 \in \mathcal{P}^1$ for which (3.26) holds with equality, we then need to show that $R^{p_1}_{jt\omega} \in \left[0, \frac{\varrho_{jt\omega} + \sqrt{\varrho_{jt\omega}}}{1-\varrho_{jt\omega}}\right]$. Note that if $R_{jt\omega}$ becomes positive via constraints (3.18) and (3.23), then we can write the following:

$$0 \leq R^{p_1}_{jt\omega} \approx R_{jt\omega} = \frac{\varrho_{jt\omega}}{1-\varrho_{jt\omega}} \leq \frac{\varrho_{jt\omega} + \sqrt{\varrho_{jt\omega}}}{1-\varrho_{jt\omega}}$$

This proves that $\forall j \in \mathcal{J}, t \in \mathcal{T}, \omega \in \Omega, \exists p_1 \in \mathcal{P}^1$ for which, at optimality, (3.26) holds with equality. ∎

3.4 Solution Approach

By setting $|\Omega| = |\mathcal{T}| = |\mathcal{N}_{jk}| = |\mathcal{S}| = |\mathcal{B}| = 1$, it can be shown that the reformulated model **[LIPM]** is essentially a variation of the *fixed charge network flow problem* which is already known to be an $\mathcal{NP}$-hard problem [12, 65]. Therefore, state-of-the-art commercial solvers (e.g., Gurobi, CPLEX) will find it difficulty to solve large instances of **[LIPM]**, as we also experienced in our computational results discussed in Section 5.5.3. To alleviate this computational challenge, we propose a parallelized hybrid decomposition algorithm based on *constraint generation* algorithm embedded with a *sample average approximation* algorithm and a *modified*

L-shaped algorithm, in order to solve the model to optimum (or near-optimum) in a reasonable timeframe.

3.4.1 Constraint Generation Algorithm

Model **[LIPM]** generates a pool of constraints given by the equations (3.26) and (3.28). Evaluating the model by considering all these constraints at a time can be considered extremely challenging. Therefore, we introduce the *constraint generation* (CG) algorithm [153, 143] that can efficiently and effectively solve model **[LIPM]** despite being generating large number of constraints at once. Essentially, the algorithm starts by solving model **[LIPM]** with a subset of constraints obtained from equations (3.26) and (3.28) while additional constraints are added to **[LIPM]** per requirement. The algorithm terminates upon reaching the optimality gap to an acceptable threshold limit. In case if the termination criterion is not met, a new set of constraints are generated and added to **[LIPM]** and the process continues. The algorithm is detailed as follows:

Let ν**[LIPM]** be the objective function value of problem **[LIPM]** and $(\mathbf{Y}^q, \mathbf{X}^q, \mathbf{H}^q, \mathbf{U}^q)$ be it's optimal solution. For any iteration q, we let LB^q and UB^q to represent the lower and upper bound of the original problem **[IPM]**. We can then obtain the *lower* and *upper* bound of the optimal objective function value of problem **[IPM]** as follows:

$$
\begin{aligned}
LB^q &= \nu\textbf{[LIPM]}(\mathcal{P}_1^q, \mathcal{P}_2^q) \\
&= \sum_{t\in\mathcal{T}}\Bigg\{\sum_{s\in\mathcal{S}}\sum_{j\in\mathcal{J}}\Bigg(\sum_{n\in\mathcal{N}_{jk}}\sum_{k\in\mathcal{K}_j}\psi_{st}Y_{snjkt} + \sum_{m\in\mathcal{M}}\sum_{b\in\mathcal{B}}\eta_{mbt}Y_{mbsjt}\Bigg) \\
&\quad + \sum_{\omega\in\Omega}\rho_\omega\Bigg(\sum_{(e,f)\in(\mathcal{I}\bigcup\mathcal{K},\mathcal{J}\bigcup\mathcal{G})} c_{meft}X_{meft\omega} + \sum_{(i,g)\in(\mathcal{I},\mathcal{G})} c_{migt}X_{migt\omega} \\
&\quad + \sum_{b\in\mathcal{B}}\sum_{s\in\mathcal{S}}\sum_{n\in\mathcal{N}_{jk}}\sum_{(j,k)\in(\mathcal{J},\mathcal{K})} c_{mbsjkt}X_{mbsnjkt\omega} + \sum_{j\in\mathcal{J}\bigcup\mathcal{K}} h_{mjt}H_{mjt\omega} \\
&\quad + \sum_{g\in\mathcal{G}}\pi_{mgt}U_{mgt\omega} + \sum_{j\in\mathcal{J}} c^o_{jt}R_{jt\omega} + \sum_{k\in\mathcal{K}} c^o_{kt}W_{kt\omega}\Bigg)\Bigg\}
\end{aligned} \tag{3.32}
$$

$$
\begin{aligned}
UB^q &= \sum_{t\in\mathcal{T}}\Bigg\{\sum_{s\in\mathcal{S}}\sum_{j\in\mathcal{J}}\Bigg(\sum_{n\in\mathcal{N}_{jk}}\sum_{k\in\mathcal{K}_j}\psi_{st}Y_{snjkt} + \sum_{m\in\mathcal{M}}\sum_{b\in\mathcal{B}}\eta_{mbt}Y_{mbsjt}\Bigg) + \sum_{\omega\in\Omega}\rho_\omega\Bigg(\\
&\quad \sum_{(e,f)\in(\mathcal{I}\bigcup\mathcal{K},\mathcal{J}\bigcup\mathcal{G})} c_{meft}X_{meft\omega} + \sum_{(i,g)\in(\mathcal{I},\mathcal{G})} c_{migt}X_{migt\omega} + \\
&\quad \sum_{b\in\mathcal{B}}\sum_{s\in\mathcal{S}}\sum_{n\in\mathcal{N}_{jk}}\sum_{(j,k)\in(\mathcal{J},\mathcal{K})} c_{mbsjkt}X_{mbsnjkt\omega} + \sum_{j\in\mathcal{J}\bigcup\mathcal{K}} h_{mjt}H_{mjt\omega} + \sum_{g\in\mathcal{G}}\pi_{mgt}U_{mgt\omega} \\
&\quad + \sum_{j\in\mathcal{J}} c^o_{jt}\Bigg(\frac{\sum_{m\in\mathcal{M}}\sum_{b\in\mathcal{B}}\sum_{s\in\mathcal{S}}\sum_{n\in\mathcal{N}_{jk}}\sum_{k\in\mathcal{K}}X_{mbsnjkt\omega}}{\bar{c}_{jt} - \sum_{m\in\mathcal{M}}\sum_{b\in\mathcal{B}}\sum_{s\in\mathcal{S}}\sum_{n\in\mathcal{N}_{jk}}\sum_{k\in\mathcal{K}}X_{mbsnjkt\omega}}\Bigg) \\
&\quad + \sum_{k\in\mathcal{K}} c^o_{kt}\Bigg(\frac{\sum_{m\in\mathcal{M}}\sum_{g\in\mathcal{G}}X_{mkgt\omega}}{\bar{c}_{kt} - \sum_{m\in\mathcal{M}}\sum_{g\in\mathcal{G}}X_{mkgt\omega}}\Bigg)\Bigg)\Bigg\}
\end{aligned} \tag{3.33}
$$

The validity of the lower and upper bound, provided by equations (3.32) and (3.33), are given below in **Proposition 2** and **Proposition 3**.

Proposition 2 *For any given subset of points* $\{R^{p_1}_{jt\omega}\}_{\mathcal{P}_1^q\subset\mathcal{P}^1}$ *and* $\{W^{p_2}_{kt\omega}\}_{\mathcal{P}_2^q\subset\mathcal{P}^2}$, (3.32) *provides the lower bound of the optimal objective function value of* **[IPM]**.

Proof: Since **[LIPM]**$(\mathcal{P}_1^q, \mathcal{P}_2^q)$ is the relaxed version of problem **[LIPM]**, ν**[LIPM]**$(\mathcal{P}_1^q, \mathcal{P}_2^q)$ provides a valid lower bound to the optimal objective function value of problem

[LIPM]. Let ν**[LIPM]** and ν**[IPM]** to be the optimal objective function value obtained from solving **[LIPM]** and **[IPM]**, respectively. Therefore, we can state that ν**[LIPM]**$(\mathcal{P}_1^q, \mathcal{P}_2^q) \leq \nu$**[LIPM]**. Now, **[LIPM]** itself is an approximation of problem **[IPM]** which implies that ν**[LIPM]**$(\mathcal{P}_1^q, \mathcal{P}_2^q)$ will also serve as a valid lower bound of the optimal objective of the original problem **[IPM]**. Therefore, we see that the following relationship holds: ν**[LIPM]**$(\mathcal{P}_1^q, \mathcal{P}_2^q) \leq \nu$**[LIPM]**$\leq \nu$**[IPM]**. ■

Proposition 3 *For any given subset of points* $\{R_{jt\omega}^{p_1}\}_{\mathcal{P}_1^q \subset \mathcal{P}^1}$ *and* $\{W_{kt\omega}^{p_2}\}_{\mathcal{P}_2^q \subset \mathcal{P}^2}$, (3.33) *provides the upper bound of the optimal objective function value of* **[IPM]**.

Proof: Problem **[LIPM]**$(\mathcal{P}_1^q, \mathcal{P}_2^q)$ includes all the constraints of original problem **[IPM]**; therefore, any solution feasible to **[LIPM]**$(\mathcal{P}_1^q, \mathcal{P}_2^q)$ will also be a feasible solution to **[IPM]**. This implies that the objective function value of **[LIPM]** (i.e., ν**[LIPM]**), evaluated at $(\mathbf{Y}^q, \mathbf{X}^q, \mathbf{H}^q, \mathbf{U}^q)$ (shown in (3.33)), provides an upper bound to the optimal objective value of problem **[IPM]**. This completes the proof. ■

At the beginning of the CG algorithm subsets $\mathcal{P}_1^q \subset \mathcal{P}^1$ and $\mathcal{P}_2^q \subset \mathcal{P}^2$ of cuts are generated where $\mathcal{P}_1^{q=1}$ and $\mathcal{P}_2^{q=1}$ can be empty or may contain some chosen initial points. Let $\{R_{jt\omega}^{p_1}\}_{\mathcal{P}_1^q \subset \mathcal{P}^1}$ and $\{W_{kt\omega}^{p_2}\}_{\mathcal{P}_2^q \subset \mathcal{P}^2}$ be the initial set of points in $\mathcal{P}_1^q \subset \mathcal{P}^1$ and $\mathcal{P}_2^q \subset \mathcal{P}^2$, respectively. These points are used to generate initial subset of cuts that are essentially used to approximate the congestion functions $f(R_{jt\omega})$ and $f(W_{kt\omega})$, respectively. Having these cuts, the resulting solution of the problem **[LIMP]** provides a valid lower bound (LB^q) of the original problem **[IMP]** (proof can be found in **Proposition 1**). Next, this solution is utilized in equation (3.33) to obtain an upper bound (UB^q) (proof can be found in **Proposition 2**) of the CG

algorithm. The algorithm terminates when the gap between the UB^q and LB^q falls below a prespecified threshold limit ϵ. If the termination criterion is not met, we generate new sets of points $\{R_{jt\omega}^{p_{new}}\}$ and $\{W_{kt\omega}^{p_{new}}\}$ utilizing the current solution as follows:

$$R_{jt\omega}^{p_{new}} = \frac{\sum_{m\in\mathcal{M}}\sum_{b\in\mathcal{B}}\sum_{s\in\mathcal{S}}\sum_{n\in\mathcal{N}_{jk}}\sum_{k\in\mathcal{K}} X_{mbsnjkt\omega}^{q}}{\bar{c}_{jt} - \sum_{m\in\mathcal{M}}\sum_{b\in\mathcal{B}}\sum_{s\in\mathcal{S}}\sum_{n\in\mathcal{N}_{jk}}\sum_{k\in\mathcal{K}} X_{mbsnjkt\omega}^{q}}$$

and

$$W_{kt\omega}^{p_{new}} = \frac{\sum_{m\in\mathcal{M}}\sum_{g\in\mathcal{G}} X_{mkgt\omega}^{q}}{\bar{c}_{kt} - \sum_{m\in\mathcal{M}}\sum_{g\in\mathcal{G}} X_{mkgt\omega}^{q}}$$

The pseudo-code of the CG algorithm is given in **Algorithm 1**.

Algorithm 1: Constraint Generation Algorithm

Initialize, $q \leftarrow 1$, ϵ, $UB^q \leftarrow +\infty$, $LB^q \leftarrow -\infty$

$terminate \leftarrow false$

Choose an initial set of points $\{R^{p_1}_{jt\omega}\}_{\mathcal{P}^q_1 \subset \mathcal{P}^1}$ and $\{W^{p_2}_{kt\omega}\}_{\mathcal{P}^q_2 \subset \mathcal{P}^2}$

while $terminate =$ ***false*** **do**

Solve **[LIPM]**$(\mathcal{P}^q_1, \mathcal{P}^q_2)$ to obtain ν**[LIPM]** $(\mathcal{P}^q_1, \mathcal{P}^q_2)$ and $(\mathbf{Y}^q, \mathbf{X}^q, \mathbf{H}^q, \mathbf{U}^q)$

Update the lower bound: $LB^q \leftarrow \nu$**[LIPM]** $(\mathcal{P}^q_1, \mathcal{P}^q_2)$

Update the upper bound: UB^q using equation (3.33)

if $\frac{(UB^q - LB^q)}{UB^q} \leq \epsilon$ **then**

$terminate \leftarrow$ **true**

else

Generate new points:

$$R^{p_{new}}_{jt\omega} = \frac{\sum_{m\in\mathcal{M}} \sum_{b\in\mathcal{B}} \sum_{s\in\mathcal{S}} \sum_{n\in\mathcal{N}_{jk}} \sum_{k\in\mathcal{K}} X^q_{mbsnjkt\omega}}{\bar{c}_{jt} - \sum_{m\in\mathcal{M}} \sum_{b\in\mathcal{B}} \sum_{s\in\mathcal{S}} \sum_{n\in\mathcal{N}_{jk}} \sum_{k\in\mathcal{K}} X^q_{mbsnjkt\omega}}$$

$$W^{p_{new}}_{kt\omega} = \frac{\sum_{m\in\mathcal{M}} \sum_{g\in\mathcal{G}} X^q_{mkgt\omega}}{\bar{c}_{kt} - \sum_{m\in\mathcal{M}} \sum_{g\in\mathcal{G}} X^q_{mkgt\omega}}$$

$$R^{p_1,q+1}_{jt\omega} = R^{p_1,q}_{jt\omega} \bigcup \{R^{p_{new}}_{jt\omega}\}$$

$$W^{p_2,q+1}_{kt\omega} = W^{p_2,q}_{kt\omega} \bigcup \{W^{p_{new}}_{kt\omega}\}$$

end

$q \leftarrow q + 1$

end

Proposition 4 *The proposed CG algorithm can be solved in a finite number of iterations.*

Proof: In model **[LIPM]**, variable $\{X_{mbsnjkt\omega}\}$ is bounded by constraints (3.18)-(3.20). This implies that the values of $\{R_{jt\omega}\}_{\forall j\in\mathcal{J}, t\in\mathcal{T}, \omega\in\Omega}$ will also be bounded,

essentially ensured via constraints (3.23). To prove that the CG algorithm is terminated in a finite number of iterations, we eventually need to show that the $\{R_{jt\omega}^{p_{new}}\}_{\forall j\in\mathcal{J},t\in\mathcal{T},\omega\in\Omega}$ values are not repeated in coming iterations. Let us define q as an intermediate iteration of the CG algorithm when $UB^q > LB^q$. If $(\mathbf{Y}^q, \mathbf{X}^q, \mathbf{H}^q, \mathbf{U}^q)$ be the solution to **[LIPM]**$(\mathcal{P}_1^q, \mathcal{P}_2^q)$, then the new point generated in this iteration would be:

$$R_{jt\omega}^{p_{new}} = \left(\frac{\sum_{m\in\mathcal{M}}\sum_{b\in\mathcal{B}}\sum_{s\in\mathcal{S}}\sum_{n\in\mathcal{N}_{jk}}\sum_{k\in\mathcal{K}} X_{mbsnjkt\omega}^q}{\bar{c}_{jt} - \sum_{m\in\mathcal{M}}\sum_{b\in\mathcal{B}}\sum_{s\in\mathcal{S}}\sum_{n\in\mathcal{N}_{jk}}\sum_{k\in\mathcal{K}} X_{mbsnjkt\omega}^q}\right) \quad \forall j\in\mathcal{J}, t\in\mathcal{T}, \omega\in\Omega$$

Now consider that the $\{R_{jt\omega}^{p_{new}}\}_{\forall j\in\mathcal{J},t\in\mathcal{T},\omega\in\Omega}$ values match with one of the values already generated in the prior iterations. The following relationship can be obtained from constraints (3.25):

$$\begin{aligned}
&\frac{R_{jt\omega}^{p_{new}}}{(1+R_{jt\omega}^{p_{new}})} \le \frac{1}{(1+R_{jt\omega}^{p_{new}})^2} R_{jt\omega}^q + \frac{(R_{jt\omega}^{p_{new}})^2}{(1+R_{jt\omega}^{p_{new}})^2} \\
\Rightarrow \quad & R_{jt\omega}^{p_{new}}(1+R_{jt\omega}^{p_{new}}) \le R_{jt\omega}^q + (R_{jt\omega}^{p_{new}})^2 \\
\Rightarrow \quad & R_{jt\omega}^{p_{new}} + (R_{jt\omega}^{p_{new}})^2 \le R_{jt\omega}^q + (R_{jt\omega}^{p_{new}})^2 \\
\Rightarrow \quad & R_{jt\omega}^{p_{new}} \le R_{jt\omega}^q
\end{aligned}$$

With this relationship, we will have the following:

$$\begin{aligned}
LB^q = \nu\textbf{[LIPM]}(\mathcal{P}_1^q, \mathcal{P}_2^q) &= \Xi + \sum_{t\in\mathcal{T}}\sum_{j\in\mathcal{J}}\sum_{\omega\in\Omega} c_{jt}^o R_{jt\omega}^q \ge \Xi + \sum_{t\in\mathcal{T}}\sum_{j\in\mathcal{J}} c_{jt}^o R_{jt\omega}^{p_{new}} \\
&= \Xi + \sum_{t\in\mathcal{T}}\sum_{j\in\mathcal{J}}\sum_{\omega\in\Omega} c_{jt}^o \left(\frac{\sum_{m\in\mathcal{M}}\sum_{b\in\mathcal{B}}\sum_{s\in\mathcal{S}}\sum_{n\in\mathcal{N}_{jk}}\sum_{k\in\mathcal{K}} X_{mbsnjkt\omega}}{\bar{c}_{jt} - \sum_{m\in\mathcal{M}}\sum_{b\in\mathcal{B}}\sum_{s\in\mathcal{S}}\sum_{n\in\mathcal{N}_{jk}}\sum_{k\in\mathcal{K}} X_{mbsnjkt\omega}}\right) \\
\ge \max\left\{UB^q, \Xi + \sum_{t\in\mathcal{T}}\sum_{j\in\mathcal{J}}\sum_{\omega\in\Omega} c_{jt}^o \left(\frac{\sum_{m\in\mathcal{M}}\sum_{b\in\mathcal{B}}\sum_{s\in\mathcal{S}}\sum_{n\in\mathcal{N}_{jk}}\sum_{k\in\mathcal{K}} X_{mbsnjkt\omega}}{\bar{c}_{jt} - \sum_{m\in\mathcal{M}}\sum_{b\in\mathcal{B}}\sum_{s\in\mathcal{S}}\sum_{n\in\mathcal{N}_{jk}}\sum_{k\in\mathcal{K}} X_{mbsnjkt\omega}}\right)\right\} \\
\ge UB^q
\end{aligned}$$

where

$$\Xi = \sum_{t\in\mathcal{T}}\Bigg(\sum_{s\in\mathcal{S}}\sum_{j\in\mathcal{J}}\Bigg(\sum_{n\in\mathcal{N}_{jk}}\sum_{k\in\mathcal{K}_j}\psi_{st}Y_{snjkt}+\sum_{m\in\mathcal{M}}\sum_{b\in\mathcal{B}}\eta_{mbt}Y_{mbsjt}\Bigg)+\sum_{\omega\in\Omega}\rho_\omega\Bigg(\sum_{(e,f)\in(\mathcal{I}\bigcup\mathcal{K},\mathcal{J}\bigcup\mathcal{G})} c_{meft}X_{meft\omega}+\sum_{(i,g)\in(\mathcal{I},\mathcal{G})}c_{migt}X_{migt\omega}+\sum_{b\in\mathcal{B}}\sum_{s\in\mathcal{S}}\sum_{n\in\mathcal{N}_{jk}}\sum_{(j,k)\in(\mathcal{J},\mathcal{K})}c_{mbsjkt}X_{mbsnjkt\omega}+\sum_{j\in\mathcal{J}\bigcup\mathcal{K}}h_{mjt}H_{mjt\omega}+\sum_{g\in\mathcal{G}}\pi_{mgt}U_{mgt\omega}+\sum_{k\in\mathcal{K}}c^o_{kt}W_{kt\omega}\Bigg)\Bigg)$$

This violates our initial assumption $UB^q > LB^q$. This implies for any given iteration q, at least one different $\{R^{p_1}_{jt\omega}\}$ is generated, meaning that the number of values taken by $\{R^{p_1}_{jt\omega}\}$ is finite. Likewise, we can prove that for any given iteration q, at least one different $\{W^{p_2}_{kt\omega}\}$ is generated and the number of values taken by $\{W^{p_2}_{kt\omega}\}$ is finite. This proves that the CG algorithm terminates in a finite number of iterations. ∎

3.4.2 Sample Average Approximation

Model ν**[LIPM]**$(\mathcal{P}^q_1,\mathcal{P}^q_2)$ considers the stochastic nature of supply availability of the agricultural products ($\varphi_{mit\omega}$) and waterlevel condition ($\overline{w}_{jkt\omega}$) that require the evaluation of a large number of scenarios to ensure the robustness of the solution. Solving model ν**[LIPM]**$(\mathcal{P}^q_1,\mathcal{P}^q_2)$ using CG algorithm for such a large number of scenarios is still considered challenging. To overcome this computational challenge and to solve model ν**[LIPM]**$(\mathcal{P}^q_1,\mathcal{P}^q_2)$ in a reasonable timeframe, we employ a sampling technique, commonly referred to as *Sample Average Approximation* (SAA) algorithm. This technique has widely used by many researchers in different application areas including logistic and supply chain design [119, 21, 120, 107, 108],

routing [142], production-routing [1], while [66], [92], [91], [75] discussed the statistical significance and convergence properties of this algorithm.

In SAA, random samples are generated and the expected value function is approximated by the corresponding sample average function. This process is continued until a pre-specified tolerance gap is achieved. Specifically, SAA selects a sample set $\{\omega_1, \omega_2, ..., \omega_{|\mathbb{O}|}\}$ of $\mathbb{O}$ scenarios from the set of all available scenarios Ω following a probability distribution $\mathbb{P}$. Then, the corresponding $\mathbb{O}$ scenario set problems are solved repeatedly until a pre-specified tolerance gap is achieved. The lower bound of the CG algorithm is now approximated by the following SAA problem.

$$
\begin{aligned}
LB^q &= \nu\textbf{[LIPM]}(\mathcal{P}_1^{q,\mathbb{O}}, \mathcal{P}_2^{q,\mathbb{O}}) \\
&= \sum_{t\in\mathcal{T}}\Bigg(\sum_{s\in\mathcal{S}}\sum_{j\in\mathcal{J}}\Bigg(\sum_{n\in\mathcal{N}_{jk}}\sum_{k\in\mathcal{K}_j}\psi_{st}Y_{snjkt} + \sum_{m\in\mathcal{M}}\sum_{b\in\mathcal{B}}\eta_{mbt}Y_{mbsjt}\Bigg) \\
&\quad + \frac{1}{|\mathbb{O}|}\sum_{o=1}^{\mathbb{O}}\Bigg(\sum_{(e,f)\in(\mathcal{I}\bigcup\mathcal{K},\mathcal{J}\bigcup\mathcal{G})} c_{meft}X_{mefto} + \sum_{(i,g)\in(\mathcal{I},\mathcal{G})} c_{migt}X_{migto} \\
&\quad + \sum_{b\in\mathcal{B}}\sum_{s\in\mathcal{S}}\sum_{n\in\mathcal{N}_{jk}}\sum_{(j,k)\in(\mathcal{J},\mathcal{K})} c_{mbsjkt}X_{mbsnjkto} + \sum_{j\in\mathcal{J}\bigcup\mathcal{K}} h_{mjt}H_{mjto} \\
&\quad + \sum_{g\in\mathcal{G}}\pi_{mgt}U_{mgto} + \sum_{j\in\mathcal{J}} c^o_{jt}R_{jto} + \sum_{k\in\mathcal{K}} c^o_{kt}W_{kto}\Bigg)\Bigg)
\end{aligned}
\tag{3.34}
$$

With the increase in size of $\mathbb{O}$, the optimal solution of **[LIPM]**$(\mathcal{P}_1^{q,\mathbb{O}}, \mathcal{P}_2^{q,\mathbb{O}})$ and the corresponding optimal objective value ν**[LIPM]**$(\mathcal{P}_1^{q,\mathbb{O}}, \mathcal{P}_2^{q,\mathbb{O}})$ converges with probability *one* to an optimal solution of the original problem **[IPM]** [66]. However, increasing the size of $\mathbb{O}$ significantly increases the computational time associated with solving problem **[LIPM]**$(\mathcal{P}_1^q, \mathcal{P}_2^q)$. In a nutshell, there exists a trade-off

between the achieved solution quality and the computational burden associated with solving the corresponding subproblems. We now summarize the steps involved in implementing the SAA technique for solving **[LIPM]**$(\mathcal{P}_1^q, \mathcal{P}_2^q)$ as follows:

1. Generate E independent supply and waterlevel scenarios of size $|\mathbb{O}|$ i.e., $\{\varphi_e^1(\omega), \varphi_e^2(\omega), ..., \varphi_e^{|\mathbb{O}|}(\omega)\}$ and $\{\overline{w}_e^1(\omega), \overline{w}_e^2(\omega), ..., \overline{w}_e^{|\mathbb{O}|}(\omega)\}$, $\forall e = 1, ..., E$ where $\boldsymbol{\varphi} = \{\varphi_{mit\omega}, \forall m \in \mathcal{M}, i \in \mathcal{I}, t \in \mathcal{T}, \omega \in \Omega\}$, $\overline{\boldsymbol{w}} = \{\overline{w}_{jkt\omega}, \forall j \in \mathcal{J}, k \in \mathcal{K}, t \in \mathcal{T}, \omega \in \Omega\}$. After generating $\mathbb{O}$ scenarios, solve the following corresponding SAA problem:

$$\textbf{[LIPM(SAA)]}\ \underset{Y \in \mathbf{Y}}{Minimize}\ \hat{\mathbf{g}}(Y) := \sum_{t \in \mathcal{T}} \Bigg(\sum_{s \in \mathcal{S}} \sum_{j \in \mathcal{J}} \Bigg(\sum_{n \in \mathcal{N}_{jk}} \sum_{k \in \mathcal{K}_j} \psi_{st} Y_{snjkt} + \sum_{m \in \mathcal{M}} \sum_{b \in \mathcal{B}} \eta_{mbt} Y_{mbsjt} \Bigg) + \frac{1}{|\mathbb{O}|} \sum_{o=1}^{\mathbb{O}} \mathbb{Q}(\mathbf{Y}, \zeta^o) \Bigg) \quad (3.35)$$

   For $e = 1, ..., E$, let $\mathbf{v}_{\mathbb{O}}^e$ and $\hat{\mathbf{Y}}_{\mathbb{O}}^e$ represent the optimal objective value and the optimal solution of (3.35), respectively.

2. Next, we compute the *average* and *variance* of all the corresponding SAA problems, referred to as $\bar{\mathbf{v}}_E^{\mathbb{O}}$ and $\sigma^2_{\bar{\mathbf{v}}_E^{\mathbb{O}}}$, respectively.

$$\bar{\mathbf{v}}_E^{\mathbb{O}} = \frac{1}{E} \sum_{e=1}^{E} \mathbf{v}_{\mathbb{O}}^e \quad (3.36)$$

$$\sigma^2_{\bar{\mathbf{v}}_E^{\mathbb{O}}} = \frac{1}{(E-1)E} \sum_{e=1}^{E} \left(\mathbf{v}_{\mathbb{O}}^e - \bar{\mathbf{v}}_E^{\mathbb{O}} \right)^2 \quad (3.37)$$

   Note that $\bar{\mathbf{v}}_E^{\mathbb{O}}$ provides a valid statistical lower bound on the optimal objective function value ($\mathbf{v}^*$) for the original problem (3.32) i.e., $\bar{\mathbf{v}}_E^{\mathbb{O}} \geq \mathbf{v}^*$ [92].

3. Select a feasible first-stage solution $\tilde{Y} \in \mathbf{Y}$, obtained from **Step 1** of the SAA algorithm, and use the solution to estimate the objective function value of the original problem (3.32) using a reference sample $\mathbb{O}'$ as follows:

$$\hat{\mathbf{g}}(\tilde{Y}) := \sum_{t \in \mathcal{T}} \Bigg\{ \sum_{s \in \mathcal{S}} \sum_{j \in \mathcal{J}} \Bigg(\sum_{n \in \mathcal{N}_{jk}} \sum_{k \in \mathcal{K}_j} \psi_{st} \tilde{Y}_{snjkt} + \sum_{m \in \mathcal{M}} \sum_{b \in \mathcal{B}} \eta_{mbt} \tilde{Y}_{mbsjt} \Bigg) \quad (3.38)$$

$$+ \frac{1}{|\mathbb{O}'|} \sum_{o=1}^{\mathbb{O}'} \mathbb{Q}(\mathbf{Y}, \zeta^o) \Bigg\} \quad (3.39)$$

This estimator $\tilde{\mathbf{g}}_{\mathbb{O}'}(\tilde{Y})$ provides an upper bound for the optimal objective function value of the original problem (3.37). This value is updated in each iteration if the obtained value is less than that of the previous iteration. Let $\mathbb{O}'$ be a large set of randomly generated independent supply and waterlevel scenarios such that $\mathbb{O}' \gg \mathbb{O}$. The variance of $\tilde{\mathbf{g}}_{\mathbb{O}'}(\tilde{Y})$ can be estimated as follows:

$$\sigma^2_{\mathbb{O}'}(\tilde{Y}) = \frac{1}{(|\mathbb{O}'|-1)|\mathbb{O}'|}\sum_{o=1}^{\mathbb{O}'}\Bigg\{\sum_{t\in\mathcal{T}}\Bigg(\sum_{s\in\mathcal{S}}\sum_{j\in\mathcal{J}}\Bigg(\sum_{n\in\mathcal{N}_{jk}}\sum_{k\in\mathcal{K}_j}\psi_{st}\tilde{Y}_{snjkt}+\sum_{m\in\mathcal{M}}\sum_{b\in\mathcal{B}}\eta_{mbt}\tilde{Y}_{mbsjt}\Bigg)+\mathbb{Q}(\boldsymbol{\Upsilon},\zeta^o)\Bigg)-\tilde{\mathbf{g}}_{\mathbb{O}'}(\tilde{Y})\Bigg\}^2$$

4. Utilizing the estimators obtained in **Steps 2** and **3** we calculate the optimality gap ($gap_{\mathbb{O},E,\mathbb{O}'}(\tilde{Y})$) and its variance ($\sigma^2_{gap}$) as follows:

$$\begin{aligned} gap_{\mathbb{O},E,\mathbb{O}'}(\tilde{Y}) &= \bar{\mathbf{v}}^{\mathbb{O}}_E - \tilde{\mathbf{g}}_{\mathbb{O}'}(\tilde{Y}) \\ \sigma^2_{gap} &= \sigma^2_{\mathbb{O}'}(\tilde{Y}) + \sigma^2_{\bar{\mathbf{v}}^{\mathbb{O}}_E} \end{aligned}$$

The confidence interval for the optimality gap can be computed as follows:

$$\bar{\mathbf{v}}^{\mathbb{O}}_E - \tilde{\mathbf{g}}_{\mathbb{O}'}(\tilde{Y}) + z_\alpha\Big\{\sigma^2_{\mathbb{O}'}(\tilde{Y}) + \sigma^2_{\bar{\mathbf{v}}^{\mathbb{O}}_E}\Big\}^{1/2}$$

with $z_\alpha := \Phi^{-1}(1-\alpha)$, where $\Phi(z)$ represents the cumulative distribution function of the standard normal distribution.

3.4.3 L-shaped Algorithm

Step 1 of the SAA algorithm still requires solving a two-stage stochastic mixed-integer linear program **[LIPM(SAA)]**, which may still considered challenging based on the size of the problem. This motivates us to develop a modified variant of the *L-shaped algorithm* to solve **[LIPM(SAA)]** efficiently. L-shaped algorithm, proposed by Laporte and Louveaux [69], is widely used in the literature to solve a variety of network design problems such as [82, 115, 52]. In this sub-section, we first introduce the basic L-shaped algorithm followed by different accelerated

techniques, such as problem-specific valid inequalities, multi-cut, knapsack cuts, scenario grouping and mean-value cuts, to solve **[LIPM(SAA)]** efficiently.

L-shaped algorithm separates the original problem **[LIPM(SAA)]** into two simple problems: an integer *master problem* and a linear *subproblem*. Let $\Theta(\mathbf{Y})$ be the expected value of the second-stage problem of **[LIPM(SAA)]**. An equivalent formulation for **[LIPM(SAA)]** is given by **[D-LIPM]** as follows.

$$\textbf{[D-LIPM]} \underset{Y \in \mathbf{Y}}{Minimize} \sum_{t \in \mathcal{T}} \sum_{s \in \mathcal{S}} \left\{ \sum_{n \in \mathcal{N}_{jk}} \sum_{j \in \mathcal{J}} \sum_{k \in \mathcal{K}_j} \psi_{st} Y_{snjkt} + \sum_{m \in \mathcal{M}} \sum_{b \in \mathcal{B}} \sum_{j \in \mathcal{J}} \eta_{mbt} Y_{mbsjt} \right\} + \Theta(\mathbf{Y}) \tag{3.40}$$

subject to (3.2)-(3.11), (3.13)-(3.22), and (3.26)-(3.29). In each iteration of the L-Shaped algorithm, a relaxed version of problem **[D-LIPM]** is solved. Essentially, instead of minimizing $\Theta(\mathbf{Y})$, in this relaxed problem, the outer approximation of $\Theta(\mathbf{Y})$ is minimized. Birge and Louveaux [16] showed that with finite number of scenarios $|\mathcal{O}|$, $\Theta(\mathbf{Y})$ resembles a piecewise linear convex function. Therefore, the linear functions generated by the algorithm lie either on or below $\Theta(\mathbf{Y})$. With growing iterations, an improved approximation is obtained, and the process continues until an optimal solution is found. Laporte and Louveaux [69] showed that upon meeting two conditions, L-shaped method can guarantee to provide an optimal solution within a finite number of steps: *(i)* generation of valid optimality and feasibility cuts and *(ii)* $\Theta(\mathbf{Y})$ is computable with the given solutions of first-stage

variables. To approximate $\Theta(\mathbf{Y})$, we formulate model **[M-LIPM]** as an approximation of model **[D-LIPM]** as follows:

$$\textbf{[M-LIPM]} \quad \phi^r = Minimize \sum_{t\in\mathcal{T}}\sum_{s\in\mathcal{S}}\Bigg\{\sum_{n\in\mathcal{N}_{jk}}\sum_{j\in\mathcal{J}}\sum_{k\in\mathcal{K}_j}\psi_{st}Y_{snjkt} + \sum_{m\in\mathcal{M}}\sum_{b\in\mathcal{B}}\sum_{j\in\mathcal{J}}\eta_{mbt}Y_{mbsjt}\Bigg\} + \theta \tag{3.41}$$

subject to (3.2)-(3.11), and

$$\theta \geq \theta^r + \sum_{m\in\mathcal{M}}\sum_{b\in\mathcal{B}}\sum_{s\in\mathcal{S}}\sum_{j\in\mathcal{J}}\sum_{t\in\mathcal{T}}\xi^r_{mbsjt}(Y_{mbsjt} - Y^r_{mbsjt}) \quad \forall r = 1,2,3,...,R \tag{3.42}$$

Problem **[M-LIPM]** is referred to as *master problem* of the L-shaped algorithm where (3.42) are known to be *optimality cut* constraints. Let $r \in R$ be any iteration number of the L-shaped algorithm. In **[M-LIPM]**, an auxiliary free variable θ is introduced and the definitions for θ^r and ξ^r_{mbsjt} are provided below. For a given first-stage decisions $\overline{\mathbf{Y}}^r$, obtained by solving **[M-LIPM]** in iteration r, the following scenario-based subproblems **[S-LIPM(o)]** are solved.

$$\textbf{[S-LIPM(o)]} \quad \theta^r_o(\mathbf{Y},\zeta^o) = \underset{\mathbf{X,H,U}}{Minimize} \sum_{t\in\mathcal{T}}\Bigg(\sum_{(e,f)\in(\mathcal{I}\cup\mathcal{K},\mathcal{J}\cup\mathcal{G})} c_{meft}X_{mefto} + \sum_{(i,g)\in(\mathcal{I},\mathcal{G})} c_{migt}X_{migto} + \sum_{b\in\mathcal{B}}\sum_{s\in\mathcal{S}}\sum_{n\in\mathcal{N}_{jk}}\sum_{(j,k)\in(\mathcal{J},\mathcal{K})} c_{mbsjkt}X_{mbsnjkto} + \sum_{j\in\mathcal{J}\cup\mathcal{K}} h_{mjt}H_{mjto} + \sum_{g\in\mathcal{G}}\pi_{mgt}U_{mgto} + \sum_{j\in\mathcal{J}} c^o_{jt}R_{jto} + \sum_{k\in\mathcal{K}} c^o_{kt}W_{kto}\Bigg) \tag{3.43}$$

subject to (3.13)-(3.17), (3.20)-(3.22), (3.26)-(3.29), and

$$\sum_{n\in\mathcal{N}_{jk}} X_{mbsnjkto} \leq min\{\overline{w}_{jkto}, \overline{w}_b\} Y_{mbsjt} \quad \forall m \in \mathcal{M}, b \in \mathcal{B}, s \in \mathcal{S}, j \in \mathcal{J}, k \in \mathcal{K}_j, t \in \mathcal{T} \tag{3.44}$$

$$\sum_{n\in\mathcal{N}_{jk}} \sum_{k\in\mathcal{K}_j} \left(\frac{X_{mbsnjkto}}{\rho_m}\right) \leq v_b Y_{mbsjt} \forall m \in \mathcal{M}, b \in \mathcal{B}, s \in \mathcal{S}, , j \in \mathcal{J}, t \in \mathcal{T} \tag{3.45}$$

$$Y_{mbsjt} = \overline{Y}^r_{mbsjt} \quad : \xi_{mbsjto} \forall m \in \mathcal{M}, b \in \mathcal{B}, s \in \mathcal{S}, j \in \mathcal{J}, t \in \mathcal{T} \tag{3.46}$$

Let $\boldsymbol{\xi} = \{\xi^r_{mbsjto} | \forall m \in \mathcal{M}, b \in \mathcal{B}, s \in \mathcal{S}, j \in \mathcal{J}, t \in \mathcal{T}, o \in \mathcal{O}\}$ be the dual variables associated with constraints (3.46) for scenario o at iteration r of the L-shaped algorithm. In each iteration r of the L-shaped algorithm, the solutions of **[S-LIPM(o)]** are used (θ^r_o) to determine the value of θ^r as used in the optimality cut constraints in (3.42). We now use the following equations to derive the *slope coefficient* ξ^r_{mbsjt} and *intercept* θ^r for constraint (3.42).

$$\xi^r_{mbsjt} = \sum_{o\in\mathrm{O}} \rho_o \xi^r_{mbsjto} \tag{3.47}$$

$$\theta^r = \sum_{o\in\mathrm{O}} \rho_o \theta^r_o \tag{3.48}$$

Note that for any given value of $\mathbf{Y}$, constraints (3.16) ensure that the problem (3.43) is always feasible. Therefore, we did not add any feasibility cut in the master problem **[M-LIPM]**. Problem **[M-LIPM]** minimizes the outer approximation of the convex function $\Theta(\mathbf{Y})$ in **[D-LIPM]**; therefore, the objective function value of **[M-LIPM]** provides a valid lower bound for problem **[D-LIPM]**. The solution of master and scenario based subproblems provide an upper bound for the original SAA subproblem **[LIPM(SAA)]**. The L-shaped algorithm terminates when the gap

between the upper and lower bound reaches to a predetermined threshold limit. If not, an optimality cut (in the form of (3.42)) is added to **[M-LIPM]** and the algorithm continues. Let us define Z^r_{mas} such that $Z^r_{mas} = \sum_{s\in\mathcal{S}} \sum_{j\in\mathcal{J}} \sum_{t\in\mathcal{T}} \Big(\sum_{n\in\mathcal{N}_{jk}} \sum_{k\in\mathcal{K}_j} \psi_{st} Y_{snjkt} + \sum_{m\in\mathcal{M}} \sum_{b\in\mathcal{B}} \eta_{mbt} Y_{mbsjt} \Big)$. The pseudo-code of the basic L-shaped algorithm is now given in **Algorithm 2**.

We first attempt to solve **[LIPM(SAA)]** with basic L-shaped algorithm, but we observe that the algorithm finds it difficulty even in solving small-size test instances (considering the size of our real-life dataset) in a reasonable time. This motivates us to investigate additional techniques to further improve the convergence of the basic L-shaped algorithm. The aim would be to find optimum (or near-optimum) solution in solving **[LIPM(SAA)]** on realistic-test instances in a much shorter time. The following subsections present some proper accelerated techniques to improve the computational performance of the basic L-shaped algorithm.

3.4.3.1 Valid inequalities

To enhance the performance of the L-shaped algorithm, we first generate a number of valid inequalities that can be added to master problem **[M-LIPM]**. These inequalities are derived by utilizing the special structure of our problem **[IPM]**. The proposed set of valid inequalities are presented below:

- We first add *surrogate constraints*, in the form of constraints (3.49) as shown below, to problem **[M-LIPM]**. The value of σ can vary between 0.0 and 1.0 while a value of σ equal to 1.0 ensures that all the demand will be satisfied through the inland waterway ports. Essentially, constraints (3.49) can be

Algorithm 2: L-shaped Algorithm

Initialize, $r \leftarrow 1$, ϵ^L, $UB^r \leftarrow +\infty$, $LB^r \leftarrow -\infty$

$terminate \leftarrow false$

while $terminate =$ ***false*** **do**

Solve **[M-LIPM]** to obtain $\mathbf{Y}^r$, ν**[M-LIPM]**, and Z^r_{mas}

if $LB^r < \nu$***[M-LIPM]*** **then**

Update the lower bound: $LB^r \leftarrow \nu$**[M-LIPM]**

end

Solve **[S-LIPM(o)]** $\forall o \in \mathbb{O}$ to obtain $\{\xi^r_{mbsjto}\}$ and θ^r_o

Calculate $\{\xi^r_{mbsjt}\}$ and θ^r using equations (3.47) and (3.48)

if $UB^r > \theta^r + Z^r_{mas}$ **then**

Update the upper bound: $UB^r \leftarrow \theta^r + Z^r_{mas}$

end

if $\frac{(UB^r - LB^r)}{UB^r} \leq \epsilon^L$ **then**

$terminate \leftarrow$ **true**

else

add optimality cut (3.42) to **[M-LIPM]**

end

$r \leftarrow r + 1$

end

used to set a lower bound on the overall barge usage to ensure the demand for commodity $m \in \mathcal{M}$ at each time period $t \in \mathcal{T}$ is satisfied.

$$\sum_{b \in \mathcal{B}} \sum_{s \in \mathcal{S}} \sum_{j \in \mathcal{J}} Y_{mbsjt} \overline{w}_b \geq \sum_{g \in \mathcal{G}} \sigma d_{mgt} \qquad \forall m \in \mathcal{M}, t \in \mathcal{T} \qquad (3.49)$$

- While selecting between a number of barges of similar capacities, solver may encounter with symmetries that may result in elongated search times. To address this issuue, the following *lexicographic ordering constraints* [122, 63]

((3.50) and (3.51)) are generated which set priorities on barge selection. Such priorities help to break the duplications caused by the barge selection symmetry, therefore, accelerate the performance of the branch-and-bound process.

$$Y_{1,b-1,sjt} \geq Y_{1bsjt} \quad \forall b \in \mathcal{B} \setminus \{1\}, s \in \mathcal{S}, j \in \mathcal{J}, t \in \mathcal{T} \quad (3.50)$$

$$\sum_{p=1}^{m} 2^{(m-p)} Y_{p,b-1,sjt} \geq \sum_{p=1}^{m} 2^{(m-p)} Y_{pbsjt} \quad \forall m \in \mathcal{M}, b \in \mathcal{B} \setminus \{1\}, s \in \mathcal{S}, j \in \mathcal{J}, t \in \mathcal{T} \quad (3.51)$$

- Symmetries may also arise between towboats of similar capacities. Consider $\mathcal{S}_e^{'}$ as the subset of towboats of same type, i.e., $\mathcal{S}_e^{'} \subset \mathcal{S}$ and $s_e^{'} \in \mathcal{S}_e^{'}$, where $s_e^{'}$ represents a set of the members belonging to $\mathcal{S}_e^{'}$ in ascending order. Similar to constraints (3.50) and (3.51), following lexicographical ordering constraints ((3.52) and (3.53)) are applied for each $\mathcal{S}_e^{'}$ to set the priority in utilizing towboats of the same type.

$$Y_{s_e^{'}-1,njkt} \geq Y_{s_e^{'}njkt} \forall s_e^{'} \in \mathcal{S}_e^{'} \setminus \{1\}, n \in \mathcal{N}_{jk}, j \in \mathcal{J}, k \in \mathcal{K}, t \in \mathcal{T} \quad (3.52)$$

$$\psi_{s_e^{'}-1,t} Y_{s_e^{'}-1,njkt} \geq \psi_{s_e^{'}t} Y_{s_e^{'}njkt} \forall s_e^{'} \in \mathcal{S}_e^{'} \setminus \{1\}, n \in \mathcal{N}_{jk}, j \in \mathcal{J}, k \in \mathcal{K}, t \in \mathcal{T} \quad (3.53)$$

- Constraints (3.54) and (3.55) generate a lower bound on the number of barges that are required for satisfying the demand between any time interval $[t_1, t_2]$ where $t_2 \geq t_1$. If the cumulative demand over period $[t_1, t_2]$ is greater than or equal to the maximum possible inventory held ($\overline{h}_k$) or initial inventory (H_{mk0o}), then at least a certain number of barges need to be used in that specific time interval.

$$\sum_{b \in \mathcal{B}} \sum_{s \in \mathcal{S}} \sum_{j \in \mathcal{J}} \sum_{t=t_1}^{t_2} Y_{mbsjt} \geq \left\lceil \frac{\sum_{g \in \mathcal{G}} \sum_{t=t_1}^{t_2} \sigma d_{mgt} - \sum_{k \in \mathcal{K}} \overline{h}_k}{\overline{w}_b} \right\rceil \quad \forall m \in \mathcal{M}, (t_1, t_2) \in \mathcal{T}, t_2 \geq t_1 \quad (3.54)$$

$$\sum_{b \in \mathcal{B}} \sum_{s \in \mathcal{S}} \sum_{j \in \mathcal{J}} \sum_{t=t_1}^{t_2} Y_{mbsjt} \geq \left\lceil \frac{\sum_{g \in \mathcal{G}} \sum_{t=t_1}^{t_2} \sigma d_{mgt} - \sum_{k \in \mathcal{K}} \sum_{o \in \mathcal{O}} \rho_o H_{mk0o}}{\overline{w}_b} \right\rceil \quad \forall m \in \mathcal{M}, (t_1, t_2) \in \mathcal{T}, t_2 \geq t_1 \quad (3.55)$$

- Similar to constraints (3.54) and (3.55), constraints (3.56) and (3.57) set lower bounds on towboat selection between any time interval $[t_1, t_2]$ where $t_2 \geq t_1$. In both constraints, $\overline{\delta}_{\overline{s}}$ denote the capacity of the most powerful towboat $\overline{S}$.

$$\sum_{s\in\mathcal{S}}\sum_{n\in\mathcal{N}}\sum_{j\in\mathcal{J}}\sum_{k\in\mathcal{K}}\sum_{t=t_1}^{t_2} Y_{snjkt} \geq \left\lceil \frac{\sum_{m\in\mathcal{M}}\sum_{g\in\mathcal{G}}\sum_{t=t_1}^{t_2}\sigma d_{mgt} - \sum_{k\in\mathcal{K}}\overline{h}_k}{\overline{w}_b\overline{\delta}_{\overline{s}}} \right\rceil \quad \forall (t_1,t_2)\in\mathcal{T}, t_2\geq t_1 \tag{3.56}$$

$$\sum_{s\in\mathcal{S}}\sum_{n\in\mathcal{N}}\sum_{j\in\mathcal{J}}\sum_{k\in\mathcal{K}}\sum_{t=t_1}^{t_2} Y_{snjkt} \geq \left\lceil \frac{\sum_{m\in\mathcal{M}}\left(\sum_{g\in\mathcal{G}}\sum_{t=t_1}^{t_2}\sigma d_{mgt} - \sum_{k\in\mathcal{K}}\sum_{o\in\mathrm{O}}\rho_o H_{mk0o}\right)}{\overline{w}_b\overline{\delta}_{\overline{s}}} \right\rceil \quad \forall (t_1,t_2)\in\mathcal{T}, t_2\geq t_1 \tag{3.57}$$

3.4.3.2 Multicut L-shaped Algorithm

In each iteration r of the basic L-shaped algorithm, only one optimality cut is added to master problem **[M-LIPM]**. This may require several iterations before sufficient information can be gathered and passed from the subproblems to the master problem **[M-LIPM]** via constraints (3.42). To overcome this problem, Birge and Louveaux [17] propose a multi-cut L-shaped algorithm where instead of adding one optimality cut, as in the case with basic L-shaped algorithm, $|\mathrm{O}|$ number of cuts, one for each scenario subproblem **[S-LIPM(o)]**, are constructed and added to **[M-LIPM]**. The optimality cut constraint (3.42) can now be modified as follows:

$$\theta_o \geq \theta_o^r + \sum_{m\in\mathcal{M}}\sum_{b\in\mathcal{B}}\sum_{s\in\mathcal{S}}\sum_{j\in\mathcal{J}}\sum_{t\in\mathcal{T}} \xi_{mbsjto}(Y_{mbsjt} - Y^r_{mbsjt}) \quad \forall r = 1,2,3,...,R, o \tag{3.58}$$

Note that variable θ and dual parameter ξ^r_{mbsjt} are now replaced by θ_o and ξ_{mbsjto}, respectively. Accordingly, the objective function of the Benders master problem **[M-LIPM]** is now modified as follows:

$$\textbf{[MC-LIPM]}\ \phi^r = Minimize \sum_{t\in\mathcal{T}}\sum_{s\in\mathcal{S}}\left(\sum_{n\in\mathcal{N}_{jk}}\sum_{j\in\mathcal{J}}\sum_{k\in\mathcal{K}_j}\psi_{st}Y_{snjkt} + \sum_{m\in\mathcal{M}}\sum_{b\in\mathcal{B}}\sum_{j\in\mathcal{J}}\eta_{mbt}Y_{mbsjt}\right) + \sum_{o\in\mathrm{O}} p_o\theta_o \tag{3.59}$$

Note that with the introduction of multi-cuts in **[M-LIPM]**, the overall algorithm may now require less number of iterations to reach the optimality gap compared with the classical L-shaped algorithm; however, this reduction may be achieved at a cost of increasing the running time in solving the Benders master problem, primarily due to adding large number of new constraints.

3.4.3.3 Knapsack inequality

We now employ *knapsack inequalities* [119, 80] to enhance the performance of the branch and bound process and to expedite the convergence of the overall L-shaped algorithm. Addition of these cuts, along with optimality cut (3.42), essentially help state-of-the-art commercial solvers (e.g., GUROBI, CPLEX) to derive various valid inequalities that eventually help the convergence of the basic L-shaped algorithm. Let UB^r and LB^r be the *best known upper* and *lower* bounds

for the L-shaped algorithm at iteration r. The following knapsack inequalities can be added to **[M-LIPM]** in iteration $r+1$:

$$UB^r \geq \sum_{t\in\mathcal{T}}\sum_{s\in\mathcal{S}}\left(\sum_{n\in\mathcal{N}_{jk}}\sum_{j\in\mathcal{J}}\sum_{k\in\mathcal{K}_j}\psi_{st}Y_{snjkt}+\sum_{m\in\mathcal{M}}\sum_{b\in\mathcal{B}}\sum_{j\in\mathcal{J}}\eta_{mbt}Y_{mbsjt}\right)+\theta^r \quad (3.60)$$

$$LB^r \leq \sum_{t\in\mathcal{T}}\sum_{s\in\mathcal{S}}\left(\sum_{n\in\mathcal{N}_{jk}}\sum_{j\in\mathcal{J}}\sum_{k\in\mathcal{K}_j}\psi_{st}Y_{snjkt}+\sum_{m\in\mathcal{M}}\sum_{b\in\mathcal{B}}\sum_{j\in\mathcal{J}}\eta_{mbt}Y_{mbsjt}\right)+\theta \quad (3.61)$$

3.4.3.4 Scenario Bundling

The multi-cut L-shaped algorithm, discussed in subsection 3.4.3.2 [17], usually improves the computational performance of the basic L-shaped algorithm. However, adding too many cuts at each iteration, more specifically, $|\mathbb{O}|$ number of cuts, can degrade the overall performance of the L-shaped algorithm. This is primarily due to the reason that the added disaggregated cuts can significantly increase the solution time of the master problem **[M-LIPM]**. The performance further degrades over iterations, since the master problem **[M-LIPM]** now need to carry significant amount of cut information prior to the current iteration. To alleviate this challenge, we adopt a *scenario bundling* strategy [1, 46] where instead of defining model **[S-LIPM(o)]** for each scenario $o \in \mathcal{O}$, we now define each subproblem with respect to a scenario bundle **[S-LIPM(γ)]**, denoted by set $\gamma \in \Gamma$, consisting of a number of scenarios. Note that the bundling can be done by considering different criterion specific to the model (e.g., high, medium, and low supply/waterlevel scenario bundling). Let $|\mathbb{O}|$ be partitioned into $|\Gamma|$ bundles and $\rho_\gamma = \sum_{o\in\gamma}\rho_o$. We now solve model **[S-LIPM(γ)]** for each bundle $\gamma \in \Gamma$ as follows:

$$\textbf{[S-LIPM}(\gamma)\textbf{]} \quad \theta^r_\gamma(\mathbf{Y},\zeta^\gamma) = \underset{\mathbf{X,H,U}}{Minimize} \sum_{t\in\mathcal{T}}\sum_{o\in\gamma}\rho_o\Bigg(\sum_{(e,f)\in(\mathcal{I}\bigcup\mathcal{K},\mathcal{J}\bigcup\mathcal{G})} c_{meft}X_{mefto} + \sum_{(i,g)\in(\mathcal{I},\mathcal{G})} c_{migt}X_{migto} + \sum_{b\in\mathcal{B}}\sum_{s\in\mathcal{S}}\sum_{n\in\mathcal{N}_{jk}}\sum_{(j,k)\in(\mathcal{J},\mathcal{K})} c_{mbsjkt}X_{mbsnjkto} + + \sum_{j\in\mathcal{J}\bigcup\mathcal{K}} h_{mjt}H_{mjto} + \sum_{g\in\mathcal{G}}\pi_{mgt}U_{mgto} + \sum_{j\in\mathcal{J}} c^o_{jt}R_{jto} + \sum_{k\in\mathcal{K}} c^o_{kt}W_{kto}\Bigg) \tag{3.62}$$

subject to (3.13)-(3.17), (3.20)-(3.22), (3.26)-(3.29), and (3.44)-(3.46). Likewise, the master problem and the optimality cut are updated as follows:

$$\textbf{[SB-LIPM]} \quad \phi^r = Minimize \quad \sum_{t\in\mathcal{T}}\sum_{s\in\mathcal{S}}\Bigg\{\sum_{n\in\mathcal{N}_{jk}}\sum_{j\in\mathcal{J}}\sum_{k\in\mathcal{K}_j}\psi_{st}Y_{snjkt} + \sum_{m\in\mathcal{M}}\sum_{b\in\mathcal{B}}\sum_{j\in\mathcal{J}}\eta_{mbt}Y_{mbsjt}\Bigg\} + \sum_{\gamma\in\Gamma}p_\gamma\theta_\gamma \tag{3.63}$$

and

$$\theta_\gamma \geq \theta^r_\gamma + \sum_{m\in\mathcal{M}}\sum_{b\in\mathcal{B}}\sum_{s\in\mathcal{S}}\sum_{j\in\mathcal{J}}\xi_{mbsjt\gamma}(Y_{mbsjt} - Y^r_{mbsjt}) \quad \forall r = 1,2,3,...,R, \gamma\in\Gamma \tag{3.64}$$

3.4.3.5 Mean Value Cuts

Type A: The earlier iterations of the L-shaped algorithm produces low quality first-stage decisions **Y**, primarily due to lack of useful information passed from the subproblems to master problem via optimality cut constraint (3.42), which prolongs the running time of the overall algorithm. To alleviate this problem, Batun et al. [14] propose a *mean value cut* that can be added in the master problem **[M-LIPM]** in order to help obtaining a good lower bound from the earlier iterations of the algorithm. The aim is to speed up the convergence of the overall L-shaped algorithm. Essentially, a mean value cut, more specifically, referred to as *Type A*

mean value cut, is generated using the subproblems defined under a *mean-value scenario* $\bar{o}$ (a scenario comprised of the mean values of the uncertain parameters). The newly generated cut helps to strengthen the lower bound of the free variable θ in an attempt to generate high quality feasible solutions during earlier iterations of the L-shaped algorithm. To generate this inequality, the following additional parameters and decision variables are introduced:

Auxiliary parameters:

- $\bar{\varphi}_{mit}$: mean amount of product of $m \in \mathcal{M}$ available in supply site $i \in \mathcal{I}$ at time period $t \in \mathcal{T}$
- $\bar{w}_{jkt}$: mean allowable weight $\overline{w}_{jkt}$ that can be carried between the channel $(j,k) \in (\mathcal{J},\mathcal{K})$ at time period $t \in \mathcal{T}$

Auxiliary decision variables:

- $\bar{X}_{migt}$: mean amount of commodities of type $m \in \mathcal{M}$ transported along arc $(i,g) \in (\mathcal{I} \bigcup \mathcal{G})$ at time period $t \in \mathcal{T}$
- $\bar{X}_{meft}$: mean amount of commodities of type $m \in \mathcal{M}$ transported along arc $(e,f) \in (\mathcal{I} \bigcup \mathcal{K}, \mathcal{J} \bigcup \mathcal{G})$ at time period $t \in \mathcal{T}$
- $\bar{X}_{mbsnjkt}$: mean amount of commodities of type $m \in \mathcal{M}$ transported using barge $b \in \mathcal{B}$ of towboat $s \in \mathcal{S}$ of trip $n \in \mathcal{N}_{jk}$ along arc $(j,k) \in (\mathcal{J},\mathcal{K})$ at time period $t \in \mathcal{T}$
- $\bar{H}_{mjt}$: mean amount of commodities of type $m \in \mathcal{M}$ stored in port $j \in \mathcal{J} \bigcup \mathcal{K}$ at time period $t \in \mathcal{T}$
- $\bar{U}_{mgt}$: mean amount of commodities of type $m \in \mathcal{M}$ shortage in market $g \in \mathcal{G}$ at time period $t \in \mathcal{T}$

The following additional constraints are added to the master problem **[MC-LIPM]**:

$$\sum_{j\in\mathcal{J}_i}\bar{X}_{mijt}+\sum_{g\in\mathcal{G}_i}\bar{X}_{migt} \leq \bar{\varphi}_{mit}\forall m\in\mathcal{M}, i\in\mathcal{I}, t\in\mathcal{T} \tag{3.65}$$

$$\sum_{i\in\mathcal{I}_j}\bar{X}_{mijt}+(1-\alpha_m)\bar{H}_{mj,t-1} = \sum_{b\in\mathcal{B}}\sum_{s\in\mathcal{S}}\sum_{n\in\mathcal{N}_{jk}}\sum_{k\in\mathcal{K}_j}\bar{X}_{mbsnjkt}+\bar{H}_{mjt} \quad \forall m\in\mathcal{M}, j\in\mathcal{J}, t\in\mathcal{T} \tag{3.66}$$

$$\sum_{b\in\mathcal{B}}\sum_{s\in\mathcal{S}}\sum_{n\in\mathcal{N}_{jk}}\sum_{j\in\mathcal{J}_k}\bar{X}_{mbsnjkt} = \sum_{g\in\mathcal{G}_k}\bar{X}_{mkgt}+\bar{H}_{mkt}-(1-\alpha_m)\bar{H}_{mk,t-1} \quad \forall m\in\mathcal{M}, k\in\mathcal{K}, t\in\mathcal{T} \tag{3.67}$$

$$\sum_{i\in\mathcal{I}_g}\bar{X}_{migt}+\sum_{k\in\mathcal{K}_g}\bar{X}_{mkgt}+\bar{U}_{mgt} = d_{mgt}\forall m\in\mathcal{M}, g\in\mathcal{G}, t\in\mathcal{T} \tag{3.68}$$

$$\sum_{m\in\mathcal{M}}\bar{H}_{mjt} \leq \overline{h}_j\forall j\in\mathcal{J}\bigcup\mathcal{K}, t\in\mathcal{T} \tag{3.69}$$

$$\sum_{n\in\mathcal{N}_{jk}}\bar{X}_{mbsnjkt} \leq min\{\bar{w}_{jkt},\overline{w}_b\}Y_{mbsjt} \quad \forall m\in\mathcal{M}, b\in\mathcal{B}, s\in\mathcal{S}, j\in\mathcal{J}, k\in\mathcal{K}_j, t\in\mathcal{T} \tag{3.70}$$

$$\sum_{n\in\mathcal{N}_{jk}}\sum_{k\in\mathcal{K}_j}\left(\frac{\bar{X}_{mbsnjkt}}{\rho_m}\right) \leq v_bY_{mbsjt}\forall m\in\mathcal{M}, b\in\mathcal{B}, s\in\mathcal{S}, j\in\mathcal{J}, t\in\mathcal{T} \tag{3.71}$$

$$\sum_{m\in\mathcal{M}}\sum_{b\in\mathcal{B}}\sum_{s\in\mathcal{S}}\sum_{n\in\mathcal{N}_{jk}}\sum_{k\in\mathcal{K}_j}\bar{X}_{mbsnjkt} \leq \overline{c}_{jt}\forall j\in\mathcal{J}, t\in\mathcal{T} \tag{3.72}$$

$$\sum_{m\in\mathcal{M}}\sum_{g\in\mathcal{G}_k}\bar{X}_{mkgt} \leq \overline{c}_{kt}\forall k\in\mathcal{K}, t\in\mathcal{T} \tag{3.73}$$

$$\sum_{m\in\mathcal{M}}\sum_{b\in\mathcal{B}}\sum_{s\in\mathcal{S}}\sum_{n\in\mathcal{N}_{jk}}\sum_{k\in\mathcal{K}}\bar{X}_{mbsnjkt} \leq \left(\frac{\bar{R}_{jt}}{(1+\bar{R}_{jt}^{p_1})^2}\right)\overline{c}_{jt}+\left(\frac{\bar{R}_{jt}^{p_1}}{1+\bar{R}_{jt}^{p_1}}\right)^2\overline{c}_{jt} \quad \forall j\in\mathcal{J}, t\in\mathcal{T}, p_1\in\mathcal{P}^1 \tag{3.74}$$

$$\sum_{m\in\mathcal{M}}\sum_{g\in\mathcal{G}}\bar{X}_{mkgt} \leq \left(\frac{\bar{W}_{kt}}{(1+\bar{W}_{kt}^{p_2})^2}\right)\overline{c}_{kt}+\left(\frac{\bar{W}_{kt}^{p_2}}{1+\bar{W}_{kt}^{p_2}}\right)^2\overline{c}_{kt} \quad \forall k\in\mathcal{K}_j, t\in\mathcal{T}, p_2\in\mathcal{P}^2 \tag{3.75}$$

$$\bar{W}_{kt} \in \mathbb{R}^{+} \forall k \in \mathcal{K}, t \in \mathcal{T} \quad (3.76)$$

$$\bar{R}_{jt} \in \mathbb{R}^{+} \forall j \in \mathcal{J}, t \in \mathcal{T} \quad (3.77)$$

$$\bar{X}_{migt}, \bar{X}_{mjkbsnt}, \bar{X}_{mkgt}, \bar{H}_{mjt}, \bar{H}_{mkt}, \bar{U}_{mgt} \in \mathbb{R}^{+} \quad (3.78)$$

Additionally, the following lower bound strengthening cut is added to **[MC-LIPM]**:

$$\theta^{r} \geq \sum_{t \in \mathcal{T}} \Bigg(\sum_{(e,f) \in (\mathcal{I} \bigcup \mathcal{K}, \mathcal{J} \bigcup \mathcal{G})} c_{meft} \bar{X}_{meft} + \sum_{(i,g) \in (\mathcal{I}, \mathcal{G})} c_{migt} \bar{X}_{migt} + \sum_{b \in \mathcal{B}} \sum_{s \in \mathcal{S}} \sum_{n \in \mathcal{N}_{jk}} \sum_{(j,k) \in (\mathcal{J}, \mathcal{K})} c_{mbsjkt} \bar{X}_{mbsnjkt} + \sum_{j \in \mathcal{J} \bigcup \mathcal{K}} h_{mjt} \bar{H}_{mjt} + \sum_{g \in \mathcal{G}} \pi_{mgt} \bar{U}_{mgt} + \sum_{j \in \mathcal{J}} c^{o}_{jt} \bar{R}_{jt} + \sum_{k \in \mathcal{K}} c^{o}_{kt} \bar{W}_{kt} \Bigg) \quad (3.79)$$

Type B: We now generate another type of mean value cut, referred to as *Type B mean value cut*, where *scenario bundling/grouping* technique (discussed in Section 3.4.3.4) is utilized under the *mean value* framework.These cuts are derived from *mean scenario group* $\bar{\gamma}$ where $\bar{\gamma}$ denote the mean scenario from all scenario o under any specific scenario group/bundle γ. The newly generated cuts are then added to the master problem **[SB-LIPM]** in an attempt to improve the convergence of the basic L-shaped algorithm. In order to develop *multiple mean-value* cuts, the following additional parameters and decision variables are introduced:

Auxiliary parameters:

- $\varphi_{mit\bar{\gamma}}$: mean amount of product of $m \in \mathcal{M}$ available in supply site $i \in \mathcal{I}$ at time period $t \in \mathcal{T}$ under scenario group γ
- $\overline{w}_{jkt\bar{\gamma}}$: mean allowable weight $\overline{w}_{jkt}$ that can be carried between the channel $(j,k) \in (\mathcal{J}, \mathcal{K})$ at time period $t \in \mathcal{T}$ under scenario group γ

Auxiliary decision variables:

- $X_{migt\bar{\gamma}}$: average amount of commodities of type $m \in \mathcal{M}$ transported along arc $(i,g) \in (\mathcal{I} \bigcup \mathcal{G})$ at time period $t \in \mathcal{T}$ under scenario group γ
- $\bar{X}_{meft\bar{\gamma}}$: average amount of commodities of type $m \in \mathcal{M}$ transported along arc $(e,f) \in (\mathcal{I} \bigcup \mathcal{K}, \mathcal{J} \bigcup \mathcal{G})$ at time period $t \in \mathcal{T}$ under scenario group γ
- $\bar{X}_{mbsnjkt\bar{\gamma}}$: average amount of commodities of type $m \in \mathcal{M}$ transported using barge $b \in \mathcal{B}$ of towboat $s \in \mathcal{S}$ of trip $n \in \mathcal{N}_{jk}$ along arc $(j,k) \in (\mathcal{J},\mathcal{K})$ at time period $t \in \mathcal{T}$ under scenario group γ
- $\bar{H}_{mjt\bar{\gamma}}$: average amount of commodities of type $m \in \mathcal{M}$ stored in port $j \in \mathcal{J} \bigcup \mathcal{K}$ at time period $t \in \mathcal{T}$ under scenario group γ
- $\bar{U}_{mgt\bar{\gamma}}$: average amount of commodities of type $m \in \mathcal{M}$ shortage in market $g \in \mathcal{G}$ at time period $t \in \mathcal{T}$ under scenario group γ

Utilizing these new variables and parameters, the following set of constraints are formulated and accordingly added to the master problem **[M-LIPM]**.

$$\sum_{j\in\mathcal{J}_i} X_{mijt\bar{\gamma}} + \sum_{g\in\mathcal{G}_i} X_{migt\bar{\gamma}} \leq \varphi_{mit\bar{\gamma}} \forall m \in \mathcal{M}, i \in \mathcal{I}, t \in \mathcal{T} \quad (3.80)$$

$$\sum_{i\in\mathcal{I}_j} X_{mijt\bar{\gamma}} + (1-\alpha_m) H_{mj,t-1,o} = \sum_{b\in\mathcal{B}} \sum_{s\in\mathcal{S}} \sum_{n\in\mathcal{N}_{jk}} \sum_{k\in\mathcal{K}_j} X_{mbsnjkt\bar{\gamma}} + H_{mjt\bar{\gamma}} \quad \forall m \in \mathcal{M}, j \in \mathcal{J}, t \in \mathcal{T} \quad (3.81)$$

$$\sum_{b\in\mathcal{B}} \sum_{s\in\mathcal{S}} \sum_{n\in\mathcal{N}_{jk}} \sum_{j\in\mathcal{J}_k} X_{mbsnjkt\bar{\gamma}} = \sum_{g\in\mathcal{G}_k} X_{mkgt\bar{\gamma}} + H_{mkt\bar{\gamma}} - (1-\alpha_m) H_{mk,t-1,\bar{\gamma}} \quad \forall m \in \mathcal{M}, k \in \mathcal{K}, t \in \mathcal{T} \quad (3.82)$$

$$\sum_{i\in\mathcal{I}_g} X_{migt\bar{\gamma}} + \sum_{k\in\mathcal{K}_g} X_{mkgt\bar{\gamma}} + U_{mgt\bar{\gamma}} = d_{mgt} \forall m \in \mathcal{M}, g \in \mathcal{G}, t \in \mathcal{T} \quad (3.83)$$

$$\sum_{m\in\mathcal{M}} H_{mjt\bar{\gamma}} \leq \overline{h}_j \forall j \in \mathcal{J} \bigcup \mathcal{K}, t \in \mathcal{T} \quad (3.84)$$

$$\sum_{n\in\mathcal{N}_{jk}} X_{mbsnjkt\bar{\gamma}} \leq min\{\overline{w}_{jkt\bar{\gamma}}, \overline{w}_b\} Y_{mbsjt} \forall m \in \mathcal{M}, b \in \mathcal{B}, s \in \mathcal{S}, j \in \mathcal{J}, k \in \mathcal{K}_j, t \in \mathcal{T} \quad (3.85)$$

$$\sum_{n\in\mathcal{N}_{jk}} \sum_{k\in\mathcal{K}_j} \left(\frac{X_{mbsnjkt\bar{\gamma}}}{\rho_m} \right) \leq v_b Y_{mbsjt} \forall m \in \mathcal{M}, b \in \mathcal{B}, s \in \mathcal{S}, j \in \mathcal{J}, t \in \mathcal{T} \quad (3.86)$$

$$\sum_{m\in\mathcal{M}} \sum_{b\in\mathcal{B}} \sum_{s\in\mathcal{S}} \sum_{n\in\mathcal{N}_{jk}} \sum_{k\in\mathcal{K}_j} X_{mbsnjkt\bar{\gamma}} \leq \overline{c}_{jt} \forall j \in \mathcal{J}, t \in \mathcal{T} \quad (3.87)$$

$$\sum_{m\in\mathcal{M}} \sum_{g\in\mathcal{G}_k} X_{mkgt\bar{\gamma}} \leq \overline{c}_{kt} \forall k \in \mathcal{K}, t \in \mathcal{T} \quad (3.88)$$

$$\sum_{m\in\mathcal{M}} \sum_{b\in\mathcal{B}} \sum_{s\in\mathcal{S}} \sum_{n\in\mathcal{N}_{jk}} \sum_{k\in\mathcal{K}} X_{mbsnjkt\bar{\gamma}} \leq \left(\frac{R_{jt\bar{\gamma}}}{(1+R_{jt\bar{\gamma}}^{p_1})^2} \right) \overline{c}_{jt} + \left(\frac{R_{jt\bar{\gamma}}^{p_1}}{1+R_{jt\bar{\gamma}}^{p_1}} \right)^2 \overline{c}_{jt} \quad \forall j \in \mathcal{J}, t \in \mathcal{T}, p_1 \in \mathcal{P}^1 \quad (3.89)$$

$$\sum_{m\in\mathcal{M}} \sum_{g\in\mathcal{G}} X_{mkgt\bar{\gamma}} \leq \left(\frac{W_{kt\bar{\gamma}}}{(1+W_{kt\bar{\gamma}}^{p_2})^2} \right) \overline{c}_{kt} + \left(\frac{W_{kt\bar{\gamma}}^{p_2}}{1+W_{kt\bar{\gamma}}^{p_2}} \right)^2 \overline{c}_{kt} \quad \forall k \in \mathcal{K}_j, t \in \mathcal{T}, p_2 \in \mathcal{P}^2 \quad (3.90)$$

$$W_{kt\bar{\gamma}} \in \mathbb{R}^{+} \forall k \in \mathcal{K}, t \in \mathcal{T} \quad (3.91)$$

$$R_{jt\bar{\gamma}} \in \mathbb{R}^{+} \forall j \in \mathcal{J}, t \in \mathcal{T} \quad (3.92)$$

$$X_{migt\bar{\gamma}}, X_{mjkbsnt\bar{\gamma}}, X_{mkgt\bar{\gamma}}, H_{mjt\bar{\gamma}}, H_{mkt\bar{\gamma}}, U_{mgt\bar{\gamma}} \in \mathbb{R}^{+} \quad (3.93)$$

Type B mean value cut is then given by the following:

$$\begin{aligned}\theta_{\gamma} \geq \sum_{t\in\mathcal{T}} \Bigg(& \sum_{(e,f)\in(\mathcal{I}\bigcup\mathcal{K},\mathcal{J}\bigcup\mathcal{G})} c_{meft} X_{meft\bar{\gamma}} + \sum_{(i,g)\in(\mathcal{I},\mathcal{G})} c_{migt} X_{migt\bar{\gamma}} + \\ & \sum_{b\in\mathcal{B}} \sum_{s\in\mathcal{S}} \sum_{n\in\mathcal{N}_{jk}} \sum_{(j,k)\in(\mathcal{J},\mathcal{K})} c_{mbsjkt} X_{mbsnjkt\bar{\gamma}} + \sum_{j\in\mathcal{J}\bigcup\mathcal{K}} h_{mjt} H_{mjt\bar{\gamma}} + \sum_{g\in\mathcal{G}} \pi_{mgt} U_{mgt\bar{\gamma}} \\ & + \sum_{j\in\mathcal{J}} c^{o}_{jt} R_{jt\bar{\gamma}} + \sum_{k\in\mathcal{K}} c^{o}_{kt} W_{kt\bar{\gamma}} \Bigg) \end{aligned} \quad (3.94)$$

3.4.3.6 Local Branching

The earlier iterations of the L-shaped algorithm still experience slow convergence i.e., the gap between the upper and lower bound drops slowly even after the addition of all proposed cuts. To address this issue, the *local branching procedure* is adopted. This procedure was first developed by Fischetti and Lodi [41]. Later, Rei et al. (2009) [116] first demonstrated the utilization of this procedure under the classical Benders decomposition framework. Following this procedure, the feasible region is divided into a series of smaller subproblems which can be solved by any generic solver (e.g., GUROBI, CPLEX) within an acceptable time limit. The procedure begins with a feasible solution **Y** of **[M-LIMP]** that serves as a *reference point* to create *local branching subproblems*. Let k_v be a positive integer parameter.

Considering $\bar{\mathbf{Y}}^1$ be an optimal solution of the master problem **[M-LIMP]**, the feasible region of **[M-LIMP]** is divided into the following two reduced subproblems.

$$\Delta(\mathbf{Y}, \bar{\mathbf{Y}}^1) \leq k_v \quad \vee \quad \Delta(\mathbf{Y}, \bar{\mathbf{Y}}^1) \geq k_v + 1 \tag{3.95}$$

The reduced subproblem is then solved by adding the *left branching constraint* presented in the first part of constraint (3.95). After solving the local branching subproblem, depending on the status of the optimizer, one of the four cases, *(i)* optimality, *(ii)* infeasibility , *(iii)* suboptimality, and *(iv)* exceeding timelimit, might arise. If the first case (i) arises, the left branching constraint is replaced by the right branching constraint i.e., $\Delta(\mathbf{Y}, \bar{\mathbf{Y}}^1) \geq k_v + 1$, and the reference point is updated with the new solution. In case *(ii)*, the left branching constraint is replaced by the right branching constraint i.e., $\Delta(\mathbf{Y}, \bar{\mathbf{Y}}^1) \geq k_v + 1$ and a *diversification* procedure is applied by increasing the size of the feasible region by $\lceil k_v/2 \rceil$ i.e., $(k_v + \lceil k_v/2 \rceil)$. Upon occurance of case *(iii)*, we eliminate the left branching constraint, and add a *tabu* constraint $\Delta(\mathbf{Y}, \bar{\mathbf{Y}}^2) \geq 1$ where, $\bar{\mathbf{Y}}^2$ is the new reference point from the last subproblem. Then, a new subproblem is generated and solved by adding the left branching constraint $\Delta(\mathbf{Y}, \bar{\mathbf{Y}}^2) \leq k_v$. In case *(iv)*, we decrease the right hand size of the left branching constraint by one, and add *tabu cut* to eliminate $\bar{\mathbf{Y}}^2$ from further consideration. The current subproblem is then solved for finding a better solution. If not found, the diversification procedure is repeated to enlarge the size of the feasible region.

3.4.4 Implementing Parallel Processing:

The proposed algorithmic framework utilizes constraint generation (CG), sample average approximation (SAA), and the L-shaped algorithm in a nested structure along with a number of enhancement techniques introduced in section 3.4.3. To enhance the performance of this nested hybrid decomposition algorithm and to accelerate the solution process, we develop two different parallelization schemes based on *parallel computing* concept. In contrast with the conventional techniques where the subproblems of the algorithms under investigation could be solved in series, we develop a parallelization framework, utilizing the multiprocessing capabilities of the computers, to solve our proposed hybrid decomposition algorithm in parallel. Essentially, two parallelization schemes are developed which are discussed in details below.

(i) ***Scheme 1***: The first scheme applies synchronous parallelization technique under SAA algorithm. In each iteration, SAA generates $|E|$ replications of problem **[LIPM(SAA)]**. Following this scheme, each of these replications are routed to different available processors and solved in parallel utilizing the enhanced L shaped algorithm. Note that the L-shaped algorithm solves the master problem **[M-LIPM]** and scenario-based subproblems **[S-LIPM(o)]** that are the relaxed version of the equivalent formulation of **[LIPM(SAA)]**. After all the replications are solved, the solutions are aggregated and the convergence of the SAA algorithm is checked. If the obtained gap is lower than the predefined threshold limit, then the SAA algorithm is terminated; otherwise, more SAA replications are generated and the process continues. Given that the SAA algorithm is converged in any iteration, we first calculate the upper bound of the CG algorithm and then check the convergence of the CG algorithm. If the CG algorithm provides solution of the desired quality, we stop the algorithm. Otherwise, we generate new points $\{R^{new}_{jt\omega}\}$ and $\{W^{new}_{kt\omega}\}$ and continue the process. The flow chart for this parallelization scheme can be seen in Figure 3.2.

(ii) ***Scheme 2***: The second parallelization scheme applies synchronous parallelization technique under the L-shaped algorithm introduced in section 3.4.3.

In each iteration r of the L-shaped algorithm, a master problem **[M-LIPM]** and a series of scenario-based subproblems **[S-LIPM(o)]** are solved. Following this scheme, each of these scenario-based subproblems are dynamically distributed to different available processors which are finally collected and aggregated upon solution. These aggregated solutions are then utilized to generate optimality cut (3.42) and apply different enhancement techniques discussed in section 3.4.3. Upon satisfaction of convergence requirements of the L-shaped algorithm, the next replication of the SAA algorithm (i.e., problem **[LIPM(SAA)]**) is solved following the same procedure. The process is continued until all replications of any particular iteration of the SAA algorithm are solved with desired quality. If such a quality is found, the current solution is used to calculate the upper bound of the outer loop (i.e., CG algorithm) of the proposed algorithm. We then check the convergence of the CG algorithm and generate new points ($\{R^{new}_{jt\omega}\}$ and $\{W^{new}_{kt\omega}\}$) if the convergence is not at desired level. The loop repeats until the CG algorithm provides a solution of the desired quality. The flow chart for this parallelization scheme can be seen in Figure 3.3.

3.5 Experimental Results

This section presents a real-life case study on model **[IPM]** that illustrates the performance of the proposed hybrid nested decomposition algorithm and to draw important managerial insights. The model and solution algorithms are coded in python 2.7 on a desktop computer with Intel Core i7 3.6 GHz processor and 32.0 GB RAM. Optimization solver Gurobi Optimizer 6.5[2] is used to solve the proposed mathematical model. Four states from the Southeast region of the United States, namely, Arkansas (AR), Louisiana (LA), Mississippi (MS), and Tennessee (TN) are selected as a testing ground to visualize and validate the modeling results. All

[2]Available from: `http://www.gurobi.com/`

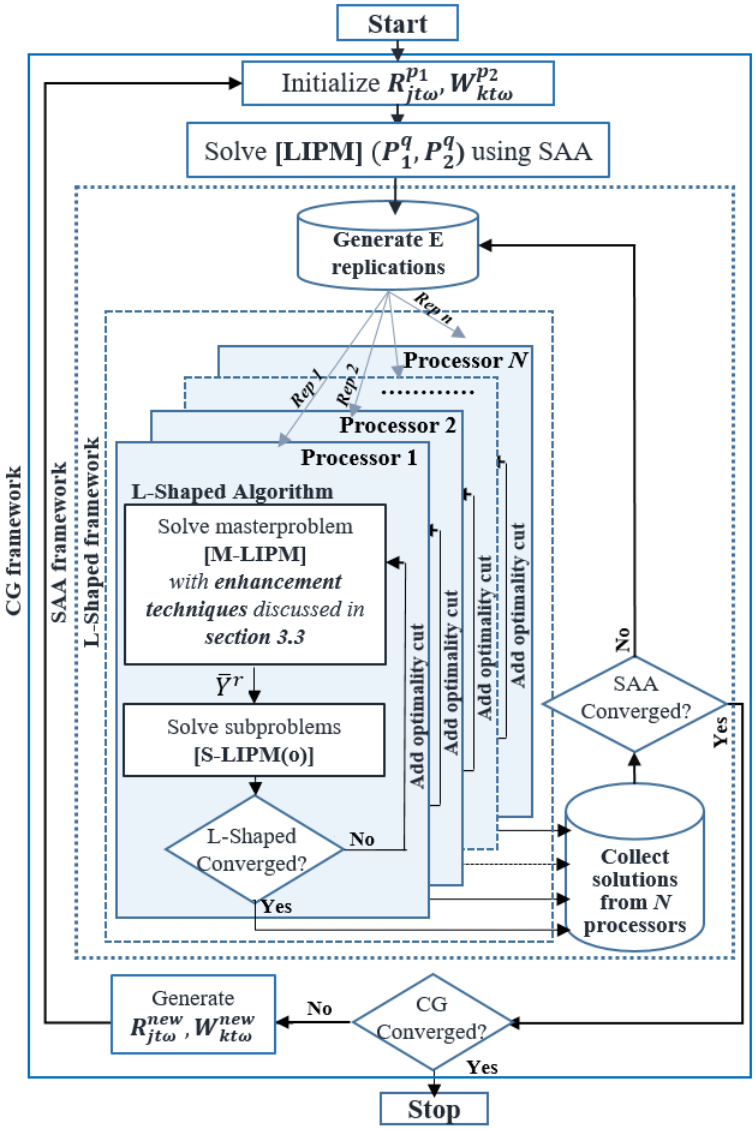

Figure 3.2

Parallelization scheme 1

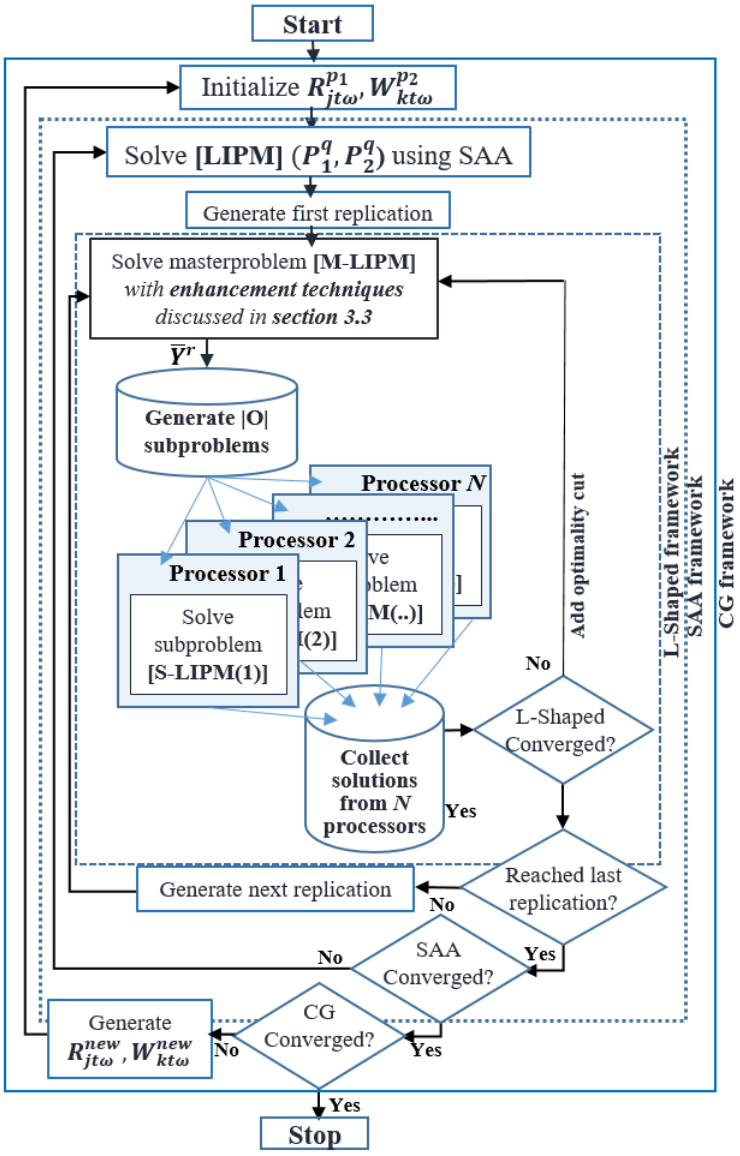

Figure 3.3

Parallelization scheme 2

costs are calculated based on 2018 dollars value. In following subsections, we briefly describe the input parameters used in this study, present the performance of the proposed solution algorithms, and summarize the managerial insights obtained from the experimental study.

3.5.1 Data Description

***Inland Waterway Port Location*:** In this study we consider a total of thirteen inland waterway ports along the Mississippi River. The geographical locations of these selected ports are shown in Figure 3.4. Among these thirteen ports, five ports, namely, the Port of Rosedale, Greenville, Vicksburg, Natchez, and the Yazoo County, are located in Mississippi. The first four of them are located alongside the Mississippi River, whereas the Port of Yazoo County stands along a stream flowing from the Mississippi River. The Port of Claiborne County is operationally unavialble [85]; therefore, we have excluded this port from further consideration. Besides, we consider few ports from Louisiana (e.g., the Port of Geismar Louisiana, Greater Baton Rouge, South Louisiana, and Gramercy) and Tennessee (e.g., the Port of Memphis, Pemiscot County, and New Madrid County), and the Port of Little Rock from Arkansas to construct the case study. All of these ports are directly connected with each other via the Mississippi River.

Figure 3.4

Inland waterway port locations along the Mississippi River

***Supply Data*:** This case study considers four commodities to be transported from their supply sites to demand locations via the transportation network under consideration. These selected commodities are rice, corn, woodchips, and fertilizer. The annual supply distribution (in 1,000 tons) of these four commodities in the test region can be seen in Figure 3.5. Suppliers located within a radius of 60 miles from the selected ports are only considered for the study. Among the selected commodities the first two, rice and corn, are highly seasonal in nature. These commodities are not available throughout the year. More specifically, rice is available only between August and October of each year whereas the harvesting period of corn starts from mid-July and ends by early December of each year [133]. The avaibality of woodchips remain fairly stable throughout the year except three months during the winter (December to February) [133]. Fertilizer is available throughout the year. The test region produces 6.3 and 113.8 million tons of rice and corn per year from 42 and 59 different counties, respectively [135]. On the other hand, 8.3 and 0.4 million tons of woodchips and fertilizer are supplied from 31 and 22 different counties, respectively [136, 137].

***Demand Data*:** In this study a total of 43 industries in Mississippi are considered as demand points for the selected commodities. These facilities are located near to any of the inland waterway ports under consideration. The annual demand for these commodities are set as 3.8, 68.3, 8.3, and 0.37 million tons of rice, corn, woodchips, and fertilizer, respectively [135, 137]. The location and distribu-

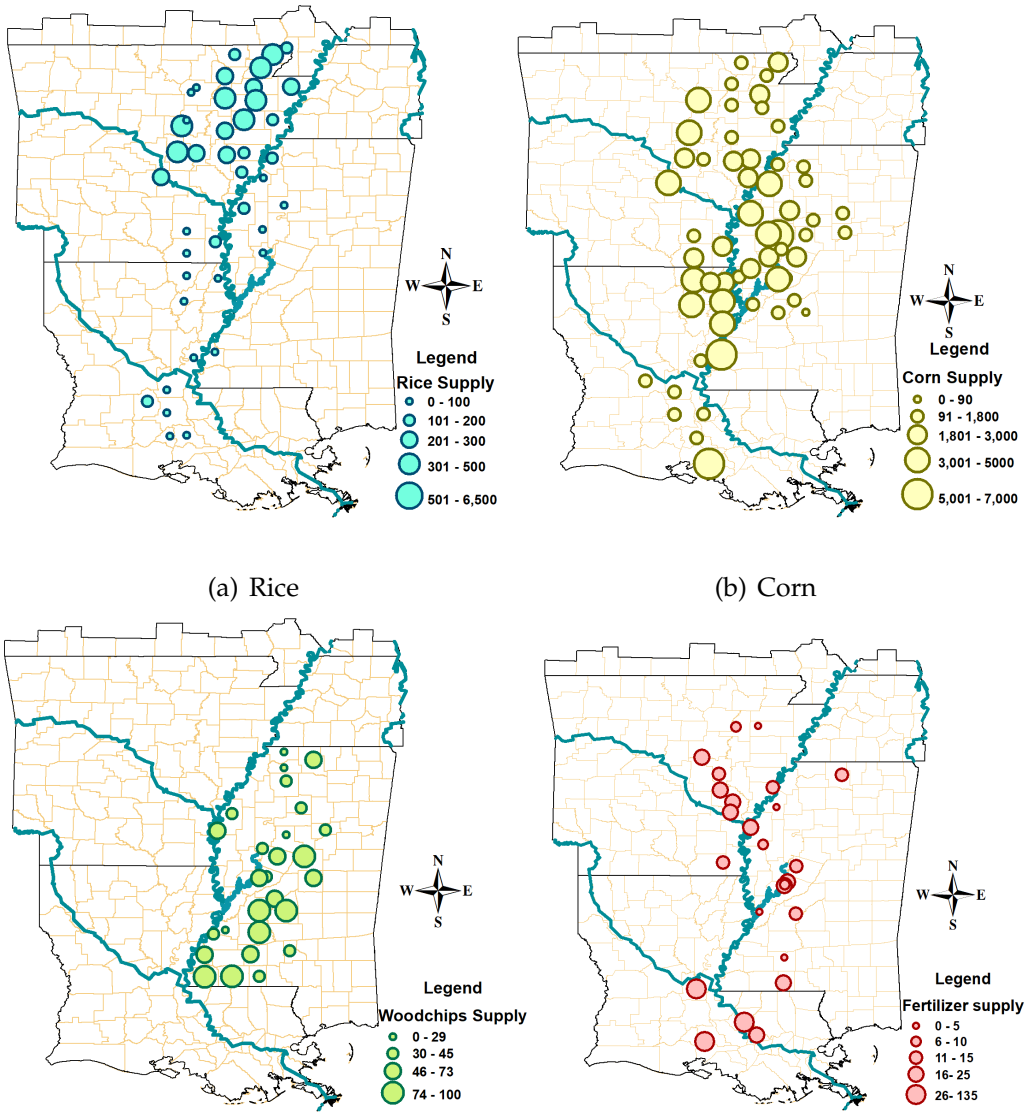

(a) Rice (b) Corn

(c) Woodchips (d) Fertilizer

Figure 3.5

Supply availability for (a) rice, (b) corn, (c) fertilizer, and (d) woodchips in the test region (in 1,000 tons)

tion of demand points for all the four commodities in Mississippi are presented in Figure 3.6.

***Transportation Costs*:** This study considers two transportation modes: *trucks* and *barges* for transporting commodities from their sources to destinations. Our study assumes that trucks will be used to transport commodities between supply sites $i \in \mathcal{I}$ to origin ports $j \in \mathcal{J}$ and destination ports $k \in \mathcal{K}$ to markets $g \in \mathcal{G}$. Additionally, trucks are also considered as useful alternatives to perform direct commodity transportation between supply sites $i \in \mathcal{I}$ and markets $g \in \mathcal{G}$. A semi truck with 25 tons of load capacity can be used to serve this purpose. The fixed cost (e.g., loading and unloading cost) and variable cost (e.g., fuel cost) associated with using any of such trucks can be \$5/ton and \$1.20/mile/truckload, respectively [36]. On the other hand, origin ports $j \in \mathcal{J}$ and destination ports $k \in \mathcal{K}$ are the two available set of points between which waterway transportation is primarily conducted with the association of barges and towboats. The capacity of towboats are considered as a maximum ($\overline{\delta}_s$) of 15 barges while utilizing towboats incur a fixed loading and unloading cost (ψ_{st}) of \$244.38 [138]. The barges are considered having a maximum design capacity ($\overline{w}_b$) of 1,500 tons each [138]. Barge usage cost is set as \$0.017/mile/ton, adopted from a study of Gonzales et al. [48].

***Waterlevel Fluctuations*:** Waterlevel fluctuation is one of the most prominent problem typically experiences by the inland waterway transportation system. Differ-

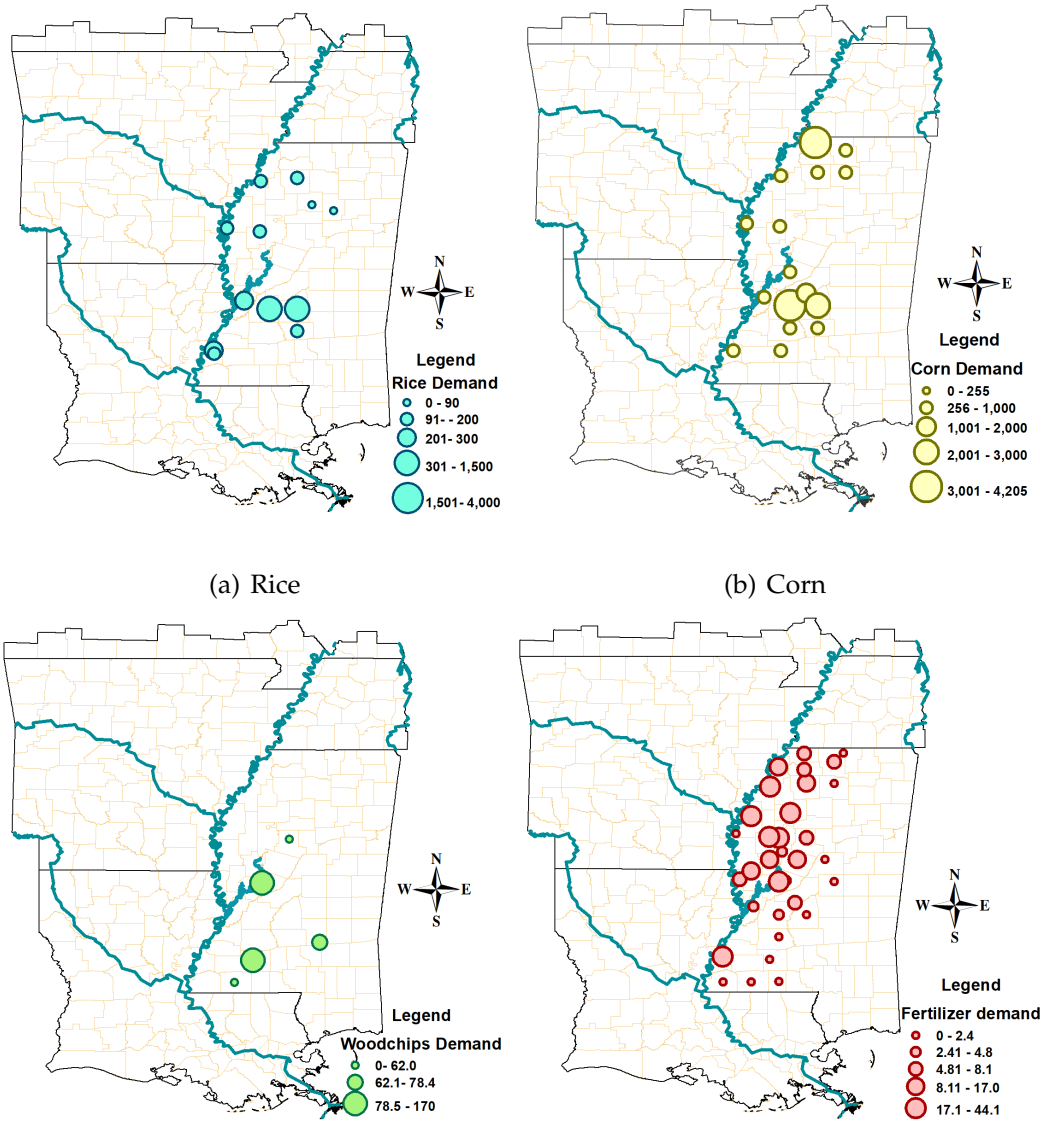

(a) Rice

(b) Corn

(c) Woodchips

(d) Fertilizer

Figure 3.6

Demand for (a) rice, (b) corn, (c) fertilizer, and (d) woodchips in the test region (in 1,000 tons)

ent waterbodies all over the world (e.g., Yangtze River at China [94], Rhine River at Europe [94], Tagliamento River at Europe [131], and many others) experience this unavoidable phenomenon in different time period of the year. The Mississippi River also experiences significant waterlevel fluctuations in different time period of a year which seriously impact the inland waterway port operations. For instance, the lower Mississippi River possess better flow compared to the upper Mississippi River; therefore, the load carrying capacity of this segment of the river is more sound and reliable compared to the upper Mississippi River. On the other hand, it is evident from the historical records that the waterlevel of this portion of river experiences significant variations year round that impacts the barge traffic flowing through this waterway. Often this fluctuation becomes extremely significant even in different weeks on the same month. A demonstration of waterlevel fluctuations between Port of Rosedale and Port of Greenville from July, 2016 to June, 2017 is provided in Figure 3.7 [139]. Each data point in Figure 3.7 shows the *water stage*[3] variation (e.g., minimum, maximum, and average waterlevel) per week as reported by the US Army Corps of Engineers [139]. We can notice from the figure that between the middle of August and end of December of a calender year, the waterlevel drops become more prominent, showing the maximum during the first three weeks of October (week 14-16 in Figure 3.7). Other than these specific periods, the water stage generally remains above the desired level of 14.2

[3]Water stage is a popular measure of waterlevel in a river stream with respect to a reference height

feet for other time periods, except in May when the level reaches to 42 feet, which is higher than the flood level (37 feet) [139].

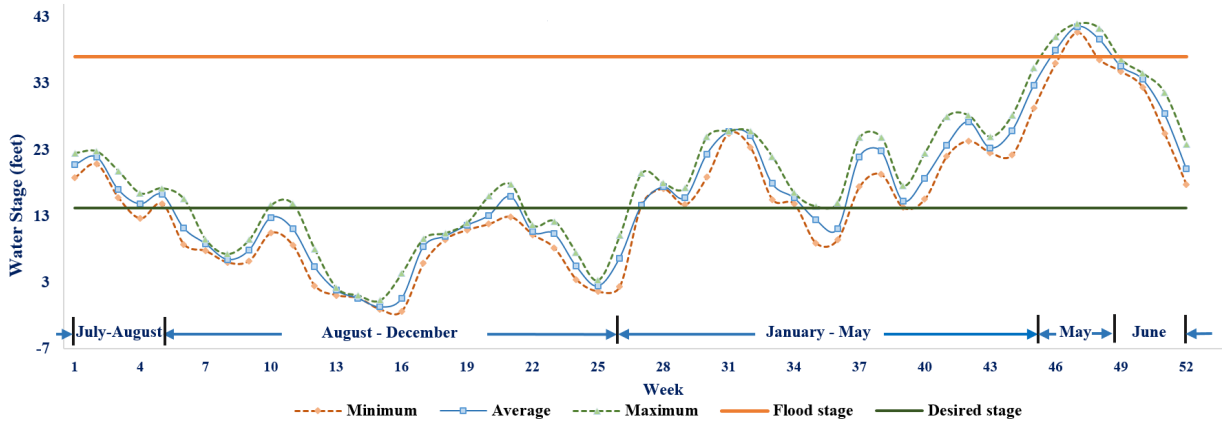

Figure 3.7

Demonstration waterlevel fluctuations between Port of Rosedale and Port of Greenville from July, 2016 to June, 2017 [139]

3.5.2 Real-life Case Study

This subsection illustrates how the proposed model and solution approaches can be used to derive important managerial insights from solving a real-world problem. In order to show the impact of different key input parameters, a number of experiments are conducted. This section provides a comprehensive summary of the experimental results.

The first set of experiments examine the impact of water level fluctuation ($\overline{w}_{jkt\omega}$) on overall system performance. Depending on the observations in Figure 3.7, we generate four different waterlevel scenarios considering $\pm 20\%$ and $\pm 40\%$ changes in base mean waterlevel ($\overline{w}_{jkt\omega}$) fluctuations. Figure 3.8 summarizes the key results of this experiment. Note that in Figure 3.8 and the following figures, $t = 1$ stands for a representative week of month July, and the following 11 months are represented in ascending order ending at $t = 12$ which is a representative week of June. Figure 3.8(a) shows that with 20% and 40% increase in mean $\overline{w}_{jkt\omega}$, barge selection (Y_{mbsjt}) drops by 8.48% and 24.14%, respectively, from the base case scenario. On the other hand, a 20% and 40% reduction in mean $\overline{w}_{jkt\omega}$ cause barges to carry less load from their design capacity which in turn rises Y_{mbsjt} selection by 13.25% and 25.33%, respectively, from the base case scenario. The peak barge usage is observed in the month of October ($t = 3$) when the waterlevel drop is most severe. Additionally, Figure 3.8(b) shows that the barge to towboat ratio (Y_{mbsjt}/Y_{snjkt}) increases with a mean reduction in $\overline{w}_{jkt\omega}$. To be specific, with 40% drop in $\overline{w}_{jkt\omega}$, this ratio reaches to a maximum of 15 barges per towboat (see $t = 2$ to 5 in Figure 3.8(b)). As evident from Figure 3.7 that the waterlevel drop is not significant between January to July. Therefore, we do not observe any significant deviations in transportation decisions for those time periods, as can be seen even for 20% and 40% increment on $\overline{w}_{jkt\omega}$ in Figures 3.8(a) and (b). To magnify the impact of congestion under different $\overline{w}_{jkt\omega}$ scenarios, few additional experiments are conducted by considering and ignoring the congestion terms in model **[IPM]**. As observed

in Figures 3.8(c) and (d), the system could utilize an additional 21.89% and 10.5% barges even in the worst (-40% change in $\overline{w}_{jkt\omega}$) and best (+40% change in $\overline{w}_{jkt\omega}$) waterlevel scenarios, respectively, if the congestion terms are dropped from model **[IPM]**. Further, it is realized that the barges are now required to adjust their weight carrying capacities according to the waterlevel conditions as illustrated in Figure 3.8(d).

The next set of experiments study the impact of system performance under different commodity supply $\phi_{mit\omega}$ scenarios. To run these experiments, we create different instances by changing the mean supply ($\overline{\phi}_{mit}$) by $\pm$25% and $\pm$50% from the base supply. Figure 3.9 illustrates the impact of $\overline{\phi}_{mit}$ changes in barge (Y_{mbsjt}) and towboat (Y_{snjkt}) selection. With 25% and 50% increase in $\overline{\phi}_{mit}$, it is observed that the Y_{mbsjt} and Y_{snjkt} selections are increased by 11.21% and 4.42%, respectively, from the base case scenario. Further, when $\overline{\phi}_{mit}$ is changed by -25%/-50%, Y_{mbsjt} and Y_{snjkt} decisions are accordingly changed by -6.7%/-15.3% and -12.05%/-15.1%, respectively, from the base case. This indicates that the selection of Y_{mbsjt} and Y_{snjkt} decisions are highly sensitive to supply availability.

The system performance is further inspected by considering and ignoring congestion (e.g., $c^o_{jt} = 0; \forall j \in \mathcal{J} \bigcup \mathcal{K}, t \in \mathcal{T}$) under $\overline{\phi}_{mit}$ changes. Moreover, to appropriately capture these cases, we create two timeframes, namely, *peak* and *low impact season*, when the supply availabilities are respectively high and low. Due to the harvesting seasons of many agricultural products (e.g., corn, rice), we select September to November as the *peak season* and other months of the year as *low*

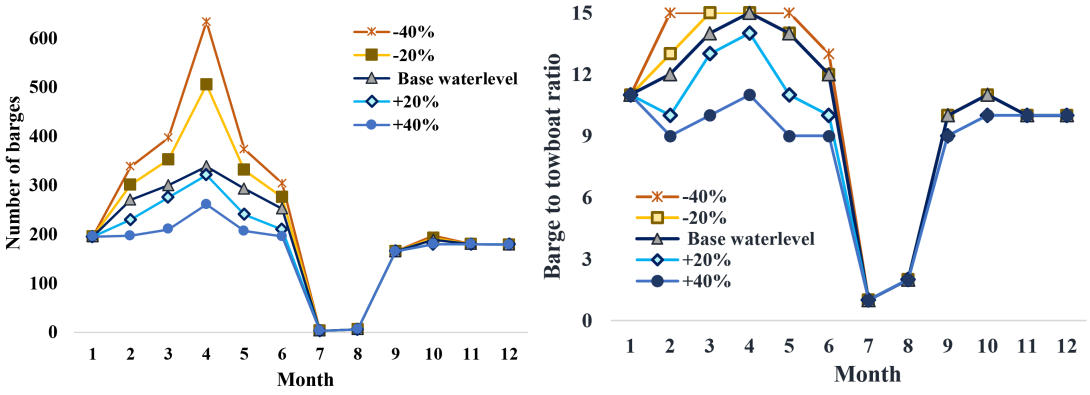

(a) Number of barges used (Y_{mbsjt})

(b) Barge to towboat ratio (Y_{mbsjt}/Y_{snjkt})

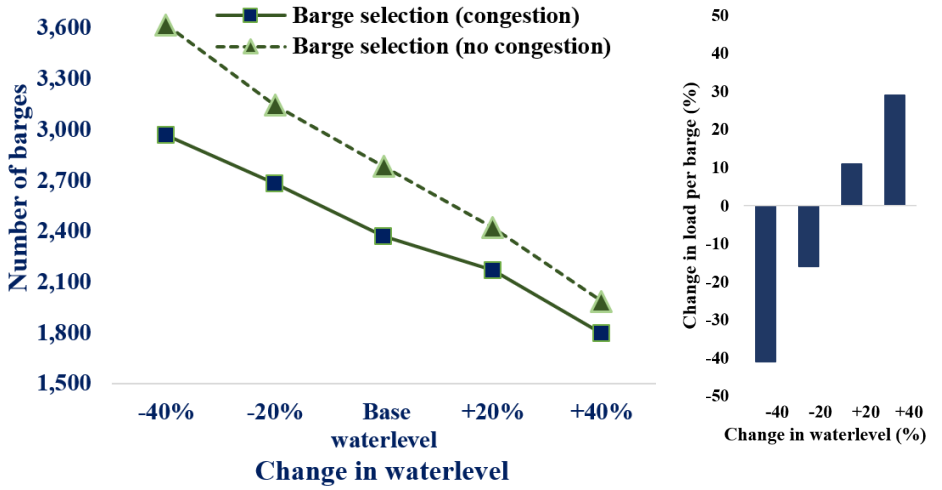

(c) Total barges used

(d) Change in load per barge

Figure 3.8

Impact of $\bar{w}_{jkt\omega}$ changes on overall system performance

impact season. Figure 3.10 demonstrates the impact of $\overline{\phi}_{mit}$ changes on overall system performance with and without considering the congestion cost. Note that in Figure 3.10, we denote $\overline{Y}_{mbsjt}$ and $\overline{U}_{mgt\omega}$ to be the average number of barges used and unsatisfied demand over the peak and low impact seasons. It is observed that compared to the base case 37.7% additional barges are now required to be used during the *peak* season if the congestion effect could be ignored. The impact is even more significant when $\overline{\phi}_{mit}$ continue to be increased (see Figure 3.10(b)). However, this number drops down to only 4.3% for the *low impact season* as can be seen in Figure 3.10(a). Figure 3.10(c) further illustrates the impact of congestion on $\overline{Y}_{mbsjt}$ and $\overline{U}_{mgt\omega}$ decisions. More specifically, we observe that $\overline{U}_{mgt\omega}$ drops with an increase in $\overline{\phi}_{mit}$ quantity. However, this drop can be as much as approximately 49.4% if the congestion terms are ignored in model **[IPM]**. To summarize, it can be observed that congestion significantly restricts the commodity transportation under all supply scenarios; therefore, additional capacity enhancements on waterways and ports might provide long term benefits in minimizing its effect and retain sound commodity transportation.

3.5.3 Performance Evaluation of the Algorithms

This section presents our computational experiences in solving model **[LIPM]** using the algorithms presented in Section 3.4. To test the performance of the solution algorithms, we first vary $|\mathcal{I}|$, $|\mathcal{J}|$, $|\mathcal{K}|$,$|\mathcal{G}|$, and $|\Omega|$ to generate 9 different problem instances. These instances are summarized in Table 3.1. We use the following cri-

teria to terminate the algorithms: (i) the optimality gap (i.e., $\epsilon = |UB - LB|/UB$) falls below a threshold value (e.g., $\epsilon = 1.0\%$); (ii) the maximum time limit (t^{max}) is reached (e.g., $t^{max} = 10,800$ CPU seconds); or (iii) the maximum iteration limit (q^{max}) is reached (e.g., $q^{max} = 100$). To help readers follow our solution approaches, the following notations are used to represent each particular variants of the proposed algorithms.

- **CG**: Constraint Generation Algorithm.
- **CG+SAA**: Hybrid algorithm combining Constraint Generation Algorithm and Sample Average Approximation discussed in Sections 3.4.1 and 3.4.2.
- **CG+SAA+L**: Hybrid decomposition algorithm combining Constraint Generation Algorithm, Sample Average Approximation, and L-shaped algorithm discussed in Sections 3.4.1-3.4.3.
- **CF-I**: Hybrid decomposition algorithm combining Constraint Generation Algorithm, Sample Average Approximation, and L-shaped algorithm with enhancements discussed in Sections 3.4.3.1–3.4.3.3, 3.4.3.6, and *Type A* Mean-value cut.
- **CF-II**: Hybrid decomposition algorithm combining Constraint Generation Algorithm, Sample Average Approximation, and L-shaped algorithm with enhancements discussed in Sections 3.4.3.1– 3.4.3.4, 3.4.3.6, and *Type B* Mean-value cut.
- **PS-I**: Parallelization scheme I discussed in Section 3.4.4.
- **PS-II**: Parallelization scheme II discussed in Section 3.4.4.
- **CF-I + PS-I**: Parallelization scheme I is applied over hybrid algorithm **CF-I**.
- **CF-I + PS-II**: Parallelization scheme II is applied over hybrid algorithm **CF-I**.
- **CF-II + PS-I**: Parallelization scheme I is applied over hybrid algorithm **CF-II**.
- **CF-II + PS-II**: Parallelization scheme II is applied over hybrid algorithm **CF-II**.

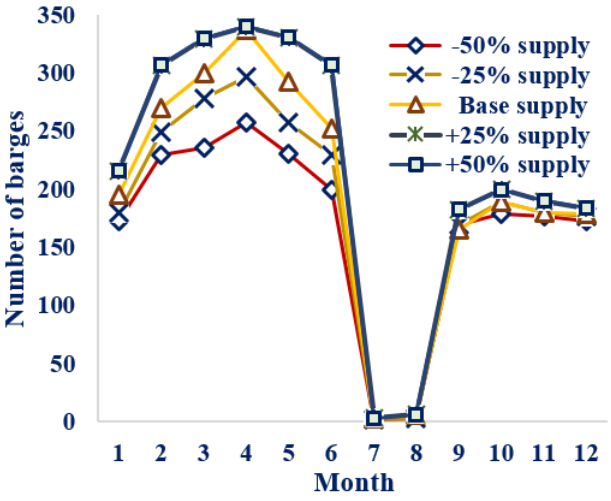

(a) Barge selection (Y_{mbsjt})

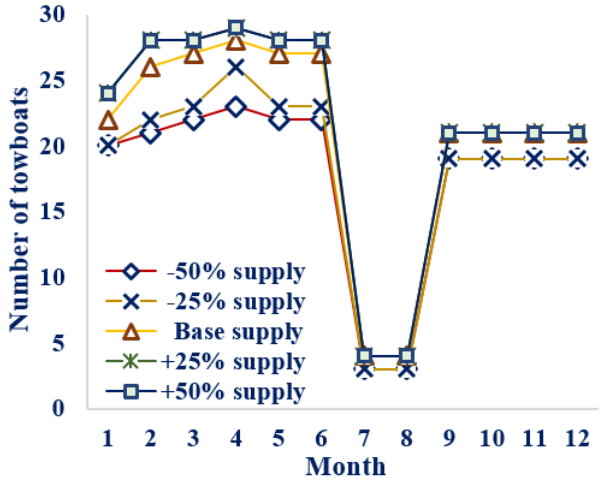

(b) Towboat selection (Y_{snjkt})

Figure 3.9

Impact of supply ($\overline{\phi}_{mit}$) changes on (a) barge and (b) towboat selection

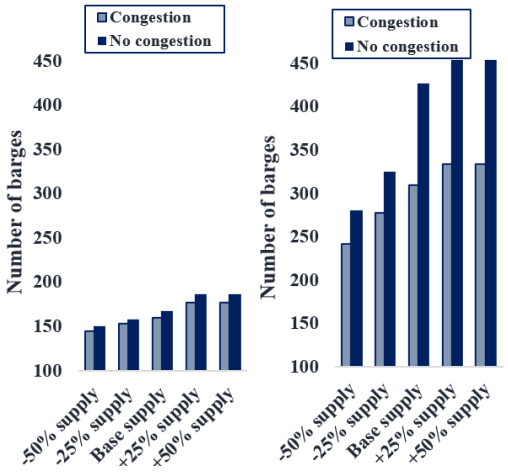

(a) $\overline{Y}_{mbsjt}$ in *low impact season*

(b) $\overline{Y}_{mbsjt}$ in *peak season*

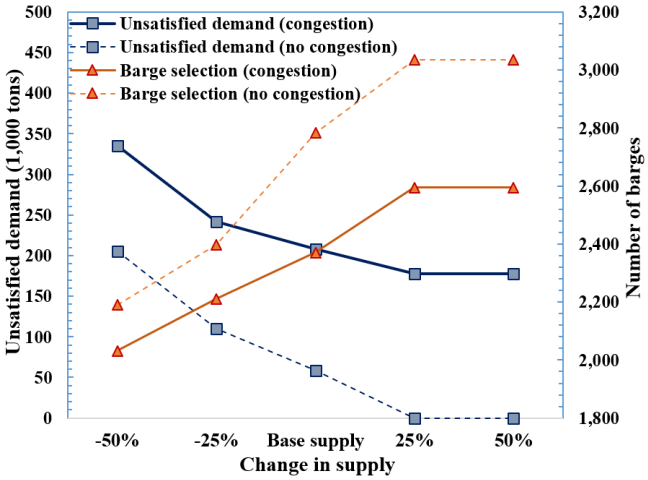

(c) Changes in $\overline{\phi}_{mit}$ on $\overline{Y}_{mbsjt}$ and $\overline{U}_{mgt\omega}$

Figure 3.10

Impact of supply ($\overline{\phi}_{mit}$) changes on $\overline{Y}_{mbsjt}$ and $\overline{U}_{mgt\omega}$ decisions

Table 3.1

Problem size and test instances

Instance No.	$\|\mathcal{I}\|$	$\|\mathcal{J}\|$	$\|\mathcal{K}\|$	$\|\mathcal{G}\|$	$\|\mathcal{M}\|$	$\|\mathcal{B}\|$	$\|\mathcal{S}\|$	$\|\mathcal{N}_{jk}\|$	$\|\mathcal{T}\|$	$\|\Omega\|$	Binary variables	Continuous variables	Total variables	No. of constraints
1	40	4	4	20	4	15	10	10	12	20	48,000	24,067,200	24,115,200	2,981,280
2	40	4	4	20	4	15	10	10	12	30	48,000	36,100,800	36,148,800	4,456,800
3	40	4	4	20	4	15	10	10	12	40	48,000	48,134,400	48,182,400	5,932,320
4	60	8	8	30	4	15	10	10	12	20	134,400	94,627,200	94,761,600	10,584,384
5	60	8	8	30	4	15	10	10	12	30	134,400	141,940,800	142,075,200	15,825,024
6	60	8	8	30	4	15	10	10	12	40	134,400	189,254,400	189,388,800	21,065,664
7	83	13	5	43	4	15	10	10	12	20	259,200	98,333,280	98,592,480	11,502,636
8	83	13	5	43	4	15	10	10	12	30	259,200	147,499,920	147,759,120	17,196,156
9	83	13	5	43	4	15	10	10	12	40	259,200	196,666,560	196,925,760	22,889,676

The first set of experiments study the impact of different variants of the proposed algorithms discussed in Section 3.4 without parallelization i.e., approaches **CG**, **CG+SAA**, **CG+SAA+L**, **CF-I**, and **CF-II**, respectively. Table 3.2 summarizes the computational results obtained from this set of experiments. Note that in reporting the computational results in Table 3.2 and as well as in the following tables, we highlight the algorithm which produces the smallest running time given all the instances are solved by other algorithms under investigation within the pre-specified optimality gap. However, if such a quality solution is not found within the maximum time or iteration limit, then the algorithm with the smallest optimality gap is highlighted. We now summarizes the key observations from Table 3.2 below:

- Results in Table 3.2 indicate that the basic **CG** algorithm is only able to solve 1 out of 9 problem instances within the pre-specified termination criteria. For the remaining instances (instances 2-9), Gurobi gets *out of memory* (OOM) in solving model **[LIPM]**. The computation performance improves slightly when **SAA** algorithm is integrated with the **CG** algorithm, namely, the **CG+SAA** algorithm. With this hybrid technique, we now can able to solve an additional instance (instance 2) within the pre-specified termination criteria, but the status of 5 out of 9 problem instances still remain *out of memory*. We further observe a slight improvement in computational performances when L-shaped algorithm is incorporated with the **CG+SAA** algorithm, namely, the **CG+SAA+L** algorithm. With this incorporation, 3 out of 9 instances are now solvable within the pre-specified termination criteria while, most importantly, none of the instances get out of memory even though leaving with a high optimality gap within the time limit.
- Additional experiments are then conducted to examine how different accelerated techniques in the L-shaped algorithm enhance the computational performances of the **CG+SAA+L** algorithm, namely, the **CF-I** and **CF-II** algorithms. Results in Table 3.2 further indicate that on average **CF-I** and **CF-II** algorithms save 5.35% and 12.54% computational time, respectively, over the **CG+SAA+L** algorithm. Additionally, the average optimality gap of the **CF-I** and **CF-II** algorithms now drop down to 6.04% and 4.51%, respectively,

from 16.99% as reported by the **CG+SAA+L** algorithm. Note that the difference between **CF-I** and **CF-II** algorithms is the incorporation of the scenario bundling technique as discussed in section 3.4.3.4. To summarize, algorithm **CF-II** demonstrates high computational performance over **CF-II** but leaves with high optimality gap in solving problem **[LIPM]** within the pre-specified time limit.

Table 3.2

Experimental result for all cuts presented in section

Instance	**CG**			**CG+SAA**			**CG+SAA+L**			**CF-I**			**CF-II**		
No.	$t(sec)$	$\epsilon(\%)$	q	$t(sec)$	$\epsilon(\%)$	q	$t(sec)$	$\epsilon(\%)$	q	$t(sec)$	$\epsilon(\%)$	q	$t(sec)$	$\epsilon(\%)$	q
1	5,219	0.99	1	4,788	0.75	2	4,321	0.43	2	3,370	0.06	2	**3,236**	0.02	2
2	OOM			7,150	0.88	2	3,386	0.52	1	5,418	0.05	2	**4,767**	0.13	2
3	OOM			10,800	4.24	3	9,345	0.33	2	6,516	0.11	2	**5,473**	0.09	2
4	OOM			10,800	25.98	2	10,800	24.12	1	8,167	0.97	1	**6,996**	0.73	1
5	OOM			OOM			10,800	23.12	1	10,800	8.11	2	**7,913**	0.87	1
6	OOM			OOM			10,800	24.93	1	10,800	7.12	2	10,800	**5.64**	2
7	OOM			OOM			10,800	27.12	1	10,800	8.07	2	10,800	**6.12**	2
8	OOM			OOM			10,800	25.42	1	10,800	**10.42**	1	10,800	11.54	1
9	OOM			OOM			10,800	26.92	1	10,800	19.42	1	10,800	**10.19**	1
Average	5,219	0.99	1	8,385	7.96	2	9,095	16.99	1	8,608	6.04	2	**7,954**	**4.51**	2

OOM: out of memory

Realizing from the results in Table 3.2 that even though algorithms **CF-I** and **CF-II** demonstrate high potential, on average 50% instances still remain unsolved within the pre-specified time limit. Hence, we employ different parallelization techniques, namely, the **PS-I** and **PS-II** algorithms, to further improve the computational performances of the **CF-I** and **CF-II** algorithms. The results are reported in

Tables 3.3 and 3.4, respectively. The key findings from these computational results are summarized below:

- As evidenced from the results in Table 3.3 that the incorporation of Parallelization scheme I (**PS-I** algorithm) in **CF-I** algorithm, namely, the **CF-I+PS-I** algorithm, significantly drops the optimality gap and running time of the basic **CF-I** algorithm. On average, we observe a drop in running time by 52.9% while producing an optimality gap of 0.36% by **CF-I+PS-I** over the **CF-I** algorithm. Most importantly, algorithm **CF-I+PS-I** is now capable of solving all the problem instances reported in Table 4.1 by obeying the pre-specified termination criteria. Note that even though the incorporation of Parallelization scheme II (**PS-II** algorithm) in **CF-I** algorithm, namely, the **CF-I+PS-II** algorithm, slightly improves the computation performances (both in running time and optimality gap) of the basic **CF-I** algorithm, 4 out of 9 instances still left with high optimality gap.

- Similar observations can also be made with the **CF-II** algorithm (shown in Table 3.4) when both Parallelization schemes I and II are incorporated with the **CF-II** algorithm, namely, the **CF-II+PS-I** and **CF-II+PS-II** algorithms. Yet again we observe that algorithm **CF-II+PS-I** is capable of solving all the problem instances reported in Table 3.1 in less than 1% optimality gap while solving problem **[LIPM]** approximately twice faster than the **CF-II** algorithm. On the other hand, the **CF-II+PS-II** algorithm, even though drops the average optimality gap of the **CF-II** algorithm from 4.15% to 2.43%, still unable to solve 4 out of 9 problem instances by obeying the pre-specified termination criteria.

- Our final observations can be made between the **CF-I+PS-I** and **CF-II+PS-I** algorithms where it is evident from the results in Tables 3.3 and 3.4 that **CF-II+PS-I** slightly outperforms **CF-I+PS-I** with respect to both running time and optimality gap produced by the algorithms. Even though both **CF-I+PS-I** and **CF-II+PS-I** algorithms are now capable of solving all the problem instances reported in Table 3.1 in less than 1% optimality gap, algorithm **CF-II+PS-I** saves an additional 8.8% running time in solving problem **[LIPM]** while producing the optimality gaps reported by Tables 3.3 and 3.4, respectively. To summarize, algorithm **CF-II+PS-I** seems to offer high quality solutions consistently within our tested experimental range.

Table 3.3

Experimental results for **CF-I** under different parallelization schemes

Instance	**CF-I**			**CF-I+PS-I**			**CF-I+PS-II**		
No.	$t(sec)$	$\epsilon(\%)$	q	$t(sec)$	$\epsilon(\%)$	q	$t(sec)$	$\epsilon(\%)$	q
1	3,370	0.06	2	**927**	0.03	2	2,759	0.06	2
2	5,418	0.05	2	**1,449**	0.08	2	4,851	0.39	2
3	6,516	0.11	2	**1,873**	0.42	2	5,697	0.42	2
4	8,167	0.98	1	**2,287**	0.16	1	7,292	0.06	1
5	10,800	8.12	2	**4,631**	0.10	2	8,942	0.80	1
6	10,800	7.12	2	**6,153**	0.56	2	10,800	3.22	2
7	10,800	8.08	2	**4,123**	0.49	1	10,800	3.89	2
8	10,800	10.43	1	**9,071**	0.50	2	10,800	14.53	1
9	10,800	19.43	1	**10,214**	0.87	2	10,800	17.65	1
Average	8,608	6.04	2	**4,550**	0.36	2	8,082	4.56	2

Table 3.4

Experimental results for **CF-II** under different parallelization schemes

Instance	**CF-II**			**CF-II+PS-I**			**CF-II+PS-II**		
No.	$t(sec)$	$\epsilon(\%)$	q	$t(sec)$	$\epsilon(\%)$	q	$t(sec)$	$\epsilon(\%)$	q
1	3,236	0.02	2	**895**	0.11	2	2,515	0.03	2
2	4,767	0.14	2	**1,289**	0.20	2	4,107	0.06	2
3	5,473	0.09	2	**1,607**	0.26	2	4,752	0.27	2
4	6,996	0.74	1	**1,995**	0.12	1	5,894	0.16	1
5	7,913	0.87	1	**3,279**	0.22	1	6,589	0.30	1
6	10,800	5.65	2	**5,817**	0.44	2	10,800	4.19	2
7	10,800	8.12	2	**3,998**	0.27	1	10,800	3.71	2
8	10,800	11.55	1	**8,469**	0.30	2	10,800	5.53	1
9	10,800	10.20	1	**9,979**	0.38	2	10,800	7.65	1
Average	7,954	4.15	2	**4,148**	0.26	2	7,451	2.43	2

3.6 Conclusion and Future Research Directions

This paper proposes a two-stage stochastic non-linear programming model to design and manage an inland waterway transportation-based logistics network while stochastic nature of commodity supply and water-level fluctuations are taken into consideration. The model is designed to jointly optimize trip-wise towboat and barge assignment decisions and different supply chain decisions (e.g., inventory management, transportation decisions) in such a way that the congestion as well as the overall system cost can be minimized under uncertainty. We present a parallelized hybrid nested decomposition algorithm to solve our proposed model. Results indicate that the presented parallelization schemes with hybrid nested decomposition algorithm can efficiently solve our proposed optimization model in a timely manner. We utilize few Southeast US States as a testbed to visualize and validate the modeling results. A number of managerial insights, including the impact of uncertain water level fluctuation and supply, and port congestion on the inland waterway transportation network, are drawn from the case study.

To summarize, the major contributions of this study include: (i) proposing a multi-commodity, multi-time period two-stage stochastic non-linear programming model that not only optimizes the inland waterway port operations but also minimizes the overall system cost considering the impacts of congestion under supply uncertainty; (ii) presenting and testing an efficient hybrid nested decomposition algorithm combining Constraint Generation Algorithm, Sample Average Approximation, and an enhanced L-shaped Algorithm to solve realistic-size

network design problems; (iii) developing and testing different parallelization schemes to parallelize the proposed nested decomposition algorithm; and (iv) drawing managerial insights from a real-life case study. Note that the proposed methodologies can be adopted to efficiently solve different stochastic optimization problems. Further, the managerial insights obtained from this study may help decision makers to design and manage a cost-efficient inland waterway-based supply chain network under uncertainty.

This study can be extended in several research directions. First, it would be interesting to see how the detailed consideration of barge and tow routing, scheduling, and re-positioning issues impact the inland waterway port operations. Next, the impacts of port operations under both natural (e.g., hurricane, tornado) and/or human-induced (e.g., cyber attack) disruptions also need to be investigated. These issues will be addressed in future studies.

CHAPTER 4

SOLVING A STOCHASTIC INLAND WATERWAY PORT MANAGEMENT PROBLEM USING A PARALLELIZED HYBRID DECOMPOSITION ALGORITHM

4.1 Introduction

Inland waterway ports are indispensable components of a nation's overall transportation system and to the economy. In the U.S., the annual GDP (Gross Domestic Product) contribution of these ports are approximately 15 billion dollars while creating more than 250,000 annual employment opportunities from this transportation sector [89]. Apart from these benefits, inland waterway ports greatly contribute to a nation's rural industrial and agricultural development [84]. However, despite of their substantial potentiality, this segment of transportation system is frequently impacted by many factors that hurts its productivity, including but not limited to high water level fluctuations, congestion, aging infrastructure, delays caused by scheduled and unscheduled closures of locks (primarily due to maintenance activities), and many others [140]. For instance, in the early 2011, a severe flood affected the inland waterway system of the U.S., causing a total damage of approximately $8.5 billions. However, in the very next year, waterways experienced severe drought causing a number of barges to run aground [140]. Consider-

ing the severity and frequency of this vital inland waterway-specific issue and the long term sustainment of this transportation sector, developing reliable optimization models that account for different factors which frequently impact the inland waterway port operations (e.g., waterway fluctuations, commodity supply fluctuations, barge/towboat maintenance and availability, delays in locks) are of utmost importance.

Inland waterway transportation holds some distinctive properties which makes it different from the seaports. To mention a few, these ports generally handle barge traffic drafting up to 9 feet only, are located primarily near smaller bodies of water (e.g., rivers and canals), usually land intensive, and/or handle smaller counts of larger users and a large number of smaller users [84]. Additionally, the water level at the port channels and any part of the waterway, connecting two inland waterway ports, undergo severe fluctuations in different time periods of the year [139]. Depending on the severity of this fluctuation, these ports, including the waterway itself, often experience disruptions, such as drought and flood that may tremendously impact or even cease the port operations for a prolonged period of time. Further, these ports commute heavy volume of highly seasonal and perishable commodities (e.g., rice, corn, woodchips, soybean). The seasonality of the commodities coupled with time varying waterway conditions excessively delay the port operations, which directly impacts the operational planning of the ports under consideration. All these prevalent challenges restrict the optimization models available in the literature for the maritime transportation to be directly applicable

for the inland waterway ports. Therefore, in order to ensure long term sustainment of the inland waterway ports, sophisticated optimization models need to be developed that best capture the unique characteristics of this cost efficient, reliable, and environmentally-friendly transportation sector.

Among different variants of the waterway port-specific problems, a number of research develops optimization models to address diversified seaport-related problems, such as ship routing and scheduling [29], inventory routing [5], berth allocation and scheduling [141], empty container re-positioning [43], sailing speed optimization [141], bunker consumption [145], emission consideration [141], disruption [126, 56], port delays [148], and many others. Few researchers attempted to develop simulation models to address those similar problems (e.g., [125, 44]). Even though deep penetration to seaport research is observed, inland waterway ports did not receive much attention from the research community. A few studies has been carried out that characterize and model the specifics of *deep draft inland ports*, capable of handling container cargos and ships; however, almost no research has been conducted to date that puts specific considerations to model *shallow draft inland ports*[1]. Realizing their significance on the overall transportation system and economy, better understanding of the shallow draft inland waterway ports is imperative in order to successfully design and manage a sound and efficient inland waterway transportation network.

[1]The ports that are unable to handle barges/vessels drafting more than 9 feet are known as *shallow draft inland ports*. *Deep draft inland ports*, on the other hand, are the ones that can handle barges/vessels drafting more than 9 feet.

To fill this research gap, this study proposes a mathematical model that realistically captures different inland waterway port-related issues (e.g., water level fluctuations, barge/towboat assignments and availabilities, weight and volumetric capacity restrictions of barges, product mix restrictions, storage restrictions) under a same decision making framework and illustrates their impacts on designing and managing an inland waterway transportation network. More specifically, we propose a capacitated, multi-commodity, multi-period, two-stage stochastic mixed-integer linear programming model that jointly optimizes trip-wise barge and towboat assignment decisions along with different crucial supply chain decisions (e.g., inventory management, transportation decisions) with a goal of minimizing the overall system cost under water level and commodity supply uncertainty.

The proposed mathematical model is an extension of a fixed charged, uncapacitated network flow problem, which is already known to be an $\mathcal{NP}$-hard problem [74]. To alleviate this challenge and to obtain solutions within a limited computational time, we develop a highly customized parallelized hybrid decomposition algorithm which combines Sample Average Approximation with an enhanced Progressive Hedging (PH) and Nested Decomposition (ND) algorithm. Several techniques are used to enhance the PH algorithm, such as penalty parameter updating, global and local heuristics, and scenario bundling techniques. On the other hand, techniques, such as problem-specific valid inequalities, strengthened Benders and Lagrangian cuts, are used to enhance the performance of the ND algo-

rithm. To the end, two parallelization schemes are proposed to parallelize the entire hybrid decomposition algorithm. Extensive computational experiments are presented to demonstrate how the parallelized hybrid decomposition algorithm effectively and efficiently solves the proposed mathematical model.

Apart from proposing the mathematical model and solution approaches, we demonstrate a real-life application by utilizing the inland waterway transportation network along the lower Mississippi River. The outcome of this study provides a number of managerial insights, such as the impact of water level fluctuations on towboat and barge selection and commodity supply fluctuations on overall system performance, which may effectively aid decision makers to design a cost-efficient shallow draft inland waterway transportation network.

this paper is organized as follows. Section 4.2 provides a comprehensive review of the related works and distinguish our work with the existing literature. Section 4.3 discusses the problem and introduces the proposed mathematical model. The decomposition algorithms used to solve our proposed model are outlined in Section 4.4. Section 4.5 presents a real life case study and discusses the computational performances of the proposed algorithms. Finally, Section 4.6 concludes this study and discusses future research directions.

4.2 Literature Review

Deep draft inland waterway ports have received tremendous attention from the research community in the last years. Different researchers have studied several

realistic aspects of the deep draft inland waterway ports, including barge and tow-boat routing and repositioning problem, berth allocation, port disruption, delays in locks and dams, and few others. This section provides a comprehensive review on these specific research problems and distinguishes our work from the existing literature.

Berth allocation problem is a common problem that typically experiences by both seaports and inland waterway ports. To date, few researchers have attempted to solve this problem for the deep draft inland waterway ports. For instance, Grubivsic et al. [50] solve a berth layout design problem to minimize the overall vessel waiting time. Depuy et al. [30] consider several factors, such as fleet location capacity, total volume of barges, and average handling time, to optimally allocate barge volume to different fleet locations. Arango et al. [11] adopt a combined simulation-optimization approach to solve a berth allocation problem.

In addition to this research challenge, another stream of research studies how the performances of locks and dams impact the deep draft inland waterway transportation network. For instance, Ting and Schonfeld [130] utilize a simulation-optimization framework to decide how much capacity increment is required for the locks so that the costs associated with tow delays can be minimized. Wang and Schonfeld [147] also adopt a combined simulation-optimization approach to schedule the investment decisions for lock reconstruction and rehabilitation. Most recently, Tan et al. [127] propose an optimization model that jointly optimizes ship

schedule and sailing speed for the deep draft inland shipping services under uncertain dam transit time.

Another stream of research focuses on optimizing the barge routing and empty container repositioning problem for the deep draft inland waterway ports. One such study is conducted by Braekers et al. [20] where the authors optimize barge routing and empty container repositioning between a sea port and few hinterland ports. The extension of this work [19] includes vessel capacity and round trip service frequency to the barge routing and empty container repositioning problem. Marass [76] proposes a mixed-integer linear programming (MILP) model to optimize the transport routes of chartered container ships or tows for an inland waterway port. Most recently, An et al. [9] formulate a mixed-integer nonlinear programming (MINLP) model to solve an empty container repositioning shipping network design problem.

Realizing that a port may fail either due to natural (e.g., hurricane, tornado) or human-induced (e.g., cyber-attack) disaster, few studies focus on identifying the resiliency of a deep draft inland waterway port. For instance, Baroud et al. [13] convert different stochastic resilience-based component importance measures into an optimization framework to determine the important waterway links and the precedence of link recovery in case of a disaster. Oztanriseven and Nachtman [102] develop a simulation-based approach to estimate the potential economic impacts of inland waterways disruption response. The authors utilize McClellan-Kerr Arkansas River navigation system as a testbed to visualize and validate the

simulation results. Hosseini and Barker [59, 58] propose a Bayesian network to model the infrastructure resilience of an inland waterway port. Other studies related to inland waterway ports include the consideration of port-specific economic analysis [4], optimal dredging scheduling and investment decisions [113], the efficiency of inland waterway container terminals [152], tug scheduling between seaport to inland ports [157], and carbon emission [155].

Different from the studies discussed above, our study captures different realistic shallow draft inland waterway port-related features (e.g., water level fluctuation, delay in locks and dams, towboat and barge assignment decisions, barge availability and maintenance) and magnifies their impact on the overall supply chain system performance. Note that till now a number of existing studies in the literature consider inland waterway ports as a medium of transportation while designing a supply chain network, examples including but not limited to biomass supply chain (e.g., [109]), coal supply chain (e.g., [35]), grain supply chain (e.g., [31]), and many other application areas. However, very few studies have captured the true characteristics of the inland waterway transportation (e.g., water level fluctuation, barge/towboat assignment decisions, barge availability and maintenance) while solving a network designing problem. Our study captures one of the most important and impactful features of the shallow waterway transportation network, water level fluctuation. Proper consideration of this issue can significantly help obtain reliable tripwise commodity transportation decisions under an extremely uncertain situation. Water level issues are well studied in maritime

transportation [93, 24, 114]. However, in the case of inland waterway transportation, not much research attempts are observed that put specific focus on this issue. Few studies discuss the impact of water level issue from an economic perspective, such as [77, 100]. These studies investigate the impact of climate change and water level on different economical factors of inland waterway transportation, such as price per tonne transported, average annual shipping costs, average operating costs, and freight prices per tonne, rather than considering the problem from a real-life transportation network viewpoint. Hence, it is obvious that proper modeling efforts, that capture different realistic features, need to be made in order to design a reliable inland waterway transportation network.

4.3 Problem Description and Mathematical Model Formulation

This section presents a capacitated, multicommodity, multiperiod, two-stage stochastic programming model formulation to efficiently design and manage an inland waterway-based logistics network taking the stochastic, time-variant nature of commodity supply and water-level fluctuations into account. The main objective of the model is to optimize a number of inland waterway port-related operational decisions (e.g., towboat and barge assignment, inventory, and commodity transportation decisions) under uncertainty and in such a way that the overall system cost can be minimized. Figure 4.1 illustrates a simplified logistics network consisting of two origin ports and three destination ports.

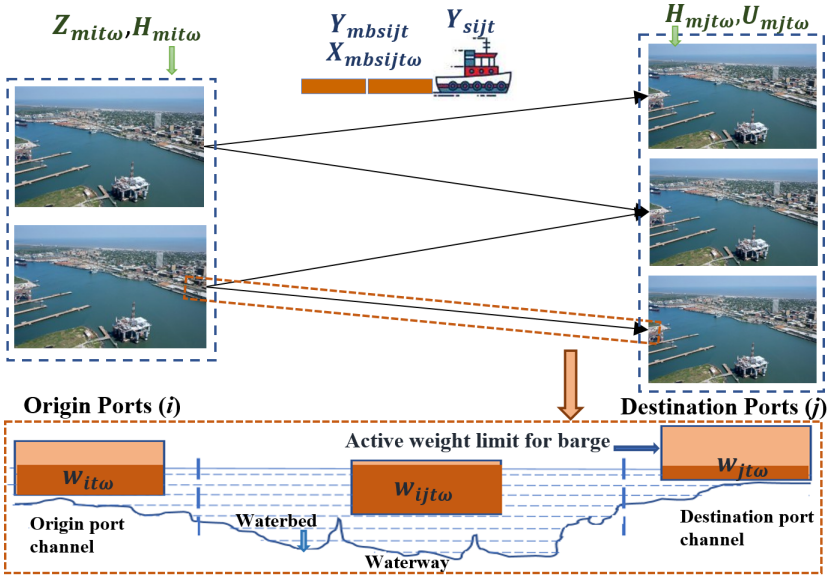

Figure 4.1

Illustration of an inland waterway transportation network

Let us first denote a logistics network $G = (\mathcal{N}, \mathcal{A})$ where $\mathcal{N}$ be the set of nodes and $\mathcal{A}$ be the set of arcs connecting the nodes within the logistics network. Set $\mathcal{N}$ consists of a set of origin and destination inland waterway ports, denoted by $\mathcal{I} = \{1, 2, 3, ..., I\}$ and $\mathcal{J} = \{1, 2, 3, ..., J\}$, respectively. The network requires to transport a set of commodities $\mathcal{M} = \{1, 2, 3, ..., M\}$ through the two origin and destination ports over a predetermined time periods, denoted by set $\mathcal{T} = \{1, 2, 3, ..., T\}$. In order to handle the appropriate interconnections between each origin and destination port, we introduce two subsets $\mathcal{I}_j$ and $\mathcal{J}_i$ in our model. The first subset $\mathcal{I}_j$ denotes the subset of origin ports connected to destination port

$j \in \mathcal{J}$ while the second subset $\mathcal{J}_i$ denotes the subset of destination ports connected to origin port $i \in \mathcal{I}$. To handle different stochastic scenarios (e.g., commodity supply, water-level fluctuations), scenario set $\omega \in \Omega$ is introduced where ρ_ω defines the probability of a given realization and $\rho_\omega \geq 0$ and $\sum_{\omega \in \Omega} \rho_\omega = 1$.

Inland waterway ports handle a number of agricultural products which are highly seasonal in nature, such as corn, rice, and woodchips. To exemplify, rice becomes available only between August to October in a given calendar year. Likewise, corn is harvested between mid-July to late November of each year [133]. This seasonality coupled with stochastic availability of agricultural products create a serious challenge for decision makers to plan and manage the port operations. Let us assume that the origin ports $i \in \mathcal{I}$ are supplied with a stochastic amount of commodity $\varphi_{mit\omega}$ of type $m \in \mathcal{M}$ at time period $t \in \mathcal{T}$ under scenario $\omega \in \Omega$. Depending on the demand, these commodities need to be transported in different destination ports via an inland waterway transportation network, which utilizes an association of barges and towboats to carry these commodities. Let $\mathcal{S} = \{1, 2, 3, ..., \overline{S}\}$ be the set of towboats and $\mathcal{B} = \{1, 2, 3, ..., B\}$ be the set of barges available to carry commodities between any pair $(i, j) \in (\mathcal{I}, \mathcal{J})$ of the origin-destination ports. Set $\mathcal{S}$ is arranged depending on the capabilities of the towboats such that towboat 1 in set $\mathcal{S}$ represents the least powerful towboat while $\overline{S}$ represents the most powerful towboat. Based on the capabilities, we denote $\overline{\delta}_s$ and $\underline{\delta}_s$ to be the maximum and minimum number of barges that can be carried out by any particular towboat $s \in \mathcal{S}$. Let ψ_{st} to denote the fixed cost associated with using a towboat $s \in \mathcal{S}$ at

time period $t \in \mathcal{T}$. Further, loading and unloading commodity $m \in \mathcal{M}$ in barge $b \in \mathcal{B}$, having weight carrying capacity $\overline{w}_b$ and volumetric capacity v_b, at time period $t \in \mathcal{T}$ incurs a fixed cost of η_{mbt}. Let c_{mbsijt} to denote the unit transportation cost of commodity $m \in \mathcal{M}$ using barge $b \in \mathcal{B}$ connected with towboat $s \in \mathcal{S}$ along arc $(i,j) \in (\mathcal{I},\mathcal{J})$ at time period $t \in \mathcal{T}$. Since the barges and towboats are required to go through periodic maintenance, we capture these factors by introducing two binary availability parameters a_{bit} and a_{sit}, respectively.

Each port $i \in \mathcal{I} \bigcup \mathcal{J}$ is assumed to carry inventory, restricted by maximum commodity storage capacity of $\overline{h}_i$. The inventory holding cost for commodity $m \in \mathcal{M}$ in port $i \in \mathcal{I} \bigcup \mathcal{J}$ at time period $t \in \mathcal{T}$ is denoted by h_{mit}. We also capture the deterioration rate of carrying commodity $m \in \mathcal{M}$ between two consecutive time periods by introducing parameter α_m. The waterway depth at port channel or throughout the waterbody may vary in different time period of the year depending upon the amount of sediment, silt, or mud accumulated in the waterbed. If such accumulation is too intense at any portion of the waterway (e.g., near ports or between two connecting ports), it increases the height of the waterbed which results in a decrease in the waterdepth. This waterdepth reduction can sometimes be too intense that it seriously impacts the transportation of shallow draft water vessels through the waterway. Resultantly, the barges need to carry commodities below to their designed weight carrying capacities, $\overline{w}_b$, to avoid being stuck at any point of their navigational waterway. Let us define $w_{it\omega}$ and $w_{jt\omega}$ to denote the maximum weight carrying capacity at port channel $i \in \mathcal{I} \bigcup \mathcal{J}$

and $w_{ijt\omega}$ to be the allowable weight that can be carried through the waterway between port pair $(i,j) \in (\mathcal{I},\mathcal{J})$ at time period $t \in \mathcal{T}$ under scenario $\omega \in \Omega$. Therefore, the *maximum effective weight* that a barge $m \in \mathcal{M}$ can carry under this restriction would be the *minimum* weight between the weight capacity near origin and destination ports, namely, $w_{it\omega}$ and $w_{jt\omega}$, and the channel between each origin-destination ports $(i,j) \in (\mathcal{I},\mathcal{J})$, namely, $w_{ijt\omega}$, i.e., $min\{\overline{w}_{ijt\omega}, \overline{w}_b\}$ where $\overline{w}_{ijt\omega} := min\{w_{it\omega}, w_{ijt\omega}, w_{jt\omega}\}$. Considering the uncertainty associated with this restriction, we consider $\overline{w}_{ijt\omega}$ to be a stochastic parameter in our proposed model formulation. Finally, we assume that the commodity demand at destination ports, denoted by d_{mjt}, can be satisfied either through the inland waterway transportation network or via an external source by paying a unit penalty cost of π_{mjt}. We now summarize the following notations for our proposed mathematical model formulation.

Sets:

- $\mathcal{I}$: set of origin ports, $i \in \mathcal{I}$
- $\mathcal{J}$: set of destination ports, $j \in \mathcal{J}$
- $\mathcal{M}$: set of commodities, $m \in \mathcal{M}$
- $\mathcal{S}$: set of towboats, $s \in \mathcal{S}$
- $\mathcal{B}$: set of barges, $b \in \mathcal{B}$
- $\mathcal{T}$: set of time periods, $t \in \mathcal{T}$
- $\mathcal{I}_j$: set of origin ports connected to destination port j, $\forall j \in \mathcal{J}$
- $\mathcal{J}_i$: set of destination ports connected to origin port i, $\forall i \in \mathcal{I}$

- Ω: set of possible scenarios ω, $\forall \omega \in \Omega$

Parameters:

- $\varphi_{mit\omega}$: supply availability of product $m \in \mathcal{M}$ in port $i \in \mathcal{I}$ at time period $t \in \mathcal{T}$ under scenario $\omega \in \Omega$
- ψ_{st}: fixed cost of using towboat $s \in \mathcal{S}$ at time period $t \in \mathcal{T}$
- η_{mbt}: fixed cost for loading and unloading commodity $m \in \mathcal{M}$ in barge $b \in \mathcal{B}$ at time period $t \in \mathcal{T}$
- c_{mbsijt}: unit cost of transporting commodity $m \in \mathcal{M}$ along arc $(i,j) \in (\mathcal{I},\mathcal{J})$ using barge $b \in \mathcal{B}$ of towboat $s \in \mathcal{S}$ at time period $t \in \mathcal{T}$
- $\overline{h}_i$: commodity storage capacity at port $i \in \mathcal{I} \bigcup \mathcal{J}$
- d_{mjt}: demand for commodity of type $m \in \mathcal{M}$ in port $j \in \mathcal{J}$ at time period $t \in \mathcal{T}$
- α_m: deterioration of commodity $m \in \mathcal{M}$
- a_{sit}, a_{bit}: binary availability of towboat and barge at port $i \in \mathcal{I}$ in time period $t \in \mathcal{T}$
- $\overline{\delta}_s$, $\underline{\delta}_s$: maximum/minimum number of barges to carry by towboat $s \in \mathcal{S}$
- $\overline{\delta}_{\overline{s}}$: capacity of the most powerful towboat $\overline{s} \in \mathcal{S}$
- $\overline{w}_{ijt\omega}$: the minimum of $\{w_{it\omega}, w_{ijt\omega}, w_{jt\omega}\}$ where $w_{it\omega}$ and $w_{jt\omega}$ indicate the maximum weight carrying capacity at port $i \in \mathcal{I} \bigcup \mathcal{J}$ and $w_{ijt\omega}$ the allowable weight that can be carried between the channel $(i,j) \in (\mathcal{I},\mathcal{J})$ at time period $t \in \mathcal{T}$ under scenario $\omega \in \Omega$. The last weight ($w_{ijt\omega}$) depends on the depth of the waterway and should not exceed the minimal water-level between the origin-destination ports
- ρ_m: density of commodity $m \in \mathcal{M}$
- v_b: volume capacity of barge $b \in \mathcal{B}$
- $\overline{w}_b$: weight capacity of a barge $b \in \mathcal{B}$
- h_{mit}: unit inventory holding cost for commodity $m \in \mathcal{M}$ in port $i \in \mathcal{I} \bigcup \mathcal{J}$ at time period $t \in \mathcal{T}$
- θ_{it}: total number of barges available in port $i \in \mathcal{I}$ at time period $t \in \mathcal{T}$

- π_{mjt}: unit penalty cost of not satisfying demand for commodity $m \in \mathcal{M}$ in port $j \in \mathcal{J}$ at time period $t \in \mathcal{T}$
- γ_{mit}: procurement cost of commodity $m \in \mathcal{M}$ in port $i \in \mathcal{I}$ at time period $t \in \mathcal{T}$
- t_l, t_u: average loading and unloading time of a barge
- Δ: average delay in locks
- l_{ij}: number of locks between origin port $i \in \mathcal{I}$ and destination port $j \in \mathcal{J}$
- d_{ij}: distance between origin port $i \in \mathcal{I}$ and destination port $j \in \mathcal{J}$
- $\bar{v}_{st}$: average speed of towboat $s \in \mathcal{S}$ at time period $t \in \mathcal{T}$
- $\bar{t}_{ij}$: allowable transport time limit between each origin port $i \in \mathcal{I}$ to destination port $j \in \mathcal{J}$
- ρ_ω: probability of scenario $\omega \in \Omega$

First Stage Decision Variables:

- Y_{sijt}: 1 if a towboat $s \in \mathcal{S}$ is used in arc $(i,j) \in (\mathcal{I}, \mathcal{J})$ at time period $t \in \mathcal{T}$; 0 otherwise
- Y_{mbsijt}: 1 if commodity $m \in \mathcal{M}$ is carried on barge $b \in \mathcal{B}$ of towboat $s \in \mathcal{S}$ from port $i \in \mathcal{I}$ to port $j \in \mathcal{J}$ at time period $t \in \mathcal{T}$; 0 otherwise

Second Stage Decision Variables:

- Z_{mitw}: amount of commodities of type $m \in \mathcal{M}$ processed at port $i \in \mathcal{I}$ at time period $t \in \mathcal{T}$ under scenario ω
- $X_{mbsijtw}$: amount of commodities of type $m \in \mathcal{M}$ transported using barge $b \in \mathcal{B}$ of towboat $s \in \mathcal{S}$ along arc $(i,j) \in (\mathcal{I}, \mathcal{J})$ at time period $t \in \mathcal{T}$ under scenario $\omega \in \Omega$
- H_{mitw}: amount of commodities of type $m \in \mathcal{M}$ stored in port $i \in \mathcal{I} \bigcup \mathcal{J}$ at time period $t \in \mathcal{T}$ under scenario $\omega \in \Omega$
- U_{mjtw} amount of commodities of type $m \in \mathcal{M}$ shortage in destination port $j \in \mathcal{J}$ at time period $t \in \mathcal{T}$ under scenario $\omega \in \Omega$

We now introduce the following first- and second-stage decision variables for our proposed two-stage stochastic programming model formulation. The first-stage decision variables $\mathbf{Y}^1 := \{Y_{sijt} | \forall s \in \mathcal{S}, i \in \mathcal{I}, j \in \mathcal{J}_i, t \in \mathcal{T}\}$ and $\mathbf{Y}^2 := \{Y_{mbsijt} | \forall m \in \mathcal{M}, b \in \mathcal{B}, s \in \mathcal{S}, i \in \mathcal{I}, j \in \mathcal{J}, t \in \mathcal{T}\}$ determine which towboat to use between an origin-destination pair in a given time period and which barge to use for carrying any particular product at any given origin port, respectively, i.e.,

$$Y_{sijt} = \begin{cases} 1 & \text{if a towboat } s \text{ is used between ports } (i,j) \in (\mathcal{I},\mathcal{J}) \text{ at time period } t \\ 0 & \text{otherwise;} \end{cases}$$

$$Y_{mbsijt} = \begin{cases} 1 & \text{if barge } b \text{ connected to towboat } s \text{ is used to carry commodity } m \\ & \text{between port } i \text{ and } j \text{ in time period } t \\ 0 & \text{otherwise;} \end{cases}$$

For notation simplicity, we define $\mathbf{Y}$ as $\mathbf{Y} := \mathbf{Y}^1 \bigcup \mathbf{Y}^2$. The second-stage decision variables $\mathbf{X} := \{X_{mbsijt\omega} | \forall m \in \mathcal{M}, b \in \mathcal{B}, s \in \mathcal{S}, (i,j) \in (\mathcal{I},\mathcal{J}), t \in \mathcal{T}, \omega \in \Omega\}$ to denote the amount of commodities of type $m \in \mathcal{M}$ transported using barge $b \in \mathcal{B}$ of towboat $s \in \mathcal{S}$ along arc $(i,j) \in (\mathcal{I},\mathcal{J})$ at time period $t \in \mathcal{T}$ under scenario $\omega \in \Omega$; $\mathbf{H} := \{H_{mit\omega} | \forall m \in \mathcal{M}, i \in \mathcal{I} \bigcup \mathcal{J}, t \in \mathcal{T}, \omega \in \Omega\}$ to denote the amount of commodities of type $m \in \mathcal{M}$ stored in port $i \in \mathcal{I} \bigcup \mathcal{J}$ at time period $t \in \mathcal{T}$ under scenario $\omega \in \Omega$; and $\mathbf{U} := \{U_{mjt\omega}\}$ to denote the amount of commodities of type $m \in \mathcal{M}$ shortage in destination port $j \in \mathcal{J}$ at time period $t \in \mathcal{T}$ under scenario $\omega \in \Omega$.

It needs to be noted here that the inland waterway transportation frequently impacted by the possible delays experienced by the barges in locks between two connecting ports. To simplify the modeling process, in this study we ignore the congestion occurred in the locks. Instead, we capture this delay through a feasible time limit, denoted by $\bar{t}_{ij}$. The introduction of $\bar{t}_{ij}$ provides a time window for towboats to deliver the commodities between each source-destination pair which otherwise will not be economical/feasible if violated. Let Δ, l_{ij}, and d_{ij} to represent the average delay in locks, the number of locks, and actual waterway distance between each origin-destination port $(i,j) \in (\mathcal{I},\mathcal{J})$. We further denote $\bar{v}_{st}$ to be the average speed of a towboat $s \in \mathcal{S}$ and t_l and t_u to be the average loading and unloading time for a barge. The total travel time for a towboat $s \in \mathcal{S}$ between each origin-destination port $(i,j) \in (\mathcal{I},\mathcal{J})$ at time $t \in \mathcal{T}$ can now be approximated as: $\left\{ \sum_{m\in\mathcal{M}} \sum_{b\in\mathcal{B}} (t_l + t_u) Y_{mbsijt} + (\frac{d_{ij}}{\bar{v}_{st}} + \Delta l_{ij}) Y_{sijt} \right\}$, while this travel time is assumed to be restricted by a feasible time limit $\bar{t}_{ij}$.

We now introduce the objective function of our proposed two-stage stochastic programming mathematical formulation, referred to as **[IWT]**. Note that the decisions about towboat and barge selection (**Y**) are made prior to a realization of any stochastic event. However, after the stochasticity is revealed, a number of second-stage decisions, such as transportation (**X**), storage (**H**), and shortage (**U**) decisions, are made. Our proposed mathematical model is introduced below.

[IWT] $$\underset{\mathbf{Y}}{Minimize} \sum_{s\in\mathcal{S}}\sum_{i\in\mathcal{I}}\sum_{j\in\mathcal{J}_i}\sum_{t\in\mathcal{T}}\left(\psi_{st}Y_{sijt} + \sum_{m\in\mathcal{M}}\sum_{b\in\mathcal{B}}\eta_{mbt}Y_{mbsit}\right) + \sum_{\omega\in\Omega}\rho_\omega \mathbb{Q}(\mathbf{Y},\omega) \tag{4.1}$$

subject to

$$\sum_{m\in\mathcal{M}} Y_{mbsijt} \leq 1 \qquad \forall b\in\mathcal{B}, s\in\mathcal{S}, i\in\mathcal{I}, j\in\mathcal{J}_i, t\in\mathcal{T} \tag{4.2}$$

$$\underline{\delta}_s Y_{sijt} \leq \sum_{m\in\mathcal{M}}\sum_{b\in\mathcal{B}} Y_{mbsijt} \leq \bar{\delta}_s Y_{sijt} \qquad \forall s\in\mathcal{S}, i\in\mathcal{I}, j\in\mathcal{J}_i, t\in\mathcal{T} \tag{4.3}$$

$$\sum_{m\in\mathcal{M}}\sum_{b\in\mathcal{B}}\sum_{s\in\mathcal{S}}\sum_{j\in\mathcal{J}} Y_{mbsijt} \leq \theta_{it} \qquad \forall i\in\mathcal{I}, t\in\mathcal{T} \tag{4.4}$$

$$\sum_{j\in\mathcal{J}_i}\sum_{s\in\mathcal{S}} Y_{sijt} \leq \tau_{it} \qquad \forall i\in\mathcal{I}, t\in\mathcal{T} \tag{4.5}$$

$$\sum_{j\in\mathcal{J}_i} Y_{sijt} \leq a_{sit} \qquad \forall s\in\mathcal{S}, i\in\mathcal{I}, t\in\mathcal{T} \tag{4.6}$$

$$\sum_{m\in\mathcal{M}}\sum_{s\in\mathcal{S}} Y_{mbsijt} \leq a_{bit} \qquad \forall b\in\mathcal{B}, i\in\mathcal{I}, j\in\mathcal{J}_i, t\in\mathcal{T} \tag{4.7}$$

$$\sum_{m\in\mathcal{M}}\sum_{b\in\mathcal{B}}(t_l + t_u)Y_{mbsijt} \leq \bar{t}_{ij} - \left(\frac{d_{ij}}{v_{st}} + \Delta l_{ij}\right)Y_{sijt} \forall s\in\mathcal{S}, i\in\mathcal{I}, j\in\mathcal{J}_i, t\in\mathcal{T} \tag{4.8}$$

$$Y_{mbsijt} \in \{0,1\} \quad \forall m\in\mathcal{M}, b\in\mathcal{B}, s\in\mathcal{S}, i\in\mathcal{I}, j\in\mathcal{J}_i, t\in\mathcal{T} \tag{4.9}$$

$$Y_{sijt} \in \{0,1\} \quad \forall s\in\mathcal{S}, i\in\mathcal{I}, j\in\mathcal{J}_i, t\in\mathcal{T} \tag{4.10}$$

with $\mathbb{Q}(\mathbf{Y},\omega)$ being the solution of the following second-stage problem:

$$\mathbb{Q}(\mathbf{Y},\omega) = \underset{\mathbf{X,H,U}}{Minimize} \sum_{t\in\mathcal{T}}\sum_{m\in\mathcal{M}}\left(\sum_{i\in\mathcal{I}\bigcup\mathcal{J}} h_{mit}H_{mit\omega} + \sum_{b\in\mathcal{B}}\sum_{s\in\mathcal{S}}\sum_{(i,j)\in(\mathcal{I},\mathcal{J})} c_{mbsijt}X_{mbsijt\omega} + \sum_{i\in\mathcal{I}}\gamma_{mit}Z_{mit\omega} + \sum_{j\in\mathcal{J}}\pi_{mjt}U_{mjtw}\right) \tag{4.11}$$

subject to

$$Z_{mit\omega} \leq \varphi_{mit\omega} \forall m \in \mathcal{M}, i \in \mathcal{I}, t \in \mathcal{T}, \omega \in \Omega \quad (4.12)$$

$$Z_{mit\omega} + (1-\alpha_m) H_{mi,t-1,\omega} = \sum_{b\in\mathcal{B}} \sum_{s\in\mathcal{S}} \sum_{j\in\mathcal{J}_i} X_{mbsijt\omega} + H_{mit\omega} \quad \forall m \in \mathcal{M}, i \in \mathcal{I}, t \in \mathcal{T}, \omega \in \Omega \quad (4.13)$$

$$\sum_{b\in\mathcal{B}} \sum_{s\in\mathcal{S}} \sum_{i\in\mathcal{I}_j} X_{mbsijt\omega} + (1-\alpha_m) H_{mj,t-1,\omega} = d_{mjt} + H_{mjt\omega} - U_{mjtw} \quad \forall m \in \mathcal{M}, j \in \mathcal{J}, t \in \mathcal{T}, \omega \in \Omega \quad (4.14)$$

$$\sum_{m\in\mathcal{M}} H_{mit\omega} \leq \overline{h}_i \forall i \in \mathcal{I} \bigcup \mathcal{J}, t \in \mathcal{T}, \omega \in \Omega \quad (4.15)$$

$$X_{mbsijt\omega} \leq min\{\overline{w}_{ijt\omega}, \overline{w}_b\} Y_{mbsijt} \forall m \in \mathcal{M}, b \in \mathcal{B}, s \in \mathcal{S}, i \in \mathcal{I}, j \in \mathcal{J}_i, t \in \mathcal{T}, \omega \in \Omega \quad (4.16)$$

$$\left(\frac{X_{mbsijt\omega}}{\rho_m}\right) \leq v_b Y_{mbsijt} \forall m \in \mathcal{M}, b \in \mathcal{B}, s \in \mathcal{S}, i \in \mathcal{I}, j \in \mathcal{J}_i, t \in \mathcal{T}, \omega \in \Omega \quad (4.17)$$

$$X_{mbsijt\omega}, H_{mit\omega}, H_{mjt\omega}, Z_{mit\omega} \in \mathbb{R}^+ \quad (4.18)$$

The objective function (4.1) minimizes the first-stage costs and the expected second-stage costs. The first two terms in (4.1) represent the fixed costs associated with using towboats and loading and unloading commodities into the barges. Constraints (4.2) restrict the loading of one commodity $m \in \mathcal{M}$ in a given barge $b \in \mathcal{B}$ at time period $t \in \mathcal{T}$. Constraints (4.3) restrict the minimum ($\underline{\delta}_s$) and maximum ($\overline{\delta}_s$) number of barges that can be connected with a given towboat $s \in \mathcal{S}$ at any time period $t \in \mathcal{T}$. Constraints (4.4) and (4.5) set the maximum availability of

barges and towboats in a given port $i \in \mathcal{I}$ at time period $t \in \mathcal{T}$ to θ_{it} and τ_{it}, respectively. The unavailability of barges and towboats due to period maintenance activities are captured by binary parameters a_{sit} and a_{bit} at constraints (4.6) and (4.7), respectively. Constraints (4.8) set total travel time restriction for a towboat $s \in \mathcal{S}$ between each origin-destination port $(i, j) \in (\mathcal{I}, \mathcal{J})$ at time period $t \in \mathcal{T}$. Finally, constraints (4.9) and (4.10) set integrality restrictions for barge and towboat selections.

The second-stage objective function (4.11) consists of four terms: the first term represents the costs associated with storing commodities at the source and destination ports; the second term represents the transportation costs of flowing commodities within the inland waterway transportation network; last two terms in the objective function, respectively, capture the commodity processing costs at any origin port and the commodity shortage costs at any destination port. Constraints (4.12) restrict the commodity processing capability of an origin port $i \in \mathcal{I}$ in time period $t \in \mathcal{T}$ under scenario $\omega \in \Omega$ to a given availability $\varphi_{mit\omega}$. Constraints (4.13) are the flow balance constraints for origin ports $i \in \mathcal{I}$, indicating that all the processed commodity $m \in \mathcal{M}$ can be either stored or transported to a destination port $j \in \mathcal{J}_i$ at time period $t \in \mathcal{T}$. Constraints (4.14) maintain flow balance at destination ports $j \in \mathcal{J}$ in time period $t \in \mathcal{T}$. These constraints indicate that the demand (d_{mjt}) for commodity $m \in \mathcal{M}$ at any destination port $j \in \mathcal{J}$ in time period $t \in \mathcal{T}$ can be satisfied either via the origin ports, stored inventory, or via an external source while the balance can be stored in the destination port's inventory for

future use. The inventory storage restriction at any port $i \in \mathcal{I} \bigcup \mathcal{J}$ is imposed via constraints (4.15). Constraints (4.16) and (4.17) set weight and volumetric capacity restriction for a given barge $b \in \mathcal{B}$ carrying commodity $m \in \mathcal{M}$ between each origin-destination port $(i, j) \in (\mathcal{I}, \mathcal{J})$ at time period $t \in \mathcal{T}$. Finally, constraints (4.18) represent the standard non-negativity constraints.

4.4 Solution Approach

By setting $|\Omega| = |\mathcal{T}| = |\mathcal{S}| = |\mathcal{B}| = 1$, problem **[IWT]** can be reduced to a *fixed charge network flow problem* which is already known to be an $\mathcal{NP}$-hard problem [12, 65]. Therefore, we find it difficulty to solve the large instances of **[IWT]** using commercial solvers, such as Gurobi. To overcome this computational burden, we propose a parallelized hybrid decomposition algorithm combining Sample Average Approximation (SAA) algorithm with an enhanced Progressive Hedging (PH) algorithm. The techniques used to enhance the PH algorithm are penalty parameter updating, global and local heuristics, scenario bundling, and a nested decomposition algorithm. The aim of adopting all the solution techniques is to generate quality solutions in solving large instances of problem **[IWT]** in a reasonable computational time.

4.4.1 Sample Average Approximation

To generate reliable solutions, problem **[IWT]** needs to be investigated with a large number of scenarios which may pose serious challenge from solution standpoint. To alleviate this challenge, we adopt *Sample Average Approximation* (SAA) method [119, 107]. SAA is a well known technique that has been widely used in solv-

ing problems in diversified application areas, including logistic and supply chain design, vehicle routing, production-routing, and many others. Following this procedure, we generate a SAA problem by selecting a set of random samples from the set of available scenarios. More specifically, we randomly generate a small sample of size N from the scenario set Ω (where $N \ll \Omega$) and approximate the recourse function with the sample average function $\frac{1}{N}\sum_{n\in N} \mathbb{Q}(\mathbf{Y}, n)$. Problem **[IWT]** can now be approximated by the following SAA problem:

$$\underset{Y\in\mathbf{Y}}{Minimize} \quad \left\{ \hat{\mathbf{g}}(Y) := \sum_{t\in\mathcal{T}} \left(\sum_{s\in\mathcal{S}} \sum_{i\in\mathcal{I}} \sum_{j\in\mathcal{J}_i} \left(\psi_{st} Y_{sijt} + \sum_{m\in\mathcal{M}} \sum_{b\in\mathcal{B}} \eta_{mbt} Y_{mbsijt} \right) \right. \right. \\ \left. \left. + \frac{1}{N} \sum_{n=1}^{N} \mathbb{Q}(\mathbf{Y}, n) \right\} \right. \tag{4.19}$$

For sufficiently large sample size N, problem (4.19) converges to the optimal solution of the original model **[IWT]** with a probability of 1.0 [66]. However, with an increase in N, the computational time required to solve problem (4.19) becomes excessively large. In practice, there exists a trade-off between the achieved solution quality and the computational burden associated with solving the large scenario subproblems. Next, we summarize the steps involved in implementing the SAA technique to solve problem **[IWT]** as follows:

1. Generate E independent samples of product supply and water level scenarios of size N i.e., $\{\varphi_e^1(\omega), \varphi_e^2(\omega), ..., \varphi_e^N(\omega)\}$ and $\{\overline{w}_e^1(\omega), \overline{w}_e^2(\omega), ..., \overline{w}_e^N(\omega)\}$, $\forall e = 1, 2, ..., E$, where $\boldsymbol{\varphi} = \{\varphi_{mit\omega} | \forall m \in \mathcal{M}, i \in \mathcal{I}, t \in \mathcal{T}, \omega \in \Omega\}$, $\overline{\mathbf{w}} =$

$\{\overline{w}_{ijt\omega} | \forall i \in \mathcal{I}, j \in \mathcal{J}, t \in \mathcal{T}, \omega \in \Omega\}$ and solve the corresponding SAA problem:

$$\textbf{[IWT(SAA)]} \underset{Y \in \mathbf{Y}}{Minimize} \Bigg\{ \hat{\mathbf{g}}(Y) : = \sum_{t \in \mathcal{T}} \Bigg(\sum_{s \in \mathcal{S}} \sum_{i \in \mathcal{I}} \sum_{j \in \mathcal{J}_i} \Bigg(\psi_{st} Y_{sijt} + \sum_{m \in \mathcal{M}} \sum_{b \in \mathcal{B}} \eta_{mbt} Y_{mbsijt} \Bigg) + \frac{1}{|N|} \sum_{n=1}^{N} \mathbb{Q}(\mathbf{Y}, n)) \Bigg\} \tag{4.20}$$

This SAA problem is solved for each replication $e = 1, ..., E$. Consider $\mathbf{v}_N^e$ and $\hat{\mathbf{Y}}_N^e$ to be the optimal objective value and the optimal solution of (4.20), respectively.

2. In the next step, we compute the *average* of the optimal objective values of the SAA problems, denoted by $\bar{v}_E^N$, by solving E replications. We further denote $\sigma^2_{\bar{v}_E^N}$ to be the *variance* of all the corresponding SAA problems. We then obtain the following:

$$\bar{v}_E^N = \frac{1}{E} \sum_{e=1}^{E} v_N^e; \quad \sigma^2_{\bar{v}_E^N} = \frac{1}{(E-1)E} \sum_{e=1}^{E} (v_N^e - \bar{v}_E^N)^2$$

Parameter $\bar{v}_E^N$ is an unbiased estimator of the optimal objective value of **[IWT]**, denoted by v^*, which shall satisfy this property $\bar{v}_E^N \leq v^*$. This implies that $\bar{v}_E^N$ provides a statistical lower bound for the optimal objective value of problem **[IWT]** and $\sigma^2_{\bar{v}_E^N}$ is the estimator of the variance of this lower bound.

3. Next, a feasible first-stage solution $\tilde{Y}_N^e \in \mathbf{Y}$ is chosen and utilized to evaluate problem **[IWT]** with a newly generated reference sample size N' ($N' \gg N$) as follows:

$$\tilde{g}_{N'}(\tilde{Y}) := \sum_{s \in \mathcal{S}} \sum_{i \in \mathcal{I}} \sum_{j \in \mathcal{J}_i} \sum_{t \in \mathcal{T}} \Bigg(\psi_{st} \tilde{Y}_{sijt} + \sum_{m \in \mathcal{M}} \sum_{b \in \mathcal{B}} \eta_{mbt} \tilde{Y}_{mbsijt} \Bigg) + \frac{1}{N'} \sum_{n=1}^{N'} \mathbb{Q}(\mathbf{Y}, n) \tag{4.21}$$

Here, the estimator $\tilde{g}_{N'}(\tilde{Y})$ provides a valid upper bound for the original problem **[IWT]**. The variance of $\tilde{g}_{N'}(\tilde{Y})$ is obtained as follows:

$$\sigma^2_{N'}(\tilde{Y}) = \frac{1}{(N'-1)N'} \sum_{n=1}^{N'} \Bigg\{ \sum_{s \in \mathcal{S}} \sum_{i \in \mathcal{I}} \sum_{j \in \mathcal{J}_i} \sum_{t \in \mathcal{T}} \Bigg(\psi_{st} \tilde{Y}_{sijt} + \sum_{m \in \mathcal{M}} \sum_{b \in \mathcal{B}} \eta_{mbt} \tilde{Y}_{mbsijt} \Bigg) + \mathbb{Q}(\mathbf{Y}, n) - \tilde{g}_{N'}(\tilde{Y}) \Bigg\}^2$$

4. Through the estimators calculated in **Steps 2** and **3**, the optimality gap, $gap_{N,E,N'}(\tilde{Y})$, and its variance, σ^2_{gap}, are calculated as follows:

$$gap_{N,E,N'}(\tilde{Y}) = \tilde{g}_{N'}(\tilde{\mathcal{Y}}) - \bar{v}^N_E$$
$$\sigma^2_{gap} = \sigma^2_{N'}(\tilde{Y}) + \sigma^2_{\bar{v}^N_E}$$

The confidence interval for the optimality gap, $gap_{N,E,N'}(\tilde{Y})$, is obtained as follow:

$$\tilde{g}_{N'}(\tilde{\mathcal{Y}}) - \bar{v}^N_E + z_\alpha \left\{ \sigma^2_{N'}(\tilde{Y}) + \sigma^2_{\bar{v}^N_E} \right\}^{1/2}$$

where $z_\alpha = \Phi^{-1}(1-\alpha)$, and $\Phi(z)$ is the cumulative distribution function of the standard normal distribution.

4.4.2 Progressive Hedging Algorithm

The first step of the SAA algorithm requires solving a two-stage stochastic mixed integer linear programming model **[IWT(SAA)]** with N scenarios. Although the size of this model is considerably lower than the original problem **[IWT]**, i.e., $N \ll |\Omega|$, depending on the size of $|\mathcal{I}|, |\mathcal{J}|$, and $|\mathcal{T}|$, solving such model can still be considered challenging. In order to address this challenge, we employ Progressive Hedging (PH) algorithm that decomposes problem **[IWT(SAA)]** by scenarios [117, 95]. The cornerstone of this algorithm is *scenario decomposition* technique (based on the augmented Lagrangian relaxation scheme) which is utilized to solve a number of individual scenario subproblems. Interested readers may review the work by [144, 150] to gain a comprehensive overview of the PH implementation.

In problem **[IWT(SAA)]**, constraints (4.16) and (4.17) link the first-stage decision variables with the second-stage decision variables. These constraints also restrict problem **[IWT(SAA)]** to be separable by scenarios. To overcome this challenge, we introduce two new copy variables, namely, $\{Y_{mbsijtn}\}_{\forall m\in\mathcal{M}, b\in\mathcal{B}, s\in\mathcal{S}, i\in\mathcal{I}, j\in\mathcal{J}}$,

$_{t\in\mathcal{T},n\in\mathcal{N}} \in \{0,1\}$ and $\{Y_{sijtn}\}_{\forall s\in\mathcal{S},(i,j)\in(\mathcal{I},\mathcal{J}),t\in\mathcal{T},n\in\mathcal{N}} \in \{0,1\}$, which will allow problem **[IWT(SAA)]** to be decomposable by scenarios. Problem **[IWT(SAA)]** can now be modified as follows:

$$\underset{\mathbf{Y},\mathbf{H},\mathbf{X},\mathbf{Z},\mathbf{U}}{Minimize}\frac{1}{N}\sum_{n=1}^{N}\left\{\sum_{s\in\mathcal{S}}\sum_{i\in\mathcal{I}}\sum_{j\in\mathcal{J}_i}\sum_{t\in\mathcal{T}}\left(\psi_{st}Y_{sijtn}+\sum_{m\in\mathcal{M}}\sum_{b\in\mathcal{B}}\eta_{mbt}Y_{mbsijtn}\right)+\mathbb{Q}(\mathbf{Y},n)\right\} \quad (4.22)$$

subject to (4.12)-(4.15), (4.18), and

$$\sum_{m\in\mathcal{M}} Y_{mbsijtn} \leq 1 \forall b\in\mathcal{B}, s\in\mathcal{S}, i\in\mathcal{I}, j\in\mathcal{J}_i, t\in\mathcal{T}, n\in N \quad (4.23)$$

$$\underline{\delta}_s Y_{sijtn} \leq \sum_{m\in\mathcal{M}}\sum_{b\in\mathcal{B}} Y_{mbsitn} \leq \overline{\delta}_s Y_{sijtn} \forall s\in\mathcal{S}, i\in\mathcal{I}, j\in\mathcal{J}_i, t\in\mathcal{T}, n\in N \quad (4.24)$$

$$\sum_{m\in\mathcal{M}}\sum_{b\in\mathcal{B}}\sum_{s\in\mathcal{S}}\sum_{j\in\mathcal{J}_i} Y_{mbsijtn} \leq \theta_{it} \forall i\in\mathcal{I}, t\in\mathcal{T}, n\in N \quad (4.25)$$

$$\sum_{j\in\mathcal{J}_i}\sum_{s\in\mathcal{S}} Y_{sijtn} \leq \tau_{it} \forall i\in\mathcal{I}, t\in\mathcal{T}, n\in N \quad (4.26)$$

$$\sum_{j\in\mathcal{J}_i} Y_{sijtn} \leq a_{sit} \forall s\in\mathcal{S}, i\in\mathcal{I}, t\in\mathcal{T}, n\in N \quad (4.27)$$

$$\sum_{m\in\mathcal{M}}\sum_{s\in\mathcal{S}} Y_{mbsijtn} \leq a_{bit} \forall b\in\mathcal{B}, i\in\mathcal{I}, j\in\mathcal{J}_i, t\in\mathcal{T}, n\in N \quad (4.28)$$

$$\sum_{m\in\mathcal{M}}\sum_{b\in\mathcal{B}}(t_l+t_u)Y_{mbsijtn} \leq \overline{t}_{ij}-\left(\frac{d_{ij}}{v_{st}}+\Delta l_{ij}\right)Y_{sijtn} \quad \forall s\in\mathcal{S}, i\in\mathcal{I}, j\in\mathcal{J}_i, t\in\mathcal{T}, n\in N \quad (4.29)$$

$$X_{mbsijtn} \leq min\{\overline{w}_{ijtn}, \overline{w}_b\}Y_{mbsijtn} \forall m\in\mathcal{M}, b\in\mathcal{B}, \quad s\in\mathcal{S}, i\in\mathcal{I}, j\in\mathcal{J}_i, t\in\mathcal{T}, n\in N \quad (4.30)$$

$$\left(\frac{X_{mbsijtn}}{\rho_m}\right) \leq v_b Y_{mbsijtn} forall m\in\mathcal{M}, b\in\mathcal{B}, s\in\mathcal{S}, \quad \imath\in\mathcal{I}, j\in\mathcal{J}_i, t\in\mathcal{T}, n\in N \quad (4.31)$$

$$Y_{mbsijtn} = Y_{mbsijtn'} \forall (n,n')\in N, n\neq n' \quad (4.32)$$

$$Y_{sijtn} = Y_{sijtn'} \forall (n,n')\in N, n\neq n' \quad (4.33)$$

$$Y_{mbsijtn} \in \{0,1\} \forall m \in \mathcal{M}, b \in \mathcal{B}, s \in \mathcal{S}, i \in \mathcal{I}, j \in \mathcal{J}_i, t \in \mathcal{T}, n \in N \quad (4.34)$$

$$Y_{sijtn} \in \{0,1\} \forall s \in \mathcal{S}, i \in \mathcal{I}, j \in \mathcal{J}_i, t \in \mathcal{T}, n \in N \quad (4.35)$$

Constraints (4.32) and (4.33) are referred to as *nonanticipativity* constraints which not only link the first- and second-stage decision variables but also force all the scenarios to yield same values for each first-stage decision variables. Additionally, these constraints restrict problem (4.22) to be separable by scenarios. To overcome this problem, we introduce two new variables,

$\{\bar{Y}_{mbsijt}\}_{\forall m \in \mathcal{M}, b \in \mathcal{B}, s \in \mathcal{S}, i \in \mathcal{I}, j \in \mathcal{J}_i, t \in \mathcal{T}} \in \{0,1\}$ and $\{\bar{Y}_{sijt}\}_{\forall s \in \mathcal{S}, (i,j) \in (\mathcal{I},\mathcal{J}), t \in \mathcal{T}} \in \{0,1\}$, referred to as "overall design vectors". With the introduction of this two variables, constraints (4.32) and (4.33) can now be replaced with the following set of constraints:

$$Y_{mbsijtn} = \bar{Y}_{mbsijt} \forall m \in \mathcal{M}, b \in \mathcal{B}, s \in \mathcal{S}, i \in \mathcal{I}, j \in \mathcal{J}_i, t \in \mathcal{T}, n \in N \quad (4.36)$$

$$Y_{sijtn} = \bar{Y}_{sijt} \forall s \in \mathcal{S}, i \in \mathcal{I}, j \in \mathcal{J}_i, t \in \mathcal{T}, n \in N \quad (4.37)$$

$$\bar{Y}_{mbsijt}, \bar{Y}_{sijt} \in \{0,1\} \qquad \forall m \in \mathcal{M}, b \in \mathcal{B}, s \in \mathcal{S}, (i,j) \in (\mathcal{I},\mathcal{J}), t \in \mathcal{T}$$

Constraints (4.36) and (4.37) can be relaxed using the *augmented Lagrangian strategy*, proposed by Rockafellar and Wets [117], and yield the following objective function:

$$\underset{Y\in\mathbf{Y},\mathbf{H},\mathbf{X},\mathbf{Z},\mathbf{U}}{Minimize} \quad \frac{1}{N}\sum_{n=1}^{N}\sum_{t\in\mathcal{T}}\Bigg\{\sum_{s\in\mathcal{S}}\sum_{i\in\mathcal{I}}\sum_{j\in\mathcal{J}_i}\Bigg(\psi_{st}Y_{sijtn}+\sum_{m\in\mathcal{M}}\sum_{b\in\mathcal{B}}\eta_{mbt}Y_{mbsijtn}\Bigg)+\mathbb{Q}(\mathbf{Y},n)+$$
$$\sum_{s\in\mathcal{S}}\sum_{i\in\mathcal{I}}\sum_{j\in\mathcal{J}_i}\Bigg(\sum_{m\in\mathcal{M}}\sum_{b\in\mathcal{B}}\zeta_{mbsijtn}(Y_{mbsijtn}-\bar{Y}_{mbsijt})+\frac{1}{2}\sum_{m\in\mathcal{M}}\sum_{b\in\mathcal{B}}\vartheta(Y_{mbsijtn}$$
$$-\bar{Y}_{mbsijt})^2+\beta_{sijtn}(Y_{sijtn}-\bar{Y}_{sijt})+\frac{1}{2}\theta(Y_{sijtn}-\bar{Y}_{sijt})^2\Bigg)\Bigg\}$$

where $\{\zeta_{mbsijtn}\}_{\forall m\in\mathcal{M},b\in\mathcal{B},s\in\mathcal{S},i\in\mathcal{I},j\in\mathcal{J}_i,t\in\mathcal{T},n\in N}$ and $\{\beta_{sijtn}\}_{\forall s\in\mathcal{S},i\in\mathcal{I},j\in\mathcal{J}_i,t\in\mathcal{T},n\in N}$ define the Lagrangian multipliers for the relaxed constraints and ϑ and θ are the penalty ratios. Since variables $\{Y_{mbsijtn}\}_{\forall m\in\mathcal{M},b\in\mathcal{B},\ s\in\mathcal{S},i\in\mathcal{I},j\in\mathcal{J}_i,t\in\mathcal{T},n\in N}$, and $\{\bar{Y}_{mbsijtn}\}$ $_{\forall m\in\mathcal{M},b\in\mathcal{B},s\in\mathcal{S},i\in\mathcal{I},j\in\mathcal{J}_i,t\in\mathcal{T},n\in N}$ are binary, quadratic term $\sum_{s\in\mathcal{S}}\sum_{i\in\mathcal{I}}\sum_{j\in\mathcal{J}_i}\sum_{t\in\mathcal{T}}\theta(Y_{sijtn}-\bar{Y}_{sijt})^2$ can now be reduced as follows:

$$\sum_{s\in\mathcal{S}}\sum_{i\in\mathcal{I}}\sum_{j\in\mathcal{J}_i}\sum_{t\in\mathcal{T}}\theta(Y_{sijtn}-\bar{Y}_{sijt})^2=\sum_{s\in\mathcal{S}}\sum_{i\in\mathcal{I}}\sum_{j\in\mathcal{J}_i}\sum_{t\in\mathcal{T}}\Big(\theta(Y_{sijtn})^2-2\theta Y_{sijtn}\bar{Y}_{sijt}+\theta(\bar{Y}_{sijt})^2\Big)$$
$$\approx\sum_{s\in\mathcal{S}}\sum_{i\in\mathcal{I}}\sum_{j\in\mathcal{J}_i}\sum_{t\in\mathcal{T}}\Big(\theta Y_{sijtn}-2\theta Y_{sijtn}\bar{Y}_{sijt}+\theta\bar{Y}_{sijt}\Big)$$

Similarly, we can also simplify the quadratic term $\sum_{m\in\mathcal{M}}\sum_{b\in\mathcal{B}}\sum_{s\in\mathcal{S}}\sum_{i\in\mathcal{I}}\sum_{j\in\mathcal{J}_i}$ $\sum_{t\in\mathcal{T}}\vartheta(Y_{mbsijtn}-\bar{Y}_{mbsijt})^2$ and yield the following objective function:

$$\underset{\mathbf{Y,H,X,Z,U}}{Minimize} \quad \frac{1}{N}\sum_{n=1}^{N}\sum_{t\in\mathcal{T}}\Bigg\{\sum_{s\in\mathcal{S}}\sum_{i\in\mathcal{I}}\sum_{j\in\mathcal{J}_i}\Bigg((\psi_{st}+\beta_{sijtn}-\theta\bar{Y}_{sijt}+\frac{\theta}{2})Y_{sijtn}+\sum_{m\in\mathcal{M}}\sum_{b\in\mathcal{B}}(\eta_{mbt}$$
$$+\zeta_{mbsijtn}-\vartheta\bar{Y}_{mbsijt}+\frac{\vartheta}{2})Y_{mbsijtn}\Bigg)+\mathbb{Q}(\mathbf{Y},n)-\sum_{s\in\mathcal{S}}\sum_{i\in\mathcal{I}}\sum_{j\in\mathcal{J}}\beta_{sijtn}\bar{Y}_{sijt}+$$
$$\frac{1}{2}\sum_{s\in\mathcal{S}}\sum_{i\in\mathcal{I}}\sum_{j\in\mathcal{J}}\theta\bar{Y}_{sijt}-\sum_{m\in\mathcal{M}}\sum_{b\in\mathcal{B}}\sum_{s\in\mathcal{S}}\sum_{i\in\mathcal{I}}\sum_{j\in\mathcal{J}}\zeta_{mbsijtn}\bar{Y}_{mbsijt}$$
$$+\frac{1}{2}\sum_{m\in\mathcal{M}}\sum_{b\in\mathcal{B}}\sum_{s\in\mathcal{S}}\sum_{i\in\mathcal{I}}\sum_{j\in\mathcal{J}}\vartheta\bar{Y}_{mbsijt}\Bigg\} \tag{4.38}$$

With fixed values of the overall plan $\{\bar{Y}_{mbsijt}\}_{\forall m\in\mathcal{M},b\in\mathcal{B},s\in\mathcal{S},i\in\mathcal{I},j\in\mathcal{J}_i,t\in\mathcal{T}}$ and $\{\bar{Y}_{sijt}\}_{\forall s\in\mathcal{S},i\in\mathcal{I},j\in\mathcal{J}_i,t\in\mathcal{T}}$, the last part of the objective function (4.38) becomes constant. This will allow the subproblems to be separable by scenarios $n \in N$. The revised subproblem now becomes:

$$[\textbf{IWT-PHA(}\boldsymbol{n}\textbf{)}]\underset{\mathbf{Y,H,X,Z,U}}{Minimize} \sum_{s\in\mathcal{S}}\sum_{i\in\mathcal{I}}\sum_{j\in\mathcal{J}_i}\sum_{t\in\mathcal{T}}\Bigg\{(\psi_{st}+\beta_{sijtn}-\theta\bar{Y}_{sijt}+\frac{\theta}{2})Y_{sijtn}+\sum_{m\in\mathcal{M}}\sum_{b\in\mathcal{B}}($$
$$\eta_{mbt}+\zeta_{mbsijtn}-\vartheta\bar{Y}_{mbsijt}+\frac{\vartheta}{2})Y_{mbsijtn}\Bigg\}+\mathbb{Q}(\mathbf{Y},n) \tag{4.39}$$

subject to (4.12)-(4.15), (4.18), (4.23)-(4.31), (4.34), and (4.35). Let r be the current iteration of the PH algorithm. We let $\{\zeta^r_{mbsijtn}\}$ and $\{\beta^r_{sijtn}\}$ to denote the Lagrangian multipliers and ϑ^r and β^r to be the penalty parameters at iteration r of the PH algorithm. In the basic PH implementation, N deterministic subproblems [**IWT-PHA(*n*)**] are solved and the consensus parameters $\{\bar{Y}^r_{mbsijt}\}_{\forall m\in\mathcal{M},b\in\mathcal{B},s\in\mathcal{S},i\in\mathcal{I},j\in\mathcal{J}_i,t\in\mathcal{T}}$ and $\{\bar{Y}^r_{sijt}\}_{\forall s\in\mathcal{S},i\in\mathcal{I},j\in\mathcal{J}_i,t\in\mathcal{T}}$ are obtained. If the total gap between the binary variables, i.e., $\{Y^r_{mbsijtn}\}$ and $\{Y^r_{sijtn}\}$, and the consensus parameters. i.e., $\{\bar{Y}^r_{mbsijt}\}$ and $\{\bar{Y}^r_{sijt}\}$, falls below a threshold limit, the algorithm

terminates; otherwise, we update the values of $\{\zeta^r_{mbsijtn}\}, \{\beta^r_{sijtn}\}, \vartheta^r$, and θ^r using equations (4.40)-(4.43) and the process continues.

$$\zeta^r_{mbsijtn} \longleftarrow \zeta^{r-1}_{mbsijtn} + \vartheta^{r-1}(Y^r_{mbsijtn} - \bar{Y}^{r-1}_{mbsijt})$$
$$\forall m \in \mathcal{M}, b \in \mathcal{B}, s \in \mathcal{S}, i \in \mathcal{I}, j \in \mathcal{J}_i, t \in \mathcal{T} \quad (4.40)$$

$$\vartheta^r \longleftarrow \Delta\vartheta^{r-1} \quad (4.41)$$

$$\beta^r_{sijtn} \longleftarrow \beta^{r-1}_{sijtn} + \theta^{r-1}(Y^r_{sijtn} - \bar{Y}^r_{sijt}) \forall s \in \mathcal{S}, (i,j) \in (\mathcal{I}, \mathcal{J}), t \in \mathcal{T} \quad (4.42)$$

$$\theta^r \longleftarrow \Delta\theta^{r-1} \quad (4.43)$$

In the first iteration, the values of $\{\zeta^{r=0}_{mbsijtn}\}$ and $\{\beta^{r=0}_{sijtn}\}$ are set to zero for each scenario $n \in N$. Penalty parameters $\{\vartheta^{r=0}\}$ and $\{\theta^{r=0}\}$ are initialized with a fixed positive number which eventually turns into $\{\vartheta^r, \theta^r\} \rightarrow \infty$ with the progression of the PH algorithm. The constant parameter Δ is set to a value grater than 1 i.e., $\Delta > 1$. A pseudo-code of the basic Progressive hedging algorithm is provided in **Algorithm 1**.

Termination criteria: The PH algorithm terminates upon satisfying one of the following conditions:

- $\frac{1}{N}\sum_{n\in N}\sum_{s\in\mathcal{S}}\sum_{i\in\mathcal{I}}\sum_{t\in\mathcal{T}}\sum_{j\in\mathcal{J}_i}\Big(\sum_{m\in\mathcal{M}}\sum_{b\in\mathcal{B}}|Y^r_{mbsitn} - \bar{Y}^{r-1}_{mbsit}| + |Y^r_{sijtn} - \bar{Y}^{r-1}_{sijt}|\Big) \leq \epsilon$; where ϵ is a pre-specified tolerance gap.
- 10 consecutive non-improvement iterations.
- Maximum iteration limit is reached (i.e., $iter^{max} = 500$)
- Maximum time limit is reached (i.e., $t^{max} = 10,800$ CPU seconds)

4.4.3 Enhanced Progressive Hedging Algorithm

4.4.3.1 Penalty Parameter Updating

The performance of the basic PH algorithm is highly sensitive to the values set for the penalty parameters ϑ^r and θ^r. Prior studies, such as [22, 60], show that if conservative values are set for the penalty parameters, then the algorithm converges to a near optimal solution, but with an expense of high computational time. On the contrary, if the values of ϑ^r and θ^r are set too high, then the algorithm quickly converges to a suboptimal solution. To overcome this problem, we utilize the *dynamic penalty parameter adjustment* approach proposed by Hvattum and Lokketangen [61]. This approach dynamically adjusts the penalty parameters ϑ^r and θ^r based on the computational performances of the PH algorithm from prior iterations. Let Δ_1^r, Δ_3^r and Δ_2^r, Δ_4^r be the indicators of the convergence rates in the *dual* and *primal space*, respectively. The penalty parameters ϑ^r and θ^r are now dynamically updated as follows:

$$
\begin{aligned}
\Delta_1^r &= \sum_{m\in\mathcal{M}} \sum_{b\in\mathcal{B}} \sum_{s\in\mathcal{S}} \sum_{(i,j)\in(\mathcal{I},\mathcal{J})} \sum_{t\in\mathcal{T}} \sum_{n\in N} (Y^r_{mbsijtn} - \bar{Y}^r_{mbsijt})^2 \\
\Delta_2^r &= \sum_{m\in\mathcal{M}} \sum_{b\in\mathcal{B}} \sum_{s\in\mathcal{S}} \sum_{(i,j)\in(\mathcal{I},\mathcal{J})} \sum_{t\in\mathcal{T}} (\bar{Y}^r_{mbsijt} - \bar{Y}^{r-1}_{mbsijt})^2 \\
\Delta_3^r &= \sum_{s\in\mathcal{S}} \sum_{(i,j)\in(\mathcal{I},\mathcal{J})} \sum_{t\in\mathcal{T}} \sum_{n\in N} (Y^r_{sijtn} - \bar{Y}^r_{sijt})^2 \\
\Delta_4^r &= \sum_{s\in\mathcal{S}} \sum_{(i,j)\in(\mathcal{I},\mathcal{J})} \sum_{t\in\mathcal{T}} (\bar{Y}^r_{sijt} - \bar{Y}^{r-1}_{sijt})^2
\end{aligned}
$$

$$\vartheta^r = \begin{cases} \Gamma\vartheta^{r-1} & if\ \ \Delta_1^r - \Delta_1^{r-1} > 0 \\ \frac{1}{\Gamma}\vartheta^{r-1} & else\ if\ \ \Delta_2^r - \Delta_2^{r-1} > 0 \\ \vartheta^{r-1} & Otherwise \end{cases} ; \quad \theta^r = \begin{cases} \Gamma\theta^{r-1} & if\ \ \Delta_3^r - \Delta_3^{r-1} > 0 \\ \frac{1}{\Gamma}\theta^{r-1} & else\ if\ \ \Delta_4^r - \Delta_4^{r-1} > 0 \\ \theta^{r-1} & Otherwise \end{cases}$$

where Γ is a constant parameter whose value is set to $\Gamma > 1$.

4.4.3.2 Global and Local Heuristic Strategies

We adopt two heuristic strategies, *global* and *local* heuristics as proposed by Crainic et al. [26], to further accelerate the convergence of the basic PH algorithm. The underlying concept of these strategies are to modify the barge loading/unloading cost η_{mbt} and towboat usage cost ψ_{st} in such a way that help to guide fixing few decision variables and eventually accelerates the convergence of the basic PH algorithm. The first strategy is referred to as *global heuristic* since this strategy updates η_{mbt} and ψ_{st} at the end of each PHA iteration r. On the other hand, in *local heuristic*, cost parameters η_{mbt} and ψ_{st} are adjusted within the scenario level.

As discussed in section 4.4.2, problem [**IWT-PHA(*n*)**] consists of N deterministic sub-problems. Following **Algorithm 1**, we collect consensus parameters $\{\bar{Y}^r_{mbsijt}\}$ $\forall m\in\mathcal{M}, b\in\mathcal{B}, s\in\mathcal{S}, i\in\mathcal{I}, t\in\mathcal{T}$ and $\{\bar{Y}^r_{sijt}\}\forall s\in\mathcal{S}, i\in\mathcal{I}, j\in\mathcal{J}_i, t\in\mathcal{T}$ at the end of each iteration r. The higher value of $\{\bar{Y}^r_{mbsijt}\}$ signifies that barge $b \in \mathcal{B}$ is used with towboat $s \in \mathcal{S}$ to transport commodity $m \in \mathcal{M}$ between origin-destination pair $(i, j) \in (\mathcal{I}, \mathcal{J})$ at time period $t \in \mathcal{T}$ in *most* of the previous iterations. In contrary, a lower value of $\{\bar{Y}^r_{mbsijt}\}$ indicates that this decision was not a favorable selection in most of the previous iterations. Similar conclusion can be made for $\{\bar{Y}^r_{sijt}\}$ as well. Let $\bar{a}$ and $\underline{a}$ be two parameters indicating the upper and lower threshold values for $\{\bar{Y}^r_{mbsijt}\}$.

If $\{\bar{Y}^r_{mbsijt}\}$ yields the value greater than $\bar{a}$, then decreasing the value of η_{mbt} will motivate the sub-problems to select more barges in the following iterations. Similarly, two other thresholds $\bar{b}$ and $\underline{b}$ can be defined as the upper and lower limit for $\{\bar{Y}^r_{sijt}\}$ and same decision strategy can be applied for this consensus parameter as well. These cost adjustment strategies will help to fix the decision of using barges and towboats to either one or zero which will eventually help to reduce the size of the overall problem. The adjustment strategy is given below:

$$\eta^r_{mbt} = \begin{cases} \kappa\eta^{r-1}_{mbt} & if \;\; \bar{Y}^{r-1}_{mbsijt} < \bar{a} \\ \frac{1}{\kappa}\eta^{r-1}_{mbt} & if \;\; \bar{Y}^{r-1}_{mbsijt} > \underline{a} \\ \eta^{r-1}_{mbt} & Otherwise \end{cases} ; \quad \psi^r_{st} = \begin{cases} \kappa\psi^{r-1}_{st} & if \;\; \bar{Y}^{r-1}_{sijt} < \bar{b} \\ \frac{1}{\kappa}\psi^{r-1}_{st} & if \;\; \bar{Y}^{r-1}_{sijt} > \underline{b} \\ \psi^{r-1}_{st} & Otherwise \end{cases}$$

where η^r_{mbt} denotes the *modified cost* of loading and unloading barge $b \in \mathcal{B}$ with commodity $m \in \mathcal{M}$ in time period $t \in \mathcal{T}$ and ψ^r_{st} to be the *modified cost* of using towboat $s \in \mathcal{S}$ in time period $t \in \mathcal{T}$ in the *r-th* of the PH iteration. The values of $\bar{a}$, $\underline{a}$, $\bar{b}$, and $\underline{b}$ are set to be any values form the range $0.7 < (\bar{a}, \bar{b}) < 1$ and $0 < (\underline{a}, \underline{b}) < 0.3$. Finally, the constant parameter κ is set to be any value greater than 1.0.

The performance of the global heuristic strategy can be further improved by modifying the fixed cost of using barges and towboats locally within the scenario level. The modification of the fixed costs only impact the sub-problem at scenario n of a particular iteration r; therefore, this strategy is referred to as *local heuristic* [26]. Following this strategy, if the gap between the binary variables and the corresponding consensus parameters, i.e., $|Y^{r-1}_{mbsijtn} - \bar{Y}^r_{mbsit}|$ and $|Y^{r-1}_{sijtn} - \bar{Y}^r_{sijt}|$, are

sufficiently large for any scenario $n \in N$ of a particular iteration, then the fixed cost of using barges and towboats are adjusted. The local adjustment strategy is presented below:

$$\eta^{r}_{mbtn} = \begin{cases} \kappa \eta^{r-1}_{mbtn} & if \;\; |Y^{r-1}_{mbsijtn} - \bar{Y}^{r}_{mbsijt}| \geq a^{far} \;\; and \;\; Y^{r-1}_{mbsijtn} = 0 \\ \frac{1}{\kappa} \eta^{r-1}_{mbtn} & if \;\; |Y^{r-1}_{mbsijtn} - \bar{Y}^{r}_{mbsijt}| \geq a^{far} \;\; and \;\; Y^{r-1}_{mbsijtn} = 1 \\ \eta^{r-1}_{mbtn} & Otherwise \end{cases}$$

$$\psi^{r}_{stn} = \begin{cases} \kappa \psi^{r-1}_{stn} & if \;\; |Y^{r-1}_{sijtn} - \bar{Y}^{r}_{sijt}| \geq b^{far} \;\; and \;\; Y^{r-1}_{sijtn} = 0 \\ \frac{1}{\kappa} \psi^{r-1}_{stn} & if \;\; |Y^{r-1}_{sijtn} - \bar{Y}^{r}_{sijt}| \geq b^{far} \;\; and \;\; Y^{r-1}_{sijtn} = 1 \\ \psi^{r-1}_{stn} & Otherwise \end{cases}$$

where η^{r}_{mbtn} and ψ^{r}_{stn} represent, respectively, the adjusted fixed cost associated with using barges and towboats under scenario $n \in N$ in the *r-th* iteration of the PH algorithm; κ is a constant parameter whose value is set to $\kappa > 1$; a^{far} and b^{far} are threshold values at which local adjustment to the η^{r}_{mbtn} and ψ^{r}_{stn} are made and are, respectively, set in the following range: $0.5 < a^{far} < 1$ and $0.5 < b^{far} < 1$.

4.4.3.3 Scenario Bundling

The performance of the PH algorithm can be improved even further by grouping the scenarios and then solve [**IWT-PHA(*n*)**] for each scenario group, commonly referred to as *scenario bundling/grouping* technique [1]. Following this technique, instead of solving PH subproblems for each individual scenario, a set of bundles are created from the scenarios, and the PH subproblems are then solved for each scenario bundle $l \in \mathcal{L}$. Scenario bundling can be done in many ways which would

be more specific to the model (e.g., grouping/bundling high, medium, and low supply/water level scenarios). Let us partition set N into $|\mathcal{L}|$ bundles where the probability of each bundle, denoted by ρ_l, will be $\rho_l = \sum_{n \in l} \rho_n$. Problem **[IWT-PHA(*n*)]** is now solved for each bundle $l \in \mathcal{L}$ as follows:

$$[\textbf{IWT-PHA(}l\textbf{)}] \underset{\mathbf{Y,H,X,Z,U}}{Minimize} \Bigg\{ \sum_{s \in \mathcal{S}} \sum_{i \in \mathcal{I}} \sum_{j \in \mathcal{J}_i} \sum_{t \in \mathcal{T}} \Bigg((\psi_{st} + \beta_{sijtl} - \theta \bar{Y}_{sijt} + \frac{\theta}{2}) Y_{sijtl} + \sum_{m \in \mathcal{M}} \sum_{b \in \mathcal{B}} (\eta_{mbt} + \zeta_{mbsijtl} - \vartheta \bar{Y}_{mbsijt} + \frac{\vartheta}{2}) Y_{mbsijtl} \Bigg\} + \sum_{n \in l} \frac{\rho_n}{P_l} \Big(\mathbb{Q}(\mathbf{Y}, n) \Big) \quad (4.44)$$

subject to (4.12)-(4.15), (4.18), (4.23)-(4.31), (4.34), and (4.35). Note that the definitions for $\{Y_{mbsijtl}\}$ and $\{Y_{sijtl}\}$ will remain same as **[IWT(PHA)]** but for each scenario bundle $l \in \mathcal{L}$.

4.4.4 Nested Decomposition Algorithm

Even though the computational burden in solving problem **[IWT-PHA(*n*)]** now reduced significantly, the problem can still be considered challenging depending upon the size of $|\mathcal{I}|$, $|\mathcal{J}|$, $|\mathcal{M}|$, $|\mathcal{B}|$, $|\mathcal{S}|$, and $|\mathcal{T}|$. To address this challenge, we employ another decomposition technique, commonly referred to as *nested decomposition* (ND) algorithm [70], to further reduce the problem size for **[IWT-PHA(*n*)]**. This algorithm utilizes the concept of Stochastic Dual Dynamic Integer Programming (SDDiP), which is commonly used to solve multi-stage stochastic integer programming problems with binary state variables, and are capable of converging in a finite number of iterations [158].

Recall that problem **[IWT-PHA(*n*)]** includes constraints (4.13) and (4.14) which connect inventory storage decisions between multiple time periods. These *linking*

constraints restrict problem **[IWT-PHA(*n*)]** to be decomposable by time period $t \in \mathcal{T}$, which otherwise would significantly reduce the size of the overall problem. To overcome this problem, we introduce *duplicating variables* $\mathbf{H}_1^{prev} := \{H_{mitn}^{prev} | \forall m \in \mathcal{M}, i \in \mathcal{I}, t \in \mathcal{T}, n \in N\}$ and $\mathbf{H}_2^{prev} := \{H_{mjtn}^{prev} | m \in \mathcal{M}, j \in \mathcal{J}, t \in \mathcal{T}, n \in N\}$ for each linking variables $\{H_{mi,t-1,n}\}$ and $\{H_{mj,t-1,n}\}$ and replace constraints (4.13) and (4.14) by the following set of constraints:

$$Z_{mitn} + (1 - \alpha_m) H_{mitn}^{prev} = \sum_{b \in \mathcal{B}} \sum_{s \in \mathcal{S}} \sum_{j \in \mathcal{J}_i} X_{mbsijtn} + H_{mitn} \quad \forall m \in \mathcal{M}, i \in \mathcal{I}, t \in \mathcal{T}, t > 1 \quad (4.45)$$

$$\sum_{b \in \mathcal{B}} \sum_{s \in \mathcal{S}} \sum_{i \in \mathcal{I}_j} X_{mbsijtn} + (1 - \alpha_m) H_{mjtn}^{prev} = d_{mjt} + H_{mjtn} \quad \forall m \in \mathcal{M}, j \in \mathcal{J}, t \in \mathcal{T}, t > 1 \quad (4.46)$$

$$H_{mitn}^{prev} = \hat{H}_{mi,t-1,n} \leftarrow \mu_{mitn} \in \mathbb{R}^{|\mathcal{M}|+|\mathcal{I}|+|\mathcal{T}|-1} \quad \forall m \in \mathcal{M}, i \in \mathcal{I}, t \in \mathcal{T}, t > 1 \quad (4.47)$$

$$H_{mjtn}^{prev} = \hat{H}_{mj,t-1,n} \leftarrow \mu_{mjtn} \in \mathbb{R}^{|\mathcal{M}|+|\mathcal{J}|+|\mathcal{T}|-1} \quad \forall m \in \mathcal{M}, j \in \mathcal{J}, t \in \mathcal{T}, t > 1 \quad (4.48)$$

$$H_{mitn}^{prev}, H_{mjtn}^{prev} \in \mathbb{R}^+ \quad (4.49)$$

where $\{H_{mitn}^{prev}\}_{\forall m \in \mathcal{M}, i \in \mathcal{I} \cup \mathcal{J}, n \in N}$ is a duplicating variable representing $\{H_{mi,t-1,n}\}_{\forall m \in \mathcal{M}, i \in \mathcal{I} \cup \mathcal{J}, n \in N}$ and $\{\hat{H}_{mi,t-1,n}\}_{\forall m \in \mathcal{M}, i \in \mathcal{I} \cup \mathcal{J}, n \in N}$ is the solution for $\{H_{mitn}\}_{\forall m \in \mathcal{M}, i \in \mathcal{I} \cup \mathcal{J}, n \in N}$ at time period $t - 1$, which is fixed when solving for time period t and $\{\mu_{mitn}\}_{\forall m \in \mathcal{M}, i \in \mathcal{I} \cup \mathcal{J}, t \in \mathcal{T}, n \in N}$ are Lagrangian multipliers which are unrestricted in

sign. With this, problem **[IWT-PHA(*n*)]** can now be decomposable by time period $t \in \mathcal{T}$ which is shown below:

$$[\textbf{IWT-ND}(\boldsymbol{n,t})] \underset{\mathbf{Y,H,X,Z,U}}{Minimize} O_t := \sum_{s\in\mathcal{S}}\sum_{i\in\mathcal{I}}\sum_{j\in\mathcal{J}_i}\Big\{(\psi_{st}+\beta_{sijtn}-\theta\bar{Y}_{sijt}+\frac{\theta}{2})Y_{sijtn}+$$
$$\sum_{m\in\mathcal{M}}\sum_{b\in\mathcal{B}}(\eta_{mbt}+\zeta_{mbsijtn}-\vartheta\bar{Y}_{mbsijt}+\frac{\vartheta}{2})Y_{mbsijtn}\Big\}+\mathbb{Q}(\mathbf{Y},t,n)+\kappa_t \quad (4.50)$$

subject to constraints (4.12), (4.15), (4.23)-(4.35), (4.45)-(4.49), and

$$\kappa_t \geq \hat{O}_{t+1,q}+\sum_{m\in\mathcal{M}}\sum_{i\in\mathcal{I}}\mu_{mi,t+1,nq}(\hat{H}_{mitnq}-H_{mitn})+\sum_{m\in\mathcal{M}}\sum_{j\in\mathcal{J}}\mu_{mj,t+1,nq}(\hat{H}_{mjtnq}-$$
$$H_{mjtn})\forall q \quad (4.51)$$

where κ_t defines a *cost to go function*. In each iteration q of the ND algorithm, problem (4.50) needs to be solved separately and sequentially for each time period $t \in \mathcal{T}$, and the future cost cuts (4.51) are added in **[IWT-ND(*n,t*)]** from the following iterations $q+1$. Essentially, problem **[IWT-ND(*n,t*)]** is solved through successive *forward* and *backward* pass in each iteration q of the ND algorithm. The forward pass yields a feasible upper bound, denoted by UB_q, while the backward pass, which generates cuts from the relaxed subproblems, provides a valid lower bound for the original problem **[IWT-PHA(*n*)]**. The process is continued till the gap between the upper and lower bound falls below a pre-specified tolerance level ϵ_{ND}. Figure 4.2 delineates the steps involved in solving **[IWT-PHA(*n*)]** using the ND algorithm.

Forward Pass: The purpose of the *forward pass* is to generate a valid upper bound, UB_q, for the full problem. In this step, the optimization model is solved sequen-

tially for each consecutive time period by using the solution obtained from the previous time period. The upper bound UB_q is calculated as follows:

$$UB_q = \sum_{t \in \mathcal{T}} (\hat{O}_{tq} - \hat{k}_t) \qquad \forall q \tag{4.52}$$

It is obvious from (4.52) that the sum of the optimal solutions of the forward pass subproblems in any iteration q, $\hat{O}_{tq}$, minus the cost-to-go approximations, $\hat{k}_t$, for all time periods of that iteration q provides a valid upper bound for the full problem **[IWT-PHA(*n*)]**.

Backward Pass: After solving all the forward subproblems for each time period $t \in \mathcal{T}$, the process of solving **[IWT-PHA(*n*)]** using the *backward pass* initiates. Backward pass solves the subproblems in descending order of the time periods and generates cuts from the solutions of the future periods. These are cumulative cuts but specific to each time period $t \in \mathcal{T}$. This means that the cuts are added in each iteration q, whenever a new backward pass subproblem for each time period t is solved and are then kept in the following forward passes. These cuts provide approximations to predict the cost-to-go functions within the planning horizon. Cuts, added in the backward pass of each iteration q, are still kept in the forward pass until the gap between the upper and lower bound reaches to a pre-specified tolerance level ϵ_{ND}. The fixed variables stored in the forward pass, $\hat{H}_{mi,t,nq}$ and $\hat{H}_{mj,t,nq}$, are also used in the backward pass. The lower bound, LB_q, is then calculated as follows:

$$LB_q = \hat{O}_{1,q} \qquad \forall q \tag{4.53}$$

Here, the solution of the first time period (i.e., t=1) provides a valid lower bound to the total cost since it contains only a subset of the constraints from the original problem **[IWT-PHA(*n*)]**.

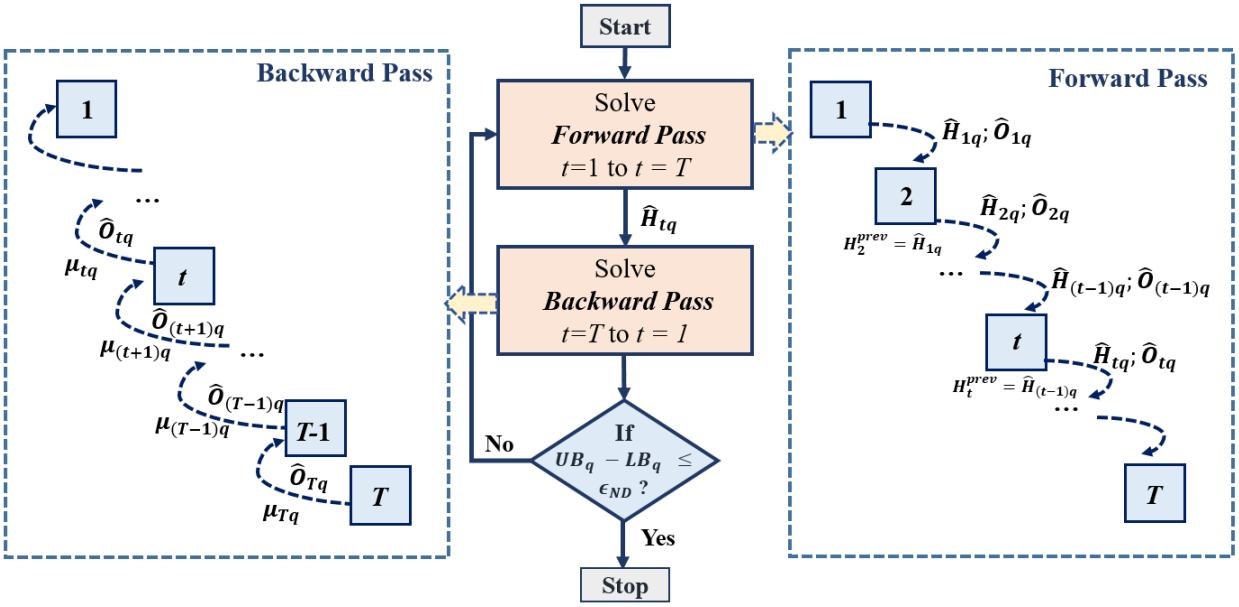

Figure 4.2

Nested decomposition algorithm

4.4.4.1 Valid Inequalities:

To enhance the performance of the ND algorithm, we first derive a number of valid inequalities by utilizing the special structure of our problem [**IWT**] and then added to problem [**IWT-ND(*n*,*t*)**]. The proposed set of valid inequalities are presented below:

- Constraint (4.54) provides a lower bound on the overall barge usage to ensure the demand satisfaction for commodity $m \in \mathcal{M}$ at each time period $t \in \mathcal{T}$. These constraints are known to be as *surrogate constraints*. The value of σ can vary between 0.0 and 1.0. When $\sigma = 1.0$, all the demand are required to be satisfied through the inland waterway port network.

$$\sum_{b\in\mathcal{B}}\sum_{s\in\mathcal{S}}\sum_{i\in\mathcal{I}}\sum_{j\in\mathcal{J}} Y_{mbsijt}\overline{w}_b \geq \sum_{j\in\mathcal{J}} \sigma d_{mjt} \qquad \forall m \in \mathcal{M}, t \in \mathcal{T} \tag{4.54}$$

- While choosing between a number of barges of similar capacities, symmetries may occur which may elongate the search time for the solver. To address this issue, we add the following *lexicographic ordering constraints* (4.55) and (4.56) which set priorities on the barge selection. Such priorities help to break the duplications caused by the barge selection symmetry, which thereby accelerate the performance of the branch-and-bound process.

$$Y_{1,b-1,sijt} \geq Y_{1bsijt} \forall b \in \mathcal{B} \setminus \{1\}, s \in \mathcal{S}, i \in \mathcal{I}, j \in \mathcal{J}, t \in \mathcal{T} \tag{4.55}$$

$$\sum_{p=1}^{m} 2^{(m-p)} Y_{p,b-1,sijt} \geq \sum_{p=1}^{m} 2^{(m-p)} Y_{pbsijt} \forall m \in \mathcal{M}, b \in \mathcal{B} \setminus \{1\}, s \in \mathcal{S}, i \in \mathcal{I}, j \in \mathcal{J}, t \in \mathcal{T} \tag{4.56}$$

- Symmetries may also arise in the case of towboat selection. Consider $\mathcal{S}'_e$ as the subset of towboats of same type, i.e., $\mathcal{S}'_e \subset \mathcal{S}$ and $s'_e \subset \mathcal{S}'_e$ where s'_e represents a set of the members belonging to $\mathcal{S}'_e$ in ascending order. Similar to constraints (4.55) and (4.56), following lexicographical ordering constraints (4.57) and (4.58) are applied for each $\mathcal{S}$ to set the priority in utilizing towboats of the same type.

$$Y_{s'_e-1,ijt} \geq Y_{s'_e,ijt} \forall s'_e \in \mathcal{S}'_e \setminus \{1\}, i \in \mathcal{I}, j \in \mathcal{J}, t \in \mathcal{T} \tag{4.57}$$

$$\psi_{s'_e-1,t} Y_{s'_e-1,ijt} \geq \psi_{s'_e,t} Y_{s'_e,ijt} \forall s'_e \in \mathcal{S}'_e \setminus \{1\}, i \in \mathcal{I}, j \in \mathcal{J}, t \in \mathcal{T} \tag{4.58}$$

- Constraints (4.59) generate a lower bound on the number of barges that are required for satisfying the demand at any time period $t \in \mathcal{T} \setminus \{1\}$. If the cumulative demand over period t is greater than or equal to minimum of the maximum possible inventory held $(\overline{h}_j)$ and initial inventory H^{prev}_{mjt}, then at least a certain number of barges need to be used in that specific time period t.

$$\sum_{b\in\mathcal{B}}\sum_{s\in\mathcal{S}}\sum_{i\in\mathcal{I}}\sum_{j\in\mathcal{J}} Y_{mbsijt} \geq \left\lceil \frac{\sum_{j\in\mathcal{J}} \sigma d_{mjt} - min\{\sum_{j\in\mathcal{J}} H^{prev}_{mjt}, \sum_{j\in\mathcal{J}} \overline{h}_j\}}{\overline{w}_b} \right\rceil$$
$$\forall m \in \mathcal{M}, t \in \mathcal{T} \setminus \{1\} \quad (4.59)$$

4.4.4.2 Benders cut:

Standard ND algorithm is designed to solve convex optimization problems for which different cuts, such as Benders cuts, can be generated in a much simplified way, i.e., using the objective value and the Lagrange multiplier of the constraints (4.47) and (4.48), which provides better convergence. Since we are applying the ND algorithm for solving non-convex, MILP problems, Benders cuts cannot be applied directly. Therefore, to generate a valid Benders cut, the subproblems need to be convexified or relaxed appropriately. Let $\hat{O}^{LP}_{t,q}$ be the objective of the relaxed subproblem at time period $t \in \mathcal{T}$. Benders cuts can now be generated as follows:

$$k_{t-1} \geq \hat{O}^{LP}_{t,q} + \sum_{m\in\mathcal{M}}\sum_{i\in\mathcal{I}} \mu^{LP}_{mi,t,nq}(\hat{H}_{mi,t-1,nq} - H_{mi,t-1,n}) + \sum_{m\in\mathcal{M}}\sum_{j\in\mathcal{J}} \mu^{LP}_{mj,t,nq}(\hat{H}_{mj,t-1,nq} - H_{mj,t-1,n}) \ \forall q \quad (4.60)$$

Note that Benders cut is the weakest of the possible cuts; however, it has the advantage of being easily and quickly computed. It works well for the tighter formulation when the solution of the linear relaxation is close to the actual solution of the MILP.

4.4.4.3 Lagrangian cut:

The performance of the ND algorithm can also be enhanced by adding Lagrangian cuts. These cuts are generated by obtaining Lagrangian relaxation of [**IWT-ND(*n*,*t*)**]

which yields the convex hull of the noncomplicating constraints. First, we dualize the linking constraints (4.47) and (4.48) and then penalize their violation in the objective function by the vector of Lagrange multipliers, $\{\mu_{mitnq}\}$ and $\{\mu_{mjtnq}\}$, respectively. These Lagrangian multipliers are unrestricted in sign. The following relaxed subproblem is then obtained:

$$\underset{\mathbf{Y},\mathbf{H},\mathbf{X},\mathbf{Z},\mathbf{U}}{Minimize} \quad O_{tq}^{LR} := \sum_{s\in\mathcal{S}}\sum_{i\in\mathcal{I}}\sum_{j\in\mathcal{J}_i}\Big\{(\psi_{st}+\beta_{sijtn}-\theta\bar{Y}_{sijt}+\frac{\theta}{2})Y_{sijtn}+\sum_{m\in\mathcal{M}}\sum_{b\in\mathcal{B}}(\eta_{mbt}+\zeta_{mbsijtn}-\vartheta\bar{Y}_{mbsijt}+\frac{\vartheta}{2})Y_{mbsijtn}\Big\}+\mathbb{Q}(\mathbf{Y},t,n)+\kappa_t-\sum_{m\in\mathcal{M}}\Big\{\sum_{i\in\mathcal{I}}\mu_{mitnq}(H_{mitn}^{prev}-\hat{H}_{mi,t-1,n})+\sum_{j\in\mathcal{J}}\mu_{mjtnq}(H_{mjtn}^{prev}-\hat{H}_{mj,t-1,n})\Big\} \tag{4.61}$$

subject to constraints (4.12), (4.15), (4.23)-(4.31), (4.34), (4.35), (4.45)-(4.46), (4.49), and (4.51).

With Lagrange multiplier values closer to their optimal, tighter approximation is obtained and stronger cuts are generated. The optimal values of the Lagrange multipliers, $\{\mu_{mitnq}\}$ and $\{\mu_{mjtnq}\}$, can be obtained by solving the following subproblem:

$$\underset{\mu_{mitnq},\mu_{mjtnq}}{Maximize} \quad O_{tq}^{LD} = \Big\{\underset{\mathbf{Y},\mathbf{H},\mathbf{X},\mathbf{Z},\mathbf{U}}{Minimize}\ O_{tq}^{LR} = \sum_{s\in\mathcal{S}}\sum_{i\in\mathcal{I}}\sum_{j\in\mathcal{J}_i}\Big\{(\psi_{st}+\beta_{sijtn}-\theta\bar{Y}_{sijt}+\frac{\theta}{2})Y_{sijtn}+\sum_{m\in\mathcal{M}}\sum_{b\in\mathcal{B}}(\eta_{mbt}+\zeta_{mbsijtn}-\vartheta\bar{Y}_{mbsijt}+\frac{\vartheta}{2})Y_{mbsijtn}\Big\}+\mathbb{Q}(\mathbf{Y},t,n)+\kappa_t-\sum_{m\in\mathcal{M}}\Big\{\sum_{i\in\mathcal{I}}\mu_{mitnq}(H_{mitn}^{prev}-\hat{H}_{mi,t-1,n})+\sum_{j\in\mathcal{J}}\mu_{mjtnq}(H_{mjtn}^{prev}-\hat{H}_{mj,t-1,n})\Big\}\Big\} \tag{4.62}$$

subject to constraints (4.12), (4.15), (4.23)-(4.31), (4.34), (4.35), (4.45)-(4.46), (4.49), and (4.51).

The coefficients obtained through solving the maximization problem (4.62), are used to generate Lagrangian cut (4.63) for any fixed time period $t \in \mathcal{T}$.

$$\begin{aligned} k_{t-1} \geq \hat{O}^{LD}_{tq} &+ \sum_{m\in\mathcal{M}}\sum_{i\in\mathcal{I}} \mu^{LD}_{mitnq}(\hat{H}_{mi,t-1,nq} - H_{mi,t-1,n}) \\ &+ \sum_{m\in\mathcal{M}}\sum_{j\in\mathcal{J}} \mu^{LD}_{mjtnq}(\hat{H}_{mj,t-1,nq} - H_{mj,t-1,n}) \quad \forall q \end{aligned} \tag{4.63}$$

The maximization problem in (4.62) can, however, be computationally expensive. Therefore, we adapt the Lagrange multipliers for each of the sub-problems of the Backward Pass using the sub-gradient method. The Backward Pass steps under the ND algorithm with the application of Lagrangean cuts are listed below.

For time period $t = T, ..., 1$ in iteration q:

Step 1. Solve the original MILP subproblem in (4.50) to get the actual objective value, O_{tq}.

Step 2. Solve the LP relaxation of the MILP subproblem and store the dual variables, $\{\mu^{LP}_{mitnq}\}$ and $\{\mu^{LP}_{mjtnq}\}$.

Step 3. Use the dual variables from the LP relaxation as an initial guess for the Lagrange multipliers.

Step 4. Solve the Lagrangean subproblem (4.61) to obtain the optimal value O^{LR}_{tq}.

Step 5. Check the following stopping criterion, where ϵ_2 and ϵ_3 are pre-specified tolerances:

(a) If $(O_{tq} - O^{LR}_{tq}) \leq \epsilon_2$; store the optimal O^{LR}_{tq} and multipliers $\{\mu^{LP}_{mitnq}\}$ and $\{\mu^{LP}_{mjtnq}\}$ and go to the next subproblem, $t-1$, by adding the appropriate future cost cuts.

(b) If no significant progress can be achieved after re-solving the Lagrangean relaxation in a successive number of iterations, i.e., if $|O_{tq}^{LR,old} - O_{tq}^{LR}| \leq \epsilon_3$ where $O_{tq}^{LR,old}$ is the solution of the Lagrangean Relaxation in the previous step of the subgradient method, no further effort should be made to decrease the duality gap of this subproblem in this iteration. Store the optimal O_{tq}^{LR} and multipliers $\{\mu_{mitnq}^{LP}\}$ and $\{\mu_{mjtnq}^{LP}\}$ and go to the next subproblem, $t-1$, by adding the appropriate future cost cuts.

Step 6. If the stopping criteria are not met, update the set of multipliers using the subgradient method and go back to **Step 3**.

$$\mu_{mitnq}^{LP} = \mu_{mitnq}^{LP} + step_{tq}(\hat{H}_{mi,t-1,n} - H_{mitn}^{prev})$$
$$\mu_{mjtnq}^{LP} = \mu_{mjtnq}^{LP} + step_{tq}(\hat{H}_{mj,t-1,n} - H_{mjtn}^{prev})$$
$$\text{where} \quad step_{tq} = \frac{O_{tq} - O_{tq}^{LR}}{\sum_{m\in\mathcal{M}}[\sum_{i\in\mathcal{I}}(\hat{H}_{mi,t-1,n} - H_{mitn}^{prev})^2 + \sum_{j\in\mathcal{J}}(\hat{H}_{mj,t-1,n} - H_{mjtn}^{prev})^2]}$$

4.4.4.4 Strengthened Benders cut:

As discussed earlier, depending on the structure and tightness of the MILP problem, Benders cut can be weak and may require large number of iterations to converge. Generating Lagrangean cuts , on the other hand, requires longer computational time. To mitigate this challenge, Zou et al. [158] propose another set of cuts, known as *strengthened Benders cut*, which is a compromise between Benders and Lagrangean cuts and does not suffer from potential performance issues of the two previous cuts. Generation of strengthened Benders cut is similar to the Lagrangean cut. However, it does not use the subgradient method to adjust the corresponding multipliers. This cut uses the coefficients obtained from solving the first Lagrangean relaxation after the initialization of the multipliers using LP relax-

ation shown in (4.64). The strengthened benders cut for problem (4.50) is shown below:

$$k_{t-1} \geq \hat{O}^{LR}_{tq} + \sum_{m\in\mathcal{M}}\sum_{i\in\mathcal{I}} \mu^{LP}_{mitnq}(\hat{H}_{mi,t-1,nq} - H_{mi,t-1,n}) + \sum_{m\in\mathcal{M}}\sum_{j\in\mathcal{J}} \mu^{LP}_{mjtnq}(\hat{H}_{mj,t-1,nq} - H_{mj,t-1,n}) \quad \forall q \tag{4.64}$$

These cuts are at least as tight as the Benders cut and usually can be generated in less time compared to Lagrangean cuts [158].

4.4.5 Implementing Parallel Processing:

The proposed hybrid decomposition algorithm developed in this study utilizes the SAA, the enhanced PH, and the ND algorithm in a nested structure. In addition to this noble algorithmic framework, we develop two different variants of parallelization schemes by utilizing the *parallel computing* concept. These schemes are developed with a view to further enhance the overall performance of the nested decomposition algorithm. The main difference between the conventional algorithm and the parallelized algorithms is that conventional algorithms solve the respective subproblems in series, whereas our proposed parallelization frameworks are designed to solve the subproblems of our nested hybrid decomposition algorithm in parallel. Essentially, the parallelization is conducted via utilizing the computers multiprocessing capabilities. Our proposed parallelization schemes are detailed below.

(i) ***Scheme 1***: The first parallelization scheme applies synchronous parallelization technique under the SAA algorithm. Note that in each iteration of the SAA, $|E|$ replications of problem **[IWT(SAA)]** are generated. Parallelization *Scheme 1* assigns each of these replications to different available processors

and solves the subproblems in parallel by utilizing the enhanced PH algorithm which is also hybridized with the ND algorithm. After all the replications are solved, the solutions are aggregated and the convergence of the SAA algorithm is evaluated. If the obtained gap is lower than the predefined threshold limit, then the SAA algorithm is terminated; otherwise, more SAA replications are generated and the process continues until the SAA is converged to a desired optimality gap. The flow chart for this parallelization scheme can be seen in Figure 4.3.

(ii) ***Scheme 2***: The second parallelization scheme applies synchronous parallelization technique under the PH algorithm introduced in section 4.4.2. In each PH iteration r, the algorithm solves a series of scenario-based subproblems **[IWT-PHA(*n*)]**. Utilizing this scheme, each of these scenario-based subproblems are dynamically assigned to different available processors which are finally collected and aggregated upon solution. These aggregated solutions are then utilized to check the convergence of the PH algorithm. If the algorithm converges, the corresponding first-stage solutions are then fixed and evaluated under a large sample space in SAA to obtain the upper bound for the overall problem.The process continues until the SAA algorithm provides a solution of the desired quality. The flow chart for this parallelization scheme can be seen in Figure 4.4.

4.5 Experimental Results

This section presents a real-life case study and the computational performance in solving model **[IWT]** using the proposed nested decomposition algorithm. We use the inland waterway ports located in four southeast U.S. states, namely, Arkansas (AR), Louisiana (LA), Mississippi (MS), and Tennessee (TN) as a testing ground to visualize and validate the modeling results. A number of managerial insights are drawn that casts valuable insights on designing a robust inland waterway transportation network. The model and all the solution approaches are coded in python 2.7 on a desktop with Intel Core i7 3.6 GHz processor and 32.0 GB RAM. Optimization solver Gurobi Optimizer 6.5[2] is used throughout the solution pro-

[2]Available from: `http://www.gurobi.com/`

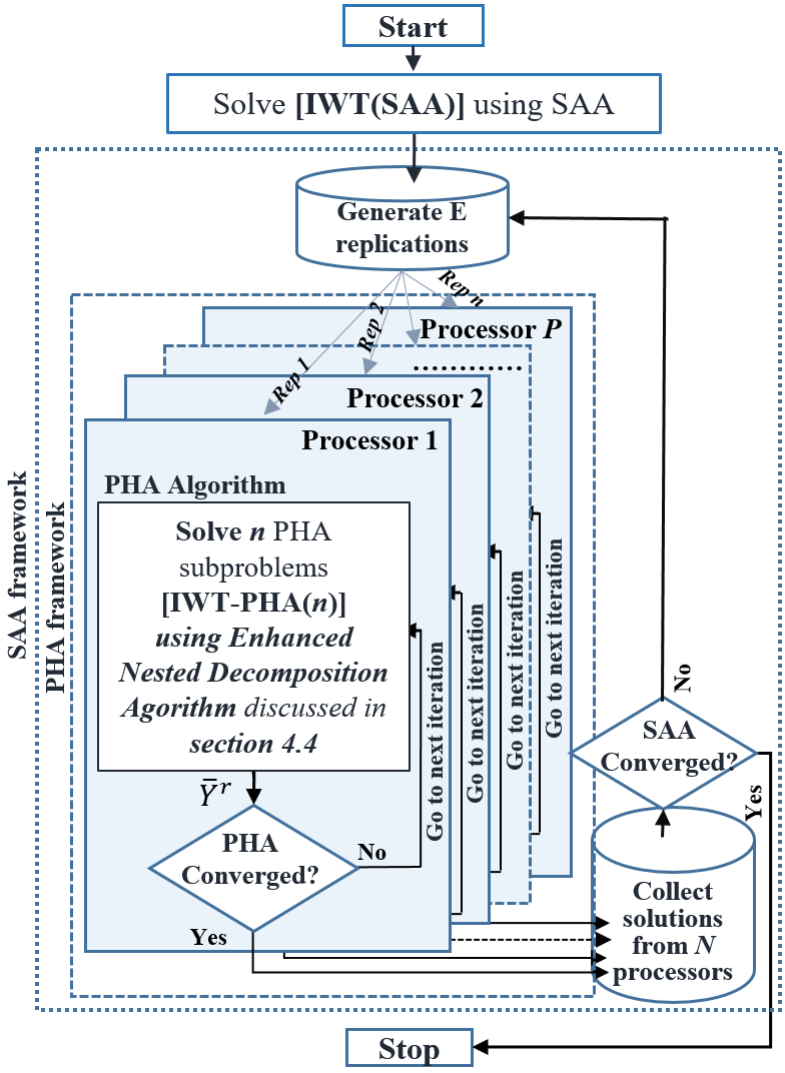

Figure 4.3

Parallelization *scheme I*

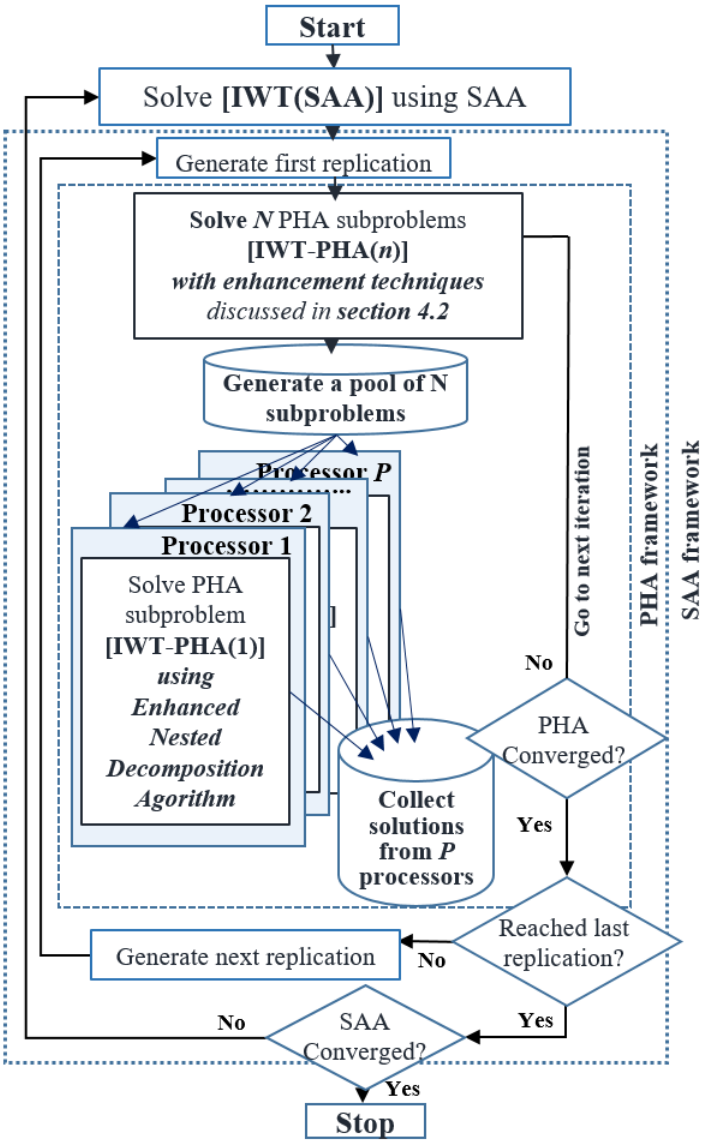

Figure 4.4

Parallelization *scheme II*

cess. Following subsections provides a brief description of the network used in this study, reports the computational performance of the proposed solution algorithms, and summarizes the managerial insights obtained from the case study.

4.5.1 Data Description

This study considers a total of 13 inland waterway ports which are located alongside Mississippi River. Among selected ports, the Port of Rosedale, Port of Greenville, Port of Vicksburg, Port of Natchez, and Port of Yazoo County are located in Mississippi; the Port of Geismar Louisiana, Port of Greater Baton Rouge, Port of South Louisiana, and Port of Gramercy are located in Louisiana; Port of Little Rock is located in Arkansas; and the Port of Memphis, Pemiscot County Port, and New Madrid County Port are located in Tennessee state. The geographical location of these selected ports can be visualized in Figure 4.5. All these ports are connected with each other via the Mississippi River. The Port of Claiborne County is operationally unavialble; therefore, we exclude this port from consideration in our study [85]. Additionally, in this study we consider four commodities, rice, corn, woodchips, and fertilizer, to be transported from the origin ports to the destination ports. In next few subsections we added the detailed information about the supply and demand distribution, transportation cost, and water level fluctuation pertaining to this test region.

4.5.1.1 Supply and demand data:

In this study we consider four commodities, rice, corn, woodchips, and fertilizer, to be transported from the origin ports to the destination ports. The suppliers of

Figure 4.5

Inland waterway port locations along the Mississippi River

these commodities are selected in such a way that they locate within a radius of 60 miles from any of the selected ports. The supply availability information for each port, $\varphi_{mit\omega}$, are then aggregated by considering the minimum distance between suppliers to all origin ports. The supply availability of the selected products (in 1,000 tons) can be seen in Figure 4.6. Each year the test region produces 6.3 and 113.8 million tons of rice and corn from 42 and 59 different counties, respectively [135]. On the other hand, the woodchips and fertilizer have an yearly availability of 8.3 and 0.4 million tons which are supplied from 31 and 22 different counties to ports, respectively [136, 137]. Note that the supply of the selected products, except fertilizer, are highly seasonal in nature. Rice becomes available only between August and October of each year whereas corn is harvested only between mid-July to early December of each year [133]. Likewise, woodchips remain available year-round except three months during the winter (December to February) [133].

This study considers five ports along the Mississippi River which can be used as destination ports to satisfy the demand of 43 industries located nearby the ports. The yearly demand distribution of these ports are shown in Figure 4.7. The annual demand of rice, corn, woodchips, and fertilizers in our testing region are 3.8, 68.3, 8.3, and 0.37 million tons, respectively [135, 137].

4.5.1.2 Transportation cost:

The towboats used in the Mississippi River are capable of carrying up to 15 barges [138]; therefore, we set $\overline{\delta}_{\bar{s}} = 15$. The fixed cost of using a towboat (ψ_{st}) is set to be as \$244.38 [138]. The unit commodity transportation cost (c_{mbsijt}) between each

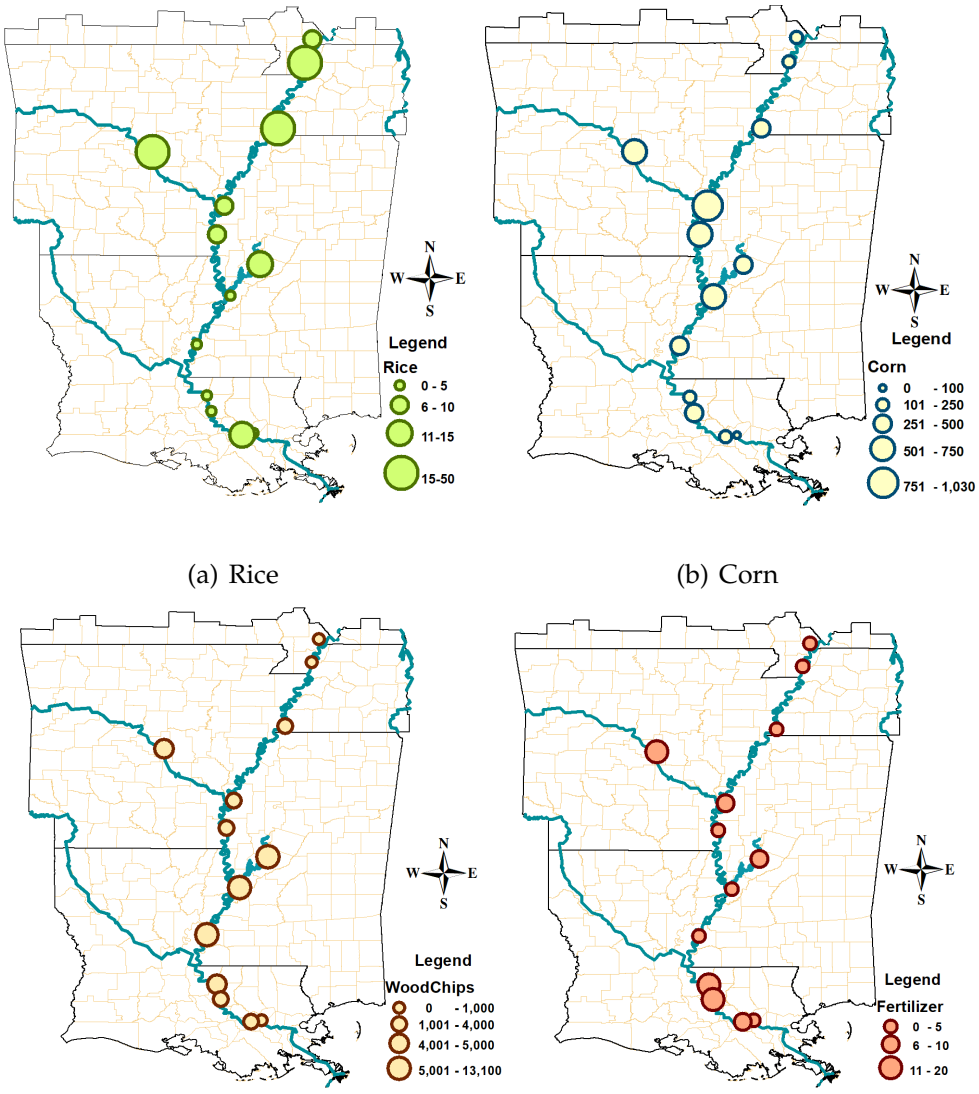

(a) Rice

(b) Corn

(c) Woodchips

(d) Fertilizer

Figure 4.6

Supply availability for (a) rice, (b) corn, (c) fertilizer, and (d) woodchips in the test region (in 1,000 tons)

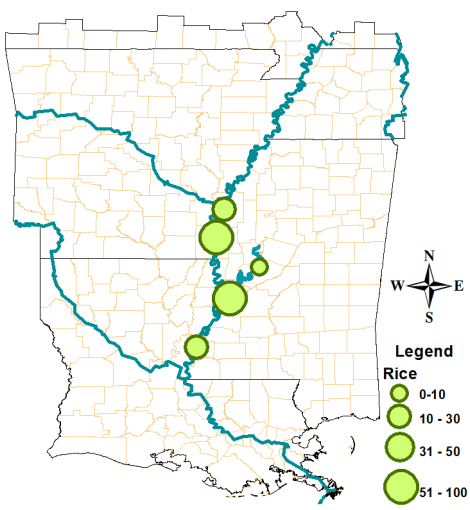

(a) Rice

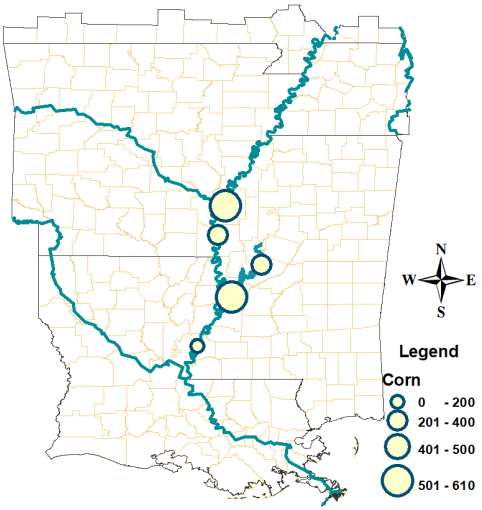

(b) Corn

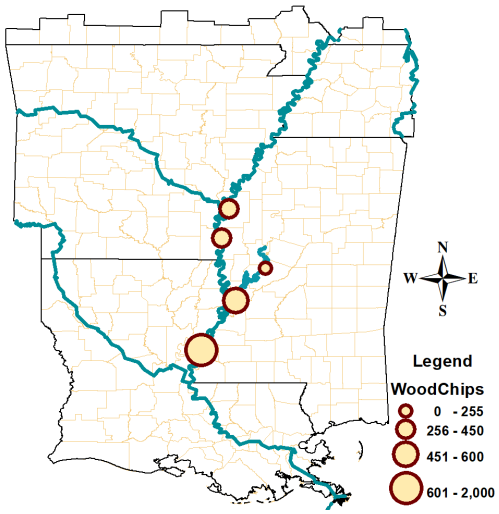

(c) Woodchips

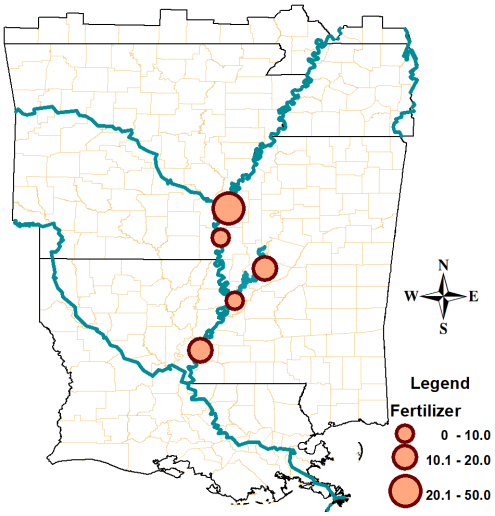

(d) Fertilizer

Figure 4.7

Demand of (a) rice, (b) corn, (c) fertilizer, and (d) woodchips in the test region (in 1,000 tons)

source-destination pair is set to be as \$0.017 /mile/ton [48]. All costs are adjusted based on the 2019 dollars value.

4.5.1.3 Water level fluctuations:

The Mississippi River experiences significant water level fluctuations in different time period of the year. A demonstration of water level fluctuations between the Port of Rosedale and Port of Greenville from July, 2016 to June, 2017 is provided in Figure 4.8 [139]. Each point on Figure 4.8 indicates the water stage of the Mississippi River on a weekly basis. It can be observed from the figure that the water level drops between mid-August till the end of December while reaches to the maximum during the first three weeks in October. Other than these specific time periods, the water stage generally remains stable for the rest of the year (above 14.2 feet), except in May when the level reaches to 42 feet, which is higher than the flood level.

4.5.2 Performance Evaluation of the Algorithms

This subsection presents our computational experiences in solving model **[IWT]** using the algorithms presented in Section 2.4. To test the performance of the solution algorithms, we first vary $|\mathcal{I}|$, $|\mathcal{J}|$, $|\mathcal{M}|$,$|\mathcal{S}|$, and $|\mathcal{T}|$ to generate 9 different problem instances. The description of these instances are summarized in Table 4.1. We use the following criteria to terminate the algorithms: (i) the optimality gap (i.e., $\epsilon = |UB - LB|/UB$) falls below a threshold value (e.g., $\epsilon = 1.0\%$); (ii) the

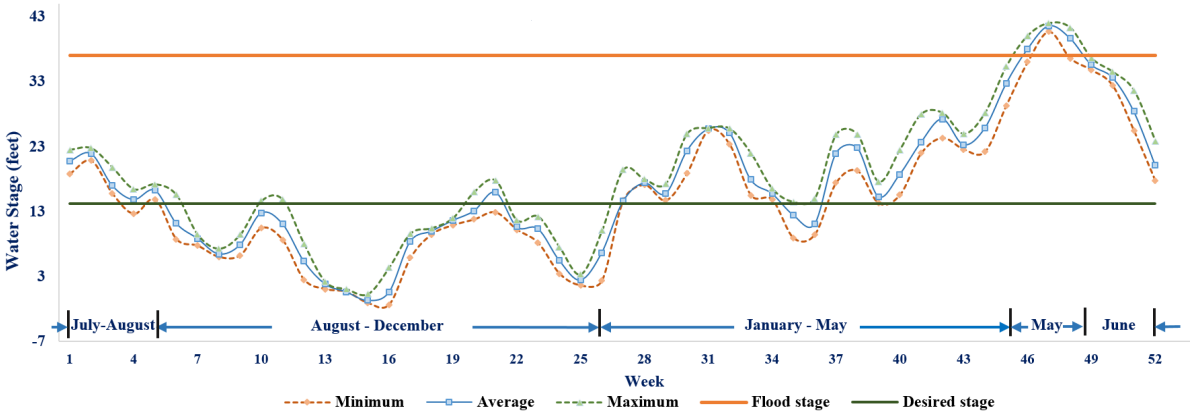

Figure 4.8

Demonstration of water level fluctuations between Port of Rosedale and Port of Greenville from July, 2016 to June, 2017 [139]

maximum time limit (t^{max}) is reached (e.g., $t^{max} = 10,800$ CPU seconds); or (iii) the maximum iteration limit (q^{max}) is reached (e.g., $q^{max} = 100$). To help the readers follow our solution approaches, the following notations are used to represent each particular variants of the proposed algorithms.

- **PHA**: Progressive Hedging Algorithm.
- **PHA+HR**: Enhanced Progressive Hedging Algorithm with application of Heuristics strategies discussed in Section 4.4.3.2.
- **PHA+HR+SB**:Enhanced Progressive Hedging Algorithm with application of both Heuristics strategies and Scenario Bundling techniques discussed in Sections 4.4.3.2 and 4.4.3.3.
- **HD**: Hybrid decomposition algorithm combining Sample Average Approximation and Enhanced Progressive Hedging Algorithm **(PHA+HR)**.
- **HND-I**: Hybrid decomposition algorithm combining Sample Average Approximation, Enhanced Progressive Hedging Algorithm **(PHA+HR)**, and basic Nested Decomposition algorithm.

- **HND-II**: Hybrid decomposition algorithm combining Sample Average Approximation, Enhanced Progressive Hedging Algorithm **(PHA+HR)**, and Enhanced Nested Decomposition algorithm with enhancements discussed in Sections 4.4.4.1- 4.4.4.2.
- **HND-III**: Hybrid decomposition algorithm combining Sample Average Approximation, Enhanced Progressive Hedging Algorithm **(PHA+HR)**, and Enhanced Nested Decomposition algorithm with enhancements discussed in Sections 4.4.4.1– 4.4.4.3.
- **HND-IV**: Hybrid decomposition algorithm combining Sample Average Approximation, Enhanced Progressive Hedging Algorithm **(PHA+HR)**, and Enhanced Nested Decomposition algorithm with enhancements discussed in Sections 4.4.4.1– 4.4.4.4.
- **PS-I**: Parallelization scheme I discussed in Section 4.4.5.
- **PS-II**: Parallelization scheme II discussed in Section 4.4.5.
- **HND-IV + PS-I**: Parallelization scheme I is applied over hybrid algorithm **HND-IV**.
- **HND-IV + PS-II**: Parallelization scheme II is applied over hybrid algorithm **HND-IV**.

The first two sets of experiments investigate the computational performance between Gurobi and different variants of the Progressive Hedging algorithm in solving model **[IWT]** under scenario sizes N = 20 and 30. The computational results obtained from this set of experiments are summarized in Table 4.2 and 4.3. Note that while reporting the computational results in Tables 4.2 and 4.3 and all the following tables, the algorithm that solves a particular instance within the prespecified optimality gap and in the smallest running time is highlighted. However, if such a quality solution cannot be obtained within the predefined time or iteration limit, we highlight the algorithm with the smallest optimality gap. The key observations obtained from these two tables are summarized below.

- Results in Table 4.2 indicate that Gurobi is only able to solve the first two out of 9 problem instances by obeying the pre-specified termination criteria. In Instance 4, Gurobi ends with a large optimality gap within the time limit. For the remaining instances (instances 3, 5-9), Gurobi fails to provide a feasible solution within the time limit. With the **PHA**, only instances 1 and 4 are now solvable by obeying the pre-specified termination criteria. However, it is realized that the **PHA** is capable of providing high quality feasible solutions (on average 2.54%) within the time limit for most of the problem instances except instances 6 and 9. The performance of the **PHA** slightly improves with the incorporation of both global and local heuristics (**PHA+HR**) and scenario bundling techniques (**PHA+HR+SB**). Among all variants of the **PHA**, algorithm **PHA+HR+SB** provides the lower optimality gap (on average 1.17%) with an average running time of 9,292 CPU seconds.

- Table 4.3 shows the results for Gurobi and different variants of the **PHA** in solving model **[IWT]** with N =30 scenarios. Gurobi, in this specific case, experiences even more difficulties in solving the selected instances. Gurobi is now able to solve only 1 instance, compared to 2 in N =20, by obeying the pre-specified termination criteria. With the **PHA**, high quality feasible solutions can be obtained in a number of instances (6/9 instances). Even though no additional instances can be solved within the time limit, the enhanced variant of the **PHA**, namely, **PHA+HR** and **PHA+HR+SB** approaches, are capable of marginally dropping the optimality gap and running time over **PHA**. In overall, algorithm **PHA+HR+SB** demonstrates the superior computational performance (with respect to both optimality gap and running time) over other techniques investigated in Table 4.3 in solving model **[IWT]** and within our tested instances.

The next set of experiments tests the computational performance of the proposed hybrid algorithms (**HD**, **HND-I**, **HND-II**, **HND-III**, and **HND-IV**) that are generated through different combinations of **SAA**, **PHA**, and **ND** algorithms along with their various enhancement techniques. To run the experiments, we set N = 20 and N' = 200. Table 4.4 summarizes the computational performance of these hybrid algorithms with Gurobi. Results in Table 4.4 clearly shows that all hybrid algorithms, namely, **HD**, **HND-I**, **HND-II**, **HND-III**, and **HND-IV**, demonstrate higher computational performance over Gurobi. Among different enhancement techniques, algorithm **HND-IV** provides the best solution with respect to run-

ning time and optimality gap. However, algorithm **HND-IV** fails to solve 7 out of 9 problem instances by obeying the pre-specified termination criteria and left with an average optimality gap of 8.09%. Therefore, we employ paralellization schemes **PS-I** and **PS-II** to further enhance the computational performance of this algorithm. The results are reported in Table 4.5. The key findings from these computational results are summarized below:

- The results in Table 4.5 show that incorporating Parallelization scheme I (**PS-I** algorithm) in **HND-IV** significantly drops the optimality gap and running time of the algorithm. On average, algorithm **HND-IV + PS-I** drops the running time by 53.15% over algorithm **HND-IV** while the reduction in running time is achieved with an average optimality gap of 0.55%. Except the last instance, this algorithm successfully solves all the problem instances reported in Table 4.1 by obeying the pre-specified termination criteria.
- For the case with algorithm **HND-IV + PS-II** in Table 4.5, we also observe notable improvements for most of the instances compared to the basic **HND-IV** algorithm. The average running time of this algorithm is now dropped by 35.1% over algorithm **HND-IV**. Note that this improvement in running time is achieved with an average optimality gap of 0.92%. Despite these notable improvements, algorithm **HND-IV + PS-II** is still unable to solve three instances (instance 6, 8, and 9) by obeying the pre-specified termination criteria.
- Our final observation is made between algorithms **HND-IV + PS-I** and **HND-IV + PS-II**. Clearly, algorithm **HND-IV + PS-I** outperforms algorithm **HND-IV + PS-II** with respect to both running time and optimality gap in most of the instances, except three instances (instance 2, 4, and 9). To further demonstrate the computational benefit of using the **HND-IV + PS-I** algorithm, we run another set of experiments by varying different water level ($\bar{w}_{ijt\omega}$) and supply ($\phi_{mit\omega}$) scenarios as shown in Table 4.6. Note that the results in Table 4.6 are demonstrated for instance 7 only which represents the base case scenario. The results clearly indicate that even though with an increase in $\bar{w}_{ijt\omega}$ and $\phi_{mit\omega}$ scenarios, the running time for both the parallelization schemes increases, algorithm **HND-IV + PS-I** still consistently produces high quality solutions within our tested experimental range.

Algorithm 1: Progressive Hedging Algorithm

Initialize, $r \leftarrow 1$, ϵ, $\{\zeta^r_{mbsijtn}\}_{\forall m\in\mathcal{M},b\in\mathcal{B},s\in\mathcal{S},i\in\mathcal{I},j\in\mathcal{J}_i,t\in\mathcal{T},n\in N} \leftarrow 0$, $\nu^r \leftarrow \nu^0$,

$\{\beta^r_{sijtn}\}_{\forall s\in\mathcal{S},(i,j)\in(\mathcal{I},\mathcal{J}),t\in\mathcal{T},n\in N} \leftarrow 0$, $\theta^r \leftarrow \theta^0$

terminate $\leftarrow$ **false**

while (*terminate* $=$ **false**) **do**

for $n = 1$ to N

Solve [**IWT-PHA(*n*)**] and obtain $\{Y^r_{mbsijtn}\}_{\forall m\in\mathcal{M},b\in\mathcal{B},s\in\mathcal{S},i\in\mathcal{I},j\in\mathcal{J},t\in\mathcal{T}}$ and

$\{Y^r_{sijtn}\}_{\forall s\in\mathcal{S}(i,j)\in(\mathcal{I},\mathcal{J}),t\in\mathcal{T}}$

end for

Calculate the consensus parameter:

$\bar{Y}^r_{mbsijt} \leftarrow \frac{1}{N}\sum_{n=1}^{N} Y^r_{mbsijtn}; \forall m \in \mathcal{M}, b \in \mathcal{B}, s \in \mathcal{S}, i \in \mathcal{I}, j \in \mathcal{J}_j, t \in \mathcal{T}$

$\bar{Y}^r_{sijt} \leftarrow \frac{1}{N}\sum_{n=1}^{N} Y^r_{sijt}; \forall s \in \mathcal{S}, (i,j) \in (\mathcal{I},\mathcal{J}), t \in \mathcal{T}$

if $(r > 1)$ **then**

Update the largangian parameter:

$$\zeta^r_{mbsijtn} \longleftarrow \zeta^{r-1}_{mbsijtn} + \vartheta^{r-1}(Y^r_{mbsijtn} - \bar{Y}^{r-1}_{mbsijt}) \quad \forall m \in \mathcal{M}, b \in \mathcal{B}, s \in \mathcal{S}, i \in \mathcal{I}, j \in \mathcal{J}, t \in \mathcal{T}$$

$$\beta^r_{sijtn} \longleftarrow \beta^{r-1}_{sijtn} + \theta^{r-1}(Y^r_{sijtn} - \bar{Y}^r_{sijt}) \quad \forall s \in \mathcal{S}, (i,j) \in (\mathcal{I},\mathcal{J}), t \in \mathcal{T}$$

Update the penalty parameter:

$$\vartheta^r \longleftarrow \Delta\vartheta^{r-1} \text{ and } \Delta > 1 \,; \theta^r \longleftarrow \Delta\theta^{r-1} \text{ and } \Delta > 1$$

end if

if $(\{|Y^r_{mbsijtn} - \bar{Y}^r_{mbsijt}| + |Y^r_{sijt} - \bar{Y}^r_{sijt}|\}_{\forall m\in\mathcal{M},b\in\mathcal{B},s\in\mathcal{S},(i,j)\in(\mathcal{I},\mathcal{J}),t\in\mathcal{T}} \leq \epsilon)$ **then**

terminate $\leftarrow$ **true**

end if

$r \leftarrow r + 1$

end while

Table 4.1

Problem size and test instances

	Instance No.	$\|\mathcal{I}\|$	$\|\mathcal{J}\|$	$\|\mathcal{M}\|$	$\|\mathcal{B}\|$	$\|\mathcal{S}\|$	$\|\mathcal{T}\|$	Binary variables	Continuous variables	Total variables	No. of constraints
	1	4	3	2	15	6	12	26,784	26,256	53,040	69,372
Small	2	4	3	3	15	8	24	105,984	104,688	210,672	252,672
	3	4	3	4	15	10	36	263,520	261,216	524,736	601,740
	4	8	4	2	15	6	12	71,424	69,696	141,120	184,464
Medium	5	8	4	3	15	8	24	282,624	278,208	560,832	672,384
	6	8	4	4	15	10	36	702,720	694,656	1,397,376	1,602,000
	7	12	5	2	15	6	12	133,920	130,416	264,336	345,348
Large	8	12	5	3	15	8	24	529,920	520,848	1,050,768	1,259,328
	9	12	5	4	15	10	36	1,317,600	1,300,896	2,618,496	3,001,140

Table 4.2

Experimental result for basic and enhanced PHA algorithm (N=20)

	Gurobi		**PHA**			**PHA+HR**			**PHA+HR+SB**		
Instance	$t(sec)$	$\epsilon(\%)$	$t(sec)$	$\epsilon(\%)$	r	$t(sec)$	$\epsilon(\%)$	r	$t(sec)$	$\epsilon(\%)$	r
1	**954**	0.11	3,246	0.8	46	3,198	0.85	45	1,364	0.51	12
2	8,987	0.27	10,800	1.68	31	10,800	1.47	30	**10,574**	0.91	9
3	TL[1]	-	10,800	4.26	11	10,800	3.37	10	10,800	**2.03**	2
4	10,800	21.4	10,463	0.41	33	10,147	0.79	31	**9,956**	0.62	21
5	TL	-	10,800	4.19	9	10,800	3.22	9	10,800	**1.69**	3
6	TL	-	TL	-	-	TL	-	-	TL	-	-
7	TL	-	10,800	2.12	15	10,800	1.36	14	**10,756**	0.94	5
8	TL	-	10,800	4.35	6	10,800	3.31	6	10,800	**1.49**	1
9	TL	-	OOM[2]	-	-	OOM	-	-	TL	-	-
Average	6,913	7.17	9,672	2.54	21.57	9,620	2.05	20.71	**9,292**	1.17	7.57

[1]TL: No feasible solution within time limit

[2]OOM: Out of memory

Table 4.3

Experimental result for basic and enhanced PHA algorithm (N=30)

	Gurobi		**PHA**			**PHA+HR**			**PHA+HR+SB**		
Instance	$t(sec)$	$\epsilon(\%)$	$t(sec)$	$\epsilon(\%)$	r	$t(sec)$	$\epsilon(\%)$	r	$t(sec)$	$\epsilon(\%)$	r
1	**852**	0.25	5,764	0.9	44	5,447	0.81	43	2,165	0.91	11
2	TL	-	10,800	1.83	20	10,800	1.28	19	**10,671**	0.84	5
3	TL	-	10,800	5.34	6	10,800	4.63	6	10,800	**2.41**	2
4	10,800	56.66	10,800	4.56	25	10,800	3.76	23	10,800	**1.42**	14
5	TL	-	10,800	5.37	7	10,800	4.31	6	10,800	**3.08**	2
6	TL	-	OOM	-	-	OOM	-	-	TL	-	-
7	TL	-	10,800	4.88	11	10,800	3.94	10	10,800	**1.97**	3
8	TL	-	OOM	-	-	OOM	-	-	TL	-	-
9	OOM	-	OOM	-	-	OOM	-	-	OOM	-	-
Average	5,826	28.45	9,960	3.81	18.66	9,907	3.12	17.83	**9,339**	1.77	6.16

Table 4.4

Experimental result for Hybrid Nested Decomposition algorithm.

Instance	Gurobi		HD			HND-I			HND-II			HND-III			HND-IV		
	$t(sec)$	$\epsilon(\%)$	$t(sec)$	$\epsilon(\%)$	r	$t(sec)$	$\epsilon(\%)$	r	$t(sec)$	$\epsilon(\%)$	r	$t(sec)$	$\epsilon(\%)$	r	$t(sec)$	$\epsilon(\%)$	r
1	3,521	0.19	10,800	10.65	16	1,196	0.36	1	741	0.16	3	787	0.24	2	**313**	0.12	1
2	TL	-	10,800	11.78	10	10,800	11.25	1	10,800	3.56	16	10,800	2.06	11	10,800	**1.60**	11
3	TL	-	10,800	16.85	3	TL	-	-	10,800	**4.17**	8	10,800	4.18	6	10,800	4.24	6
4	TL	-	10,800	27.14	13	10,800	1.63	5	912	0.94	3	474	0.07	1	**346**	0.44	1
5	TL	-	10,800	31.02	4	10,800	70.55	1	10,800	**9.14**	10	10,800	10.21	7	10,800	9.47	7
6	OOM	-	10,800	36.54	1	TL	-	-	10,800	33.01	3	10,800	30.04	3	10,800	**26.46**	3
7	TL	-	10,800	46.11	3	10,800	15.58	1	10,800	14.34	5	10,800	12.62	4	10,800	**6.759**	4
8	OOM	-	10,800	51.23	1	TL	-	-	10,800	25.29	1	10,800	20.68	1	10,800	**15.81**	1
9	OOM	-	TL	-	-	TL	-	-	TL	-	-	TL	-	-	TL	-	-
Average	3,521	0.19	10,800	28.91	6.37	8,879	19.87	1.8	8306	11.32	5.87	8,257	10.01	4.37	**8,182**	8.09	4.25

Table 4.5

Experimental result for best algorithms under different parallelization schemes

Instance	**HND-IV**			**HND-IV + PS-I**			**HND-IV + PS-II**		
No.	$t(sec)$	$\epsilon(\%)$	r	$t(sec)$	$\epsilon(\%)$	r	$t(sec)$	$\epsilon(\%)$	r
1	313	0.12	1	**284**	0.13	2	502	0.21	2
2	10,800	4.24	11	1,050	0.21	3	**832**	0.43	2
3	10,800	1.6	7	**1,510**	0.91	2	2,105	0.87	3
4	346	0.44	1	360	0.47	2	**312**	0.71	1
5	10,800	26.46	6	**6,744**	0.86	6	7,643	0.63	6
6	10,800	9.47	3	**9,140**	0.81	6	10,800	2.57	6
7	10,800	14.34	4	**4,471**	0.25	9	9,378	0.31	7
8	10,800	15.81	1	**7,103**	0.73	11	10,800	1.64	10
9	TL	-	-	10,800	23.8	1	10,800	**20.9**	1
Average	8182	9.06	4	**3833**	0.55	5	5309	0.92	5

Table 4.6

Computational performance of the proposed parallelization schemes under different water level ($\bar{w}_{ijt\omega}$) and supply ($\phi_{mit\omega}$) scenarios

	HND-IV + PS-I			**HND-IV + PS-II**		
Scenario	$t(sec)$	$\epsilon(\%)$	r	$t(sec)$	$\epsilon(\%)$	r
-40%	**1,897**	0.39	4	6,564	0.22	5
-20%	**2,798**	0.41	6	7,958	0.29	6
Base $\bar{w}_{ijt\omega}$	**4,471**	0.25	9	9,378	0.31	7
20%	**4,519**	0.29	9	9,659	0.46	7
40%	**4,963**	0.66	10	10,800	1.62	8
-40%	**2,841**	0.23	6	7,797	0.28	6
-20%	**3,409**	0.37	7	9,190	0.19	7
Base $\phi_{mit\omega}$	**4,471**	0.25	9	9,378	0.31	7
20%	**5,491**	0.54	11	10,800	2.37	9
40%	**6,248**	0.32	13	10,723	0.98	8

4.5.3 Real-life Case Study

4.5.3.1 Impact of water level fluctuation ($\bar{w}_{ijt\omega}$) on overall system performance

This set of experiments investigate the impact of water level fluctuation ($\bar{w}_{ijt\omega}$) on the overall system performance. To run the experiments, we consider four different water level scenarios by varying $\bar{w}_{ijt\omega}$ by $\pm$20% and $\pm$40%. Figure 4.9 summarizes the key results from this set of experiments. In Figure 4.9 and the following figures, $t = 1$ stands for a representative day from January, and the fol-

lowing months are represented in an ascending order which are ended at $t = 12$ which is a representative day in December. The experimental results indicate that with 20% and 40% increase in mean $\bar{w}_{ijt\omega}$, the overall barge usage (Y_{mbsijt}) drops by approximately 10.9% and 20.1%, respectively, from the base case scenario. On the other hand, when the mean $\bar{w}_{ijt\omega}$ is dropped by 20% and 40%, then the overall barge usage is increased by 21% and 47%, respectively, from the base case scenario. This is due to the fact that when the mean $\bar{w}_{ijt\omega}$ decreases, more barges are now required with less loads compared to their design capacities to avoid being stuck in any part of the waterway. Note that the peak barge usage is observed in October $(t = 10)$ when the water level drops to it's minimum. Additionally, Figure 4.9 shows that the water level reduction causes the barge to towboat ratio (Y_{mbsijt}/Y_{sijt}) to increase. With a 40% drop in $\bar{w}_{ijt\omega}$, Y_{mbsijt}/Y_{sijt} reaches to a maximum of 11 barges per towboat in October and November ($t = 10$ and 11).

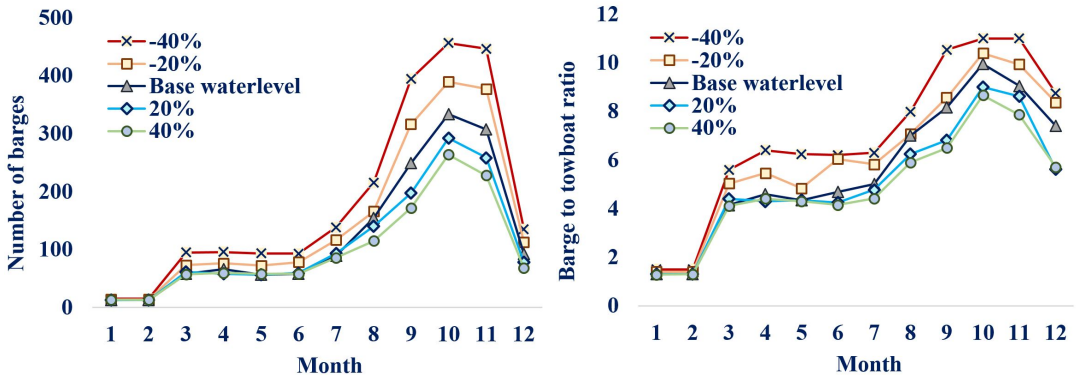

(a) Number of barges used (Y_{mbsijt}) (b) Barge to towboat ratio((Y_{mbsijt}/Y_{sijt})

Figure 4.9

Impact of $\bar{w}_{ijt\omega}$ changes on barge selection (Y_{mbsijt}) and barge to towboat ratio (Y_{mbsijt}/Y_{sijt})

4.5.3.2 Impact of commodity supply ($\phi_{mit\omega}$) changes on overall system performance

The next set of experiments study the impact of stochastic nature of the commodity supply ($\phi_{mit\omega}$) availability on the overall system performance. To run the experiments, we consider four different supply scenarios by varying mean $\phi_{mit\omega}$ by $\pm$20% and $\pm$40%. Results in Figure 4.10 show that when the mean $\phi_{mit\omega}$ increases by 20% and 40%, then the barge selection (Y_{mbsijt}) decisions are increased by 8% and 18%, respectively, from the base case scenario. On the other hand, when the mean $\phi_{mit\omega}$ drops by 20% and 40%, then the barge selection (Y_{mbsijt}) decisions are dropped by 11% and 22%, respectively, from the base case scenario. Similar to the previous experiment, the peak barge usage is observed in October (t = 10)

when the water level drop is the minimum. Figure 4.10(b) illustrates that with an increase in mean $\phi_{mit\omega}$ by 40%, on average 3 more barges are now required to be connected with a towboat during the peak demand season (t = 10). In Figure 4.10(c), we observe that the unsatisfied demand (U_{mjt}) reaches to +45% and +86% with the reduction in $\phi_{mit\omega}$ by 20% and 40%, respectively. Finally, we observe that the overall inventory storage increases with an increase in mean $\phi_{mit\omega}$ (see Figure 4.10(d)). It is interesting to note that in order to avoid the peak water level drop season (October) and to satisfy the customer demand, the system utilizes a high storage of commodities in the ports on September ($t = 9$).

4.6 Conclusion and Future Research Directions

This paper proposes a two-stage stochastic programming model to design and manage an inland waterway transportation network with appropriate considerations of the stochasticity associated with commodity supply and water level fluctuations. A parallelized hybrid decomposition algorithm is introduced to solve the proposed optimization model. Computational results indicate that the proposed algorithm is capable of producing high quality solutions consistently in a timely manner. In order to visualize and validate the modeling results, we demonstrate a real-life case study by utilizing few inland waterway ports from the down Mississippi River. A number of managerial insights are drawn from the numerical experiments, including the impact of stochastic commodity supply and water level fluctuations on the inland waterway port operations.

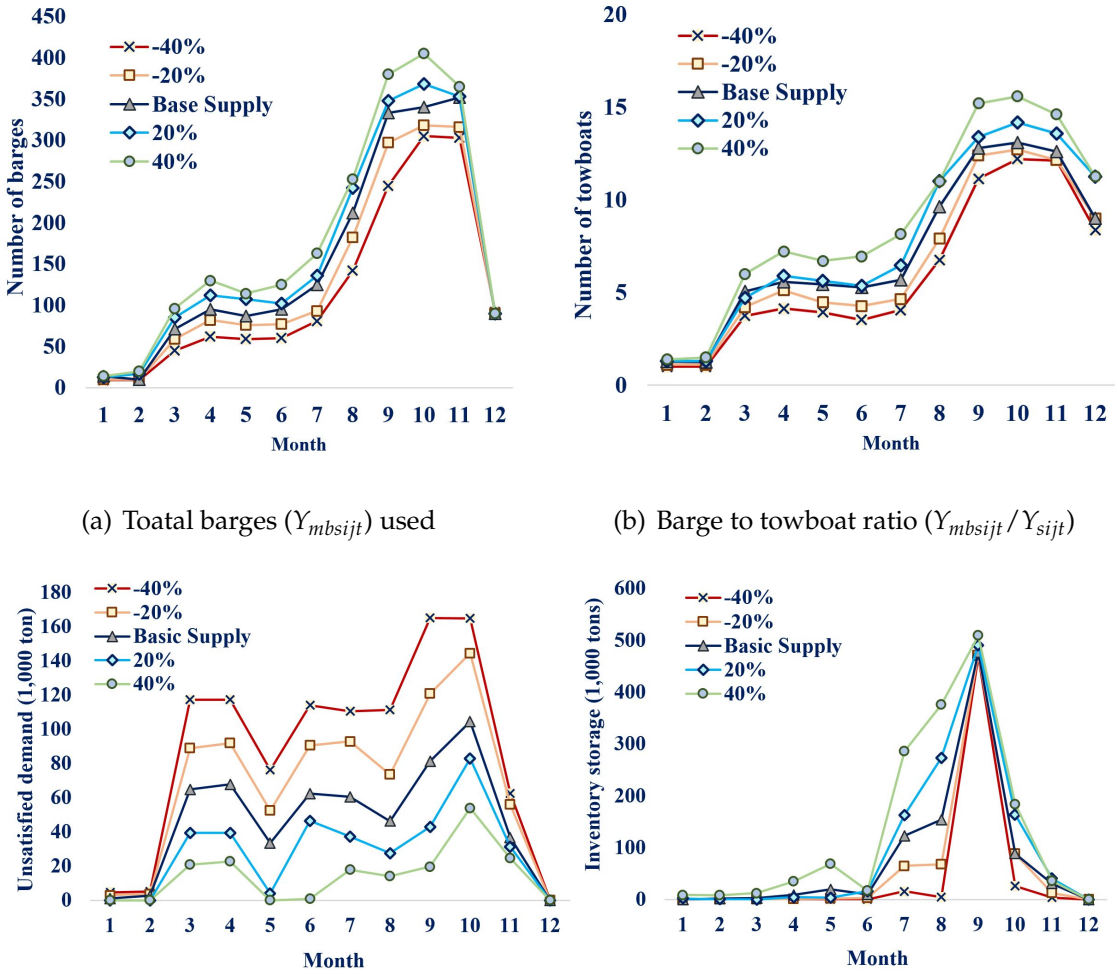

(a) Toatal barges (Y_{mbsijt}) used

(b) Barge to towboat ratio (Y_{mbsijt}/Y_{sijt})

(c) Unsatisfied demand (U_{mjt})

(d) Inventory storage (H_{mit}, H_{mjt})

Figure 4.10

Impact of $\phi_{mit\omega}$ changes on overall system performance.

To summarize, the major contributions of this study include: (i) proposing a multi-commodity, multi-time period two-stage stochastic mixed-integer linear programming model to minimize the inland waterway port operations under stochastic commodity supply and water level fluctuations; (ii) introducing and testing an efficient hybrid decomposition algorithm, combining Sample Average Approximation, and an enhanced Progressive Hedging and Nested Decomposition algorithm, to efficiently solve realistic-size network design problems in a reasonable timeframe; (iii) developing and testing different parallelization schemes to parallelize the proposed hybrid decomposition algorithm; and (iv) obtaining managerial insights from a real-life case study. Note that the proposed methodologies can be adopted to efficiently solve other stochastic optimization problems. We believe the managerial insights obtained from this study will help policy makers to design and manage a robust and cost-efficient inland waterway-based supply chain network under uncertainty.

This study opens up numerous avenues for future research. Detailed considerations of barge and towboat routing, scheduling, and re-positioning issues can be made to analyze the impact of these issues on the inland waterway port operations. Further, the impact of inland waterway port operations under both natural (e.g., hurricane, tornado) and/or human-induced (e.g., cyber attack) disruptions can also be investigated. Future studies will address these issues.

CHAPTER 5

A BENDER'S BASED NESTED DECOMPOSITION ALGORITHM TO SOLVE A STOCHASTIC INLAND WATERWAY PORT MANAGEMENT PROBLEM CONSIDERING PERISHABLE PRODUCT

5.1 Introduction

Inland waterway ports are the hearts of inland waterway transportation. While ensuring the most cost efficient and environmentally friendly means of transportation, these ports support the access to the inland waterways and play a critical role in nations overall waterway transportation system. In the United States, these ports contribute about 15 billion dollars to the country's total GDP (Gross Domestic Product) along with offering above 250,000 employment opportunities annually [89]. Additionally, these ports play a critical role in industrial and agricultural development of remote rural areas [84]. However, despite of their substantial potentiality, numerous factors, such as, water level fluctuation, dredging issues, congestion, delays caused by scheduled and unscheduled closures of locks, and aging infrastructure are imposing substantial threats to their overall productivity [140]. Also, it is worth mentioning that inland waterway transportation system is utilized to transport mostly perishable products such as corn and soybeans. There-

fore, the combined impact of these aforementioned factors can lead to a significant commodity loss at ports that might discourage the potential users of this network.

A number of features of Inland waterway ports make them well distinguishable from the *seaports*. To mention a few, these ports are generally located primarily near smaller bodies of water, handle barge traffic drafting upto 9 feet only, and handle smaller counts of larger users and a large number of smaller users [84]. Additionally, the varying precipitation levels in different periods of a year causes severe fluctuations in the active water level at port channels and any part of the waterway connecting two inland waterway ports [139, 94, 90]. Depending on the intensity of this fluctuation, disruptions such as droughts and floods can be experienced that may even cease port operations for a prolonged period of time. Another distinguishing property of inland waterway ports is that these ports handle high volume of perishable products that are seasonal in nature and can significantly deteriorate with the progression of time. Therefore, this perishability issue coupled with the stochastic water-level fluctuations, and highly uncertain supply impose an unique challenge which restrict the optimization models available in the literature for the maritime transportation to be directly applicable for the inland waterway ports. Therefore, in order to ensure long term sustainment of the inland waterway ports, sophisticated optimization models need to be developed that best capture the unique characteristics of this cost efficient, reliable, and environmentally-friendly transportation sector.

Multiple research have been conducted to date that develop optimization models to address wide variant of seaport-related problems, such as ship routing and scheduling [29, 68], inventory routing [5], berth allocation and scheduling [27, 141], empty container re-positioning [20], sailing speed optimization [73, 141], bunker consumption [145], emission consideration [141], and disruption [43, 126]. Some researchers develop simulation models to address similar problems (e.g., [118, 125, 121, 44]). However, compared to the seaport literature, inland waterway ports did not receive much attention from the research community. A few studies has been conducted to characterize and model the specifics of *deep draft inland ports*, capable of handling container cargos and ships; however, almost no research attempts has been made that specifically considers the *shallow draft inland ports*[1] related issues. Considering their remarkable contributions to the overall transportation system and the economy, creating better understanding of the shallow draft inland waterway ports is imperative in order to successfully design and manage a sound and efficient inland waterway transportation network.

To fulfill this gap, this study proposes a mathematical model to capture the prevalent issues related to inland waterway port (e.g., waterlevel fluctuations, barge/towboat assignments, inventory decisions, and port delays) and combine them under the same decision making framework that magnifies their impacts on designing and managing a sound, robust inland waterway transportation net-

[1]The ports that is unable to handle barges/vessels drafting more than 9 feet are known as *shallow draft inland ports*. *Deep draft inland ports*, on the other hand, are the ones that can handle barges/vessels drafting more than 9 feet.

work. We propose a capacitated, multi-commodity, multi-period, two-stage stochastic mixed-integer linear programming model that jointly optimizes trip-wise barge and towboat assignment decisions along with crucial supply chain decisions (e.g., inventory management, transportation decisions) under uncertainty in such a way that the overall system cost can be minimized. Our proposed model efficiently captures a number of realistic issues that appropriately characterize the shallow draft inland waterway port operations, such as towboat and barge availability, weight and volumetric capacity restriction of barges, dredging issues, shelf life of commodities, product mix restrictions, storage restrictions at ports, trip restrictions between origin-destination ports, congestion issues, delays in locks and dams, and many others.

Our proposed mathematical model is an extension of the traditional fixed charged, uncapacitated network flow problem which is already known to be an $\mathcal{NP}$-hard problem [74]. Therefore, to cope with the computational challenge in solving this model we develop a highly customized nested decomposition algorithm. This algorithm combines enhanced Benders decomposition algorithm under Sample Average Approximation framework to effectively solve the large instances of our proposed model within a reasonable time frame.

Apart from proposing the mathematical model and solution approaches, we demonstrate a real life application of our proposed model considering the inland waterway transportation network along the lower Mississippi river. The outcome of this study provides a number of managerial insights, such as the impact of wa-

ter level fluctuations on towboat and barge selection, and impact of commodity deterioration rate on overall system performance, which can effectively aid decision makers to design a reliable and cost-efficient shallow draft inland waterway transportation network under uncertainty[2]

The remainder of this paper is organized as follows. Section 5.2 provides a comprehensive review the related works. In Section 5.3 the problem statement and the proposed mathematical model formulation is introduced. The decomposition algorithms used to solve our proposed model are outlined in Section 5.4. Section 5.5 presents a real life case study and summarizes the key managerial insights and the computational performances of the proposed algorithms obtained by solving the case study. Section 5.6 concludes the study with discussing some future research avenues.

5.2 Literature review

The deep draft inland waterway ports have been gaining the focus from the research community over several years. Different researchers have studied multiple realistic issues such as barge and towboat routing and repositioning, berth allocation, port disruption, and delays in locks and dams related to deep-draft inland waterway ports. This section provides a comprehensive overview of these studies, highlights the research gap, and explains the key contributions of our work compared to the existing literature.

[2]This article has recently been accepted in International Journal of Production Economics [2].

Alike seaports, inland waterway ports also experience berth allocation problem. Few researchers have studied this problem for deep-draft inland waterway ports. For example, Grubivsic et al. [50] solve a berth layout design problem with an objective to minimize the overall vessel waiting time at deep-draft inland waterway ports. Depuy et al.[30] consider fleet location capacity, the total volume of barges, and average handling time to ensure optimal berth allocation. Arango et al.[11] adopted a combined simulation-optimization approach to solve this problem. Another research develops two mathematical models for modeling the berth allocation problem and adopts a tree search procedure to solve these models [51].

Another research scheme investigates the cascading impcats of lock and dam delays on the inland waterway transportation network including deep draft inland ports. Ting and Schonfeld [130] use a simulation-optimization framework to determine the optimal capacity for lock and dams so that the costs associated with the tow delays can be minimized. Similarly, the research by Wang and Schonfeld [147] use a combined simulation-optimization approach to determine an optimal strategy to schedule the investment decisions for lock reconstruction and rehabilitation. Ting and Schonfeld [129] develop an integrated tow control algorithm that can reduce the tow delays associated with a series of locks.

Barge routing and empty container repositioning problems are another prevalent areas in deep draft inland waterway port research. These problems are generally addressed together in the existing literature. Braekers et al. [20] solves the barge routing and empty container repositioning problem between a seaport and

few hinterland ports. Later, this research has been extended to include the vessel capacity and round trip service frequency [19]. Marass [76] develops a mixed-integer linear programming (MILP) model to optimize the the transport routes of chartered container ships or tows for an inland waterway port. Davidovic et al. [28] discuss a barge and container ship routing problem and propose a guided local search technique to solve the problem. Most recently, An et al. [9] proposed a MINLP model to solve the empty container repositioning problem for the shipping network.

Different natural (e.g., hurricane, tornado) or human-induced (e.g., cyber-attack) disasters may interrupt or cease the port operations for an extended period of time [54, 57] and impact the overall supply chain [7, 55, 53]. Realizing this situation, a few studies develops models to measure the resiliency of a deep draft inland waterway port. Among those studies, Baroud et al. [13] determine the important waterway links and the precedence of link recovery in case of a disaster by convering different stochastic resilience-based component importance measures into an optimization model. Oztanriseven and Nachtman [87] adopted a simulation approach to determine the potential economic impacts of inland waterways disruption response. This research uses the McClellan-Kerr Arkansas River navigation system as a testbed to visualize and validate the simulation results. Pant et al. [103] propose a dynamic, multi-regional interdependency model to investigate the impact of disruptions on the waterway networks, including both ports and waterway links. Another study [59] propose a Bayesian network based approach

to model the infrastructure resilience of an inland waterway port. Other related research in this area include port-specific economic analysis [4, 87, 151, 67], determining optimal dredging schedule and investment decisions [86, 113, 18], investigating the efficiency of inland waterway container terminals [152], tug scheduling between seaport to inland ports [39, 45, 157], and carbon emission considerations [155, 71, 25].

Different from the studies mentioned above, our study considers different shallow draft inland waterway port related issues such as optimal transportation of perishable products considering their shelf life, waterlevel fluctuation, delay in locks and dams, optimal towboat and barge assignment, barge availability and maintenance considerations under uncertainty. Some existing studies consider shallow draft inland waterway ports as a tier while designing a different supply chain networks such as biomass supply chain (e.g., [107, 81, 80]), coal supply chain (e.g., [35, 47, 62]), grain supply chain (e.g., [88, 10, 31]), and many others. However, very few other studies [99, 96, 98, 97] solely focused on the shallow draft inland waterway ports, where the [99] and [96] characterize the shallow draft inland waterway ports and demonstrate methodologies to analyzes the competitiveness of a given port among a set ports. The next studies [98, 97] consider few shallow draft inland waterway port related issues and develop MILP model to optimize the resource usage, and barge and towboat assignment decisions under a deterministic setting. The shelf life of commodities and stochasticity associated with waterlevel fluctuation and commodity availability were not considered in that model. Our

study fills this literature gap by considering all these crucial factors (e.g., shelf life of commodities, stochastic waterlevel fluctuation, and uncertain commodity availability) along with capturing the true characteristics of the inland waterway transportation. Few studies [37, 93, 24, 114] consider the water level fluctuation issues for maritime ports. However, in the case of inland waterway transportation, not much research attempts are observed that penetrate on this specific issue. Further, the commodity loss due to the limited shelf life of agricultural commodities is also ignored in the current literature the impact of which can be very significant on the optimal transportation and resource allocation decisions at ports under uncertain supply conditions. This signifies that the proper modeling efforts, that capture the aforementioned realistic features, need to be made in order to design a reliable inland waterway transportation network.

5.3 Problem Description and Model Formulation

This section presents a capacitated, multicommodity, multi-time period, two-stage, stochastic programming model formulation to efficiently design and manage an inland waterway transportation-based logistics network considering the stochastic, time-variant nature of commodity supply and water-level fluctuations. The model is effectively designed to capture the possible loss in perishable commodities governed by prolonged storage and delayed transportation. Let us consider an inland waterway transportation network $G = (\mathcal{D}, \mathcal{A})$ where $\mathcal{D}$ be the set of nodes and $\mathcal{A}$ denotes the set of arcs that connects different tiers of the network. Set $\mathcal{D}$

consists of a set of origin ports $\mathcal{I}$, from which commodities are shipped and a set of destination ports $\mathcal{J}$ that receive and process the shipped commodities. Figure 5.1 illustrates a simplified inland waterway transportation network consisting of two origin ports and three destination ports.

Network G transports a set of agricultural commodities $\mathcal{M} = \{1, 2, 3, ..., M\}$ through its two tiers (origin ports and destination ports) over a predetermined set of time periods $\mathcal{T} = \{1, 2, 3, ..., T\}$. Subsets $\mathcal{I}_j$ and $\mathcal{J}_i$ are introduced in our model where, set $\mathcal{I}_j$ consists of the subset of origin ports connected to port $j \in \mathcal{J}$ and $\mathcal{J}_i$ represents the subset of destination ports connected to origin port $i \in \mathcal{I}$. Further, we introduce the scenario set $\omega \in \Omega$ that stands for different commodity supply and water-level fluctuation scenarios. Given ρ_ω as the probability of any particular realization, the sum of the all realizations of any sample space Ω should be 1, i.e., $\sum_{\omega \in \Omega} \rho_\omega = 1$.

Inland waterway transportation network primarily transports agricultural commodities such as corn, rice, and soybean the supply of which are highly seasonal in nature. For instance, in the U.S. corn is harvested between mid-July to late November of each calander year [133]. Moreover, knowing the seasonality associated with commodity harvesting, their estimated supply availability by season are also not same for each year. In fact, this amount is highly stochastic in nature. Therefore, to realistically capture this issue we assume that each origin port $i \in \mathcal{I}$ is provided with a stochastic amount $\varphi_{mit\omega}$ of commodity $m \in \mathcal{M}$ at time period

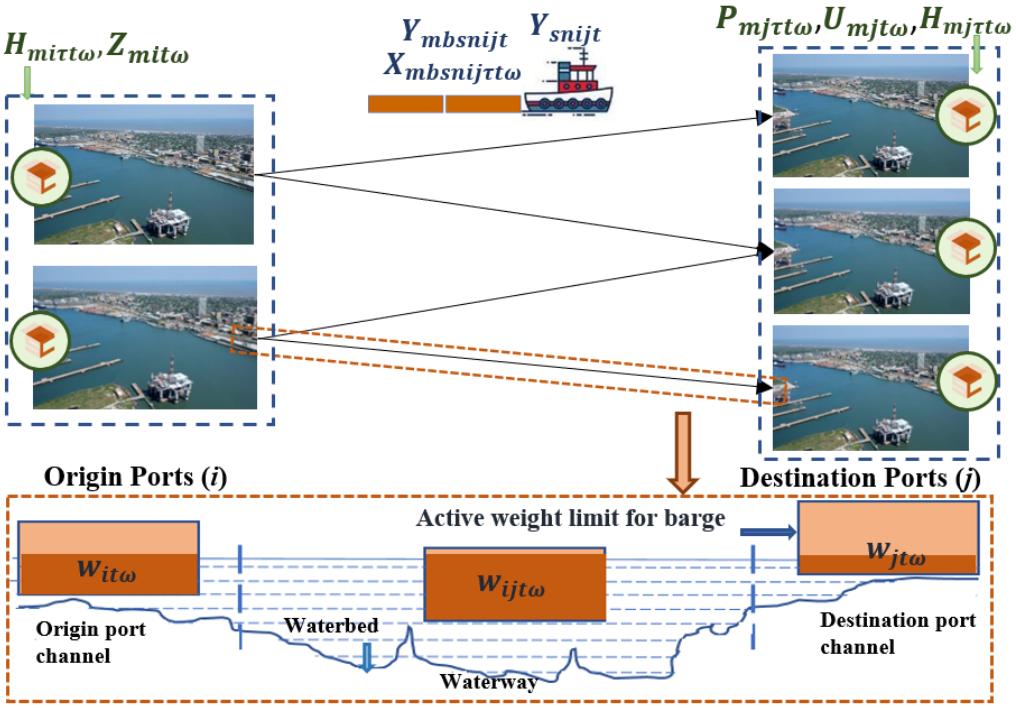

Figure 5.1

Illustration of a inland waterway transportation network

$t \in \mathcal{T}$ under scenario $\omega \in \Omega$. These commodities will be transported through different arcs $\mathcal{A}$ of network G and used to serve the demand at destination ports $j \in \mathcal{J}$. The inland waterway commodity transportation is done by the association of barges and towboats. Let $\mathcal{B} = \{1, 2, 3, ..., B\}$ and $\mathcal{S} = \{1, 2, 3, ..., \overline{S}\}$ respectively represent the set of barges and the set of towboats that can be used to transport commodities between any port pair $(i, j) \in (\mathcal{I}, \mathcal{J})$. Set $\mathcal{S}$ is a ordered set where the first element of the set, i.e., towboat 1 in set $\mathcal{S}$ represents the least powerful towboat and towboat $\overline{S}$ be the most powerful one. Based on their capabilities we denote $\overline{\delta}_s/\underline{\delta}_s$ to be the maximum/minimum number of barges that can/should be carried out by any particular towboat $s \in \mathcal{S}$. In any time period t, the fixed cost of using any towboat $s \in \mathcal{S}$ and the loading and unloading cost for commodity $m \in \mathcal{M}$ to barge $b \in \mathcal{B}$ is denoted as ψ_{st} and η_{mbt}. Further, we consider the commodity carrying capacity of barges through two different parameters $\overline{w}_b$ and v_b where the former one represent the weight carrying capacity and the later one stands for volumetric capacity of barge b, respectively. The unit transportation cost of commodity $m \in \mathcal{M}$ using barge $b \in \mathcal{B}$ connected to towboat $s \in \mathcal{S}$ of trip $n \in \mathcal{N}_{ij}$ along arc $(i, j) \in (\mathcal{I}, \mathcal{J})$ at time period $t \in \mathcal{T}$ that was procured at time period $\tau \in \mathcal{T}$ is denoted by $c_{mbsnij\tau t}$ where $\tau \leq t$. Additionally to account for the periodic maintenance requirements for barges and towboats, two binary availability parameters a_{bit} and a_{sit} are defined that denote the availability of any barge and towboat in any port i at any particular time period t, respectively.

Each port $i \in \mathcal{I} \bigcup \mathcal{J}$ is assumed to have inventory, restricted by a maximum commodity storage capacity of $\overline{h}_i$. The inventory holding cost for commodity $m \in \mathcal{M}$ in port $i \in \mathcal{I} \bigcup \mathcal{J}$ between time periods $\tau \in \mathcal{T}$ and $t \in \mathcal{T}$ under scenario $\omega \in \Omega$ is denoted as $h_{mi\tau t}$ ($\tau \leq t$). We also capture the deterioration rate of carrying commodity $m \in \mathcal{M}$ in any port inventory between two consecutive time periods $\tau \in \mathcal{T}$ and $t \in \mathcal{T}$ by introducing parameter $\alpha_{m\tau t}$. The active weight capacity of any barge between any specific port pairs at any given time $t \in \mathcal{T}$ is defined using parameters $w_{it\omega}$, $w_{jt\omega}$, and $w_{ijt\omega}$, where $w_{it\omega}$ and $w_{jt\omega}$ denote the maximum weight carrying capacity at port channel $i \in \mathcal{I} \bigcup \mathcal{J}$ at time period $t \in \mathcal{T}$ under scenario $\omega \in \Omega$ and $w_{ijt\omega}$ is the allowable weight that can be carried through the waterway between the same port pair $(i, j) \in (\mathcal{I}, \mathcal{J})$ at time period $t \in \mathcal{T}$ under scenario $\omega \in \Omega$. Essentially, the waterway depth at port channel or throughout the waterbody may vary in different time periods of the year depending upon the amount of sediment, silt, or mud accumulated in the waterbed. If such accumulation is too intense at any portion of the waterway (e.g., near ports or between two connecting ports), it increases the height of the waterbed resulting in a decrease in the waterdepth. This waterdepth reduction can sometimes be too intense that it seriously impacts the transportation of shallow draft water vessels through the waterway. Resultantly, the barges need to carry commodities below to their designed weight carrying capacity of $\overline{w}_b$ to avoid being stuck at any point of their navigational waterway. Therefore, the *maximum effective weight* that a barge $m \in \mathcal{M}$ can carry under this restriction would be the *minimum* weight between

the weight capacity near origin and destination ports, namely, $w_{it\omega}$ and $w_{jt\omega}$, and the channel between each origin-destination ports $(i,j) \in (\mathcal{I},\mathcal{J})$, namely, $w_{ijt\omega}$, i.e., $min\{\overline{w}_{ijt\omega}, \overline{w}_b\}$ where $\overline{w}_{ijt\omega} := min\{w_{it\omega}, w_{ijt\omega}, w_{jt\omega}\}$. Considering the unpredictability of accurately estimating this restriction, we consider $\overline{w}_{ijt\omega}$ as a stochastic parameter in our proposed model formulation. Further, we define a set of possible trips along arc $(i,j) \in (\mathcal{I},\mathcal{J})$ as $\mathcal{N}_{ij}$. As discussed earlier, due to stochastic weight carrying capacity of barges, in certain time periods more trips are needed to support commodity transportation. This is captured through the parameter τ_{ijt} that represents the number of possible trips between each source-destination ports. Finally, we assume that the commodity demand at destination ports, denoted by d_{mjt}, can be satisfied either through barge transportation from the origin ports or via an external source by paying a unit penalty cost of π_{mjt}. We now summarize the following notations for our proposed mathematical model formulation.

Sets:

- $\mathcal{I}$: set of origin ports, $i \in \mathcal{I}$
- $\mathcal{J}$: set of destination ports, $j \in \mathcal{J}$
- $\mathcal{M}$: set of commodities, $m \in \mathcal{M}$
- $\mathcal{S}$: set of towboats, $s \in \mathcal{S}$
- $\mathcal{B}$: set of barges, $b \in \mathcal{B}$
- $\mathcal{N}_{ij}$: set of trips along arc (i,j) $\in (\mathcal{I},\mathcal{J}), n \in \mathcal{N}_{ij}$
- $\mathcal{T}$: set of time periods, $t \in \mathcal{T}$
- $\mathcal{I}_j$: set of origin ports connected to destination port j, $\forall j \in \mathcal{J}$
- $\mathcal{J}_i$: set of destination ports connected to origin port i, $\forall i \in \mathcal{I}$
- Ω: set of possible scenarios ω, $\forall \omega \in \Omega$

Parameters:

- ψ_{st}: fixed cost of using towboat $s \in \mathcal{S}$ at time period $t \in \mathcal{T}$
- η_{mbt}: fixed cost for loading and unloading commodity $m \in \mathcal{M}$ in barge $b \in \mathcal{B}$ at time period $t \in \mathcal{T}$
- $c_{mbsnij\tau t\omega}$: unit cost of transporting commodity $m \in \mathcal{M}$ along arc $(i,j) \in (\mathcal{I},\mathcal{J})$ using barge $b \in \mathcal{B}$ of towboat $s \in \mathcal{S}$ in trip $n \in \mathcal{N}_{ij}$ at time period $t \in \mathcal{T}$ that were purchased at time period $\tau \in \mathcal{T}$ under scenario $\omega \in \Omega$, where $\tau < t$
- γ_{mit}: procurement cost of commodity $m \in \mathcal{M}$ in port $i \in \mathcal{I}$ at time period $t \in \mathcal{T}$
- $h_{mi\tau t\omega}$: unit inventory holding cost for commodity $m \in \mathcal{M}$ in port $i \in \mathcal{I} \bigcup \mathcal{J}$ between time period time period $\tau \in \mathcal{T}$ and $t \in \mathcal{T}$ under scenario $\omega \in \Omega$, where $\tau < t$
- π_{mjt}: unit penalty cost of not satisfying demand for commodity $m \in \mathcal{M}$ in port $j \in \mathcal{J}$ at time period $t \in \mathcal{T}$
- $\varphi_{mit\omega}$: supply availability of product $m \in \mathcal{M}$ in port $i \in \mathcal{I}$ at time period $t \in \mathcal{T}$ under scenario $\omega \in \Omega$
- $\overline{h}_i$: commodity storage capacity at port $i \in \mathcal{I} \bigcup \mathcal{J}$
- $\alpha_{m\tau t}$: deterioration rate of commodity $m \in \mathcal{M}$ due to storing between time period $\tau \in \mathcal{T}$ and $t \in \mathcal{T}$ under scenario $\omega \in \Omega$, where $\tau < t$
- a_{sit}, a_{bit}: binary availability of towboat s and barge b at port $i \in \mathcal{I}$
- $\overline{\delta}_s$, $\underline{\delta}_s$: maximum/minimum number of barges to carry by towboat $s \in \mathcal{S}$
- $\overline{\delta}_{\overline{s}}$: capacity of the most powerful towboat $\overline{s} \in \mathcal{S}$
- $\overline{w}_b$: weight capacity of a barge $b \in \mathcal{B}$
- $\overline{w}_{ijt\omega}$: the minimum of $\{w_{it\omega}, w_{ijt\omega}, w_{jt\omega}\}$ where $w_{it\omega}$ and $w_{jt\omega}$ indicate the maximum weight carrying capacity at port $i \in \mathcal{I} \bigcup \mathcal{J}$ and $w_{ijt\omega}$ the allowable weight that can be carried between the channel $(i,j) \in (\mathcal{I},\mathcal{J})$ at time period $t \in \mathcal{T}$ under scenario $\omega \in \Omega$. The last weight ($w_{ijt\omega}$) depends on the depth of the waterway and should not exceed the minimal water-level between the origin-destination ports
- ρ_m: density of commodity $m \in \mathcal{M}$
- v_b: volume capacity of barge $b \in \mathcal{B}$

- θ_{it}: total number of barges available in port $i \in \mathcal{I}$ at time period $t \in \mathcal{T}$
- t_l, t_u: average loading and unloading time of a barge
- Δ: average delay in locks
- l_{ij}: number of locks between origin port $i \in \mathcal{I}$ and destination port $j \in \mathcal{J}$
- d_{ij}: distance between origin port $i \in \mathcal{I}$ and destination port $j \in \mathcal{J}$
- $\bar{v}_{st}$: average speed of towboat $s \in \mathcal{S}$ at time period $t \in \mathcal{T}$
- $\bar{t}_{ij}$: allowable transport time limit between each origin port $i \in \mathcal{I}$ to destination port $j \in \mathcal{J}$
- τ_{ijt}: maximum number of trips that can be made along arc $(i,j) \in (\mathcal{I}, \mathcal{J})$ at time period t
- d_{mjt}: demand for commodity of type $m \in \mathcal{M}$ in port $j \in \mathcal{J}$ at time period $t \in \mathcal{T}$
- ρ_ω: probability of scenario $\omega \in \Omega$

First Stage Decision Variables:

- Y_{snijt}: 1 if a towboat $s \in \mathcal{S}$ is used in arc $(i,j) \in (\mathcal{I}, \mathcal{J})$ in trip $n \in \mathcal{N}_{ij}$ at time period $t \in \mathcal{T}$; 0 otherwise
- $Y_{mbsnijt}$: 1 if commodity $m \in \mathcal{M}$ is carried on barge $b \in \mathcal{B}$ of towboat $s \in \mathcal{S}$ to serve trip $n \in \mathcal{N}_{ij}$ between port $i \in \mathcal{I}$ and port $j \in \mathcal{J}$ at time period $t \in \mathcal{T}$; 0 otherwise

Second Stage Decision Variables:

- Z_{mitw}: amount of commodities of type $m \in \mathcal{M}$ processed at port $i \in \mathcal{I}$ at time period $t \in \mathcal{T}$ under scenario ω
- $X_{mbsnij\tau tw}$: amount of commodities of type $m \in \mathcal{M}$ that were purchased at time period τ and transported $t \in \mathcal{T}$ using barge $b \in \mathcal{B}$ of towboat $s \in \mathcal{S}$ for trip $n \in \mathcal{N}_{ij}$ along arc $(i,j) \in (\mathcal{I}, \mathcal{J})$ under scenario $\omega \in \Omega$, where $(\tau, t) \in \mathcal{T} | \tau \leq t$
- $H_{mi\tau tw}$: amount of commodities of type $m \in \mathcal{M}$ stored in port $i \in \mathcal{I} \bigcup \mathcal{J}$ between time period τ and t under scenario $\omega \in \Omega$, where $(\tau, t) \in \mathcal{T} | \tau \leq t$
- U_{mjtw}: amount of commodities of type $m \in \mathcal{M}$ shortage in destination port $j \in \mathcal{J}$ at time period $t \in \mathcal{T}$ under scenario $\omega \in \Omega$

- $P_{mj\tau tw}$: Satisfied demand of commodities of type $m \in \mathcal{M}$ in destination port $j \in \mathcal{J}$ with commodities purchased at time period τ and transported $t \in \mathcal{T}$ under scenario $\omega \in \Omega$, where $(\tau, t) \in \mathcal{T} | \tau \leq t$

Following first and second-stage decision variables are defined for our proposed two-stage stochastic programming model formulation. Decision variables $\mathbf{Y}^1 := \{Y_{snijt} | \forall s \in \mathcal{S}, n \in \mathcal{N}_{ij}, i \in \mathcal{I}, j \in \mathcal{J}_i, t \in \mathcal{T}\}$ and $\mathbf{Y}^2 := \{Y_{mbsnijt} | \forall m \in \mathcal{M}, b \in \mathcal{B}, s \in \mathcal{S}, n \in \mathcal{N}_{ij}, i \in \mathcal{I}, j \in \mathcal{J}, t \in \mathcal{T}\}$ are first-stage variables that respectively determine which towboat to use between any origin-destination pair in a given time period and which barge to use for carrying any particular product at any given origin port, respectively, i.e.,

$$Y_{snijt} = \begin{cases} 1 & \text{if a towboat } s \text{ is used in trip } n \in \mathcal{N}_{ij} \text{ between ports } (i,j) \in (\mathcal{I}, \mathcal{J}) \\ & \text{at time period } t \\ 0 & \text{otherwise;} \end{cases}$$

$$Y_{mbsnijt} = \begin{cases} 1 & \text{if barge } b \text{ connected to towboat } s \text{ is used in trip } n \in \mathcal{N}_{ij} \text{ to carry} \\ & \text{commodity } m \text{ between port } i \text{ and } j \text{ at time period } t \\ 0 & \text{otherwise;} \end{cases}$$

The second-stage decision variables include $\mathbf{Z} := \{Z_{mitw} | \forall m \in \mathcal{M}, i \in \mathcal{I}, t \in \mathcal{T}, \omega \in \Omega\}$ to denote the amount of commodities of type $m \in \mathcal{M}$ processed at port $i \in \mathcal{I}$ at time period $t \in \mathcal{T}$ under scenario ω ; $\mathbf{X} := \{X_{mbsnij\tau t\omega} | \forall m \in \mathcal{M}, b \in \mathcal{B}, s \in \mathcal{S}, n \in \mathcal{N}_{ij}, (i,j) \in (\mathcal{I}, \mathcal{J}), (\tau, t) \in \mathcal{T} | \tau \leq t, \omega \in \Omega\}$ to denote the amount of commodities of type $m \in \mathcal{M}$ that came in origin port $i \in \mathcal{I}$ at time period $\tau \in \mathcal{T}$ and to port $j \in \mathcal{J}$ at time period $t \in \mathcal{T}$ under scenario $\omega \in \Omega$ using barge $b \in \mathcal{B}$

and towboat $s \in \mathcal{S}$ at trip $n \in \mathcal{N}_{ij}$; $\mathbf{H} := \{H_{mi\tau t\omega} | \forall m \in \mathcal{M}, i \in \mathcal{I} \bigcup \mathcal{J}, (\tau, t) \in \mathcal{T} | \tau \leq t, \omega \in \Omega\}$ to denote the amount of commodities of type $m \in \mathcal{M}$ stored in port $i \in \mathcal{I} \bigcup \mathcal{J}$ between time period τ to t and under scenario $\omega \in \Omega$; $\mathbf{P} := \{P_{mj\tau tw} | \forall m \in \mathcal{M}, j \in \mathcal{J}, (\tau, t) \in \mathcal{T} | \tau \leq t, \omega \in \Omega\}$ amount of demand satisfaction for commodity $m \in \mathcal{M}$ in destination port $j \in \mathcal{J}$ with commodities purchased at time period τ and transported at time period $t \in \mathcal{T}$ under scenario $\omega \in \Omega$, where $(\tau, t) \in \mathcal{T} | \tau \leq t$; and $\mathbf{U} := \{U_{mjt\omega}\}$ to denote the amount of commodities of type $m \in \mathcal{M}$ shortage in destination port $j \in \mathcal{J}$ at time period $t \in \mathcal{T}$ under scenario $\omega \in \Omega$. For notational simplicity, we define $\mathbf{Y}$ as $\mathbf{Y} := \mathbf{Y}^1 \bigcup \mathbf{Y}^2$.

Analyzing the prevalent issues of inland waterway transportation network it is clearly noticeable that the barge transportation through this network is very frequently impacted by the delays in locks between two connecting ports. To capture this issue, we model barge delays through a feasible time limit, denoted by $\bar{t}_{ij}$, instead of developing highly complex nonlinear model to explicitly capture lock congestion. The introduction of $\bar{t}_{ij}$ provides a feasible time window for towboats to deliver the commodities between each source-destination pair. Violating this time window will be uneconomical and sometimes infeasible considering the commodity transportation requirement. Let Δ, l_{ij}, and d_{ij} represent the average delay in locks, the number of locks, and the actual waterway distance between each origin-destination port $(i, j) \in (\mathcal{I}, \mathcal{J})$. Further, we define $\bar{v}_{st}$ as the average speed of a towboat $s \in \mathcal{S}$ and t_l and t_u as the average loading and unloading time for a barge. The total travel time for a towboat $s \in \mathcal{S}$ between each

origin-destination port $(i,j) \in (\mathcal{I},\mathcal{J})$ at time $t \in \mathcal{T}$ can now be approximated as: $\left\{ \sum_{m\in\mathcal{M}} \sum_{b\in\mathcal{B}} (t_l + t_u) Y_{mbsnijt} + (\frac{d_{ij}}{\bar{v}_{st}} + \Delta l_{ij}) Y_{snijt} \right\}$, while this travel time is assumed to be restricted by a feasible time limit $\bar{t}_{ij}$.

$$\textbf{[PIM]} \quad \underset{\mathbf{Y}}{Minimize} \sum_{s\in\mathcal{S}} \sum_{n\in\mathcal{N}_{ij}} \sum_{i\in\mathcal{I}} \sum_{j\in\mathcal{J}_i} \sum_{t\in\mathcal{T}} \left(\psi_{st} Y_{snijt} + \sum_{m\in\mathcal{M}} \sum_{b\in\mathcal{B}} \eta_{mbt} Y_{mbsnijt} \right) + \sum_{\omega\in\Omega} \rho_\omega \mathbb{Q}(\mathbf{Y},\omega) \tag{5.1}$$

subject to

$$\sum_{m\in\mathcal{M}} Y_{mbsnijt} \leq 1 \forall b \in \mathcal{B}, s \in \mathcal{S}, n \in \mathcal{N}_{ij}, i \in \mathcal{I}, j \in \mathcal{J}_i, t \in \mathcal{T} \tag{5.2}$$

$$\sum_{S\in\mathcal{S}} Y_{snijt} \leq 1 \forall n \in \mathcal{N}_{ij}, i \in \mathcal{I}, j \in \mathcal{J}_i, t \in \mathcal{T} \tag{5.3}$$

$$\underline{\delta}_s Y_{snijt} \leq \sum_{m\in\mathcal{M}} \sum_{b\in\mathcal{B}} Y_{mbsnijt} \leq \bar{\delta}_s Y_{snijt} \forall s \in \mathcal{S}, n \in \mathcal{N}_{ij}, i \in \mathcal{I}, j \in \mathcal{J}_i, t \in \mathcal{T} \tag{5.4}$$

$$\sum_{m\in\mathcal{M}} \sum_{b\in\mathcal{B}} \sum_{s\in\mathcal{S}} \sum_{n\in\mathcal{N}_{ij}} \sum_{j\in\mathcal{J}} Y_{mbsnijt} \leq \theta_{it} \forall i \in \mathcal{I}, t \in \mathcal{T} \tag{5.5}$$

$$\sum_{S\in\mathcal{S}} \sum_{n\in\mathcal{N}_{ij}} Y_{snijt} \leq \tau_{ijt} \forall i \in \mathcal{I}, j \in \mathcal{J}_i, t \in \mathcal{T} \tag{5.6}$$

$$\sum_{n\in\mathcal{N}_{ij}} \sum_{j\in\mathcal{J}_i} Y_{snijt} \leq a_{sit} \forall s \in \mathcal{S}, i \in \mathcal{I}, t \in \mathcal{T} \tag{5.7}$$

$$\sum_{m\in\mathcal{M}} \sum_{s\in\mathcal{S}} \sum_{n\in\mathcal{N}_{ij}} Y_{mbsnijt} \leq a_{bit} \forall b \in \mathcal{B}, i \in \mathcal{I}, j \in \mathcal{J}_i, t \in \mathcal{T} \tag{5.8}$$

$$\sum_{m\in\mathcal{M}} \sum_{b\in\mathcal{B}} (t_l + t_u) Y_{mbsnijt} + \left(\frac{d_{ij}}{v_{st}} + \Delta l_{ij} \right) Y_{snijt} \leq \bar{t}_{ij} \forall n \in \mathcal{N}_{ij}, s \in \mathcal{S}, i \in \mathcal{I}, j \in \mathcal{J}_i, t \in \mathcal{T} \tag{5.9}$$

$$Y_{mbsnijt} \in \{0,1\} \forall m \in \mathcal{M}, b \in \mathcal{B}, s \in \mathcal{S}, n \in \mathcal{N}_{ij}, i \in \mathcal{I}, j \in \mathcal{J}_i, t \in \mathcal{T} \tag{5.10}$$

$$Y_{snijt} \in \{0,1\} \forall s \in \mathcal{S}, n \in \mathcal{N}_{ij}, n \in \mathcal{N}_{ij}, i \in \mathcal{I}, i \in \mathcal{I}, j \in \mathcal{J}_i, t \in \mathcal{T} \quad (5.11)$$

with $\mathbb{Q}(\mathbf{Y}, \omega)$ being the solution of the following second-stage problem:

$$\mathbb{Q}(\mathbf{Y}, \omega) = \underset{\mathbf{X,H,U}}{Minimize} \sum_{t \in \mathcal{T}} \sum_{m \in \mathcal{M}} \left(\sum_{i \in \mathcal{I} \bigcup \mathcal{J}} \sum_{\tau=1}^{t} h_{mi\tau t} H_{mi\tau t\omega} + \sum_{b \in \mathcal{B}} \sum_{s \in \mathcal{S}} \sum_{n \in \mathcal{N}_{ij}} \sum_{(i,j) \in (\mathcal{I},\mathcal{J})} \right.$$
$$\left. \sum_{\tau=1}^{t} c_{mbsnij\tau t} X_{mbsnij\tau t\omega} + \sum_{i \in \mathcal{I}} \gamma_{mit} Z_{mit\omega} + \sum_{j \in \mathcal{J}} \pi_{mjt} U_{mjtw} \right) \quad (5.12)$$

Subject to

$$Z_{mit\omega} \leq \varphi_{mit\omega} \forall m \in \mathcal{M}, i \in \mathcal{I}, t \in \mathcal{T}, \omega \in \Omega \quad (5.13)$$

$$Z_{mit\omega} - \sum_{b \in \mathcal{B}} \sum_{s \in \mathcal{S}} \sum_{n \in \mathcal{N}_{ij}} \sum_{j \in \mathcal{J}_i} X_{mbsnijtt\omega} = H_{mitt\omega} \forall m \in \mathcal{M}, i \in \mathcal{I}, t \in \mathcal{T}, \omega \in \Omega \quad (5.14)$$

$$(1 - \alpha_{m\tau(t-1)}) H_{mi\tau(t-1)\omega} = H_{mi\tau t\omega} - \sum_{b \in \mathcal{B}} \sum_{s \in \mathcal{S}} \sum_{n \in \mathcal{N}_{ij}} \sum_{j \in \mathcal{J}_i} X_{mbsnij\tau t\omega} \forall m \in \mathcal{M},$$
$$i \in \mathcal{I}, (\tau, t) \in \mathcal{T} | \tau \leq t-1, \omega \in \Omega \quad (5.15)$$

$$\sum_{b \in \mathcal{B}} \sum_{s \in \mathcal{S}} \sum_{\in \mathcal{N}_{ij}} \sum_{i \in \mathcal{I}_j} X_{mbsnijtt\omega} = P_{mjtt\omega} + H_{mjtt\omega} \forall m \in \mathcal{M},$$
$$j \in \mathcal{J}, t \in \mathcal{T}, \omega \in \Omega \quad (5.16)$$

$$\sum_{b \in \mathcal{B}} \sum_{s \in \mathcal{S}} \sum_{\in \mathcal{N}_{ij}} \sum_{i \in \mathcal{I}_j} X_{mbsnij\tau t\omega} - P_{mj\tau t\omega} = H_{mj\tau t\omega} - (1 - \alpha_{m\tau(t-1)}) H_{mj\tau(t-1)\omega} \forall m \in \mathcal{M},$$
$$j \in \mathcal{J}, (\tau, t) \in \mathcal{T} | \tau \leq t-1, \omega \in \Omega \quad (5.17)$$

$$\sum_{m \in \mathcal{M}} \sum_{\tau=1}^{t} H_{mi\tau t\omega} \leq \overline{h}_i \forall i \in \mathcal{I} \bigcup \mathcal{J}, t \in \mathcal{T}, \omega \in \Omega \quad (5.18)$$

$$\sum_{\tau=1}^{t} P_{mj\tau t\omega} + U_{mjt\omega} = d_{mjt} \forall m \in \mathcal{M}, j \in \mathcal{J}, t \in \mathcal{T}, \omega \in \Omega \quad (5.19)$$

$$\sum_{\tau=1}^{t} X_{mbsnij\tau t\omega} \leq min\{\overline{w}_{ijt\omega}, \overline{w}_b\} Y_{mbsnijt} \forall m \in \mathcal{M}, b \in \mathcal{B}, s \in$$
$$\mathcal{S}, n \in \mathcal{N}_{ij}, i \in \mathcal{I}, j \in \mathcal{J}_i, t \in \mathcal{T}, \omega \in \Omega \quad (5.20)$$

$$\sum_{\tau=1}^{t} X_{mbsnij\tau t\omega} \leq \rho_m v_b Y_{mbsnijt} \forall m \in \mathcal{M}, b \in \mathcal{B}, s \in \mathcal{S}, n \in \mathcal{N}_{ij}, i \in \mathcal{I}, j \in \mathcal{J}_i,$$

$$t \in \mathcal{T}, \omega \in \Omega \quad (5.21)$$

$$X_{mbsnij\tau t\omega}, H_{mi\tau t\omega}, H_{mj\tau t\omega}, Z_{mit\omega}, P_{mj\tau t\omega}, U_{mjt\omega} \in \mathbb{R}^{+} \quad (5.22)$$

The objective function (5.1) sums up the first-stage costs and the expected second-stage costs. The first two terms in (5.1) represent the fixed costs of using towboats and loading and unloading commodities into the barges. Constraints (5.2) handles the product mix issues stating only one commodity of type $m \in \mathcal{M}$ can be loaded to a given barge $b \in \mathcal{B}$ in time period $t \in \mathcal{T}$. Constraints (5.3) ensures that that at any time period t each towboat can use only one of the available trips. Constraints (5.4) restrict the minimum ($\underline{\delta}_s$) and maximum ($\overline{\delta}_s$) number of barges that can be connected with a given towboat $s \in \mathcal{S}$ at any time period $t \in \mathcal{T}$. The maximum barge usage at any given port $i \in \mathcal{I}$ considering the available barges (θ_{it}) at that port in time period $t \in \mathcal{T}$ is handled through constraints (5.5). Additionally, through constraints (5.6) the towboat usage between each origin destination port $(i, j) \in (\mathcal{I}, \mathcal{J})$ at time $t \in \mathcal{T}$ is restricted to a maximum τ_{ijt}. Further, we use (5.7) and (5.8) to captures the effect of periodic availability of barge and towboat in inland waterway transportation network. Due to aging and other related issues, barges and towboats needs to have periodic maintenance at different time periods of the year. If such activity occurs for any barge $b \in \mathcal{B}$ or towboat $s \in \mathcal{S}$ at any time $t \in \mathcal{T}$ the respective barge and towboat become unavailable in that

time period. This unavailability issue is captured through binary parameters a_{sit} and a_{bit} in constraints (5.7) and (5.8). Further, the total travel time restriction for a towboat $s \in \mathcal{S}$ between each origin destination port $(i, j) \in (\mathcal{I}, \mathcal{J})$ at time $t \in \mathcal{T}$ is captured through constraints (5.9). Finally, constraints (5.10) and (5.11) set the integrality constraints.

The second stage problem intends to minimize the inventory storage cost, commodity transportation cost, procurement cost, and third party commodity supply cost (equation (5.12)). Among the second stage constraints, constraints (5.13) restrict the processing of commodity $m \in \mathcal{M}$ according to its availability $\varphi_{mit\omega}$ at port $i \in \mathcal{I}$ in time period $t \in \mathcal{T}$ under scenario $\omega \in \Omega$. Constraints (5.14) and (5.15) are flow balance constraints for commodity storage and transportation at origin port $i \in \mathcal{I}$. Similarly, combination of constraints (5.16) and (5.17) balances the commodity flow and inventory at destination port $j \in \mathcal{J}$. Constraints (5.18) set the commodity storage restriction for origin and destination ports $i \in (\mathcal{I} \cup \mathcal{J})$. Constraints (5.19) ensure that, at any time period $t \in \mathcal{T}$, the demand for commodity $m \in \mathcal{M}$ at destination port $j \in \mathcal{J}$ must be satisfied either through the waterway transportation network or from a third-party supplier. Further, we use constraints (5.20) to match the amount of commodity transportation based on stochastic waterway condition and the barge wight capacity; constraints (5.21) to match the amount of commodity transportation following the volumetric capacity of the barge. Finally, we add constraints (5.22) as standard non-negativity constraints.

5.4 Solution Approach

By setting $|\Omega| = |\mathcal{T}| = |\mathcal{S}| = |\mathcal{B}| = 1$, model **[PIM]** can be reduced to a *fixed charge network flow problem* which is a proven $\mathcal{NP}$-hard problem [12, 65]. This implies that, model **[PIM]** is also $\mathcal{NP}$-hard from solution viewpoint, therefore, commercial solvers, such as CPLEX and Gurobi are unable to solve large-scale instances of this problem. In order to overcome this computational burden, we propose a hybrid algorithm combining the Sample average approximation (SAA) technique with an enhanced Benders decomposition algorithm to solve model **[PIM]** within a reasonable time frame. The next few subsections discuss the structural details of this algorithm.

5.4.1 Sample Average Approximation

The uncertain availability of agricultural products ($\varphi_{mit\omega}$) and highly unpredictable water level fluctuations ($\overline{w}_{ijt\omega}$) require the investigation of large number of scenarios to guarantee a robust network design solution. However, solving **[PIM]** for a large number of scenarios is computationally challenging and requires significant time and computational efforts. Therefore, to address this issue we apply *Sample Average Approximation*(**SAA**) method in solving large instances of model **[PIM]**. SAA is a well-known technique and has been widely adopted in different application areas [119, 1]. Interested readers may review the studies by [66] and [92] to get detailed understanding about the statistical evaluation (e.g., validation and error analysis, stopping rules) and convergence properties of the SAA.

Following the SAA algorithm, take a random sample from the set of all available scenarios and generate SAA problem for that sample scenarios. More specifically, we select a sample of E scenarios from the scenario set Ω ($E << \Omega$), and approximate the recourse function with the sample average function $\frac{1}{E}\sum_{e\in E} \mathbb{Q}(\mathbf{Y},\omega)$. The problem **[PIM]** can be approximated by the following SAA problem:

$$\underset{Y\in\mathbf{Y}}{Minimize}\left\{\hat{\mathbf{g}}(Y) : \sum_{t\in\mathcal{T}}\left(\sum_{s\in\mathcal{S}}\sum_{n\in\mathcal{N}_{ij}}\sum_{i\in\mathcal{I}}\sum_{j\in\mathcal{J}_i}\left(\psi_{st}Y_{snijt} + \sum_{m\in\mathcal{M}}\sum_{b\in\mathcal{B}}\eta_{mbt}Y_{mbsnijt}\right)\right.\right.$$
$$\left.\left. + \frac{1}{|E|}\sum_{e=1}^{E}\mathbb{Q}(\mathbf{Y},e)\right\}\right. \quad (5.23)$$

For a sufficiently large sample size E, problem (5.23) converges to the optimal solution of original model **[PIM]** with a probability of 1.0 [66]. However, with large E, the computational time in solving problem (5.23) becomes significantly high. Therefore, in estimating E, an evident trade-off exists between the achieved solution quality and the computational burden to solve large scale SAA subproblems. Now we summarize the steps involved in applying the SAA technique to solve model **[PIM]**:

1. Generate R independent sample of product supply and water level scenarios of size $|E|$ i.e., $\{\varphi_r^1(\omega), \varphi_r^2(\omega), ..., \varphi_r^E(\omega)\}$ and $\{\overline{w}_r^1(\omega), \overline{w}_r^2(\omega), ..., \overline{w}_r^E(\omega)\}$, $\forall r = 1, 2, ..., R$, where $\varphi = \{\varphi_{mit\omega}, \forall m \in \mathcal{M}, i \in \mathcal{I}, t \in \mathcal{T}, \omega \in \Omega\}$, $\overline{w} = \{\overline{w}_{ijt\omega}, \forall i \in \mathcal{I}, j \in \mathcal{J}, t \in \mathcal{T}, \omega \in \Omega\}$. Now solve the corresponding SAA problem and obtain the approximated lower bound for the algorithm:

$$\underset{Y\in\mathbf{Y}}{Minimize}\left\{\hat{\mathbf{g}}(Y) := \sum_{t\in\mathcal{T}}\left(\sum_{s\in\mathcal{S}}\sum_{n\in\mathcal{N}_{ij}}\sum_{i\in\mathcal{I}}\sum_{j\in\mathcal{J}_i}\left(\psi_{st}Y_{snijt} + \sum_{m\in\mathcal{M}}\sum_{b\in\mathcal{B}}\eta_{mbt}Y_{mbsnijt}\right)\right.\right.$$
$$\left.\left. + \frac{1}{E}\sum_{e=1}^{E}\mathbb{Q}(\mathbf{Y},e)\right\}\right. \quad (5.24)$$

   This SAA problem is solved for each replication $r = 1, ..., R$. Let $\mathbf{v}_E^r$ and $\hat{\mathbf{Y}}_E^r$ denote the optimal objective value and the optimal solution of (5.24), respectively.

2. In the next step we compute the *average* of the optimal objective values of all SAA problems, $\bar{v}_R^E$. Next, we define $\sigma^2_{\bar{v}_R^E}$ as the *variance* of all corresponding SAA problems. We obtain:

$$\bar{v}_R^E = \frac{1}{R}\sum_{r=1}^{R} v_E^r; \quad \sigma^2_{\bar{v}_E^R} = \frac{1}{(R-1)R}\sum_{r=1}^{R}(v_E^r - \bar{v}_R^E)^2$$

Parameter $\bar{v}_R^E$ is an unbiased estimator of the optimal objective value of **[PIM]**. Let us denote the optimal objective value of **[PIM]** as v^*, $\bar{v}_R^E$ satisfies the property, $\bar{v}_R^E < v^*$. Therefore, $\bar{v}_R^E$ provides a statistical lower bound of the original model **[PIM]** and $\sigma^2_{\bar{v}_R^E}$ is the estimator of the variance of this lower bound.

3. Now from the obtained first-stage solutions from R replications, we pick any solution $\hat{Y}_E^r \in Y$. We use this solution $\hat{Y}_E^r$ to evaluate problem **[PIM]** with a newly generated reference sample of size E' ($E' << E$) as follows:

$$\tilde{g}_{E'}(\tilde{Y}) = \sum_{s\in\mathcal{S}}\sum_{n\in\mathcal{N}_{ij}}\sum_{i\in\mathcal{I}}\sum_{j\in\mathcal{J}_i}\sum_{t\in\mathcal{T}}\left(\psi_{st}\tilde{Y}_{snijt} + \sum_{m\in\mathcal{M}}\sum_{b\in\mathcal{B}}\eta_{mbt}\tilde{Y}_{mbsnijt}\right) + \frac{1}{|E'|}\sum_{e=1}^{E'}\mathrm{Q}(\mathbf{Y}, e) \quad (5.25)$$

Here, the estimator $\tilde{g}_{E'}(\tilde{Y})$ provides an upper bound for the main problem **[PIM]**. The variance of $\tilde{g}_{E'}(\tilde{Y})$ is obtained as follows:

$$\sigma^2_{E'}(\tilde{Y}) = \frac{1}{(E'-1)E'}\sum_{e=1}^{E'}\left\{\sum_{s\in\mathcal{S}}\sum_{n\in\mathcal{N}_{ij}}\sum_{i\in\mathcal{I}}\sum_{j\in\mathcal{J}_i}\sum_{t\in\mathcal{T}}\left(\psi_{st}\tilde{Y}_{snijt} + \sum_{m\in\mathcal{M}}\sum_{b\in\mathcal{B}}\eta_{mbt}\tilde{Y}_{mbsnijt}\right) + \mathrm{Q}(\mathbf{Y}, e) - \tilde{g}_{E'}(\tilde{Y})\right\}$$

4. Through the estimators calculated in last two steps, the optimality gap $gap_{E,R,E'}(\tilde{Y})$ and its variance σ^2_{gap} is calculated as follows:

$$gap_{E,R,E'}(\tilde{Y}) = \tilde{g}_{E'}(\tilde{\mathcal{Y}}) - \bar{v}_R^E$$
$$\sigma^2_{gap} = \sigma^2_{E'}(\tilde{Y}) + \sigma^2_{\bar{v}_R^E}$$

The confidence interval for the optimality gap, $gap_{E,R,E'}(\tilde{Y})$ is obtained as follows:

$$\tilde{g}_{E'}(\tilde{\mathcal{Y}}) - \bar{v}_R^E + z_\alpha\{\sigma^2_{E'}(\tilde{Y}) + \sigma^2_{\bar{v}_R^E}\}^{1/2}$$

where $z_\alpha = \Phi^{-1}(1-\alpha)$, and $\Phi(z)$ is the cumulative distribution function of the standard normal distribution.

5.4.2 Benders Decomposition Algorithm

The step1 of SAA algorithm requires solving a two-stage stochastic mixed-integer linear programming model with $|E|$ scenarios. Depending on the size of $|\mathcal{M}|, |\mathcal{B}|, |\mathcal{S}|, |\mathcal{N}|, |\mathcal{I}|, |\mathcal{J}|$ and $|\mathcal{T}|$ problem (5.23) can still be computationally expensive. To address this issue, we employ a well-known partitioning method, *Benders Decomposition* Algorithm [15], to solve the SAA problem. In Benders decomposition algorithm, the original problem is decomposed into two parts: an integer *master problem* and a linear *subproblems*. Before introducing the subproblems, let us first present the underlying Benders reformulation for model **[PIM(SAA)]** as follows:

$$\underset{Y\in\mathbf{Y}}{Minimize}\Bigg\{\sum_{t\in\mathcal{T}}\sum_{s\in\mathcal{S}}\sum_{n\in\mathcal{N}_{ij}}\sum_{i\in\mathcal{I}}\sum_{j\in\mathcal{J}_i}\Bigg(\psi_{st}Y_{snijt}+\sum_{m\in\mathcal{M}}\sum_{b\in\mathcal{B}}\eta_{mbt}Y_{mbsnijt}\Bigg) + \frac{1}{E}\sum_{e=1}^{E}\mathbf{SP}_e(\mathbf{X},\mathbf{H},\mathbf{U},\mathbf{Z}|\hat{\mathbf{Y}}^1,\hat{\mathbf{Y}}^2)\Bigg\} \tag{5.26}$$

Subject to (5.2)-(5.11) and (5.13)-(5.22). We present $\mathbf{SP}_e(\mathbf{X},\mathbf{H},\mathbf{U},\mathbf{Z}|\hat{\mathbf{Y}}^1,\hat{\mathbf{Y}}^2)$ as the scenario-specific subproblem. For given values of $\hat{\mathbf{Y}}^1 := \{Y_{mbsnijt}|\forall m \in \mathcal{M}, b \in \mathcal{B}, s \in \mathcal{S}, n \in \mathcal{N}_{ij}, i \in \mathcal{I}, j \in \mathcal{J}_i, t \in \mathcal{T}\}$ and $\hat{\mathbf{Y}}^2 := \{Y_{snijt}|\forall s \in \mathcal{S}, n \in \mathcal{N}_{ij}, i \in \mathcal{I}, j \in \mathcal{J}_i, t \in \mathcal{T}\}$ problem **[PIM(SAA)]** can be reduced to the following *primal subproblem* that includes only continuous variables $\mathbf{X},\mathbf{H},\mathbf{U},\mathbf{Z}$ as follows:

$$\mathbf{SP}_e(\mathbf{X},\mathbf{H},\mathbf{U},\mathbf{Z}|\hat{\mathbf{Y}}^1,\hat{\mathbf{Y}}^2) Minimize\Bigg\{\sum_{t\in\mathcal{T}}\sum_{m\in\mathcal{M}}\Bigg(\sum_{i\in\mathcal{I}\bigcup\mathcal{J}}\sum_{\tau=1}^{t}h_{mi\tau t}H_{mi\tau te}+\sum_{i\in\mathcal{I}}\gamma_{mit}Z_{mite} + \sum_{j\in\mathcal{J}}\pi_{mjt}U_{mjte}+\sum_{b\in\mathcal{B}}\sum_{s\in\mathcal{S}}\sum_{n\in\mathcal{N}_{ij}}\sum_{(i,j)\in(\mathcal{I},\mathcal{J})}\sum_{\tau=1}^{t}c_{mbsnij\tau t}X_{mbsnij\tau te}\Bigg)\Bigg\} \tag{5.27}$$

Subject to

$$Z_{mite} \leq \varphi_{mite} \forall m \in \mathcal{M}, i \in \mathcal{I}, t \in \mathcal{T} \quad (5.28)$$

$$Z_{mite} - \sum_{b\in\mathcal{B}} \sum_{s\in\mathcal{S}} \sum_{n\in\mathcal{N}_{ij}} \sum_{j\in\mathcal{J}_i} X_{mbsnijtte} = H_{mitte} \forall m \in \mathcal{M}, i \in \mathcal{I}, t \in \mathcal{T} \quad (5.29)$$

$$(1-\alpha_{m\tau(t-1)})H_{mi\tau(t-1)e} = \sum_{b\in\mathcal{B}} \sum_{s\in\mathcal{S}} \sum_{n\in\mathcal{N}_{ij}} \sum_{j\in\mathcal{J}_i} X_{mbsnij\tau te} + H_{mi\tau te}$$
$$\forall m \in \mathcal{M}, i \in \mathcal{I}(\tau,t) \in \mathcal{T} | \tau \leq t-1 \quad (5.30)$$

$$\sum_{b\in\mathcal{B}} \sum_{s\in\mathcal{S}} \sum_{\in\mathcal{N}_{ij}} \sum_{i\in\mathcal{I}_j} X_{mbsnijtte} = P_{mjtte} + H_{mjtte} \forall m \in \mathcal{M}, j \in \mathcal{J}, t \in \mathcal{T} \quad (5.31)$$

$$\sum_{b\in\mathcal{B}} \sum_{s\in\mathcal{S}} \sum_{\in\mathcal{N}_{ij}} \sum_{i\in\mathcal{I}_j} X_{mbsnij\tau te} = P_{mj\tau te} + H_{mj\tau te} - (1-\alpha_{m\tau(t-1)})H_{mj\tau(t-1)e}$$
$$\forall m \in \mathcal{M}, j \in \mathcal{J}, (\tau,t) \in \mathcal{T} | \tau \leq t-1 \quad (5.32)$$

$$\sum_{\tau=1}^{t} P_{mj\tau te} = d_{mjt} - U_{mjte} \forall m \in \mathcal{M}, j \in \mathcal{J}, t \in \mathcal{T} \quad (5.33)$$

$$\sum_{m\in\mathcal{M}} \sum_{\tau=1}^{t} H_{mi\tau te} \leq \overline{h}_i \forall i \in \mathcal{I} \bigcup \mathcal{J}, t \in \mathcal{T} \quad (5.34)$$

$$\sum_{\tau=1}^{t} X_{mbsnij\tau te} \leq min\{\overline{w}_{ijte}, \bar{w}_b\} Y_{mbsnijt} \forall m \in \mathcal{M}, b \in \mathcal{B},$$
$$s \in \mathcal{S}, n \in \mathcal{N}_{ij}, i \in \mathcal{I}, j \in \mathcal{J}_i, t \in \mathcal{T} \quad (5.35)$$

$$\sum_{\tau=1}^{t} X_{mbsnij\tau te} \leq \rho_m v_b Y_{mbsnijt} \forall m \in \mathcal{M}, b \in \mathcal{B}, s \in \mathcal{S},$$
$$n \in \mathcal{N}_{ij}, i \in \mathcal{I}, j \in \mathcal{J}_i, t \in \mathcal{T} \quad (5.36)$$

$$X_{mbsnij\tau te}, H_{mi\tau te}, H_{mj\tau te}, Z_{mite}, P_{mj\tau te}, U_{mjte} \in \mathbb{R}^+ \quad (5.37)$$

Let $\vartheta = \{\vartheta_{mite} \geq 0 | \forall m \in \mathcal{M}, i \in \mathcal{I}, t \in \mathcal{T}, e \in E\}$, $\kappa = \{\kappa_{mite} | \forall m \in \mathcal{M}, i \in \mathcal{I}, t \in \mathcal{T}, e \in E\}$, $\zeta = \{\zeta_{mi\tau te} | \forall m \in \mathcal{M}, i \in \mathcal{I}, (\tau,t) \in \mathcal{T} | \tau \leq t-1, e \in E\}$, $\varepsilon = \{\varepsilon_{mjte} | \forall m \in \mathcal{M}, j \in \mathcal{J}, t \in \mathcal{T}, e \in E\}$, $\beta = \{\beta_{mj\tau te} | \forall m \in \mathcal{M}, j \in \mathcal{J}, (\tau,t) \in \mathcal{T} | \tau \leq t-1, e \in E\}$, $\chi = \{\chi_{mjte} | \forall m \in \mathcal{M}, j \in \mathcal{J}, t \in \mathcal{T}, e \in E\}$, $\nu = \{\nu_{ite} \geq$

$0|\forall i \in \mathcal{I}, t \in \mathcal{T}, e \in E\}$, $\Gamma = \{\Gamma_{jte} \geq 0|\forall j \in \mathcal{J}, t \in \mathcal{T}, e \in E\}$, $\varsigma = \{\varsigma_{mbsnijte} \geq 0|\forall m \in \mathcal{M}, b \in \mathcal{B}, s \in \mathcal{S}, n \in \mathcal{N}_{ij}, i \in \mathcal{I}, j \in \mathcal{J}_i, t \in \mathcal{T}, e \in E\}$ and $\Lambda = \{\Lambda_{mbsnijte} \geq 0|\forall m \in \mathcal{M}, b \in \mathcal{B}, s \in \mathcal{S}, n \in \mathcal{N}_{ij}, i \in \mathcal{I}, j \in \mathcal{J}_i, t \in \mathcal{T}, e \in E\}$ be the vector of the dual variables associated with constraints (5.28)-(5.36). We present the dual of the primal subproblem for each scenario $e \in E$, referred to as $[\mathbf{DSP}]_e$, as follows:

$$[\mathbf{DSP}]_e := Maximize \sum_{t\in\mathcal{T}} \sum_{m\in\mathcal{M}} \Bigg(\sum_{j\in\mathcal{J}} d_{mjt}\chi_{mjte} - \sum_{i\in\mathcal{I}} \phi_{mite}\vartheta_{mite} - \sum_{b\in\mathcal{B}} \sum_{s\in\mathcal{S}} \sum_{n\in\mathcal{N}_{ij}} \sum_{j\in\mathcal{J}} \sum_{i\in\mathcal{I}} \Big(min(\overline{w}_{ijte}, \overline{b}) \hat{Y}_{mbsnijt} \varsigma_{mbsnijte} + \rho_m v_b \hat{Y}_{mbsnijt} \Lambda_{mbsnijte} \Big) \Bigg) - \sum_{t\in\mathcal{T}} \Bigg(\sum_{i\in\mathcal{I}} \overline{h}_i \nu_{ite} + \sum_{j\in\mathcal{J}} \overline{h}_j \Gamma_{jte} \Bigg) \tag{5.38}$$

Subject to

$$-\kappa_{mite} - \nu_{ite} \leq h_{mitt} \quad \forall m \in \mathcal{M}, i \in \mathcal{I}, t \in \mathcal{T} \tag{5.39}$$

$$-\kappa_{mite} + (1 - \alpha_{m\tau(t+1)})\zeta_{mi\tau(t+1)e} - \nu_{ite} \leq h_{mi\tau t} \quad \forall m \in \mathcal{M}, i \in \mathcal{I}, (\tau, t) \in \mathcal{T}|\tau = t - 1 \tag{5.40}$$

$$(1 - \alpha_{m\tau(t+1)})\zeta_{mi\tau(t+1)e} - \zeta_{mi\tau te} - \nu_{ite} \leq h_{mi\tau t} \quad \forall m \in \mathcal{M}, i \in \mathcal{I}, (\tau, t) \in \mathcal{T}|\tau < t - 1 \tag{5.41}$$

$$-\varepsilon_{mjte} - \Gamma_{jte} \leq h_{mjtt} \quad \forall m \in \mathcal{M}, j \in \mathcal{J}, t \in \mathcal{T} \tag{5.42}$$

$$-\varepsilon_{mjte} + (1 - \alpha_{m\tau(t+1)})\beta_{mj\tau(t+1)e} - \Gamma_{jte} \leq h_{mj\tau t} \quad \forall m \in \mathcal{M}, j \in \mathcal{J}, (\tau, t) \in \mathcal{T}|\tau = t - 1 \tag{5.43}$$

$$(1 - \alpha_{m\tau(t+1)})\beta_{mj\tau(t+1)e} - \beta_{mj\tau te} - \Gamma_{jte} \leq h_{mj\tau t} \quad \forall m \in \mathcal{M}, j \in \mathcal{J}, (\tau, t) \in \mathcal{T}|\tau < t - 1 \tag{5.44}$$

$$-\zeta_{mi\tau te} + \beta_{mj\tau te} - \varsigma_{mbsnijte} - \Lambda_{mbsnijte} \leq c_{mbsnij\tau t} \; \forall m \in \mathcal{M}, b \in \mathcal{B}, s \in \mathcal{S}, n \in \mathcal{N}_{ij}, i \in \mathcal{I}, j \in \mathcal{J}_i, (\tau, t) \in \mathcal{T} | \tau \leq t-1 \quad (5.45)$$

$$-\kappa_{mite} + \varepsilon_{mjte} - \varsigma_{mbsnijte} \leq c_{mbsnijtt} \forall m \in \mathcal{M}, b \in \mathcal{B}, s \in \mathcal{S}, n \in \mathcal{N}_{ij}, i \in \mathcal{I}, j \in \mathcal{J}_i, t \in \mathcal{T} \quad (5.46)$$

$$-\vartheta_{mite} + \kappa_{mite} \leq \gamma_{mit} \quad \forall m \in \mathcal{M}, i \in \mathcal{I}, t \in \mathcal{T} \quad (5.47)$$

$$\chi_{mjte} \leq \pi_{mjt} \quad \forall m \in \mathcal{M}, j \in \mathcal{J}, t \in \mathcal{T} \quad (5.48)$$

$$-\beta_{mj\tau te} + \chi_{mjte} \leq 0 \forall m \in \mathcal{M}, j \in \mathcal{J}, (\tau, t) \in \mathcal{T} | \tau \leq t-1 \quad (5.49)$$

$$-\varepsilon_{mjte} + \chi_{mjte} \leq 0 \forall m \in \mathcal{M}, j \in \mathcal{J}, t \in \mathcal{T} \quad (5.50)$$

$$\vartheta_{mite}, \nu_{ite}, \Gamma_{jte}, \varsigma_{mbsnijte} \in \mathbb{R}^+ \quad (5.51)$$

$$\kappa_{mite}, \zeta_{mi\tau te}, \varepsilon_{mjte}, \beta_{mj\tau te}, \chi_{mjte} \in \mathbb{R} \quad (5.52)$$

Now, we introduce an additional free variable Θ to the underlying Benders reformulation and define the following Benders *Master problem* [**MP**]:

$$[\mathbf{MP}] \underset{\mathbf{Y},\Theta}{Minimize} \sum_{t \in \mathcal{T}} \sum_{s \in \mathcal{S}} \sum_{n \in \mathcal{N}_{ij}} \sum_{i \in \mathcal{I}} \sum_{j \in \mathcal{J}_i} \left(\psi_{st} Y_{snijt} + \sum_{m \in \mathcal{M}} \sum_{b \in \mathcal{B}} \eta_{mbt} Y_{mbsnijt} \right) + \Theta \quad (5.53)$$

Subject to:

$$\Theta \geq \sum_{e \in E} \sum_{t \in \mathcal{T}} p_e \Bigg(\sum_{m \in \mathcal{M}} \sum_{j \in \mathcal{J}} d_{mjt} \chi_{mjte} - \sum_{m \in \mathcal{M}} \sum_{i \in \mathcal{I}} \phi_{mite} \vartheta_{mite} - \sum_{m \in \mathcal{M}} \sum_{i \in \mathcal{I}} \overline{h}_i \nu_{ite}$$

$$- \sum_{m \in \mathcal{M}} \sum_{j \in \mathcal{J}} \overline{h}_j \Gamma_{jte} - \sum_{m \in \mathcal{M}} \sum_{b \in \mathcal{B}} \sum_{s \in \mathcal{S}} \sum_{n \in \mathcal{N}_{ij}} \sum_{j \in \mathcal{J}} \sum_{i \in \mathcal{I}} \Bigg(min(\overline{w}_{ijte}, \overline{b}) \hat{Y}_{mbsnijt} \varsigma_{mbsnijte} +$$

$$\rho_m v_b \hat{Y}_{mbsnijt} \Lambda_{mbsnijte} \Bigg) \Bigg) (\vartheta, \kappa, \zeta, \varepsilon, \beta, \chi, \nu, \Gamma, \varsigma, \Lambda) \in \mathcal{P}_D \tag{5.54}$$

$$\sum_{m \in \mathcal{M}} Y_{mbsnijt} \leq 1 \forall b \in \mathcal{B}, s \in \mathcal{S}, n \in \mathcal{N}_{ij}, i \in \mathcal{I}, j \in \mathcal{J}_i, t \in \mathcal{T} \tag{5.55}$$

$$\underline{\delta}_s Y_{snijt} \leq \sum_{m \in \mathcal{M}} \sum_{b \in \mathcal{B}} Y_{mbsnijt} \leq \overline{\delta}_s Y_{snijt} \forall s \in \mathcal{S}, n \in \mathcal{N}_{ij}, i \in \mathcal{I}, j \in \mathcal{J}_i, t \in \mathcal{T} \tag{5.56}$$

$$\sum_{m \in \mathcal{M}} \sum_{b \in \mathcal{B}} \sum_{s \in \mathcal{S}} \sum_{n \in \mathcal{N}_{ij}} \sum_{j \in \mathcal{J}} Y_{mbsnijt} \leq \theta_{it} \forall i \in \mathcal{I}, t \in \mathcal{T} \tag{5.57}$$

$$\sum_{n \in \mathcal{N}_{ij}} \sum_{j \in \mathcal{J}_i} Y_{snijt} \leq a_{sit} \forall s \in \mathcal{S}, i \in \mathcal{I}, t \in \mathcal{T} \tag{5.58}$$

$$\sum_{m \in \mathcal{M}} \sum_{s \in \mathcal{S}} \sum_{n \in \mathcal{N}_{ij}} Y_{mbsnijt} \leq a_{bit} \forall b \in \mathcal{B}, i \in \mathcal{I}, j \in \mathcal{J}_i, t \in \mathcal{T} \tag{5.59}$$

$$\sum_{m \in \mathcal{M}} \sum_{b \in \mathcal{B}} (t_l + t_u) Y_{mbsnijt} + \left(\frac{d_{ij}}{v_{st}} + \Delta l_{ij} \right) Y_{snijt} \leq \overline{t}_{ij} \forall n \in \mathcal{N}_{ij}, s \in \mathcal{S}, i \in \mathcal{I}, j \in \mathcal{J}_i, t \in \mathcal{T} \tag{5.60}$$

$$\sum_{S \in \mathcal{S}} \sum_{n \in \mathcal{N}_{ij}} Y_{snijt} \leq \tau_{ijt} \forall i \in \mathcal{I}, j \in \mathcal{J}_i, t \in \mathcal{T} \tag{5.61}$$

$$\sum_{S \in \mathcal{S}} Y_{snijt} \leq 1 \forall n \in \mathcal{N}_{ij}, i \in \mathcal{I}, j \in \mathcal{J}_i, t \in \mathcal{T} \tag{5.62}$$

$$Y_{mbsnijt} \in \{0,1\} \forall m \in \mathcal{M}, b \in \mathcal{B}, s \in \mathcal{S}, n \in \mathcal{N}_{ij}, i \in \mathcal{I}, j \in \mathcal{J}_i, t \in \mathcal{T} \tag{5.63}$$

$$Y_{snijt} \in \{0,1\} \forall s \in \mathcal{S}, n \in \mathcal{N}_{ij}, i \in \mathcal{I}, j \in \mathcal{J}_i, t \in \mathcal{T} \tag{5.64}$$

Constraints (5.54) are referred to as *optimality cut* constraints where $\mathcal{P}_D$ is the set of extreme points in the feasible region of **[DSP]** and p_e is the probability of any specific scenario $e \in E$ ($p_e = \frac{1}{E}$). The objective function value of **[DSP]** bounds free variable Θ from above i.e.,

$$\Theta \geq \sum_{e\in E}\sum_{t\in\mathcal{T}} p_e\Bigg(\sum_{m\in\mathcal{M}}\sum_{j\in\mathcal{J}} d_{mjt}\chi_{mjte} - \sum_{m\in\mathcal{M}}\sum_{i\in\mathcal{I}}\phi_{mite}\vartheta_{mite} - \sum_{m\in\mathcal{M}}\sum_{i\in\mathcal{I}}\overline{h}_i\nu_{ite}$$
$$- \sum_{m\in\mathcal{M}}\sum_{j\in\mathcal{J}}\overline{h}_j\Gamma_{jte} - \sum_{m\in\mathcal{M}}\sum_{b\in\mathcal{B}}\sum_{s\in\mathcal{S}}\sum_{n\in\mathcal{N}_{ij}}\sum_{j\in\mathcal{J}}\sum_{i\in\mathcal{I}}\Bigg(min(\overline{w}_{ijte},\overline{b})\hat{Y}_{mbsnijt}\varsigma_{mbsnijte}$$
$$+\rho_m v_b\hat{Y}_{mbsnijt}\Lambda_{mbsnijte}\Bigg)\Bigg) \quad (\vartheta,\kappa,\zeta,\varepsilon,\beta,\chi,\nu,\Gamma,\varsigma,\Lambda)\in\mathcal{P}_D \quad (5.65)$$

In problem (5.27), constraints (5.33) ensure that for any feasible solution of **[MP]**, $\hat{\mathbf{Y}}$, the primal subproblems $\mathbf{SP}_e(\mathbf{X},\mathbf{H},\mathbf{U},\mathbf{Z}|\hat{\mathbf{Y}}^1,\hat{\mathbf{Y}}^2)$ will always remain feasible. Therefore, we do not add any *feasibility cut* to **[MP]**. Moreover, the parameters $h_{mi\tau t}, h_{mj\tau t}$, $c_{mbsnij\tau t}, \gamma_{mit}$ and π_{mjt} are finite, which implies that any feasible solution of primal subproblems must be bounded and based on the strong duality theory, the dual subproblems **[DSP]** will also remain feasible and bounded. Master problem **[MP]** contains large number of optimality constraints (5.54) that makes it difficult to solve. To overcome this issue, we solve a *restricted master problem* **[RMP]** in which the set $\mathcal{P}_D$ is replaced with $\mathcal{P}_D^r$, i.e., $\mathcal{P}_D^r \subset \mathcal{P}_D$, and the size of $\mathcal{P}_D^r$ increases with each iteration r. The overall algorithm is outlined below:

Let UB^r and LB^r be an upper and lower bound of the original problem **[PIM]** obtained in the r^{th} iteration of Benders decomposition algorithm. Let, $z^r_{MAS} = \sum_{s\in\mathcal{S}}\sum_{n\in\mathcal{N}_{ij}}\sum_{i\in\mathcal{I}}\sum_{j\in\mathcal{J}_i}\sum_{t\in\mathcal{T}}\left(\psi_{st}Y_{snijt} + \sum_{m\in\mathcal{M}}\sum_{b\in\mathcal{B}}\eta_{mbt}Y_{mbsnijt}\right)$ and let $\mathcal{P}_D^r$ be

the set of extreme points at iteration r. Basic Benders decomposition algorithm iteratively solves [**RMP**] to obtain the values of $\{Y^r_{snijt}\}_{s\in\mathcal{S},n\in\mathcal{N}_{ij},i\in\mathcal{I},j\in\mathcal{J}_i,t\in\mathcal{T}}$, $\{Y^r_{mbsnijt}\}_{m\in\mathcal{M},b\in\mathcal{B},s\in\mathcal{S},n\in\mathcal{N}_{ij},i\in\mathcal{I},j\in\mathcal{J}_i,t\in\mathcal{T}}$, and z^r_{MAS}. The objective function value of [**RMP**], z^r_{MP}, provides a valid lower bound for the original problem [**PIM**]. Next, the the dual subproblem **[DSP]** is solved with the fixed values of $\{\hat{Y}^r_{snijt}\}$ and $\{\hat{Y}^r_{mbsnijt}\}$. At each iteration r, the solution of the first-stage decision values z^r_{MAS} and objective function value of subproblem (z^r_{SUB}) provides a valid upper bound for the original problem [**PIM**]. The algorithm terminates if the obtained gap between the upper and lower bounds falls below a pre-specified threshold limit ϵ; otherwise $\mathcal{P}^r_D$ is updated and the optimality cut (5.54) is added to [**RMP**], if violated. The pseudo-code of algorithm is provided in Algorithm 1.

5.4.3 Enhancement of Benders Decomposition Algorithm

This section introduces a number of techniques that can enhance the computational performance of the basic Benders decomposition algorithm. These techniques include addition of problem-specific valid inequalities, different variants of multi-cut and mean-value cut, pareto-optimal cut, knapsack inequalities, and a few simple heuristic improvements (e.g., warm start). These techniques helps to generate a high quality feasible solution of problem **[PIM]** in a timely fashion.

5.4.3.1 Valid inequalities

In each iteration of Benders decomposition algorithm, we add valid inequalities to the relaxed master problem **[RMP]**. These valid inequalities are derived

by utilizing the special structure of problem **[PIM]** and can be used to accelerate the performance of the overall Benders decomposition algorithm. Following set of valid inequalities are proposed:

***Problem specific valid inequalities*:**

- *Surrogate constraints* (5.66) are proposed which provide a lower bound on the required number of barges to satisfy commodity demand $m \in \mathcal{M}$ at time period $t \in \mathcal{T}$. The value of σ can be varied between 0.0 and 1.0 and when $\sigma = 1.0$, it ensures that all demand must be satisfied through the inland waterway transportation network.

$$\sum_{b\in\mathcal{B}}\sum_{s\in\mathcal{S}}\sum_{n\in\mathcal{N}_{ij}}\sum_{i\in\mathcal{I}}\sum_{j\in\mathcal{J}_i} Y_{mbsnijt}\overline{w}_b \geq \sum_{j\in\mathcal{J}} \sigma d_{mjt} \qquad \forall m \in \mathcal{M}, t \in \mathcal{T} \tag{5.66}$$

- While choosing between multiple barges of similar capacities, symmetries may arise that will result in elongated search times for the solver. Therefore, we add *lexicographic ordering constraints* (5.67) and (5.68) to set priorities on barge selection. Such priorities help to break the duplications caused by the barge selection symmetry and accelerate the performance of the branch-and-bound process.

$$Y_{1,b-1,snijt} \geq Y_{1bsijt} \forall b \in \mathcal{B} \setminus 1, s \in \mathcal{S}, n \in \mathcal{N}_{ij}, i \in \mathcal{I}, j \in \mathcal{J}, t \in \mathcal{T} \tag{5.67}$$

$$\sum_{p=1}^{m} 2^{(m-p)} Y_{p,b-1,snijt} \geq \sum_{p=1}^{m} 2^{(m-p)} Y_{pbsijt} \forall m \in \mathcal{M}, b \in \mathcal{B} \setminus 1, s \in \mathcal{S}, n \in \mathcal{N}_{ij}, i \in \mathcal{I}, j \in \mathcal{J}, t \in \mathcal{T} \tag{5.68}$$

- Symmetries may also arise while selecting towboats. Let $\mathcal{S}'_e$ be the subset of same typed towboats, i.e., $\mathcal{S}'_e \subset \mathcal{S}$ and $s'_e \subset \mathcal{S}'_e$ where s'_e represents a set of non-decreasing order of the members belongs to $\mathcal{S}'_e$. Similar to constraints (5.67) and (5.68), lexicographic ordering constraints (5.69) and (5.70) are applied for each $\mathcal{S}'_e$ to determine the priority in utilizing towboats of the same type.

$$Y_{s'_e-1,nijt} \geq Y_{s'_e,nijt} \forall s'_e \in \mathcal{S}'_e \setminus \{1\}, n \in \mathcal{N}_{ij}, i \in \mathcal{I}, j \in \mathcal{J}, t \in \mathcal{T} \tag{5.69}$$

$$\psi_{s'_e-1,t} Y_{s'_e-1,nijt} \geq \psi_{s'_e,t} Y_{s'_e,ijt} \forall s'_e \in \mathcal{S}'_e \setminus \{1\}, n \in \mathcal{N}_{ij}, i \in \mathcal{I}, j \in \mathcal{J}, t \in \mathcal{T} \tag{5.70}$$

- Constraints (5.71) and (5.72) generate a lower bound on the required barge usage for satisfy the demand between time interval $[t_1, t_2]$. If the cumulative

demand over period $[t_1, t_2]$ is greater than or equal to the maximum possible inventory held $(\overline{h}_j)$ and initial inventory $H_{mj\tau t_1}$, then at least a certain number of barges should be used in that specific interval:

$$\sum_{b\in\mathcal{B}}\sum_{s\in\mathcal{S}}\sum_{n\in\mathcal{N}_{ij}}\sum_{i\in\mathcal{I}}\sum_{j\in\mathcal{J}}\sum_{t=t_1}^{t_2} Y_{mbsnijt} \geq \left\lceil \frac{\sum_{j\in\mathcal{J}}\sum_{t=t_1}^{t_2} d_{mjt} - \sum_{j\in\mathcal{J}} \overline{h}_j}{\overline{w}_b} \right\rceil \quad \forall m \in \mathcal{M}, (t_1, t_2) \in \mathcal{T}, t_2 \geq t_1 \tag{5.71}$$

$$\sum_{b\in\mathcal{B}}\sum_{s\in\mathcal{S}}\sum_{n\in\mathcal{N}_{ij}}\sum_{i\in\mathcal{I}}\sum_{j\in\mathcal{J}}\sum_{t=t_1}^{t_2} Y_{mbsnijt} \geq \left\lceil \frac{\sum_{j\in\mathcal{J}}\sum_{t=t_1}^{t_2} d_{mjt} - \sum_{j\in\mathcal{J}}\sum_{\tau=1}^{t_1} H_{mj\tau t_1}}{\overline{w}_b} \right\rceil \quad \forall m \in \mathcal{M}, (t_1, t_2) \in \mathcal{T}, t_2 \geq t_1 \tag{5.72}$$

Lower bounding function: Lower bounding function [112] is another class of valid inequalities providing useful information about the projected terms of the objective function of the master problem [**RMP**]. These valid inequalities can be considered as an approximated boundary of the recourse cost of scenarios in the master problem. To obtain lower bounding valid inequalities, we consider a deterministic version of model [**PIM**] and obtain its linear relaxation [**LBF**] for each scenario as follows:

$$[\mathbf{LBF}(e)] \quad v(\phi_{mite}, \overline{w}_{ijte}) := \underset{\mathbf{X,H,U,Z}}{Minimize} \sum_{t\in\mathcal{T}}\sum_{m\in\mathcal{M}}\left(\sum_{i\in\mathcal{I}\bigcup\mathcal{J}}\sum_{\tau=1}^{t} h_{mi\tau t}H_{mi\tau te} + \sum_{i\in\mathcal{I}}\gamma_{mit}Z_{mite}\right.$$
$$\left. + \sum_{j\in\mathcal{J}}\pi_{mjt}U_{mjte} + \sum_{b\in\mathcal{B}}\sum_{s\in\mathcal{S}}\sum_{n\in\mathcal{N}_{ij}}\sum_{i\in\mathcal{I}}\sum_{j\in\mathcal{J}_i}\sum_{\tau=1}^{t}(c_{mbsnij\tau t} + \frac{\psi_{st}}{\overline{\delta}_s\overline{w}_b} + \frac{\eta_{mbt}}{\overline{w}_b})X_{mbsnij\tau te}\right) \tag{5.73}$$

Subject to

$$Z_{mite} \leq \varphi_{mite} \forall m \in \mathcal{M}, i \in \mathcal{I}, t \in \mathcal{T} \quad (5.74)$$

$$Z_{mite} = \sum_{b\in\mathcal{B}} \sum_{s\in\mathcal{S}} \sum_{n\in\mathcal{N}_{ij}} \sum_{j\in\mathcal{J}_i} X_{mbsnijtte} + H_{mitte} \quad \forall m \in \mathcal{M}, i \in \mathcal{I}, t \in \mathcal{T} \quad (5.75)$$

$$(1-\alpha_{m\tau(t-1)})H_{mi\tau(t-1)e} = \sum_{b\in\mathcal{B}} \sum_{s\in\mathcal{S}} \sum_{n\in\mathcal{N}_{ij}} \sum_{j\in\mathcal{J}_i} X_{mbsnij\tau te} + H_{mi\tau te} \quad \forall m \in \mathcal{M}, i \in \mathcal{I} \quad (\tau, t) \in \mathcal{T} | \tau \leq t-1 \quad (5.76)$$

$$\sum_{b\in\mathcal{B}} \sum_{s\in\mathcal{S}} \sum_{\in\mathcal{N}_{ij}} \sum_{i\in\mathcal{I}_j} X_{mbsnijtte} = P_{mjtte} + H_{mjtte} \forall m \in \mathcal{M}, j \in \mathcal{J}, t \in \mathcal{T} \quad (5.77)$$

$$\sum_{b\in\mathcal{B}} \sum_{s\in\mathcal{S}} \sum_{\in\mathcal{N}_{ij}} \sum_{i\in\mathcal{I}_j} X_{mbsnij\tau te} = P_{mj\tau te} + H_{mj\tau te} - (1-\alpha_{m\tau(t-1)})H_{mj\tau(t-1)e} \quad \forall m \in \mathcal{M}, j \in \mathcal{J}, (\tau, t) \in \mathcal{T} | \tau \leq t-1 \quad (5.78)$$

$$\sum_{\tau=1}^{t} P_{mj\tau te} = d_{mjt} - U_{mjte} \forall m \in \mathcal{M}, j \in \mathcal{J}, t \in \mathcal{T} \quad (5.79)$$

$$\sum_{m\in\mathcal{M}} \sum_{\tau=1}^{t} H_{mi\tau te} \leq \overline{h}_i \forall i \in \mathcal{I} \bigcup \mathcal{J}, t \in \mathcal{T} \quad (5.80)$$

$$\sum_{\tau=1}^{t} X_{mbsnij\tau te} \leq min\{\overline{w}_{ijte}, \overline{w}_b\} \quad \forall m \in \mathcal{M}, b \in \mathcal{B}, s \in \mathcal{S}, n \in \mathcal{N}_{ij}, i \in \mathcal{I}, j \in \mathcal{J}_i, t \in \mathcal{T} \quad (5.81)$$

$$\sum_{\tau=1}^{t} X_{mbsnij\tau te} \leq \rho_m v_b \quad \forall m \in \mathcal{M}, b \in \mathcal{B}, s \in \mathcal{S}, n \in \mathcal{N}_{ij}, i \in \mathcal{I}, j \in \mathcal{J}_i, t \in \mathcal{T} \quad (5.82)$$

$$X_{mbsnij\tau te}, H_{mi\tau te}, H_{mj\tau te}, Z_{mite}, P_{mj\tau te}, U_{mjte} \in \mathbb{R}^+ \quad (5.83)$$

Theorem 1

Let $\overline{X}_{mbsij\tau te}, \overline{H}_{mi\tau te}, \overline{H}_{mj\tau te}, \overline{Z}_{mite}, \overline{P}_{mj\tau te}, \overline{U}_{mjte}, \overline{Y}_{snijt}$, *and* $\overline{Y}_{mbsnijt}$ *be the optimal solution of problem [**LBF**(e)];* $\overline{\vartheta}_{mit}$ *and* $\overline{\varsigma}_{mbsnijt}$ *be the dual variables associated with constraints* (5.74) *and* (5.81). *Then, equation* (5.84) *presented below is a valid cut for the Benders master problem [**RMP**]:*

$$\Theta_e \geq \sum_{t\in\mathcal{T}}\sum_{m\in\mathcal{M}}\Bigg(\sum_{i\in\mathcal{I}\bigcup\mathcal{J}}\sum_{\tau=1}^{t} h_{mi\tau t}\overline{H}_{mi\tau te} + \sum_{i\in\mathcal{I}}\gamma_{mit}\overline{Z}_{mite} + \sum_{j\in\mathcal{J}}\pi_{mjt}\overline{U}_{mjt\omega} + \sum_{b\in\mathcal{B}}\sum_{s\in\mathcal{S}}\sum_{n\in\mathcal{N}_{ij}}$$
$$\sum_{(i,j)\in(\mathcal{I},\mathcal{J})}\sum_{\tau=1}^{t} c_{mbsnij\tau t}\overline{X}_{mbsij\tau te}\Bigg) + \sum_{s\in\mathcal{S}}\sum_{n\in\mathcal{N}_{ij}}\sum_{i\in\mathcal{I}}\sum_{j\in\mathcal{J}_i}\sum_{t\in\mathcal{T}}\Bigg(\psi_{st}(\overline{Y}_{snijt} - Y_{snijt}) + \sum_{m\in\mathcal{M}}$$
$$\sum_{b\in\mathcal{B}}\eta_{mbt}(\overline{Y}_{mbsnijt} - Y_{mbsnijt})\Bigg) - \sum_{m\in\mathcal{M}}\sum_{i\in\mathcal{I}}\sum_{t\in\mathcal{T}}\alpha_1(\phi^{max}_{mit} - \phi_{mite})\overline{\vartheta}_{mit} - \sum_{m\in\mathcal{M}}\sum_{b\in\mathcal{B}}\sum_{s\in\mathcal{S}}$$
$$\sum_{n\in\mathcal{N}_{ij}}\sum_{i\in\mathcal{I}}\sum_{j\in\mathcal{J}_i}\sum_{t\in\mathcal{T}}\alpha_2(\bar{w}^{max}_{ijt} - \bar{w}_{ijte})\overline{\varsigma}_{mbsnijt} \qquad \forall e \in \Xi \quad (5.84)$$

Proof:

[**LBF**(e)] is a linear relaxation of deterministic model [**PMI**] for scenario (e), thus it provides a lower bound on its optimal cost. Therefore, at any optimal solution, following the 'wait and see" and "here and now" solution properties of stochastic programming problem [16], following relation holds among the Benders equivalent reformulation of model [**PMI**] and the objective function of model [**LBF**(e)]:

$$\sum_{s\in\mathcal{S}}\sum_{n\in\mathcal{N}_{ij}}\sum_{i\in\mathcal{I}}\sum_{j\in\mathcal{J}_i}\sum_{t\in\mathcal{T}}\Bigg(\psi_{st}Y_{snijt} + \sum_{m\in\mathcal{M}}\sum_{b\in\mathcal{B}}\eta_{mbt}Y_{mbsnijt}\Bigg) + \Theta_e \geq \sum_{t\in\mathcal{T}}\sum_{m\in\mathcal{M}}\Bigg(\sum_{i\in\mathcal{I}\bigcup\mathcal{J}}\sum_{\tau=1}^{t}$$
$$h_{mi\tau t}\overline{H}_{mi\tau te} + \sum_{i\in\mathcal{I}}\gamma_{mit}\overline{Z}_{mite} + \sum_{j\in\mathcal{J}}\pi_{mjt}\overline{U}_{mjte} + \sum_{b\in\mathcal{B}}\sum_{s\in\mathcal{S}}\sum_{n\in\mathcal{N}_{ij}}\sum_{(i,j)\in(\mathcal{I},\mathcal{J})}\sum_{\tau=1}^{t}$$
$$(c_{mbsnij\tau t} + \frac{\psi_{st}}{\overline{\delta}_s\overline{w}_b} + \frac{\eta_{mbt}}{\overline{w}_b})\overline{X}_{mbsij\tau te}\Bigg)$$

Now we have the following variable transformations:

$$\overline{Y}_{mbsnijt} \approx \frac{\sum_{\tau=1}^{t}\overline{X}_{mbsnij\tau te}}{\overline{w}_b}\forall m\in\mathcal{M}, b\in\mathcal{B}, s\in\mathcal{S}, n\in\mathcal{N}_{ij} i\in\mathcal{I}, j\in\mathcal{J}_i, t\in\mathcal{T}$$
$$\overline{Y}_{snijt} \approx \frac{\sum_{\tau=1}^{t}\sum_{m\in\mathcal{M}}\sum_{b\in\mathcal{B}}\overline{X}_{mbsnij\tau te}}{\overline{\delta}_s\overline{w}_b} \qquad \forall s\in\mathcal{S}, n\in\mathcal{N}_{ij} i\in\mathcal{I}, j\in\mathcal{J}_i, t\in\mathcal{T}$$

These translates to the following equations:

$$\sum_{s\in\mathcal{S}}\sum_{n\in\mathcal{N}_{ij}}\sum_{i\in\mathcal{I}}\sum_{j\in\mathcal{J}_i}\sum_{t\in\mathcal{T}}\left(\psi_{st}Y_{snijt}+\sum_{m\in\mathcal{M}}\sum_{b\in\mathcal{B}}\eta_{mbt}Y_{mbsnijt}\right)+\Theta_e\geq\sum_{t\in\mathcal{T}}\sum_{m\in\mathcal{M}}\left(\sum_{i\in\mathcal{I}\bigcup\mathcal{J}}\right.$$
$$\left.\sum_{\tau=1}^{t}h_{mi\tau t}\overline{H}_{mi\tau te}+\sum_{i\in\mathcal{I}}\gamma_{mit}\overline{Z}_{mite}+\sum_{j\in\mathcal{J}}\pi_{mjt}\overline{U}_{mjte}+\sum_{b\in\mathcal{B}}\sum_{s\in\mathcal{S}}\sum_{n\in\mathcal{N}_{ij}}\sum_{(i,j)\in(\mathcal{I},\mathcal{J})}\left(\right.\right.$$
$$\left.\left.\psi_{st}\overline{Y}_{mbsnijt}+\sum_{\tau=1}^{t}c_{mbsnij\tau t}\overline{X}_{mbsij\tau te}\right)\right)+\sum_{s\in\mathcal{S}}\sum_{n\in\mathcal{N}_{ij}}\sum_{(i,j)\in(\mathcal{I},\mathcal{J})}\sum_{t\in\mathcal{T}}\eta_{mbt}\overline{Y}_{snijt}$$
$$\Rightarrow\Theta_e\geq\sum_{t\in\mathcal{T}}\sum_{m\in\mathcal{M}}\left(\sum_{i\in\mathcal{I}\bigcup\mathcal{J}}\sum_{\tau=1}^{t}h_{mi\tau t}\overline{H}_{mi\tau te}+\sum_{i\in\mathcal{I}}\gamma_{mit}\overline{Z}_{mite}+\sum_{j\in\mathcal{J}}\pi_{mjt}\overline{U}_{mjte}+\sum_{b\in\mathcal{B}}\sum_{s\in\mathcal{S}}\right.$$
$$\left.\sum_{n\in\mathcal{N}_{ij}}\sum_{(i,j)\in(\mathcal{I},\mathcal{J})}\sum_{\tau=1}^{t}c_{mbsnij\tau t}\overline{X}_{mbsij\tau te}\right)+\sum_{s\in\mathcal{S}}\sum_{n\in\mathcal{N}_{ij}}\sum_{i\in\mathcal{I}}\sum_{j\in\mathcal{J}_i}\sum_{t\in\mathcal{T}}\left(\psi_{st}(\overline{Y}_{snijt}-Y_{snijt})\right.$$
$$\left.+\sum_{m\in\mathcal{M}}\sum_{b\in\mathcal{B}}\eta_{mbt}(\overline{Y}_{mbsnijt}-Y_{mbsnijt})\right) \tag{5.85}$$

Solving a [**LBF**] for each scenario may not computationally be interesting. For this reason, we propose to solve only a single problem with maximum supply and water level, i.e., $\phi_{mit}^{max}=max_{e\in E}\{\phi_{mite}\}_{m\in\mathcal{M},i\in\mathcal{I},t\in\mathcal{T}}$, $\overline{w}_{ijt}^{max}=max_{e\in E}\{\overline{w}_{ijte}\}_{i\in\mathcal{I},j\in\mathcal{J},t\in\mathcal{T}}$. The solution of this auxiliary problem provides a valid lower bound for all scenario subproblems. However, The obtained bound can be further improved for each scenario.

Let $\vartheta_{mit},\varsigma_{mbsnijt}$ be the dual variables associated with the stochastic constraints; Δ_1 and Δ_2 indicate the set of alternative optimal dual solutions for ϑ and ς, respectively; and $0\leq\alpha_1,\alpha_2\leq 0.5$. Functions $v(\phi_{mit\omega})$ and $v(\overline{w}_{ijtw})$ are piece-wise linear in ϕ and $\overline{w}$. Based on sensitivity analysis, we have:

$$v(\phi^{max}-\tilde{\phi}) \geq v(\phi^{max})-\alpha_1 max_{\vartheta\in\Delta}\vartheta^T\tilde{\phi}\geq v(\phi^{max})-\alpha_1\vartheta^T\tilde{\phi}$$
$$v(\bar{w}^{max}-\tilde{\bar{w}}) \geq v(\bar{w}^{max})-\alpha_2 max_{\varsigma\in\Delta_2}\varsigma^T\tilde{\bar{w}}\geq v(\bar{w}^{max})-\alpha_2\varsigma^T\tilde{\bar{w}}$$

Let $\tilde{\phi} = \phi^{max} - \phi_\omega$ and $\tilde{\bar{w}} = \bar{w}^{max} - \bar{w}_\omega$, therefore, we have:

$$\Theta_e \geq \sum_{t\in\mathcal{T}}\sum_{m\in\mathcal{M}}\Bigg(\sum_{i\in\mathcal{I}\bigcup\mathcal{J}}\sum_{\tau=1}^{t} h_{mi\tau t}\overline{H}_{mi\tau te} + \sum_{i\in\mathcal{I}}\gamma_{mit}\overline{Z}_{mite} + \sum_{j\in\mathcal{J}}\pi_{mjt}\overline{U}_{mjte} + \sum_{b\in\mathcal{B}}\sum_{s\in\mathcal{S}}$$
$$\sum_{n\in\mathcal{N}_{ij}}\sum_{(i,j)\in(\mathcal{I},\mathcal{J})}\sum_{\tau=1}^{t} c_{mbsnij\tau t}\overline{X}_{mbsij\tau te}\Bigg) + \sum_{s\in\mathcal{S}}\sum_{n\in\mathcal{N}_{ij}}\sum_{i\in\mathcal{I}}\sum_{j\in\mathcal{J}_i}\sum_{t\in\mathcal{T}}\Bigg(\psi_{st}(\overline{Y}_{snijt} - Y_{snijt})$$
$$+ \sum_{m\in\mathcal{M}}\sum_{b\in\mathcal{B}}\eta_{mbt}(\overline{Y}_{mbsnijt} - Y_{mbsnijt})\Bigg) - \sum_{m\in\mathcal{M}}\sum_{i\in\mathcal{I}}\sum_{t\in\mathcal{T}}\alpha_1(\phi^{max}_{mit} - \phi_{mite})\overline{\vartheta}_{mit}$$
$$- \sum_{m\in\mathcal{M}}\sum_{b\in\mathcal{B}}\sum_{s\in\mathcal{S}}\sum_{n\in\mathcal{N}_{ij}}\sum_{i\in\mathcal{I}}\sum_{j\in\mathcal{J}_i}\sum_{t\in\mathcal{T}}\alpha_2(\bar{w}^{max}_{ijt} - \bar{w}_{ijte})\overline{\varsigma}_{mbsnijt} \qquad \forall e \in E \tag{5.86}$$

This confirms the validity of the proposed inequality (5.84).

■

Cutset inequalities:

In model [**PIM**], the set of nodes and arcs are denoted by sets $\mathcal{D}$ and $\mathcal{A}$, respectively, where $\mathcal{A}$ includes all paths that connects the origin and destination ports. Based on the feasibility requirements of the problem at hand, sufficient capacity should be installed across any partition of the network including the set of towboats and barges to support the commodity flow. Let, $\overline{D} \subset \mathcal{D}$ be a nonempty subset of the the node set $\mathcal{D}$ and $\underline{D}$ be its complement, i.e., $\underline{D} = D \setminus \overline{D}$. The corresponding cutset is defined as $(\overline{D}, \underline{D}) = \{a_{ij} \in \mathcal{A} | i \in \overline{D}, j \in \underline{D}\}$. Let $M_t(\overline{D}, \underline{D}) = \{m \in \mathcal{M} | \sum_{i\in\overline{D}}\sum_{\omega\in\Omega}\phi_{mit\omega} \geq 0, \sum_{j\in\underline{D}} d_{mjt} \geq 0\}$ be the associated commodity subset for each time period t. The maximum flow over this cutset is defined as $d^{max}_{t(\overline{D},\underline{D})} = \{\sum_{m\in M_t(\overline{D},\underline{D})}\sum_{j\in\underline{D}} d_{mjt}\}$. Cutset $(\overline{D}, \underline{D})$ is a valid cutset if $d^{max}_{t(\overline{D},\underline{D})} > 0$. Now using parameters τ_{ijt}, $\bar{\delta}_s$, and $\overline{w}_b$, the capacity of each arc in a specific cutset

$(\overline{D}, \underline{D})$ for time period t can be approximated as $u_{t,a_{ij}} = \{\tau_{ijt} \times \overline{\delta}_s \times \overline{w}_b | i \in \overline{D}, j \in \underline{D}\}$.

Definition 1

$C_t \subseteq (\overline{D}, \underline{D})$ is a cover if the total capacity of the arcs in $(\overline{D}, \underline{D}) \setminus C_t$ does not support (cover) the flow of demand at time period t, i.e., $\sum_{a_{ij} \in (\overline{D}, \underline{D}) \setminus C} u_{t,a_{ij}} < d^{max}_{t(\overline{D}, \underline{D})}$

.

Definition 2

A cover set C_t is minimal if opening any arc in C_t is sufficient to cover the demand, i.e., $\sum_{a_{ij} \in (\overline{D}, \underline{D}) \setminus C} u_{t,a_{ij}} + u_{t,q_{ij}} \geq d^{max}_{t(\overline{D}, \underline{D})}, \forall q_{ij} \in C_t$.

Let $y_{a_{ij}}$ stands for the capacity of arc a_{ij} in any cover set $C_t \subseteq (\overline{D}, \underline{D})$. The cover inequality can be defined as $\sum_{a_{ij} \in C_t} y_{a_{ij}} \geq 1$ which forces to open atleast one arc from coverset C_t to meet the flow requirements. Considering the structure of problem **[PIM]**, to separate this set of inequalities, we adopt the procedure proposed by Chouman et al. [23]. For each arc in $(\overline{D}, \underline{D})$ we define three new parameters $Y^{max}_{t,a_{ij}} = \{\tau_{ijt} \times \overline{\delta}_s | i \in \overline{D}, j \in \underline{D}\}$, $Y^{RE}_{t,a_{ij}}$, and $\overline{Y}_{t,a_{ij}} = \{Y^{RE}_{t,a_{ij}} / Y^{max}_{t,a_{ij}} | i \in \overline{D}, j \in \underline{D}\}$. The first parameter represents the maximum number of barges that can be used in a given arc a_{ij} of cutset $(\overline{D}, \underline{D})$ at time period t. Parameter $Y^{RE}_{t,a_{ij}}$ reports the total number of barges selected in the current solution for the same arc a_{ij}. The third parameter represents the ratio of two previous parameters. Let $C_{1,t}$ and $C_{0,t}$ be two subsets of arcs in cutset $(\overline{D}, \underline{D})$ at time period t for which $\overline{Y}_{t,a_{ij}} \geq 1 - \epsilon_{ci}$, and $\overline{Y}_{t,a_{ij}} \leq \epsilon_{ci}$, respectively. Parameter ϵ_{ci} is a small positive number. For each time

period t, subsets $C_{1,t}$ and $C_{0,t}$ in cutset $(\overline{D}, \underline{D})$ are determined in such a way that they satisfy following condition:

$$\sum_{a \in (\overline{D},\underline{D}) \setminus (C_{1,t} \cup C_{0,t})} u_{t,a} \geq d^{max}_{t,(\overline{D},\underline{D})} - \sum_{a \in C_{1,t}} u_{t,a} > 0 \qquad \forall t \in \mathcal{T}$$

We used OpenCloseArcs algorithm (**Algorithm 2**) to determine $C_{1,t}$ and $C_{0,t}$ for the current solution of the model, i.e., $\hat{Y}_{mbsnijt}$.

Algorithm 2 uses U_t and D_t to represent the residual capacity and residual demand for each time period. Given the current solution $\hat{Y}_{mbsnijt}$, this algorithm attempts to close an arc with a small $\overline{Y}_{t,a_{ij}}$ (as measured by ϵ_{ci}) so that the residual capacity after closing that arc will still cover the residual demand D_t, i.e., $U_t - u_{t,a_{ij}} \geq D_t$. Similarly, the algorithm tries to open an arc with large $\overline{Y}_{t,a_{ij}}$ (as measured by $1 - \epsilon_{ci}$) and such that there is still some residual demand to cover. To obtain a violated cover inequality (CI) for cutset $(\overline{D}, \underline{D})$ in each time period t, if there is any, following separation problem needs to be solved:

$$Z_{sep}(t) := min \sum_{a_{ij} \in (\overline{D},\underline{D}) \setminus (C_{1,t} \cup C_{0,t})} \overline{Y}_{t,a_{ij}} Z_{a_{ij}} \tag{5.87}$$

$$s.t: \sum_{a_{ij} \in (\overline{D},\underline{D}) \setminus (C_{1,t} \cup C_{0,t})} u_{t,a_{ij}} Z_{a_{ij}} \geq \sum_{a_{ij} \in (\overline{D},\underline{D}) \setminus C_{0,t}} u_{t,a_{ij}} - d^{max}_{t,(\overline{D},\underline{D})}$$

$$Z_{a_{ij}} \in \{0,1\} \qquad \forall a_{ij} \in (\overline{D}, \underline{D}) \setminus (C_{1,t} \cup C_{0,t})$$

For each time period t, solving model (5.87) provides a cover set C_t for the restricted cutset $(\overline{D}, \underline{D}) \setminus (C_{1,t} \cup C_{0,t})$. Note that, binary variable $Z_{a_{ij}}$ takes the value one if the arc a_{ij} is selected to be in the cover C_t. Since problem (5.87) is frequently solved, the solution time for each time period and each cutset can be quite time consuming. Therefore, we use a heuristic approach [23] the basic idea

of which is to exclude the arcs with large $\overline{Y}_{t,a_{ij}}$ as much as possible from the set $(\overline{D}, \underline{D}) \setminus (C_{1,t} \cup C_{0,t})$. This increases the chance of finding a violated inequality. Following this approach, arcs are considered in a non-decreasing order of the $\overline{Y}_{t,a_{ij}}$. Once a violated CI is obtained, we can easily derive a minimal cover set by removing as many arcs as possible with large $\overline{Y}_{t,a_{ij}}$ to meet the required condition,i.e., $\sum_{a_{ij} \in C_t} \overline{Y}_{t,a_{ij}} < 1$. Once the cover set for cutset $(\overline{D}, \underline{D})$ for each time period t is obtained, we should open at least one arc from that cover. However, this does not necessarily mean that the capacity of the given arc should be used at full. Therefore, we define multiplier $Rf^t_{a_{ij}}$ as a reducing factor of maximum barge capacity assigned to an arc. Obtaining the approximated number of barges we can form the corresponding CI as follows:

$$\begin{aligned} Rf^t_{a_{ij}} &= \frac{1}{2}\left(\frac{\sum_{m \in M(\overline{D},\underline{D})} d_{mjt}}{d^{max}_{t(\overline{D},\underline{D})}} + \frac{1}{d_{ij}\sum_{j' \in \underline{D}} \frac{1}{d_{ij'}}}\right) \quad \forall t \in \mathcal{T}, a_{ij} \in C_t \\ Y^{ap}_{t,a_{ij}} &= Rf^t_{a_{ij}} Y^{max}_{t,a_{ij}} \quad \forall t \in \mathcal{T}, a_{ij} \in C_t \end{aligned}$$

$$\sum_{m \in \mathcal{M}} \sum_{b \in \mathcal{B}} \sum_{s \in \mathcal{S}} \sum_{n \in \mathcal{N}_{ij}} \sum_{a_{ij} \in \mathcal{C}_t} Y_{mbsna_{ij}t} \geq \min_{a_{ij} \in \mathcal{C}_t} \{Y^{ap}_{t,a_{ij}}\} \quad \forall t \in \mathcal{T} \tag{5.88}$$

Another family cutset inequalities is known as *minimum cardinality* inequalities. The basic idea of these inequalities is to find the minimum number of arcs in a cutset, the capacity of which are needed to cover the maximum demand of that cut set, i.e., $d^{max}_{t(\overline{D},\underline{D})}$. Let $C_{1,t}$ represent the set of open arcs in cutset $(\overline{D}, \underline{D})$ at time period t and $C_{0,t}$ be the set of closed arcs as obtained for the cover inequalities.

The arcs in $(\overline{D}, \underline{D}) \setminus (C_{1,t} \cup C_{0,t})$ are ordered in a decreasing manner, i.e., $u_{t,a_{ij}} \geq u_{t,(a+1)_{ij}}$ $\forall a_{ij} \in (\overline{D}, \underline{D}) \setminus (C_{1,t} \cup C_{0,t})$. Finally, the least number of arcs the capacities of which are required to ensure flow in the given cutset is obtained as follows:

$$l_{t,(\overline{D},\underline{D})\setminus(C_{1,t}\cup C_{0,t})} = max\left\{h : \sum_{a_{ij}=1,\ldots,h} u_{t,a_{ij}} < d^{max}_{(\overline{D},\underline{D})\setminus(C_{1,t}\cup C_{0,t})}\right\} + 1 \quad \forall t \in \mathcal{T} \quad (5.89)$$

Finding the value of $l_{t,(\overline{D},\underline{D})\setminus(C_{1,t}\cup C_{0,t})}$ for each cutset at each time period, we get the information that in how many arcs at minimum we would have flow of barges. However, this does not signify that all capacity of the arcs need to translate the result to the problem at hand, to do so we make use of the introduced reducing factor for the cover inequalities as follows:

$$\sum_{m\in\mathcal{M}}\sum_{b\in\mathcal{B}}\sum_{s\in\mathcal{S}}\sum_{n\in\mathcal{N}_{ij}}\sum_{a_{ij}\in(\overline{D},\underline{D})\setminus(C_{1,t}\cup C_{0,t})} Y_{mbsna_{ij}t} \geq l_{t,(\overline{D},\underline{D})\setminus(C_{1,t}\cup C_{0,t})} \min_{a_{ij}\in\mathcal{C}_t}\{Y^{ap}_{t,a_{ij}}\} \forall t \in \mathcal{T} (5.90)$$

5.4.3.2 Multi-cuts

Benders decomposition algorithm can be enhanced further by adding two types of *multi-cuts*, *Type-1 Benders cut* and *Type-2 Benders cut*. The application of these cuts are discussed below:

Type-1 Benders cut: The first cut in this class is the standard *multi-cut* approach. In this approach, instead of adding one optimality cut at a time as in the case of standard benders decomposition algorithm, we add scenario specific cuts one for

each scenario based subproblem [17]. Following this procedure, the optimality cut constraint (5.54) can now be modified as follows:

$$\Theta_e \geq \sum_{t\in\mathcal{T}}\sum_{m\in\mathcal{M}}\Bigg(\sum_{j\in\mathcal{J}} d_{mjt}\chi_{mjte} - \sum_{i\in\mathcal{I}}\phi_{mite}\vartheta_{mite} - \sum_{b\in\mathcal{B}}\sum_{s\in\mathcal{S}}\sum_{n\in\mathcal{N}_{ij}}\sum_{j\in\mathcal{J}}\sum_{i\in\mathcal{I}}\Bigg(min(\overline{w}_{ijte},\overline{w}_b)$$
$$\hat{Y}_{mbsnijt}\varsigma_{mbsnijte} + \rho_m v_b \hat{Y}_{mbsnijt}\Lambda_{mbsnijte}\Bigg)\Bigg) - \sum_{t\in\mathcal{T}}\Bigg(\sum_{i\in\mathcal{I}}\overline{h}_i\nu_{ite} + \sum_{j\in\mathcal{J}}\overline{h}_j\Gamma_{jte}\Bigg)$$
$$\forall e \in E, (\vartheta,\kappa,\zeta,\varepsilon,\beta,\chi,\nu,\Gamma,\varsigma,\Lambda) \in \mathcal{P}_D \qquad (5.91)$$

The only difference between Type-1 Benders cut and the original optimality cut (5.54) is that the variable Θ in (5.54) is now replaced with Θ_e. The objective function of the Benders master problem [**MP**] is modified as follows:

$$\underset{\mathbf{Y},\Theta}{Minimize}\Bigg\{\sum_{t\in\mathcal{T}}\sum_{s\in\mathcal{S}}\sum_{n\in\mathcal{N}_{ij}}\sum_{i\in\mathcal{I}}\sum_{j\in\mathcal{J}_i}\Bigg(\psi_{st}Y_{snijt} + \sum_{m\in\mathcal{M}}\sum_{b\in\mathcal{B}}\eta_{mbt}Y_{mbsnijt}\Bigg) + \sum_{e\in E} p_e\Theta_e\Bigg\} \qquad (5.92)$$

With the addition of *Type-1 Benders cut*, the Benders decomposition algorithm is expected to take fewer iterations to reach the desired optimality gap. In contrary, the presence of large number of optimality cuts in the Benders master problem requires longer time to solve. To alleviate this challenge, *scenario bundling* technique can be applied which is introduced in Type-2 Benders cut.

Type-2 Benders cut: The performance of the Benders decomposition algorithm can further be improved by applying scenario bundling technique to it [46]. In this technique rather than defining subproblems for each scenario e, we define each subproblem for a scenario bundle consisting of a number of scenarios. For instance, bundling can be done by considering different supply and waterlevel scenarios, i.e., high, medium, and low. Let $|E|$ individual scenarios are grouped

into $|L|$ bundles where each bundle is specified by l, i.e., $l \in L$ and $p_l = \sum_{e \in l} p_e$. Model [$\mathbf{DSP}_e$] is now solved for each scenario bundle $l \in L$ and optimality cut is defined for each bundle l as follows:

$$\Theta_l \geq \sum_{e \in l} p_e \Bigg(\sum_{t \in \mathcal{T}} \sum_{m \in \mathcal{M}} \Bigg(\sum_{j \in \mathcal{J}} d_{mjt} \chi_{mjte} - \sum_{i \in \mathcal{I}} \phi_{mite} \vartheta_{mite} - \sum_{b \in \mathcal{B}} \sum_{s \in \mathcal{S}} \sum_{n \in \mathcal{N}_{ij}} \sum_{j \in \mathcal{J}} \sum_{i \in \mathcal{I}} \Bigg(min(\overline{w}_{ijte}, \overline{w}_b) \hat{Y}_{mbsnijt} \varsigma_{mbsnijte} + \rho_m v_b \hat{Y}_{mbsnijt} \Lambda_{mbsnijte} \Bigg) \Bigg) - \sum_{t \in \mathcal{T}} \Bigg(\sum_{i \in \mathcal{I}} \overline{h}_i \nu_{ite} + \sum_{j \in \mathcal{J}} \overline{h}_j \Gamma_{jte} \Bigg) \Bigg)$$

$$\forall l \in L, (\vartheta, \kappa, \zeta, \varepsilon, \beta, \chi, \nu, \Gamma, \varsigma, \Lambda) \in \mathcal{P}_D \tag{5.93}$$

The benders master problem [**MP**] objective is modified as follows:

$$\underset{\mathbf{Y}}{Minimize} \Bigg\{ \sum_{t \in \mathcal{T}} \sum_{s \in \mathcal{S}} \sum_{n \in \mathcal{N}_{ij}} \sum_{i \in \mathcal{I}} \sum_{j \in \mathcal{J}_i} \Bigg(\psi_{st} Y_{snijt} + \sum_{m \in \mathcal{M}} \sum_{b \in \mathcal{B}} \eta_{mbt} Y_{mbsnijt} \Bigg) + \sum_{l \in L} p_l \Theta_l \Bigg\} \tag{5.94}$$

5.4.3.3 Pareto-optimal cuts

Addition of Pareto-optimal cuts can significantly improve the convergence of the Benders decomposition algorithm. These cuts are generated at each iteration in such a way that the cuts will be stronger and dominate over the previously generated cuts [74]. Constructing these cuts are overly relied on the solution obtained from the dual subproblem. If the primal subproblem shows degeneracy, multiple optimal solutions are obtaned from its dual, each of which can generate an optimality cut of particular strength [124]. Thus, selecting the strongest cut among all possible cuts is of high importance. Magnanti and Wong [74] explained the idea of *dominance* to select the strongest cut. Let $\mathbf{Y}^{LP}$ be the polyhedron defined by (5.55)-(5.57), (5.59)-(5.60), and $0 \leq \{Y_{mbsnijt}\}_{m \in \mathcal{M}, b \in \mathcal{B}, s \in \mathcal{S}, n \in \mathcal{N}_{ij}, i \in \mathcal{I}, j \in \mathcal{J}_i, t \in \mathcal{T}} \leq 1$ and $\mathcal{P}_D$ be the polyhedron of [**DSP**].

Definition 3

An optimality cut corresponding to $(\hat{\vartheta}, \hat{\kappa}, \hat{\zeta}, \hat{\varepsilon}, \hat{\beta}, \hat{\chi}, \hat{v}, \hat{\Gamma}, \hat{\varsigma}, \hat{\Lambda}) \in \mathcal{P}_D$ *dominates or is stronger than that corresponding to* $(\overline{\vartheta}, \overline{\kappa}, \overline{\zeta}, \overline{\varepsilon}, \overline{\beta}, \overline{\chi}, \overline{v}, \overline{\Gamma}, \overline{\varsigma}, \overline{\Lambda}) \in \mathcal{P}_D$ *if following relation holds with strict inequality for at least one point* $\hat{Y}_{mbsnijt} \in \mathbf{Y}^{LP}$ *:*

$$\sum_{e\in E} p_e \Bigg(\sum_{t\in\mathcal{T}} \sum_{m\in\mathcal{M}} \Bigg(\sum_{j\in\mathcal{J}} d_{mjt}\hat{\chi}_{mjte} - \sum_{i\in\mathcal{I}} \phi_{mite}\hat{\vartheta}_{mite} - \sum_{b\in\mathcal{B}} \sum_{s\in\mathcal{S}} \sum_{n\in\mathcal{N}_{ij}} \sum_{j\in\mathcal{J}} \sum_{i\in\mathcal{I}} \Bigg(min(\overline{w}_{ijte}, \overline{w}_b) \hat{Y}_{mbsnijt}\hat{\varsigma}_{mbsnijte} + \rho_m v_b \hat{Y}_{mbsnijt}\hat{\Lambda}_{mbsnijte} \Bigg) \Bigg) - \sum_{t\in\mathcal{T}} \Bigg(\sum_{i\in\mathcal{I}} \overline{h}_i \hat{v}_{ite} + \sum_{j\in\mathcal{J}} \overline{h}_j \hat{\Gamma}_{jte} \Bigg) \Bigg) \geq \sum_{e\in E} p_e \Bigg(\sum_{t\in\mathcal{T}} \sum_{m\in\mathcal{M}} \Bigg(\sum_{j\in\mathcal{J}} d_{mjt}\overline{\chi}_{mjte} - \sum_{i\in\mathcal{I}} \phi_{mite}\overline{\vartheta}_{mite} - \sum_{b\in\mathcal{B}} \sum_{s\in\mathcal{S}} \sum_{n\in\mathcal{N}_{ij}} \sum_{j\in\mathcal{J}} \sum_{i\in\mathcal{I}} \Bigg(min(\overline{w}_{ijte}, \overline{w}_b) \hat{Y}_{mbsnijt} \overline{\varsigma}_{mbsnijte} + \rho_m v_b \hat{Y}_{mbsnijt}\overline{\Lambda}_{mbsnijte} \Bigg) \Bigg) - \sum_{t\in\mathcal{T}} \Bigg(\sum_{i\in\mathcal{I}} \overline{h}_i \overline{v}_{ite} + \sum_{j\in\mathcal{J}} \overline{h}_j - \overline{\Gamma}_{jte} \Bigg) \Bigg)$$

$$\hat{Y}_{mbsnijt} \in \mathbf{Y}^{LP} \tag{5.95}$$

Definition 4

An optimality cut generated with dual solution $(\hat{\vartheta}, \hat{\kappa}, \hat{\zeta}, \hat{\varepsilon}, \hat{\beta}, \hat{\chi}, \hat{v}, \hat{\Gamma}, \hat{\varsigma}, \hat{\Lambda}) \in \mathcal{P}_D$ *is referred as Pareto-optimal, if it is not dominated by any other cut. Similarly, the dual solution* $(\hat{\vartheta}, \hat{\kappa}, \hat{\zeta}, \hat{\varepsilon}, \hat{\beta}, \hat{\chi}, \hat{v}, \hat{\Gamma}, \hat{\varsigma}, \hat{\Lambda})$ *is called Pareto-optimal.*

Let $ri(\mathbf{Y}^{LP})$ denote the relative interior of $\mathbf{Y}^{LP}$. Pareto-optimal dual solution can be extracted by solving an auxiliary problem [**DSP(PO)**]. Let $Y^0_{mbsnijt} \in ri(\mathbf{Y}^{LP})_{\forall m\in\mathcal{M}, b\in\mathcal{B}, s\in\mathcal{S}, n\in\mathcal{N}_{ij}, i\in\mathcal{I}, j\in\mathcal{J}_i, t\in\mathcal{T}}$ be the core point, $\overline{Y}_{mbsnijt}$ and $\overline{[\mathbf{DSP}]}_e$ respectively indicate

the optimal solution of the master problem and objective function value of dual subproblem. Problem [**DSP(PO)**] is formulated as follows:

$$[\mathbf{DSP(PO)}]_e := Maximize \sum_{t\in\mathcal{T}}\sum_{m\in\mathcal{M}}\Bigg(\sum_{j\in\mathcal{J}} d_{mjt}\chi_{mjte} - \sum_{i\in\mathcal{I}}\phi_{mite}\vartheta_{mite} - \sum_{b\in\mathcal{B}}\sum_{s\in\mathcal{S}}\sum_{n\in\mathcal{N}_{ij}}$$
$$\sum_{j\in\mathcal{J}}\sum_{i\in\mathcal{I}}\Big(min(\overline{w}_{ijte},\overline{w}_b)Y^0_{mbsnijt}\varsigma_{mbsnijte} + \rho_m v_b Y^0_{mbsnijt}\Lambda_{mbsnijte}\Big)\Bigg)$$
$$-\sum_{t\in\mathcal{T}}\Bigg(\sum_{i\in\mathcal{I}}\overline{h}_i\nu_{ite} + \sum_{j\in\mathcal{J}}\overline{h}_j\Gamma_{jte}\Bigg) \tag{5.96}$$

subject to (5.39)-(5.52) and

$$\sum_{t\in\mathcal{T}}\sum_{m\in\mathcal{M}}\Bigg(\sum_{j\in\mathcal{J}} d_{mjt}\chi_{mjte} - \sum_{i\in\mathcal{I}}\phi_{mite}\vartheta_{mite} - \sum_{b\in\mathcal{B}}\sum_{s\in\mathcal{S}}\sum_{n\in\mathcal{N}_{ij}}\sum_{j\in\mathcal{J}}\sum_{i\in\mathcal{I}}\Big(min(\overline{w}_{ijte},\overline{w}_b)$$
$$\overline{Y}_{mbsnijt}\varsigma_{mbsnijte} + \rho_m v_b\overline{Y}_{mbsnijt}\Lambda_{mbsnijte}\Big)\Bigg) - \sum_{t\in\mathcal{T}}\Bigg(\sum_{i\in\mathcal{I}}\overline{h}_i\nu_{ite} + \sum_{j\in\mathcal{J}}\overline{h}_j\Gamma_{jte}\Bigg)$$
$$= \overline{[\mathbf{DSP}]}_e \tag{5.97}$$

After solving $[\mathbf{DSP}]_e$ we obtain $\overline{[\mathbf{DSP}]}_e$ which is then used in the auxiliary problem $[\mathbf{DSP(PO)}]_e$ and the corresponding Pareto-optimal cut is derived. However, in this approach, the dependency on the auxiliary problem can have detrimental effect on the performance of overall algorithm. It doubles number of subproblems needed to be solved in each iteration of benders decomposition algorithm. Additionally, the presence of equality constraint (5.97) in $[\mathbf{DSP(PO)}]_e$ makes the auxiliary problems difficult than solving the regular subproblems.

Equality constraint (5.97) restricts the dual subproblem $[\mathbf{DSP}]_e$ to the optimal face of dual polyhedron where all the optimal solutions exist. The objective function (5.96) attempts to pick a solution among all available alternatives on the optimal face which gives the tightest cut as measured from an interior point of the

master problem. Here we utilize a novel method to decrease the complexity of auxiliary subproblem. This method is structured based on several definitions from linear programming theory.

Definition 5

An alternate optimal solution exists if at least one nonbasic variable possesses a reduced cost of zero.

When we identify that at least one alternate dual optima exists, the best one is searched to generate the cut by restricting the dual subproblem to the optimal face. Corollary 1 of linear programming theory states the way of fixing the dual subproblem to the optimal face.

Corollary 1

Variables with nonzero reduced cost maintain their current value at any alternate optimal solution.

Proof: Suppose any variable with non zero reduced cost changes its value, this mandates that the optimal objective value should also be changed. However, this statement contradicts the definition of alternate optima, therefore, the value of variables with non zero reduced cost should remain same at any alternative optimal solution. ■

If the dual value of an active constraint in an optimal solution is nonzero, from duality theory, the slack variable corresponding to the given constraint is equal to zero. Therefore, each inequality constraint with nonzero dual value should be converted into an equality, which is equivalent to fixing the slack variables with

nonzero reduced cost to zero. Using these definitions, Lemma 1 introduces an equivalent subproblem to extract Pareto-optimal cuts.

Lemma 1

Let $(\vec{\vartheta}, \vec{\kappa}, \vec{\zeta}, \vec{\varepsilon}, \vec{\beta}, \vec{\chi}, \vec{v}, \vec{\Gamma}, \vec{\varsigma}, \vec{\Lambda})$ *indicate the vector of variables with nonzero reduced cost derived from solving the* $[\boldsymbol{DSP}]_e$ *problem snd* Sl *be the slack variable of each constraint. Then, the solution of*

$$[\boldsymbol{DSP(RPO)}]_e := Maximize \sum_{t\in\mathcal{T}}\sum_{m\in\mathcal{M}}\Bigg(\sum_{j\in\mathcal{J}} d_{mjt}\chi_{mjte} - \sum_{i\in\mathcal{I}}\phi_{mite}\vartheta_{mite} - \sum_{b\in\mathcal{B}}\sum_{s\in\mathcal{S}}\sum_{n\in\mathcal{N}_{ij}} \sum_{j\in\mathcal{J}}\sum_{i\in\mathcal{I}}\Big(\min(\overline{w}_{ijte}, \overline{w}_b) Y^0_{mbsnijt}\varsigma_{mbsnijte} + \rho_m v_b Y^0_{mbsnijt}\Lambda_{mbsnijte}\Big)\Bigg) - \sum_{t\in\mathcal{T}}\Bigg(\sum_{i\in\mathcal{I}}\overline{h}_i\nu_{ite} + \sum_{j\in\mathcal{J}}\overline{h}_j\Gamma_{jte}\Bigg) \tag{5.98}$$

subject to (5.39)-(5.52) *and*

$$(\vec{\vartheta}, \vec{\kappa}, \vec{\zeta}, \vec{\varepsilon}, \vec{\beta}, \vec{\chi}, \vec{v}, \vec{\Gamma}, \vec{\varsigma}, \vec{\Lambda}, \vec{Sl}) = 0 \tag{5.99}$$

is equivalent to that obtained from the Magnanti-wong problem.

Proof: If there are multiple optimal solutions for a problem, the variables with zero reduced cost can only change their value not effecting the objective function value. Hence, if we have multiple optimal solutions for $[\mathbf{DSP}]_e$, we want to restrict $[\mathbf{DSP}]_e$ to its optimal face and the variables with nonzero reduced cost can be excluded from the corresponding dual polyhedron by fixing their values to zero. ■

Equality (5.99) fixes a set of variables with nonzero reduced cost to their current value (zero). This can be efficiently managed by the state-of-the-art optimization solvers such as CPLEX and GUROBI.

5.4.3.4 Mean-value cuts

Mean-value cut was first introduced by Batun et al. [14]. This inequality generates good lower bounds in the earlier iterations of the Benders decomposition algorithm which eventually helps to accelerate the convergence of the algorithm. The authors add a number of inequalities to the Benders master problem by utilizing the primal subproblem defined under the mean-value scenario $\bar{e}$. In this section, we first introduce the *primal-based mean-value cut* (*Type A* cut) proposed by Batun et al [14]. We then extend this cut to generate *multiple mean-value cut* (Type B cut) based on the *Type-2 Benders cut* proposed in section 5.4.3.2. Finally, alternative approaches to generate *single mean-cut* (*Type C* cut) and *multiple mean-cut* (*Type D* cut) utilizing the dual subproblem variables are proposed.

Primal-based mean-value cut

Type A cut: This approach appends a set of primal subproblem constraints to the [MP] under *mean-value scenario* $\bar{e}$ (a scenario comprising of mean values of the stochastic parameters). Additionally, to generate high quality feasible solutions during the early iterations of the Benders decomposition algorithm, an inequality is generated to strengthen the lower bound of the free variable Θ. In this purpose, following additional parameters and decision variables are introduced.

Auxiliary parameters:

- $\tilde{\phi}_{mit}$: mean supply availability of product $m \in \mathcal{M}$ in port $i \in \mathcal{I}$ at time period $t \in \mathcal{T}$

- $\tilde{w}_{ijt}$: mean allowable load that can be carried between the channel $(i,j) \in (\mathcal{I},\mathcal{J})$ at time period $t \in \mathcal{T}$

Auxiliary variables:

- $\tilde{Z}_{mit}$: mean amount of commodities of type $m \in \mathcal{M}$ processed at port $i \in \mathcal{I}$ at time period $t \in \mathcal{T}$
- $\tilde{X}_{mbsnij\tau t}$: amount of commodities of type $m \in \mathcal{M}$ that were purchased at time period τ and transported at time period $t \in \mathcal{T}$ using barge $b \in \mathcal{B}$ of towboat $s \in \mathcal{S}$ of trip $n \in \mathcal{N}_{ij}$ along arc $(i,j) \in (\mathcal{I},\mathcal{J})$, where $(\tau,t) \in \mathcal{T}|\tau \leq t$
- $\tilde{H}_{mi\tau t}$: amount of commodities of type $m \in \mathcal{M}$ stored in port $i \in \mathcal{I} \bigcup \mathcal{J}$ between time period τ and t , where $(\tau,t) \in \mathcal{T}|\tau \leq t$
- $\tilde{U}_{mjt}$: amount of commodities of type $m \in \mathcal{M}$ shortage in destination port $j \in \mathcal{J}$ at time period $t \in \mathcal{T}$
- $\tilde{P}_{mj\tau t}$: amount of demand of commodities of type $m \in \mathcal{M}$ satisfied in destination port $j \in \mathcal{J}$ with commodities purchased at time period τ and transported at time period $t \in \mathcal{T}$, where $(\tau,t) \in \mathcal{T}|\tau \leq t$

The following constraints are now added to the master problem [**MP**] :

$$\tilde{Z}_{mit} \leq \tilde{\varphi}_{mit} \forall m \in \mathcal{M}, i \in \mathcal{I}, t \in \mathcal{T} \quad (5.100)$$

$$\tilde{Z}_{mit} - \sum_{b\in\mathcal{B}} \sum_{s\in\mathcal{S}} \sum_{n\in\mathcal{N}_{ij}} \sum_{j\in\mathcal{J}_i} \tilde{X}_{mbsnijtt} = \tilde{H}_{mitt} \forall m \in \mathcal{M}, i \in \mathcal{I}, t \in \mathcal{T} \quad (5.101)$$

$$(1-\alpha_{m\tau(t-1)})\tilde{H}_{mi\tau(t-1)} = \sum_{b\in\mathcal{B}} \sum_{s\in\mathcal{S}} \sum_{n\in\mathcal{N}_{ij}} \sum_{j\in\mathcal{J}_i} \tilde{X}_{mbsnij\tau t}\tilde{H}_{mi\tau t}$$
$$\forall m \in \mathcal{M}, i \in \mathcal{I}, (\tau, t) \in \mathcal{T} | \tau \leq t-1 \quad (5.102)$$

$$\sum_{b\in\mathcal{B}} \sum_{s\in\mathcal{S}} \sum_{\in\mathcal{N}_{ij}} \sum_{i\in\mathcal{I}_j} \tilde{X}_{mbsnijtt} = \tilde{P}_{mjtt} + \tilde{H}_{mjtt} \forall m \in \mathcal{M}, j \in \mathcal{J}, t \in \mathcal{T} \quad (5.103)$$

$$\sum_{b\in\mathcal{B}} \sum_{s\in\mathcal{S}} \sum_{\in\mathcal{N}_{ij}} \sum_{i\in\mathcal{I}_j} \tilde{X}_{mbsnij\tau t} = \tilde{P}_{mj\tau t} + \tilde{H}_{mj\tau t} - (1-\alpha_{m\tau(t-1)})\tilde{H}_{mj\tau(t-1)}$$
$$\forall m \in \mathcal{M}, j \in \mathcal{J}, (\tau, t) \in \mathcal{T} | \tau \leq t-1 \quad (5.104)$$

$$\sum_{\tau=1}^{t} \tilde{P}_{mj\tau t} = d_{mjt} - \tilde{U}_{mjt} \forall m \in \mathcal{M}, j \in \mathcal{J}, t \in \mathcal{T} \quad (5.105)$$

$$\sum_{m\in\mathcal{M}} \sum_{\tau=1}^{t} \tilde{H}_{mi\tau t} \leq \overline{h}_i \forall i \in \mathcal{I} \bigcup \mathcal{J}, t \in \mathcal{T} \quad (5.106)$$

$$\sum_{\tau=1}^{t} \tilde{X}_{mbsnij\tau t} \leq min\{\tilde{w}_{ijt}, \bar{w}_b\} Y_{mbsnijt} \forall m \in \mathcal{M}, b \in \mathcal{B},$$
$$s \in \mathcal{S}, n \in \mathcal{N}_{ij}, i \in \mathcal{I}, j \in \mathcal{J}_i, t \in \mathcal{T} \quad (5.107)$$

$$\sum_{\tau=1}^{t} \tilde{X}_{mbsnij\tau t} \leq \rho_m v_b Y_{mbsnijt} \forall m \in \mathcal{M}, b \in \mathcal{B}, s \in \mathcal{S},$$
$$n \in \mathcal{N}_{ij}, i \in \mathcal{I}, j \in \mathcal{J}_i, t \in \mathcal{T} \quad (5.108)$$

$$\tilde{X}_{mbsnij\tau t}, \tilde{H}_{mi\tau t}, \tilde{H}_{mj\tau t}, \tilde{Z}_{mit}, \tilde{P}_{mj\tau t}, \tilde{U}_{mjt} \in \mathbb{R}^+ \quad (5.109)$$

In addition to the constrains discussed above, the following lower-bounding cut is also added to [**MP**]:

$$\Theta \geq \sum_{t\in\mathcal{T}}\sum_{m\in\mathcal{M}}\Bigg(\sum_{i\in\mathcal{I}\bigcup\mathcal{J}}\sum_{\tau=1}^{t} h_{mi\tau t}\tilde{H}_{mi\tau t} + \sum_{b\in\mathcal{B}}\sum_{s\in\mathcal{S}}\sum_{n\in\mathcal{N}_{ij}}\sum_{(i,j)\in(\mathcal{I},\mathcal{J})}\sum_{\tau=1}^{t} c_{mbsnij\tau t}\tilde{X}_{mbsnij\tau t}$$
$$+\sum_{i\in\mathcal{I}}\gamma_{mit}\tilde{Z}_{mit} + \sum_{j\in\mathcal{J}}\pi_{mjt}\tilde{U}_{mjt}\Bigg) \tag{5.110}$$

Type B cut: This approach appends a set of primal subproblem constraints to [**MP**] under *mean scenario bundle* $\bar{e}_l$; $l \in \mathcal{L}$. Further, free variable Θ is now modified as Θ_l which allows adding multiple cuts, one for each scenario bundle $l \in \mathcal{L}$. To generate the *primal-based multiple mean-value cut*, following additional parameters and decision variables are now introduced:

Auxiliary parameters:

- $\tilde{\phi}_{mitl}$: mean supply availability of product $m \in \mathcal{M}$ in port $i \in \mathcal{I}$ at time period $t \in \mathcal{T}$ under scenario bundle $l \in \mathcal{L}$
- $\tilde{w}_{ijtl}$: mean allowable load that can be carried between the channel $(i,j) \in (\mathcal{I},\mathcal{J})$ at time period $t \in \mathcal{T}$ under scenario bundle $l \in \mathcal{L}$

Auxiliary variables:

- $\tilde{Z}_{mitl}$: mean amount of commodities of type $m \in \mathcal{M}$ processed at port $i \in \mathcal{I}$ at time period $t \in \mathcal{T}$ under scenario bundle $l \in \mathcal{L}$
- $\tilde{X}_{mbsnij\tau tl}$: amount of commodities of type $m \in \mathcal{M}$ that were purchased at time period τ and transported at time period $t \in \mathcal{T}$ using barge $b \in \mathcal{B}$ of towboat $s \in \mathcal{S}$ of trip $n \in \mathcal{N}_{ij}$ along arc $(i,j) \in (\mathcal{I},\mathcal{J})$ under scenario bundle $l \in \mathcal{L}$, where $(\tau,t) \in \mathcal{T}|\tau \leq t$
- $\tilde{H}_{mi\tau tl}$: amount of commodities of type $m \in \mathcal{M}$ stored in port $i \in \mathcal{I}\bigcup\mathcal{J}$ between time period τ and t under scenario bundle $l \in \mathcal{L}$, where $(\tau,t) \in \mathcal{T}|\tau \leq t$

- $\tilde{U}_{mjtl}$: amount of commodities of type $m \in \mathcal{M}$ shortage in destination port $j \in \mathcal{J}$ at time period $t \in \mathcal{T}$ under scenario bundle $l \in \mathcal{L}$
- $\tilde{P}_{mj\tau tl}$: demand of commodities of type $m \in \mathcal{M}$ satisfied at destination port $j \in \mathcal{J}$ with commodities purchased at time period τ and transported $t \in \mathcal{T}$ under scenario bundle $l \in \mathcal{L}$, where $(\tau, t) \in \mathcal{T} | \tau \leq t$

Similar to the constraints (5.100)-(5.109), we now add a set of primal constraints to the Benders master problem [**MP**] one for each scenario bundle $l \in \mathcal{L}$. Additionally, lower-bounding cuts (5.111) are added to [**MP**] for each sceanrio bundle $l \in \mathcal{L}$.

$$\Theta_l \geq \sum_{t\in\mathcal{T}} \sum_{m\in\mathcal{M}} \Bigg(\sum_{i\in\mathcal{I}\bigcup\mathcal{J}} \sum_{\tau=1}^{t} h_{mi\tau t} \tilde{H}_{mi\tau tl} + \sum_{b\in\mathcal{B}} \sum_{s\in\mathcal{S}} \sum_{n\in\mathcal{N}_{ij}} \sum_{(i,j)\in(\mathcal{I},\mathcal{J})} \sum_{\tau=1}^{t} c_{mbsnij\tau t} \tilde{X}_{mbsnij\tau tl}$$
$$+ \sum_{i\in\mathcal{I}} \gamma_{mit} \tilde{Z}_{mitl} + \sum_{j\in\mathcal{J}} \pi_{mjt} \tilde{U}_{mjtl} \Bigg) \qquad l \in \mathcal{L} \tag{5.111}$$

Dual-based mean-value cut

Type C cut: In this approach, we obtain the dual subproblem solutions under a mean value scenario $\bar{e}$, and using this solution, a single inequality is added to [**MP**]. The set of dual variables, $\vartheta_{mite}, \kappa_{mite}, \zeta_{mi\tau te}, \varepsilon_{mjte}, \beta_{mj\tau te}, \chi_{mjte}, \nu_{ite}, \Gamma_{jte}, \varsigma_{mbsnijte}$, and $\Lambda_{mbsnijte}$ are now redefined for the mean value scenario $\bar{e}$ as $\overline{\vartheta}_{mit}, \overline{\kappa}_{mit}, \overline{\zeta}_{mi\tau t}, \overline{\varepsilon}_{mjt}$, $\overline{\beta}_{mj\tau t}, \overline{\chi}_{mjt}, \overline{\nu}_{it}, \overline{\Gamma}_{jt}, \overline{\varsigma}_{mbsnijt}, \overline{\Lambda}_{mbsnijt}$. In iteration $r+1$ of the Benders master problem [**MP**], following dual-based mean-value inequality can now be added solving the dual suproblem [**DSP**] for mean value scenario $\bar{e}$ at iteration r:

$$\Theta \geq \sum_{t\in\mathcal{T}} \sum_{m\in\mathcal{M}} \Bigg(\sum_{j\in\mathcal{J}} d_{mjt} \overline{\chi}_{mjt} - \sum_{i\in\mathcal{I}} \phi_{mit\bar{e}} \overline{\vartheta}_{mit} - \sum_{b\in\mathcal{B}} \sum_{s\in\mathcal{S}} \sum_{n\in\mathcal{N}_{ij}} \sum_{j\in\mathcal{J}} \sum_{i\in\mathcal{I}} \Bigg(\rho_m v_b \hat{Y}_{mbsnijt}$$
$$\overline{\Lambda}_{mbsnijt} + min(\overline{w}_{ijt\bar{e}}, \overline{b}) \hat{Y}_{mbsnijt} \overline{\varsigma}_{mbsnijt} \Bigg) \Bigg) - \sum_{t\in\mathcal{T}} \Bigg(\sum_{i\in\mathcal{I}} \overline{h}_i \overline{\nu}_{it} + \sum_{j\in\mathcal{J}} \overline{h}_j \overline{\Gamma}_{jt} \Bigg) \tag{5.112}$$

Type D cut

This approach appends a set of inequalities to the [**MP**] based on the dual subproblem solutions obtained under different mean value scenario bundles $\bar{e}_l$ where $l \in \mathcal{L}$. The set of dual variables $(\vartheta_{mite}, \kappa_{mite}, \zeta_{mi\tau te}, \varepsilon_{mjte}, \beta_{mj\tau te}, \chi_{mjte}, \nu_{ite}, \Gamma_{jte}, \varsigma_{mbsnijte}, \Lambda_{mbsnijte})$ are now redefined as $(\overline{\vartheta}_{mit\bar{e}_l}, \overline{\kappa}_{mit\bar{e}_l}, \overline{\zeta}_{mi\tau t\bar{e}_l}, \overline{\varepsilon}_{mjt\bar{e}_l}, \overline{\beta}_{mj\tau t\bar{e}_l}, \overline{\chi}_{mjt\bar{e}_l}, \overline{\nu}_{it\bar{e}_l}, \overline{\Gamma}_{jt\bar{e}_l}, \overline{\varsigma}_{mbsnijt\bar{e}_l}, \overline{\Lambda}_{mbsnijt\bar{e}_l})$ to account for holding the solutions for the mean value scenario $\bar{e}_l$. The following dual-based mean-value cut can be added to [**MP**] in $r+1^{th}$ iteration of the Benders decomposition algorithm after solving the dual subproblem [**DSP**] for mean value of scenario bundles $\bar{e}_l$ in previous iteration r:

$$\Theta_l \geq \sum_{t\in\mathcal{T}}\sum_{m\in\mathcal{M}}\Bigg(\sum_{j\in\mathcal{J}} d_{mjt}\overline{\chi}_{mjt\bar{e}_l} - \sum_{i\in\mathcal{I}}\phi_{mit\bar{e}_l}\overline{\vartheta}_{mit\bar{e}_l} - \sum_{b\in\mathcal{B}}\sum_{s\in\mathcal{S}}\sum_{n\in\mathcal{N}_{ij}}\sum_{j\in\mathcal{J}}\sum_{i\in\mathcal{I}}\Bigg(min(\overline{w}_{ijt\bar{e}_l}, \overline{b})\hat{Y}_{mbsnijt}\overline{\varsigma}_{mbsnijt\bar{e}_l} + \rho_m v_b \hat{Y}_{mbsnijt}\overline{\Lambda}_{mbsnijt\bar{e}_l}\Bigg)\Bigg) - \sum_{t\in\mathcal{T}}\Bigg(\sum_{i\in\mathcal{I}}\overline{h}_i\overline{\nu}_{it\bar{e}_l} + \sum_{j\in\mathcal{J}}\overline{h}_j\overline{\Gamma}_{jt\bar{e}_l}\Bigg) l \in \mathcal{L} \tag{5.113}$$

5.4.3.5 Knapsack inequalities

Santoso et al. [119] showed that once there is a good upper bound for Benders decomposition algorithm, adding knapsack inequalities with optimality cut (5.54) can have a considerable impact on the solution quality. In addition, adding knapsack inequalities to the master problem can aid the state-of-the-art solvers, such as CPLEX and GUROBI to derive a variety of valid inequalities from the given knapsack inequalities. Consequently, adding these inequalities might expedite the convergence of the Basic benders decomposition algorithm. Let UB^r be the

best known upper-bound found until iteration r, in the next iteration, following knapsack inequality is added to [**RMP**]:

$$UB^r \geq \sum_{t\in\mathcal{T}}\Bigg(\sum_{e\in E} p_e\Bigg(\sum_{m\in\mathcal{M}}\sum_{b\in\mathcal{B}}\sum_{s\in\mathcal{S}}\sum_{n\in\mathcal{N}_{ij}}\sum_{j\in\mathcal{J}}\sum_{i\in\mathcal{I}}(\eta_{mbt} - min(\overline{w}_{ijte}, \overline{b})\varsigma_{mbsnijte}$$
$$-\rho_m v_b \Lambda_{mbsnijte})\Upsilon_{mbsnijt} + \sum_{m\in\mathcal{M}}\Bigg(\sum_{j\in\mathcal{J}} d_{mjt}\chi_{mjte} - \sum_{i\in\mathcal{I}}\phi_{mite}\vartheta_{mite}\Bigg)$$
$$-\sum_{i\in\mathcal{I}}\overline{h}_i\nu_{ite} - \sum_{j\in\mathcal{J}}\overline{h}_j\Gamma_{jte}\Bigg) + \sum_{s\in\mathcal{S}}\sum_{n\in\mathcal{N}_{ij}}\sum_{i\in\mathcal{I}}\sum_{j\in\mathcal{J}_i}\psi_{st}\Upsilon_{snijt}\Bigg) \tag{5.114}$$

Likewise, let LB^r be an the best known lower-bound obtained until iteration r; the following knapsack inequality is added to [**RMP**] in $r+1^{th}$ iteration of the Benders decomposition algorithm:

$$LB^r \leq \sum_{t\in\mathcal{T}}\sum_{s\in\mathcal{S}}\sum_{n\in\mathcal{N}_{ij}}\sum_{i\in\mathcal{I}}\sum_{j\in\mathcal{J}_i}\Bigg(\psi_{st}\Upsilon_{snijt} + \sum_{m\in\mathcal{M}}\sum_{b\in\mathcal{B}}\eta_{mbt}\Upsilon_{mbsnijt}\Bigg) + \Theta \tag{5.115}$$

5.4.3.6 Integer cut

The basic Benders decomposition algorithm sometimes generate repetitive solutions in the earlier iterations of the algorithm. This is because in the earlier stage of this algorithm, the master problem do not receive sufficient information from the subproblems via the optimality cut (5.54). Repetitive solutions does not help the Benders decomposition algorithm to converge, rather increases the the overall running time of the algorithm. To address this issue and expedite the convergence of the algorithm, following Integer cut is added to the master problem in each iteration of the algorithm. Let $\Upsilon^r = \{(m,b,s,n,i,j,t)|\hat{\Upsilon}^r_{mbsnijt} = 1, \forall m\in\mathcal{M}, b\in\mathcal{B}, s\in\mathcal{S}, n\in\mathcal{N}_{ij}, i\in\mathcal{I}, j\in\mathcal{J}_i, t\in\mathcal{T}$ where $\hat{\Upsilon}^r_{mbsnijt}$ be the solution obtained by solving

Benders master problem in any particular iteration r. The following integer cut is added to the master problem in iteration $r+1$:

$$\sum_{(m,b,s,n,i,j,t)\in Y^r} (1 - Y_{mbsnijt}) + \sum_{(m,b,s,n,i,j,t)\notin Y^r} Y_{mbsnijt} \geq 1 \tag{5.116}$$

This inequality force the barge selection decisions to be different in $r+1^{th}$ iteration. Adding this cut speeds up the convergence of the algorithm, however, excessive addition of these cuts may cut the optimal search area and result in instability problem. Therefore, in our experiments, we added this cut until the algorithm reaches to an optimaltity gap of 10%.

5.4.3.7 Warm start strategy

Benders decomposition algorithm generate low quality solutions and suffer from zig-zagging behavior in its earlier iterations. To overcome these issues, we adopt a *warm-start strategy* (WSS) proposed by rahmaniani et al. [112] which generates an initial set of tight cuts. Different from the heuristic-based strategies, the key of this strategy is to deflect the current master solution. Let $\overline{Y}_{mbsnijt}$ be the solution of the current master problem, $Y^{start}_{mbsnijt}$ be an initial starting point, and $0 < \lambda_{ws} < 1$ be a weight factor. Given these factors we deflect the current master solution for barge selection variable using following equation, $Y^{ws}_{mbsnijt} =$

$\{\lambda_{ws}\overline{Y}_{mbsnijt} + (1-\lambda_{ws})Y^{start}_{mbsnijt}\}_{\forall m\in\mathcal{M},b\in\mathcal{B},s\in\mathcal{S},\ n\in\mathcal{N}_{ij},i\in\mathcal{I},j\in\mathcal{J}_i,t\in\mathcal{T}}$. Now to generate cuts, we use the deflected solutions $Y^{ws}_{mbsnijt}$ in the following subproblem:

$$[\textbf{DP(WSS)}] := \textit{Maximize} \sum_{t\in\mathcal{T}}\sum_{m\in\mathcal{M}}\Bigg(\sum_{j\in\mathcal{J}} d_{mjt}\chi_{mjte} - \sum_{i\in\mathcal{I}}\phi_{mite}\vartheta_{mite} - \sum_{b\in\mathcal{B}}\sum_{s\in\mathcal{S}}\sum_{n\in\mathcal{N}_{ij}}\sum_{j\in\mathcal{J}} \sum_{i\in\mathcal{I}}\Big(min(\overline{w}_{ijte},\overline{b})Y^{ws}_{mbsnijt}\varsigma_{mbsnijte} + \rho_m v_b Y^{ws}_{mbsnijt}\Lambda_{mbsnijte}\Big)\Bigg) - \sum_{t\in\mathcal{T}}\Bigg(\sum_{i\in\mathcal{I}}\overline{h}_i\nu_{ite} + \sum_{j\in\mathcal{J}}\overline{h}_j\Gamma_{jte}\Bigg) \tag{5.117}$$

subject to (5.39)-(5.52).

According to [105], if the starting solution $Y^{start}_{mbsnijt}$ satisfies the core point properties, we do not need to solve auxiliary subproblems to generate pareto-optimal cut. This is because the deflected point in this case guarantees the generation of non-dominated cuts. Additionally, the upper bound generated using the deflected solution is also valid for the LP relaxation of the problem. Therefore, while applying this strategy, no auxiliary subproblems are required to be solved. This strategy is also capable of considerably alleviating the instability issue of the MP. Further this strategy dampens the initial large steps of the algorithm through taking an average with a centered solution. Thus, the $Y^{ws}_{mbsnijt}$ and the whole procedure can also be interpreted as a stabilizing point and a stabilization strategy [40].

WSS is sensitive to the starting point values, $Y^{start}_{mbsnijt}$. Given the solution $\tilde{Y}_{mbsnijt}$ is obtained from the relaxed version of model [**LBF**] with maximum amount of supply and water level (as is defined for lower bounding function), we set the starting point as follows:

$$Y^{start}_{mbsnijt} = max\{0.5, \tilde{Y}_{mbsnijt}\}_{\forall m\in\mathcal{M},b\in\mathcal{B},s\in\mathcal{S},n\in\mathcal{N}_{ij},i\in\mathcal{I},j\in\mathcal{J}_i,t\in\mathcal{T}}$$

5.4.3.8 Heuristic improvements

As previously mentioned, the initial iterations of the Benders decomposition algorithm produce low-quality solutions to the master problem. Additionally, optimally solving the master problem **[RMP]** even with moderate sized network is challenging. The performance improves as sufficient information from the subproblem is passed to the master problem via otimality cut (5.54). To overcome this problem, we solve the **[RMP]** by initially setting a larger gap which gradually reduces with the progression of the iterations. For instance, we can initially set the optimality gap for solving the **[RMP]** as 5% which is then reduce to 1% when the gap between the upper and lower bound of the Benders decomposition algorithm falls below 10%.

5.5 Experimental Results

This section presents a real-life case study to test the performance of our proposed model **[PIM]** and draw managerial insights from it. The model and all algorithms discussed in section 2.4 are coded in Python 2.7 on a desktop computer with an Intel Core i7 3.6 GHz processor and 32.0 GB RAM. Optimization solver Gurobi Optimizer 6.5[3] is used to solve the proposed model and solution techniques. Three U.S. states alongside lower Mississippi river, namely, Arkansas (AR), Mississippi (MS), and Louisiana (LA) are considered as a testing ground to visualize and validate the modeling results. In the next few subsections, we discuss the input parameters, demonstrate the real-life case study and list the man-

[3]Available from: `http://www.gurobi.com/`

agerial insight obtained from the case study, and discuss the computational performance of the developed algorithms.

5.5.1 Data Description

5.5.1.1 Inland waterway port locations

This study considers eight inland waterway ports alongside Mississippi river. Among these selected ports, the Port of Rosedale, Port of Greenville, Port of Vicksburg, and Port of Natchez are located in Mississippi and the Port of Geismar, Port of Greater Baton Rouge, Port of South Louisiana, and Port of Gramercy are located in Louisiana. These ports are connected to each other via the Mississippi River system. The geographical locations of them are demonstrated in figure 5.2.

5.5.1.2 Supply data

In this study we consider two agricultural commodities, corn and soybean that needs to be transported through the inland waterway transportation network. Corn and soybean suppliers, located within 60 miles radius from the selected ports are considered in this case study. We then aggregate the supply availability information of these commodities for each port considering the minimum distance between suppliers to all origin ports. The supply availability of corn and soybean (in 1,000 tons) is demonstrated in Figure 5.3. The test region produces 113.8 million tons of corn and 101.6 million tons of soybean in 59 and 49 different counties each year, respectively [135]. Corn is harvested only between mid-July and

Figure 5.2

Inland waterway port locations along the Mississippi River

early December of each year and soybean is harvested between mid-October and November of each year [133].

5.5.1.3 Demand data

In this case study we consider Port of Rosedale, Port of Greenville, Port of Vicksburg, and Port of Natchez as destination ports. These ports are located in the state of Mississippi and commodities received in these ports are used to serve 43 industries located near the Mississippi River. Similar to the supply aggregation, demand at any destination port is obtained by grouping the commodity demand at industries located close to that destination port. The test region has an annual demand of corn and soybean as 68.3 and 52.3 million tons, respectively [135]. The yearly demand distribution of destination ports can be seen in Figure 5.4.

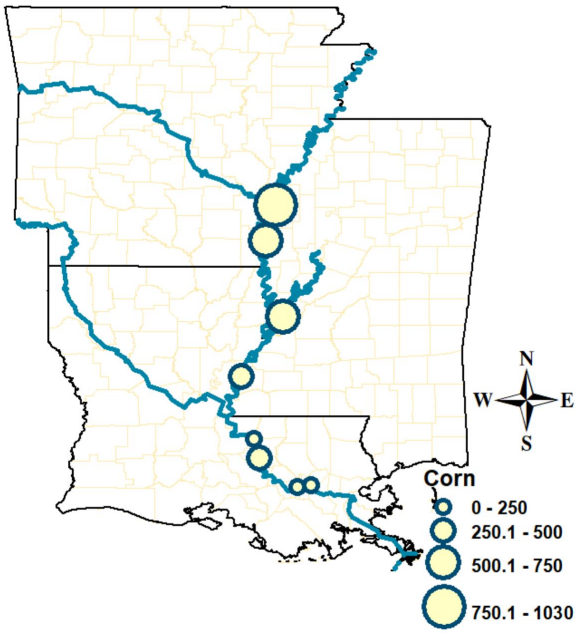

(a) Corn

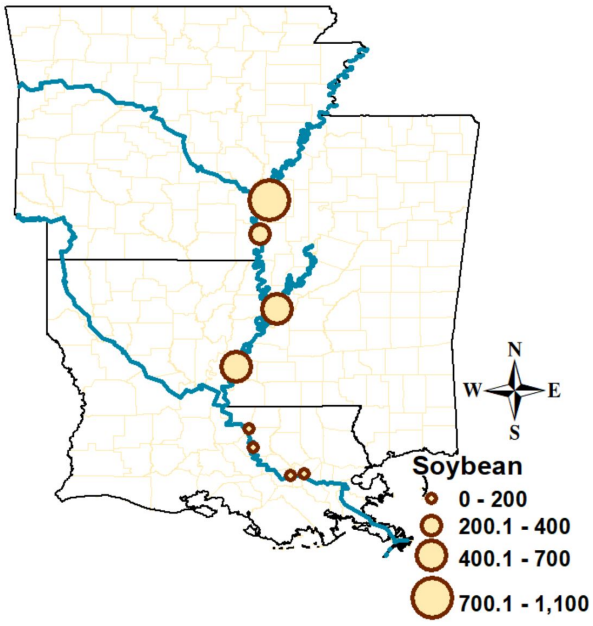

(b) Soybean

Figure 5.3

Supply availability for (a) Corn and (b) Soybean in the test region (in 1,000 tons)

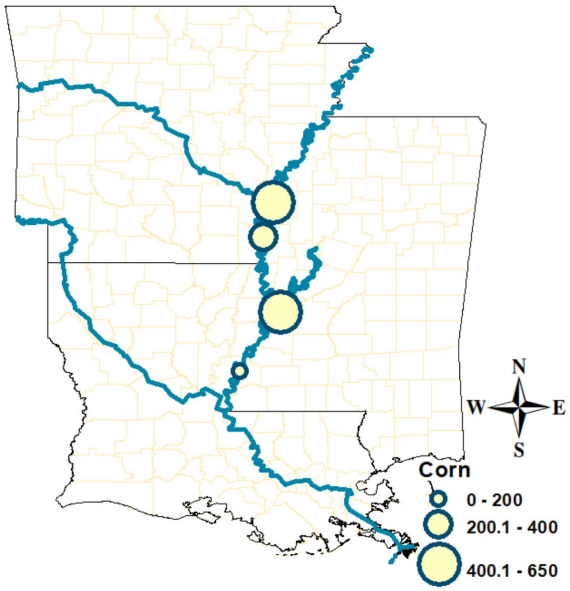

(a) Corn

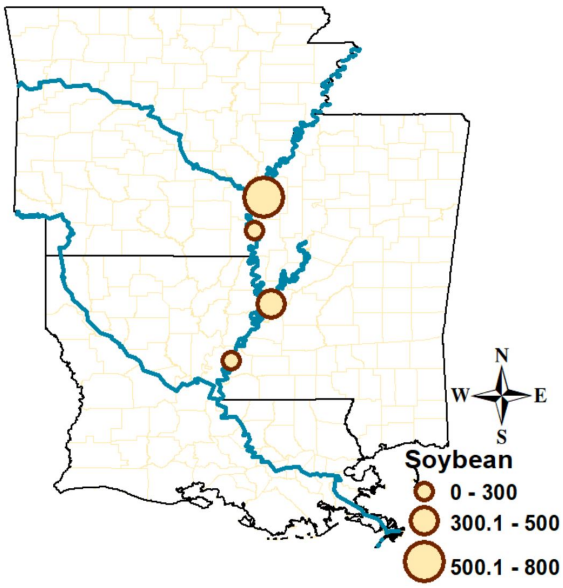

(b) Soybean

Figure 5.4

Demand of (a) Corn and (b) Soybean in the test region (in 1,000 tons)

5.5.1.4 Transportation cost

The inland waterway transportation network considered in this study includes origin ports and destination ports. Transportation between these two tiers $(i, j) \in (\mathcal{I}, \mathcal{J})$ is done using towboats and barges. Considering the capacity of the Mississippi river, the towboats here are allowed to carry a maximum of 15 barges in each trip [138] and the fixed cost of using a towboat is \$244.38 [138]. Additionally, the cost of loading and unloading commodities to each barge is set as \$15. The unit commodity transportation cost is $\$0.017/mile/ton$ [48, 110]. All costs are calculated based on 2018 dollars value.

5.5.1.5 Water-level Fluctuations

Transportation through inland waterway transportation network is seriously impacted by the uncertain water level fluctuations of the river. This is a common problem faced by different river systems all over the world, Yangtze River at China [94], Rhine River at Europe [94] and Tagliamento River at Europe [94] are few examples of this. The Mississippi river also experiences significant water level fluctuations in its different segments all over the year that imposes a serious challenge to efficiently plan and conduct barge transportation through this river. The lower portion of this river possesses sound water flow compared to the upper portion of this river, therefore, the load carrying capacity of the lower Mississippi river is more reliable compared to the upper Mississippi River. However, even this segment is not free from fluctuations. Figure 5.5 demonstrates an example

of water level fluctuations between Port of Rosedale and Port of Greenville from July 2016 to June 2017 is provided. Each point in Figure 5.5 indicates the average weekly water stage [139] at this river segment. Clearly, this figure identifies that between middle of August to the end of December of a calender year the water level drops and minimum water stage is obtained during the first three weeks of October. Except this period, the water stage generally remains above the desired level (14.2 feet) for other time periods, but in May when the water level reaches to 42 feet, which is higher than the demonstrated flood level, 37 feet.

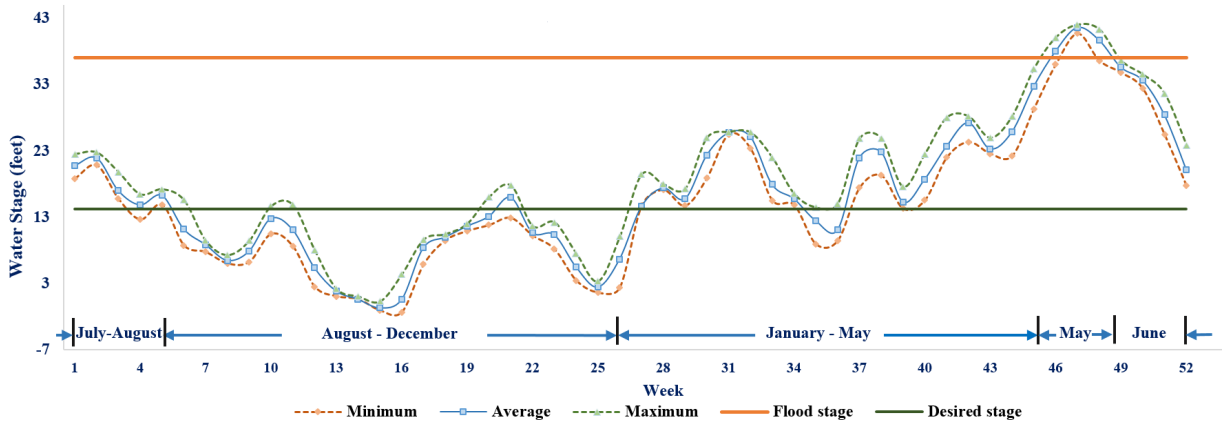

Figure 5.5

Demonstration water level fluctuations between Port of Rosedale and Port of Greenville from July, 2016 to June, 2017 [139]

5.5.2 Real-life Case Study

The highly uncertain waterway conditions coupled with urgent delivery requirement of perishable products put the policymakers in serious dilemma to perform effective and robust transportation planning for inland waterways. Therefore, to facilitate decision making and derive some key managerial insights from our proposed model **[PIM]**, in this subsection we solve our designed real life case study and perform sensitivity analysis on different key input parameters. The following sections provide a comprehensive summary about the impact of these key input parameters on model **[PIM]**.

5.5.2.1 The impact of deterioration rate $\alpha_{m\tau t}$ on the overall system performance

The deterioration of perishable commodities can significantly impact the optimal resource allocation and transportation planning of the inland waterway ports and the network under consideration. To closely analyze its impact on the overall system performance, we generate six different scenarios by considering $\pm 20\%$, $\pm 40\%$ and $\pm 60\%$ change in base deterioration rate of each commodity, i.e., corn and soybean. Figure 5.6 delineates the impacts of these changes on different key decision variables along with the overall system. The summary of the experimental outcomes is outlined below:

- With the increase in deterioration rate ($\alpha_{m\tau t}$), the overall inventory at destination ports ($H_{mj\tau t}$) decrease. More specifically, with 20%, 40%, and 60% increase in $\alpha_{m\tau t}$, $H_{mj\tau t}$ changes by -42%, -50%, and -52% respectively from the base case scenario (Figure 5.6(a)). The origin port inventory $H_{mi\tau t}$, on the other hand, slightly increases with these changes, but this impact is not much significant. In overall, 20%, 40%, and 60% increase in $\alpha_{m\tau t}$ decrease the total storage at origin and destination ports by 10.6%,11.93%, and 12.3% from the base case.

- Decreasing $\alpha_{m\tau t}$ by 20%, 40%, and 60% changes $H_{mj\tau t}$ by +2.4%,+46.2%, and +53.3% from the base case scenario (Figure 5.6(a)). Alike the $\alpha_{m\tau t}$ increment cases, decrement cases also show minimal changes to the origin port inventory $H_{mi\tau t}$. The cumulative inventory storage changes by +0.3%, +11.2%, and +12.9% from the base case scenario due to −20%, −40%, and −60% changes to the $\alpha_{m\tau t}$ (Figure 5.6(a)).

- Figure 5.6(b) represents that 20%, 40% and 60% increase in deterioration rate the overall commodity transportation through the network is reduced by 16000, 23500, and 26000 tons from the base case, which negatively impacts the demand satisfaction as well. On the other hand 20%, 40%, and 60% decrease in deterioration rate help system to transport about 3000, 14500, and 17500 tons more commodities from the base case that decreases the amount of unsatisfied demand throughout the system.

- Figure 5.6(c) demonstrates that the overall system cost experience an increase by 11.4%, 22.4%, and 32.9% from the base case cost due to +20%, +40%, and +60% change in $\alpha_{m\tau t}$. These changes increase the computational complexity of the model, therefore, we notice about +21.1%, +29.9%, and +33.2% change in solution time respectively, from the base case scenario. In contrary, −20%, −40% and −60% changes in deterioration rate change total system cost by −11.5%,24.4%, and −36.8%, with a decrease in solution time by 11.7%, 21.6%, and 26.7%, respectively from the base case scenario. This clearly signifies the importance of deterioration rate ($\alpha_{m\tau t}$) on the inland waterway transportation network.

- In overall, the amount of product stored in destination ports is highly impacted by commodity deterioration.

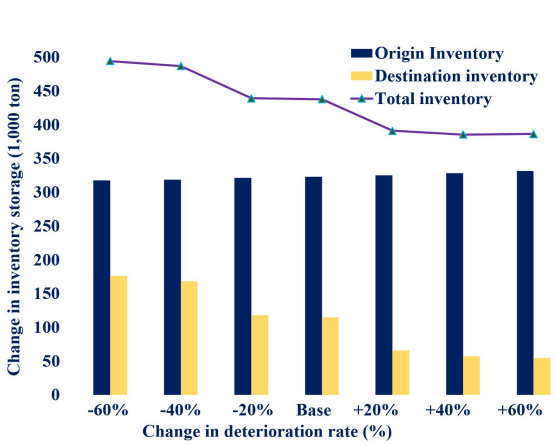

(a) Inventory Storage ($H_{mi\tau t}$, $H_{mj\tau t}$)

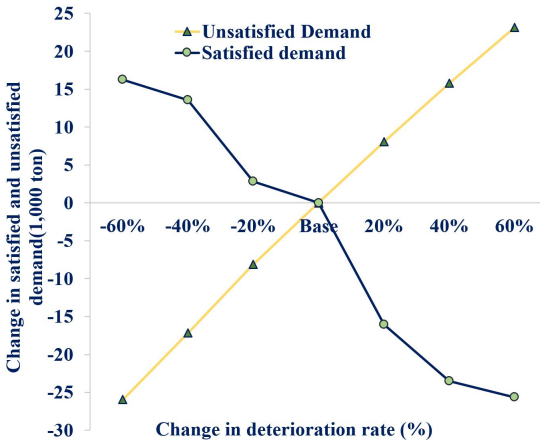

(b) Change in unsatisfied (U_{mjt}) and ($X_{mbsnij\tau t}$) satisfied demand

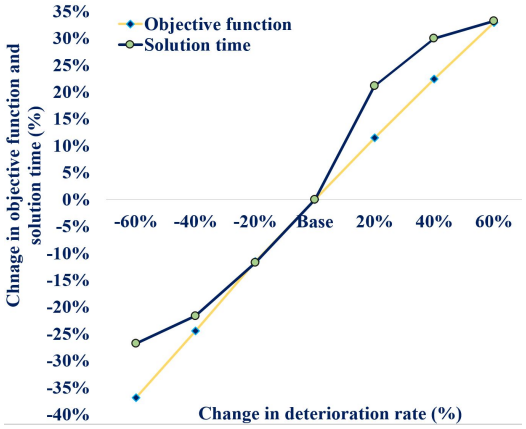

(c) Change in objective function value and Solution time

Figure 5.6

Impact of $\alpha_{m\tau t}$ changes on overall system performance.

5.5.2.2 Impact of water level fluctuation $w_{ijt\omega}$ on overall system performance

This set of experiment investigates the impact of water level fluctuation on the overall system performance. We generate six water level scenarios considering $\pm 15\%$, $\pm 30\%$ and $\pm 45\%$ change in mean water level $\bar{w}_{ijt\omega}$ and compare the results with for the base $\bar{w}_{ijt\omega}$. Our observations from this experiment are listed below:

- The results in Figure 5.7(a) indicate that with 15%, 30% and 45% increase in $\bar{w}_{ijt\omega}$ the overall barge usage drops by 13.2%,22.7%, and 28.3%, additionally, we see the reduction in the overall towboat usage by 9.8%, 18.1%, and 25.1%, respectively from the base case scenario. In contrary, 15%, 30%, and 45% decrease in mean water level $\bar{w}_{ijt\omega}$ compels the system to utilize 17.1%, 37.5%, and 60.6% more barges respectively than the base case. With these changes the system is now motivated to use 17.2%,36.8%, and 58.9% more towboats from the base case. This is because as the mean water level drops, to avoid barges being stuck in any part of the waterway, the system decides to transport less load on each barge compared to its design capacity, hence the overall barge usage raises and we need more towboats to transport these additional barges.

- Figure 5.7(b) illustrates the impact of mean water level $\bar{w}_{ijt\omega}$ on the load per barge and the load per storage. As previously mentioned, different water level condition requires barges to adjust their weight capacity. Hence, once $\bar{w}_{ijt\omega}$ is increased by 15%, 30% and 45%, the load per barge increases by $+15.1\%$, $+29.3\%$, and $+39.6\%$ respectively from the base case scenario. On the other hand, 15%, 30% and 45% reduction $\bar{w}_{ijt\omega}$ causes the barges to carry 14.6%, 29.6% and 44.3% less products from the base case scenario. Further, change in mean water level impacts the utilization of available storage capacity. With 45% increase in $\bar{w}_{ijt\omega}$ the storage capacity utilization rises by $+12.1\%$, whereas in the extreme water level case i.e., -45% this change is about -9.5%. This explains that with the higher water level, more commodities can be transported which triggers more storage requirement to support the peak demand other than using the third party supply.

- Figure 5.7(c) indicates that although increase in mean water level has no considerable effect on objective function value, with 30% and 45% decrease in mean water level, due to the the increase in unsatisfied demand, objective function value changes by $+16.3\%$, and $+33.9\%$ respectively from the base case scenario. Additionally, it can be observed that change in mean water level has a direct impact on the complexity of model, that can be measured by solution time. As mean water level decrease by 15%, 30% and 45%, the corresponding solution time change by $+43.5\%$,$+73.4\%$, and $+85.4\%$ from

the base case scenario. However, with 15%, 30% and 45% increase in mean water level, solution time drops by 34.9%, 42.1% and 47.9% from the base case scenario. This result signifies that with higher water level the model complexity reduces, therefore, less time is required to solve the model. This highlights the importance of water level($w_{ijt\omega}$) considerations on the inland waterway transportation network.

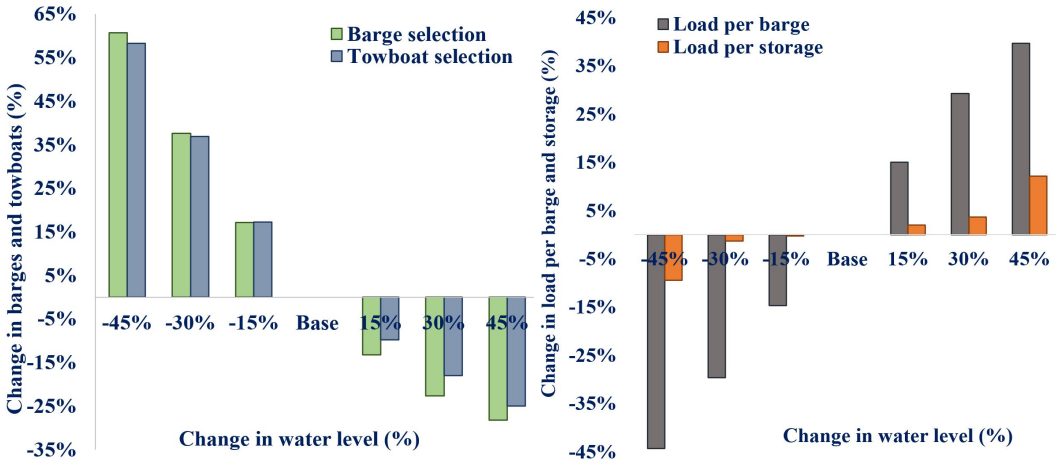

(a) Change in number of barges ($Y_{mbsnijt}$) and towboats (Y_{snijt})

(b) Change in load per barge and inventory storage

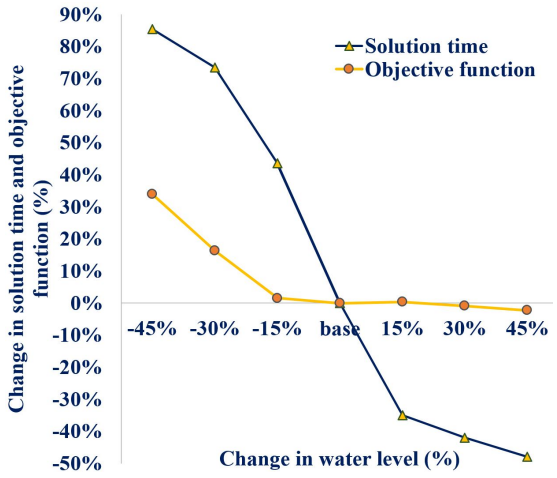

(c) Change in objective function value and Solution time

Figure 5.7

Impact of $w_{ijt\omega}$ changes on overall system performance.

5.5.3 Performance Evaluation of the Algorithms

This section presents our computational experience in solving model **[PIM]** using the algorithms presented in Section 2.4. We vary sets $|\mathcal{I}|$, $|\mathcal{J}|$, $|\mathcal{M}|$, $|\mathcal{S}|$, and $|\mathcal{T}|$ in **[PIM]** to generate 9 different problem instances, the details of these instances can be found in Table 5.1. We used following termination criterion to terminate the algorithms: (i) the optimality gap, i.e., $\epsilon = |UB - LB|/UB$ falls below a threshold value (e.g., $\epsilon = 2.0\%$); (ii) the maximum time limit, t^{max} is reached (e.g., $t^{max} = 14,400$ CPU seconds); or (iii) the maximum iteration limit, q^{max} is reached (e.g., $q^{max} = 500$). Tables 5.2, 5.3, and **??** shows the the performance of different variants of Benders decomposition algorithm. In reporting results, the column headings $\epsilon(\%)$ and $t(sec)$ respectively indicate the optimality gap and solution time. Note that, while reporting the dominant algorithm for each test instance, we highlighted the algorithm which yield the lowest solution time to solve the given instance within the predefined gap threshold ($\epsilon = 2.0\%$). If such a quality solution is not found within the stipulated time frame, the algorithm with lowest optimality gap was highlighted.

Table 5.1

Problem size and test instances

	Instance No	$\|\mathcal{I}\|$	$\|\mathcal{J}\|$	$\|\mathcal{M}\|$	$\|\mathcal{B}\|$	$\|\mathcal{S}\|$	$\|\mathcal{N}\|$	$\|\mathcal{T}\|$	Binary variables	Continuous variables	Total variables	No. of constraints
	1	4	2	2	15	6	5	4	22,320	86,768	109,088	59,200
Small	2	4	2	3	15	8	5	4	44,160	173,352	217,512	107,592
	3	4	2	4	15	10	5	4	73,200	288,736	361,936	170,384
	4	6	3	2	15	6	5	4	55,800	216,552	272,352	147,624
Medium	5	6	3	3	15	8	5	4	110,400	432,828	543,228	268,452
	6	6	3	4	15	10	5	4	183,000	721,104	904,104	425,280
	7	8	4	2	15	6	5	4	104,160	403,936	508,096	275,264
Large	8	8	4	3	15	8	5	4	206,080	807,504	1,013,584	500,688
	9	8	4	4	15	10	5	4	341,600	1,345,472	1,687,072	793,312

The first set of experiments test the performance of **Type-1** and **Type-2** cuts with and without the inclusion of *Pareto-optimal* (**PO**) cut under the Benders decomposition algorithm. Table 5.2 shows the results of these four variants of accelerated Benders decomposition algorithm. Note that all these algorithms were nested under the *Sample average approximation* (**SAA**) scheme with a sample size $E = 100$. The result shows that, incorporating **PO** cut with both **Type-1** and **Type-2** cuts significantly improve the optimality gap ϵ and reduce the run time t. Specifically, applying **PO** cut with **Type-1** cut changes the optimality gap from 12.02% to 2.15% along with saving the computational time by 5,058 CPU seconds, on average. For **Type-2** cut with **PO** these changes are 12.00% to 2.12% and 5,194, respectively. Additionally, Table 5.2 points out that the **Type-2** cut slightly domi-

nates **Type-1** cut in terms of both optimality gap and running time. Also, the **PO** cut with **Type-2** cut variant outperforms other three algorithm variants in Table 5.2.

Table 5.2

Experimental results of **Type-1** and **Type-2** cut with and without **PO** cut

	Type-1				**Type-2**			
Instance	**W/o PO**		**PO**		**W/o PO**		**PO**	
No.	$\epsilon(\%)$	$t(sec)$	$\epsilon(\%)$	$t(sec)$	$\epsilon(\%)$	$t(sec)$	$\epsilon(\%)$	$t(sec)$
1	2.42	14,400	0.88	**2,120**	2.68	14,400	0.62	2,184
2	5.39	14,400	0.12	**3,619**	5.71	14,400	1.05	3,869
3	9.36	14,400	1.95	8,144	9.07	14,400	1.89	**7,721**
4	6.65	14,400	1.82	**5,424**	6.73	14,400	1.34	5,512
5	11.78	14,400	1.42	11,239	12.14	14,400	1.64	**10,942**
6	16.24	14,400	3.17	14,400	16.78	14,400	**3.02**	14,400
7	9.97	14,400	1.19	10,332	9.54	14,400	1.48	**9,426**
8	19.62	14,400	3.41	14,400	20.46	14,400	**2.94**	14,400
9	26.78	14,400	5.42	14,400	24.96	14,400	**5.17**	14,400
Average	12.02	14,400	2.15	9,342	12.00	14,400	2.12	**9,206**

Next, we compare the computational benefits of adding **Type A**, **B**, **C**, and **D** cuts to the Benders decomposition algorithm through the results summarized in

Table 5.3. This set of experiments also uses the same **SAA** sample size i.e., $E = 100$. Additionally, all algorithm variants in Table 5.3 include *valid inequalities* and *knapsack inequalities* discussed in sections 5.4.3.1 and 5.4.3.5, respectively. Results in Table 5.3 indicate that **Type D** cut variant dominates other three cut variants in terms of solution time and quality. Even though among 9 problem instances it solves the first instance within the time limit, but for another 6 out of 8 remaining instances, this algorithm provides the best optimality gap, 10.05% on average. In summary, the addition of **Type D** cut can reduce the optimalty gap to almost one third of that produced by **Type A** and **B** cuts. Further, **Type B** and **D** cut that uses *scenario bundling* technique can make the basic Benders decomposition algorithm highly efficient and among them **Type D** shows the best result.

Table 5.3

Experimental results with **Type A**, **B**, **C**, and **D** cuts

Instance	**Type A**		**Type B**		**Type C**		**Type D**	
No.	$\epsilon(\%)$	$t(sec)$	$\epsilon(\%)$	$t(sec)$	$\epsilon(\%)$	$t(sec)$	$\epsilon(\%)$	$t(sec)$
1	7.35	14,400	1.75	12,621	5.44	14,400	1.68	**11,632**
2	14.03	14,400	2.68	14,400	11.98	14,400	**2.07**	14,254
3	24.97	14,400	9.48	14,400	21.71	14,400	**8.74**	14,400
4	17.61	14,400	**6.12**	14,400	15.08	14,400	6.76	14,400
5	32.48	14,400	11.28	14,400	32.37	14,400	**10.51**	14,400
6	44.61	14,400	15.32	14,400	43.68	14,400	**13.78**	14,400
7	30.02	14,400	**8.97**	14,400	27.30	14,400	9.07	14,400
8	41.60	14,400	19.87	14,400	43.42	14,400	**16.45**	14,400
9	49.40	14,400	24.92	14,400	49.91	14,400	**21.39**	14,400
Average	29.11	14,400	11.15	14,202	27.87	14,400	**10.05**	14,076

The experiments presented in Table 5.3 clarifies the dominance of enhanced Benders decomposition algorithm with **Type D** cut in solving the model **[PIM]**. To test the performance of other enhancement techniques discussed in section 5.4.3, first we select the enhanced Benders decomposition algorithm with **Type D** cut and add **Type-2** cut enhanced with **PO** with it which was the dominant cut in Table 5.2. We name this new algorithm variant as **TD+T2+PO**. Next, we define

few new variants by sequentially adding the integer cut with heuristics and the warm start strategy to algorithm **TD+T2+PO** and denote them as **TD+T2+PO+Int** and **TD+T2+PO+Int+WSS**. All these new algorithm variants along with **Type D** variant are tested under three different **SAA** sample sizes, $W_1 = 100$, $W_2 = 150$, and $W_3 = 200$ and the results of this experiment are reported in Tables 5.4, 5.5, and 5.6. The numerical results show that **Type D** cut variant is able to solve only the first instance out of 9 instances for all three scenario size problems under the pre-specified termination criteria. Algorithm **TD+T2+PO**, on the other hand, can efficiently solve 8 instances of model **[PIM]** with $|\Omega| = 100$ and $|\Omega| = 150$, and 7 instances of the problem with $|\Omega| = 200$. In addition, applying **TD+T2+PO** cut, the average optimality gap achieved with **Type D** cut is now changed to 1.66%, 1.75%, and 1.92% for $|\Omega| = 100$, $|\Omega| = 150$, and $|\Omega| = 200$, respectively. The solution time also drops by 41.5, 38.7, and 35.4%. Including the integer cut and heuristic improvement techniques to **TD+T2+PO** cut (**TD+T2+PO+Int** cut) we achieve a slightly better solution quality with a quicker solution time. However, this accelerating technique also could not solve the last instance of both 150 and 200 scenario problems. Finally, we apply **TD+T2+PO+Int+WSS** cut and the results show that this cut significantly improves the performance of the basic Benders decomposition algorithm and additionally it can solve all test instances under the experimental range. **TD+T2+PO+Int+WSS** cut reduces the solution time from 7,914, 8,417, and 8,906 CPU seconds to 7,570, 8,059, and 8,581 CPU seconds, which was produced by the **TD+T2+PO+Int** cut for the 100, 150, and 200 scenario

problems, respectively. This technique also slightly reduces the average optimality gap that was obtained using **TD+T2+PO+Int** technique. Further, Tables 5.4, 5.5, and 5.6 lists the results of transportation and storage related decision variables for all test instances. The average value of these transportation and storage related decisions for problem **[PIM]** with $|\Omega| = 100$, $|\Omega| = 150$, and $|\Omega| = 200$ shows almost same results with negligible difference. For example, for the 100, 150, and 200 scenario problems, the average number of barges used is equal to 1691, 1691, and 1693 which are very close. Therefore, we can realize that considering only 100 scenarios would be enough to obtain robust solutions from our proposed model, whereas with increased scenarios the model will be computationally more challenging requiring more time to solve (e.g., 200 scenarios problem takes 12% more time compared to 100 scenario problem).

Algorithm 1:The Benders decomposition algorithm

Initialization: , $r \leftarrow 1, \epsilon, UB^r \leftarrow +\infty, LB^r \leftarrow -\infty, \mathcal{P}_D^r \leftarrow 0$

$terminate \leftarrow false$

while $terminate = false$ **do**

Solve **[MP]** to obtain $\{Y^r_{snijt}\}_{s\in\mathcal{S},n\in\mathcal{N}_{ij},i\in\mathcal{I},j\in\mathcal{J}_i,t\in\mathcal{T}}$

and $\{Y^r_{mbsnijt}\}_{m\in\mathcal{M},b\in\mathcal{B},s\in\mathcal{S},n\in\mathcal{N}_{ij},i\in\mathcal{I},j\in\mathcal{J}_i,t\in\mathcal{T}}$ and z^r_{MP}

if $z^r_{MP} \geq LB^r$ **then**

$LB^r \leftarrow z^r_{MP}$

end if

For fixed $\{\hat{Y}^r_{mbsnijt}\}_{m\in\mathcal{M},b\in\mathcal{B},s\in\mathcal{S},n\in\mathcal{N}_{ij},i\in\mathcal{I},j\in\mathcal{J}_i,t\in\mathcal{T}}$ and $\{\hat{Y}^r_{snijt}\}_{s\in\mathcal{S},n\in\mathcal{N}_{ij},i\in\mathcal{I},j\in\mathcal{J}_i,t\in\mathcal{T}}$

solve **[DSP]** to obtain $(\vartheta, \kappa, \zeta, \varepsilon, \beta, \chi, \nu, \Gamma, \varsigma, \Lambda) \in \mathcal{P}_D$ and z^r_{SUB}

if $z^r_{SUB} + z^r_{MAS} < UB^r$ **then**

$UB^r \leftarrow z^r_{SUB} + z^r_{MAS}$

end if

if $\frac{UB^r - LB^r}{UB^r} \leq \epsilon$ **then**

$terminate \leftarrow true$

else

$\mathcal{P}_D^{r+1} \leftarrow \mathcal{P}_D^r \cup \{(\vartheta, \kappa, \zeta, \varepsilon, \beta, \chi, \nu, \Gamma, \varsigma, \Lambda)\}$

end if

$r \leftarrow r + 1$

end while

Algorithm 2: OpenCloseArcs algorithm

Initialization: $\forall a_{ij} \in (\overline{D}, \underline{D}), t \in \mathcal{T} : Y^{max}_{t,a_{ij}} \leftarrow \tau_{ijt} \times \overline{\delta}_s; Y^{RE}_{t,a_{ij}} \leftarrow \overline{Y}_{t,a_{ij}} = 0$

$\forall t \in \mathcal{T} : U_t \leftarrow \sum_{a_{ij} \in (\overline{D}, \underline{D})} u_{t,a_{ij}}; D_t \leftarrow d^{max}_{t(\overline{D}, \underline{D})}; \epsilon_{ci} \leftarrow 10^{-5}$

for $t \in \mathcal{T}$ **do**

  for $a_{ij} \in (\overline{D}, \underline{D})$ (in arbitrary order) **do**

    if $\{\hat{Y}_{mbsna_{ij}t}\}_{\forall m \in \mathcal{M}, b \in \mathcal{B}, s \in \mathcal{S}, n \in \mathcal{N}_{ij}} \geq 0$ **do**

      $Y^{RE}_{t,a_{ij}} \leftarrow Y^{RE}_{t,a_{ij}} + 1$

    end if

    compute $\overline{Y}_{t,a_{ij}} = \dfrac{Y^{RE}_{t,a_{ij}}}{Y^{max}_{t,a_{ij}}}$

    if $\overline{Y}_{t,a_{ij}} \leq \epsilon_{ci}$ and $U_t - u_{t,a_{ij}} \geq D_t$ **then**

      Add a_{ij} to $C_{0,t}$

      Close a_{ij} by setting $U_t \leftarrow U_t - u_{t,a_{ij}}$

    end if

    if $\overline{Y}_{t,a_{ij}} \geq 1 - \epsilon_{ci}$ and $D_t - u_{t,a_{ij}} \geq 0$ **Then**

      Add a_{ij} to $C_{1,t}$

      Open a_{ij} by setting $D_t \leftarrow D_t - u_{t,a_{ij}}$ and $U_t \leftarrow U_t - u_{t,a_{ij}}$

    end if

  end for

end for

Table 5.4

Impact of pareto-optimal cut, integer cut, warm start strategy in **Type D** cut (Part 1)

	Instance	**Type D**		**TD+T2+PO**		**TD+T2+PO+Int**		**TD+T2+PO+Int+WSS**		**Decision variables**				
	No.	$\epsilon(\%)$	$t(sec)$	$\epsilon(\%)$	$t(sec)$	$\epsilon(\%)$	$t(sec)$	$\epsilon(\%)$	$t(sec)$	$\overline{Y}_{mbsnijt}$	$\overline{Y}_{snijt}$	$\overline{X}_{mbsnijr\tau tw}$	$\overline{H}_{mi\tau tw} + \overline{H}_{mjr\tau tw}$	U_{mjtw}
	1	1.68	11,632	0.97	18,47	0.21	1,721	0.32	**1,612**	738	53	750,000	123,284	8,500
	2	2.07	14,254	1.17	33,14	0.48	3,047	0.65	**2,785**	807	59	827,762	113,446	28,500
	3	8.74	14,400	1.65	7,002	1.72	6,512	1.21	**6,231**	1,331	89	1,392,100	110,040	287,900
	4	6.76	14,400	1.41	5,089	1.32	4,794	0.85	**4,512**	1,279	92	1,304,450	195,594	227,000
$\|\Omega\|$ =100	5	10.51	14,400	1.57	9,232	1.68	8,875	1.47	**8,462**	1,381	104	1,403,955	197,814	249,830
	6	13.78	14,400	1.82	11,917	1.86	11,615	1.82	**11,023**	2,648	181	2,729,470	250,512	270,530
	7	9.07	14,400	1.67	8,612	1.89	8,374	1.43	**8,147**	1,692	126	1,735,257	481,186	51,018
	8	16.45	14,400	1.98	12,598	1.52	12,124	1.62	**11,854**	1,826	136	1,868,021	483,734	61,100
	9	21.39	14,400	2.71	14,400	1.92	14,167	1.84	**13,512**	3,517	242	3,605,719	672,334	62,424
	Average	10.05	14,076	1.66	8,223	1.4	7,914	1.24	**7,570**	1691	120	1,735,192	291,993	138,533

Table 5.5

Impact of pareto-optimal cut, integer cut, warm start strategy in **Type D** cut (Part 2)

	Instance	**Type D**		**TD+T2+PO**		**TD+T2+PO+Int**		**TD+T2+PO+Int+WSS**		**Decision variables**				
	No.	$\epsilon(\%)$	$t(sec)$	$\epsilon(\%)$	$t(sec)$	$\epsilon(\%)$	$t(sec)$	$\epsilon(\%)$	$t(sec)$	$\overline{Y}_{mbsnijt}$	$\overline{Y}_{snijt}$	$\overline{X}_{mbsnijr\tau tw}$	$\overline{H}_{mi\tau t\omega} + \overline{H}_{mjr\tau t\omega}$	$U_{mjt\omega}$
	1	1.87	12,152	0.74	2,241	1.12	2,046	0.65	**1,890**	729	52	750,000	124,529	8,500
	2	3.17	14,400	1.42	3,901	1.32	3,678	1.45	**3,412**	809	60	827,194	109860	28,517
	3	10.12	14,400	1.74	7,742	1.54	7,428	1.12	**7,049**	1,331	89	1,392,199	108200	287,800
	4	8.24	14,400	1.53	5,424	1.84	5,214	0.86	**4,994**	1,287	93	1,304,223	192898	227,013
$\|\Omega\|$ =150	5	12.32	14,400	1.69	9,756	1.51	9,521	1.61	**9,145**	1,387	104	1403,871	196016	249,763
	6	15.62	14,400	1.96	12,487	1.87	12,157	1.74	**11,587**	2,651	182	2,729,436	249861	270,563
	7	11.65	14,400	1.71	9,003	1.76	8,697	1.65	**8,435**	1,691	125	1,734,584	479414	50,821
	8	18.75	14,400	1.87	13,076	1.92	12,614	1.54	**12,145**	1,833	136	1,867,529	484539	61,135
	9	24.37	14,400	3.1	14,400	2.7	14,400	1.94	**13,876**	3,508	241	3,608,770	683391	61,109
	Average	11.79	14,150	1.75	8,670	1.73	8,417	1.39	**8,059**	1,691	120	1,735,311	29,2078	138,357

Table 5.6

Impact of pareto-optimal cut, integer cut, warm start strategy in **Type D** cut (Part 3)

	Instance	**Type D**		**TD+T2+PO**		**TD+T2+PO+Int**		**TD+T2+PO+Int+WSS**		**Decision variables**				
	No.	$\epsilon(\%)$	$t(sec)$	$\epsilon(\%)$	$t(sec)$	$\epsilon(\%)$	$t(sec)$	$\epsilon(\%)$	$t(sec)$	$\overline{Y}_{mbsnijt}$	$\overline{Y}_{snijt}$	$\overline{X}_{mbsnijr\tau tw}$	$\overline{H}_{mi\tau tw} + \overline{H}_{mjr\tau tw}$	U_{mjtw}
	1	1.68	12,784	1.45	2,612	1.51	2,418	0.84	**2,314**	730	52	750,030	124,648	8,470
	2	4.25	14,400	1.32	4,465	1.32	4,295	1.45	**3,987**	815	58	826,154	109,787	28,906
	3	12.12	14,400	1.75	8,476	1.72	8,056	1.69	**7,714**	1,330	89	1,392,004	99,558	287,995
	4	9.68	14,400	1.78	5,812	1.71	5,625	1.01	**5,341**	1,281	92	1,304,294	193,551	226,986
$\|\Omega\|$ =200	5	13.87	14,400	1.76	10,321	1.41	10,078	1.45	**9,684**	1,385	103	1,403,673	196,061	249,872
	6	17.32	14,400	1.87	13,054	1.96	12,698	1.87	**12,173**	2,647	182	2,729,414	250,663	270,588
	7	12.71	14,400	1.63	9,408	1.52	9,247	1.47	**8,914**	1,700	127	1,735,539	478,705	50,735
	8	19.96	14,400	2.37	14,126	1.87	13,345	1.26	**12,936**	1,841	143	1,867,457	487,461	61,717
	9	27.32	14,400	3.38	14,400	3.46	14,400	1.73	**14,169**	3,506	241	3,608,180	678,622	61,063
	Average	13.21	14,220	1.92	9,186	1.83	8,906	1.41	**8,581**	1,693	121	1,735,193	291,006	138,481

5.6 Conclusion and Future Research Directions

This study develops a two-stage stochastic mixed-integer linear programming model that determines the optimal resource usage and transportation related strategic and tactical decisions for an inland waterway transportation network under uncertainty. The model is designed to capture all realistic features of inland waterway transportation network including variability in water level, commodity supply, and the shelf life of commodities and provide the reliable network design solutions. Prime solutions such as the trip-wise towboat and barge assignment decisions, inventory management, and transportation decisions obtained from our model provides a reliable plan for inland ports under consideration with a minimal impact of uncertainty. We developed a nested decomposition algorithm combining the enhanced Benders decomposition algorithm with the sample average approximation method to solve our proposed optimization model in an efficient and timely manner. We demonstrate a case study considering a few Southeast US States as a ground of analysis. Additionally, sensitivity analysis is conducted that reveals the impact of various key input parameters (e.g., commodity deterioration rate and water level fluctuation) on the modeling result and reveals a number of managerial insights for policy makers and future investors.

To sum up, the major contributions of this work are as follows: (i) developing a multi-commodity, multi-time period two-stage stochastic mixed integer linear programming model to optimize the inland waterway port operations considering the perishable products, uncertain commodity supply and waterway conditions

with all realistic inland waterway related issues; (ii) presenting a novel nested decomposition combining Sample Average Approximation, and enhanced benders decomposition to solve realistic-size network design problems; (iii) extracting crucial managerial insight from a real-life case study. Note that, our proposed methodologies can also be adopted in solving different stochastic optimization problems. The managerial insights drawn from the case study will help policy makers to design and manage a robust and cost-efficient inland waterway transportation network under uncertainty

This research direct us to explore multiple research avenues. We might model the barge and towboat flows using the essence of the vehicle routing problem. Additionally, the barge and towboat routing, scheduling, and re-positioning issues can be considered to analyze the impact of them on the inland waterway port operations. Further, realizing that the inland waterway ports may experience both natural (e.g., hurricane, tornado) and/or human-induced (e.g., cyber attack) disruptions, the impact of these disruptions on inland waterway port operations can also be investigated. Future studies will address these issues.

REFERENCES

[1] Adulyasak Y., Cordeau J.-F., Jans R., "Benders decomposition for production routing under demand uncertainty," *Operations Research*, vol. 63, 2015, pp. 851–867.

[2] Aghalari A., Nur F., Marufuzzaman M., "A Benders based nested decomposition algorithm to solve a stochastic inland waterway port management problem considering perishable product," *International Journal of Production Economics*, 2020, p. 107863.

[3] Ahmadi-Javid A., Hoseinpour P., "Service System Design for Managing Interruption Risks: A Backup-Service Risk-Mitigation Strategy," *European Journal of Operational Research*, 2018.

[4] Al Enezy O., van Hassel E., Sys C., Vanelslander T., "Developing a cost calculation model for inland navigation," *Research in Transportation Business & Management*, vol. 23, 2017, pp. 64–74.

[5] Al-Khayyal F., Hwang S.J., "Inventory constrained maritime routing and scheduling for multi-commodity liquid bulk, part I: Applications and model," *European Journal of Operational Research*, vol. 176, no. 1, 2007, pp. 106–130.

[6] Alfandari L., Davidović T., Furini F., Ljubić I., Maraš V., Martin S., "Tighter MIP models for Barge Container Ship Routing.," *Omega*, vol. In press, 2017.

[7] Alfaqiri A., Hossain N.U.I., Jaradat R., Abutabenjeh S., Keating C.B., Khasawneh M.T., Pinto A.C., "A systemic approach for disruption risk assessment in oil and gas supply chains," *International Journal of Critical Infrastructures*, vol. 15, no. 3, 2019, pp. 230–259.

[8] American Society of Civil Engineers., "The economic impact Of current Investment Trends in Airports, Inland Waterways, and Marine Ports Infrastructure," Available from: `https://www.asce.org/airports_inland_waterways_and_marine_ports_report/`, 2012.

[9] An F., Hu H., Xie C., "Service network design in inland waterway liner transportation with empty container repositioning.," *European Transport Research Review*, vol. 7, no. 2, 2015, pp. 1–11.

[10] Apaiah R.K., Hendrix E.M.T., "Design of a supply chain network for pea-based novel protein foods," *Transportation Research Part D*, vol. 70, no. 3, 2005, pp. 383–391.

[11] Arango C., Cortés P., Muñuzuri J., Onieva L., "Berth allocation planning in Seville inland port by simulation and optimisation," *Advanced Engineering Informatics*, vol. 25, no. 3, 2011, pp. 452–461.

[12] Balinski M.L., "Fixed cost transportation problems," *Naval Research Logistics Quarterly*, vol. 8, 1961, pp. 41–54.

[13] Baroud H., Barker K., Ramirez-Marquez J.E. , "Importance measures for inland waterway network resilience.," *Transportation research part E*, vol. 62, 2014, pp. 55–67.

[14] Batun S., Denton B.T., Huschka T.R., Schaefer A.J., "Operating room pooling and parallel surgery processing under uncertainty.," *INFORMS Journal on Computing*, vol. 23, no. 2, 2011, pp. 220–237.

[15] Benders J.F., "Partitioning procedures for solving mixedvariables programming problems.," *Numerische Mathematik*, vol. 4, 1962, pp. 237–252.

[16] Birge J.R., Louveaux F., " Introduction to Stochastic Programming.," New York, NY, USA, 1997.

[17] Birge J.R., Louveaux F.V., "A multicut algorithm for two-stage stochastic linear programs.," *European Journal of Operational Research*, vol. 34, no. 3, 1988, p. 384392.

[18] Blazquez C.A., Adams T.M., Keillor P., "Optimization of mechanical dredging operations for sediment remediation.," *Journal of waterway, port, coastal, and ocean engineering*, vol. 127, no. 6, 2001, pp. 299–307.

[19] Braekers K., Caris A., Janssens G.K., "Optimal shipping routes and vessel size for intermodal barge transport with empty container repositioning.," *Computers in Industry*, vol. 64, no. 2, 2013, pp. 155–164.

[20] Braekers K., Janssens G., Caris A., "Determining optimal shipping routes for barge transport with empty container repositioning," *EUROSIS*, 2010.

[21] Chang M., Tseng Y., Chen J., "A scenario planning approach for the flood emergency logistics preparation problem under uncertainty.," *Transportation Research Part E: Logistics and Transportation Review*, vol. 43, no. 6, 2007, pp. 737–754.

[22] Chen C.-W., Fan Y., "Bioethanol supply chain system planning under supply and demand uncertainities.," *Transportation Research Part E*, vol. 48, 2012, pp. 150–164.

[23] Chouman M., Crainic T.G., Gendron B., "Commodity representations and cut-set-based inequalities for multicommodity capacitated fixed-charge network design," *Transportation Science*, vol. 51, no. 2, 2016, pp. 650–667.

[24] Christiansen M., Fagerholt K., Flatberg T., Haugen Ø., Kloster O., Lund E.H., "Maritime inventory routing with multiple products: A case study from the cement industry," *European Journal of Operational Research*, vol. 208, no. 1, 2011, pp. 86–94.

[25] Cornett A., Tschirky P., Knox P., Rollings S., "Moored ship motions due to passing vessels in a narrow inland waterway," *Coastal Engineering 2008: (In 5 Volumes)*, World Scientific, 2009, pp. 722–734.

[26] Crainic T.G., Fu X., Gendreau M., Rei W., Wallace S.W., "Progressive hedging-based metaheuristics for stochastic network design," *Networks*, vol. 58, 2011, pp. 114–124.

[27] Dadashi A., Dulebenets M.A., Golias M.M., Sheikholeslami A., "A novel continuous berth scheduling model at multiple marine container terminals with tidal considerations.," *Maritime Business Review*, vol. 2, no. 2, 2017, pp. 142–157.

[28] Davidovic T., Lazic J., Maras V., Stepe V., "Combinatorial formulation guided local search for inland waterway routing and scheduling," *Proceedings of 13th IASTED International Conference on Control and Applications*, 2011.

[29] De A.M., Vamsee K.R.G., Angappa S., Nachiappan T., Manoj K., "Composite particle algorithm for sustainable integrated dynamic ship routing and scheduling optimization," *Computers & Industrial Engineering*, vol. 96, 2016, pp. 201–215.

[30] Depuy G.W., Taylor G.D., Whyte T., "Barge fleet layout optimization.," *International Journal of Computer Integrated Manufacturing*, vol. 17, no. 2, 2004, pp. 97–107.

[31] DeVuyst E., Wilson W.W., Dahl B., "Longer-term forecasting and risks in spatial optimization models: The world grain trade," *Transportation Research Part E: Logistics and Transportation Review*, vol. 45, no. 3, 2009, pp. 472–485.

[32] Du Y., Chen Q., Lam J.S.L., Xu Y., Cao J.X., "Modeling the impacts of tides and the virtual arrival policy in berth allocation.," *Transportation Science*, vol. 49, no. 4, 2015, pp. 939–956.

[33] Duan G., Nur F., Alizadeh M., Chen L., Marufuzzaman M., Ma J., "Vessel routing and optimization for marine debris collection with consideration of carbon cap," *Journal of Cleaner Production*, 2020, p. 121399.

[34] Elhedhli S., Wu H., "A Lagrangean heuristic for hub-and-spoke system design with capacity selection and congestion," *INFORMS Journal on Computing*, vol. 22, no. 2, 2010, pp. 282–296.

[35] Elia J.A., Baliban R.C., Xiao X., Floudas C.A., "Optimal energy supply network determination and life cycle analysis for hybrid coal, biomass, and natural gas to liquid (CBGTL) plants using carbon-based hydrogen production," *Computers & Chemical Engineering*, vol. 35, no. 8, 2011, pp. 1399–1430.

[36] P. et al., "Strategic Assessment of Bioenergy Development in the West: Spatial analysis and supply curve development," *Final Report to the Western Governors Association, prepared by the University of California-Davis*, 2008.

[37] Fagerholt K., "A computer-based decision support system for vessel fleet schedulingexperience and future research," *Decision Support Systems*, vol. 37, no. 1, 2004, pp. 35–47.

[38] Fan L., Wilson W.W., "Impacts of congestion and stochastic variables on the network for US container imports," *Journal of Transport Economics and Policy (JTEP)*, vol. 46, no. 3, 2012, pp. 381–398.

[39] Fazi S., Fransoo J.C., Van W.T., "A decision support system tool for the transportation by barge of import containers: a case study," *Decision Support Systems*, vol. 79, 2015, pp. 33–45.

[40] Fischetti M., Ljubić I., Sinnl M., "Redesigning Benders decomposition for large-scale facility location," *Management Science*, vol. 63, no. 7, 2016, pp. 2146–2162.

[41] Fischetti M., Lodi A., "Local branching.," *Mathematical Programming*, vol. 98, 2003, pp. 23–47.

[42] Folga S., Allison T., Seda-Sanabria Y., Matheu E., Milam T., Ryan R., Peerenboom J., "A systems-level methodology for the analysis of inland waterway infrastructure disruptions.," *Journal of Transportation Security*, vol. 2, no. 4, 2009, p. 121.

[43] Francesco M.D., Lai M., Zuddas P., "Maritime repositioning of empty containers under uncertain port disruptions.," *Computers & Industrial Engineering*, vol. 64, no. 3, 2013, pp. 827–837.

[44] Fredouet C.H., "Global supply-chain securization as applied to seaport operations.," *Journal of International Logistics and Trade*, vol. 5, no. 1, 2007, pp. 57–73.

[45] Fu Q., Liu L., Xu Z., "Port resources rationalization for better container barge services in Hong Kong," *Maritime Policy and Management*, vol. 37, no. 6, 2010, pp. 543–561.

[46] Gade D., Hackebeil G., Ryan S.M., Watson J.P., Wets R.J.B., Woodruff D.L., "Obtaining lower bounds from the progressive hedging algorithm for stochastic mixed-integer programs," *Mathematical Programming*, vol. 157, no. 1, 2016, pp. 47–67.

[47] Gil E.M., Quelhas A.M., McCalley J.D., Van Voorhis T., "Modeling integrated energy transportation networks for analysis of economic efficiency and network interdependencies," *Proc. North American Power Symposium (NAPS)*, 2003.

[48] Gonzales D., Searcy E.M., Eksioglu S.D., "Cost analysis for high-volume and long-haul transportation of densified biomass feedstock.," *Transportation Research Part A*, vol. 49, 2013, pp. 48–61.

[49] Gonzalez P.H., Simonetti L., Michelon P., Martinhon C., Santos E., "A variable fixing heuristic with Local Branching for the fixed charge uncapacitated network design problem with user-optimal flow," *Computers & Operations Research*, vol. 76, 2016, pp. 134–146.

[50] Grubišić N., Hess S., Hess M., "A solution of berth allocation problem in inland waterway ports.," *Tehnički vjesnik*, vol. 21, no. 5, 2014, pp. 1135–1141.

[51] Guan Y., Cheung R.K., "The berth allocation problem: models and solution methods," *OR spectrum*, vol. 26, no. 1, 2004, pp. 75–92.

[52] Heilporn G., Cordeau J.F., Laporte G., "An integer L-shaped algorithm for the dial-a-ride problem with stochastic customer delays," *Discrete Applied Mathematics*, vol. 159, no. 9, 2011, pp. 883–895.

[53] Hossain N.U.I., El Amrani S., Jaradat R., Marufuzzaman M., Buchanan R., Rinaudo C., Hamilton M., "Modeling and assessing interdependencies between critical infrastructures using Bayesian network: A case study of inland waterway port and surrounding supply chain network," *Reliability Engineering & System Safety*, vol. 198, 2020, p. 106898.

[54] Hossain N.U.I., Jaradat R., Hosseini S., Marufuzzaman M., Buchanan R.K., "A framework for modeling and assessing system resilience using a Bayesian network: A case study of an interdependent electrical infrastructure system," *International Journal of Critical Infrastructure Protection*, vol. 25, 2019, pp. 62–83.

[55] Hossain N.U.I., Jaradat R., Marufuzzaman M., Buchanan R., Rianudo C., "Assessing and enhancing oil and gas supply chain resilience: A Bayesian network based approach," *IIE Annual Conference. Proceedings*, 2019, pp. 241–246.

[56] Hossain N.U.I., Nur F., Hosseini S., Jaradat R., Marufuzzaman M., Puryear S.M., "A Bayesian network based approach for modeling and assessing resilience: A case study of a full service deep water port," *Reliability Engineering & System Safety*, vol. 189, 2019, pp. 378–396.

[57] Hossain N.U.I., Nur F., Jaradat R., "An analytical study of hazards and risks in the shipbuilding industry," *Proceedings of the international annual conference of the American society for engineering management*, 2016, pp. 1–8.

[58] Hossain N.U.I., Nur F., Jaradat R., Hosseini S., Marufuzzaman M., Puryear S.M., Buchanan R.K., "Metrics for assessing overall performance of inland waterway ports: A bayesian network based approach," *Complexity*, vol. 2019, 2019.

[59] Hosseini S., Barker K., "Modeling infrastructure resilience using Bayesian networks: A case study of inland waterway ports.," *Computers & Industrial Engineering*, vol. 93, 2016, pp. 252–266.

[60] Huang Y., Fan Y., Chen C.-W, "An integrated bio-fuel supply chain against feedstock seasonality and uncertainty.," *Transportation Science*, vol. 48, no. 4, 2014, pp. 540–554.

[61] Hvattum L.M., Lokketangen A., "Using scenario trees and progressive hedging for stochastic inventory routing problems," *Journal of Heuristics*, vol. 15, 2009, pp. 527–557.

[62] Ibanez E., "A multiobjective optimization approach to the operation and investment of the national energy and transportation systems," 2011.

[63] Jans R., "Solving lot-sizing problems on parallel identical machines using symmetry-breaking constraints.," *INFORMS Journal on Computing*, vol. 21, 2009, pp. 123–136.

[64] Jans R., Desrosiers J., "Efficient symmetry breaking formulations for the job grouping problem.," *Computers & Operations Research*, vol. 40, no. 4, 2013, pp. 1132–1142.

[65] Kim D., Pardalos P.M., "A solution approach to the fixed charge network flow problem using a dynamic slope scaling procedure," *Operations Research Letters*, vol. 24, no. 4, 1999, pp. 195–203.

[66] Kleywegt A.J., Shapiro A., Homem-De-Mello T., "The sample average approximation method for stochastic discrete optimization.," *SIAM Journal of Optimization*, vol. 12, 2001, pp. 479–502.

[67] Konings R., "Network design for intermodal barge transport.," *Transportation Research Record: Journal of the Transportation Research Board*, , no. 1820, 2003, pp. 17–25.

[68] Lalla-Ruiz E., Shi X., Vob S., "The waterway ship scheduling problem.," *Transportation Research Part D*, vol. 60, 2016, pp. 191–209.

[69] Laporte G., Louveaux F.V., "The integer L-shaped method for stochastic integer programs with complete recourse," *Operations research letters*, vol. 13, no. 3, 1993, pp. 133–142.

[70] Lara C. L., Mallapragada D. S., Papageorgiou D. J., Venkatesh A., Grossmann I. E., "Deterministic electric power infrastructure planning: Mixed-integer programming model and nested decomposition algorithm," *European Journal of Operational Research*, vol. 271, no. 3, 2018, pp. 1037–1054.

[71] Liao C., Tseng P., Cullinane K., Lu. C., "The impact of an emerging port on the carbon dioxide emissions of inland container transport: An empirical study of Taipei port.," *Energy Policy*, vol. 38, no. 9, 2010, pp. 5251–5257.

[72] MacKenzie C.A., Barker K., Grant F.H., "Evaluating the consequences of an inland waterway port closure with a dynamic multiregional interdependence model.," *IEEE Transactions on Systems, Man, and Cybernetics-Part A: Systems and Humans*, vol. 42, no. 2, 2012, pp. 359–370.

[73] Magirou E.F., Psaraftis H.N., Bouritas T., "The economic speed of an ocean-going vessel in a dynamic setting.," *Transportation Research Part B*, vol. 76, 2015, pp. 48–67.

[74] Magnanti T.L., Wong R.T., "Accelerating Benders decomposition: Algorithmic enhancement and model selection criteria.," *Operations Research*, vol. 29, 1981, pp. 464–484.

[75] Mak W.K., Morton D.P., Wood R.K., "Monte Carlo bounding techniques for determining solution quality in stochastic programs.," *Operations Research Letters*, vol. 24, 1999, pp. 47–56.

[76] Marasš V., "Determining optimal transport routes of inland waterway container ships.," *Transportation Research Record: Journal of the Transportation Research Board*, , no. 2062, 2008, pp. 50–58.

[77] Marchand D., Sanderson M., Howe D., Alpaugh C., "Climatic change and great lakes levels the impact on shipping," *Climatic Change*, vol. 12, no. 2, 1988, pp. 107–133.

[78] M. Marufuzzaman and S. D. Ekşioğlu, "Managing congestion in supply chains via dynamic freight routing: An application in the biomass supply chain," *Transportation Research Part E: Logistics and Transportation Review*, vol. 99, 2017, pp. 54–76.

[79] Marufuzzaman M., Ekşioğlu S.D., "Designing a reliable and dynamic multimodal transportation network for biofuel supply chains," *Transportation Science*, vol. 51, no. 2, 2016, pp. 494–517.

[80] Marufuzzaman M., Ekşioğlu S.D., Li X., Wang J, "Analyzing the impact of intermodal-related risk to the design and management of biofuel supply chain," *Transportation Research Part E: Logistics and Transportation Review*, vol. 69, 2014, pp. 122–145.

[81] Marufuzzaman M., Eksioglu S.D., "Designing a Reliable and Dynamic Multi-Modal Transportation Network for Biofuel Supply Chain.," *Transportation Science*, vol. 51, no. 2, 2017, pp. 494–517.

[82] Marufuzzaman M., Eksioglu S.D., Huang Y.E., "Two-stage stochastic programming supply chain model for biodiesel production via wastewater treatment," *Computers & Operations Research*, vol. 49, 2014, pp. 1–17.

[83] Marufuzzaman M., Nur F., Bednar A.E., Cowan M., "Enhancing Benders decomposition algorithm to solve a combat logistics problem," *OR Spectrum*, vol. 42, no. 1, 2020, pp. 161–198.

[84] Miller C.R., "The evolving role of rural river ports as strategic economic development actors," *Water Resources and Rural Development*, vol. 9, 2017, pp. 28–38.

[85] Mississippi Department of Transportation, "Statewide Ports Needs And Marketing Assessment.," 2014.

[86] Nachtmann H., Mitchell K., Rainwater C., Gedik R., Pohl E., "Optimal dredge fleet scheduling within environmental work windows.," *Transportation Research Record: Journal of the Transportation Research Board*, , no. 2426, 2014, pp. 11–19.

[87] Nachtmann H., Oztanriseven F., *Economic evaluation of Arkansas inland waterways and potential disruption impacts*, Tech. Rep., Technical report, Mack-Blackwell Rural Transportation Center. Retrieved from `http://mack-blackwell.uark.edu/Research/mbtc-3029.pdf`, 2014.

[88] Nardi M.G., Sperry S.E., Davis T.D., "Grain supply chain management optimization using ARCGIS in Argentina," *2007 ESRI User Conference Proceedings*, 2007, pp. 1–23.

[89] National Research Council, *Funding and Managing the US Inland Waterways System: What Policy Makers Need to Know*, Transportation Research Board, 2015.

[90] Niagara Power Project., "Niagara river water level and flow fluctuations study final report.," Available from: `http://niagara.nypa.gov/ALP\%20working\%20documents/finalreports/html/IS23WL.htm`, 2005.

[91] Norkin V.I., Ermoliev Y.M., Ruszczynski A., "On optimal allocation of indivisibles under uncertainty.," *Operations Research*, vol. 46, 1998, pp. 381–395.

[92] Norkin V.I., Pflug G.C., Ruszczynski A., "A branch and bound method for stochastic global optimization.," *Mathematical Programming*, vol. 83, no. 3, 1998, pp. 425–450.

[93] Norstad I., Fagerholt K., Laporte G., "Tramp ship routing and scheduling with speed optimization," *Transportation Research Part C: Emerging Technologies*, vol. 19, no. 5, 2011, pp. 853–865.

[94] Notteboom T., "Container river services and gateway ports: Similarities between the Yangtze River and the Rhine River ," *Asia Pacific Viewpoint*, vol. 48, no. 3, 2007, pp. 330–343.

[95] Nur F., Aboytes-Ojeda M., Castillo-Villar K.K., Marufuzzaman M., "A Two-stage Stochastic Programming Model for Biofuel Supply Chain Network Design with Biomass Quality Implications," *IISE Transactions*, , no. just-accepted, 2020, pp. 1–55.

[96] Nur F., Marufuzzaman M., Burch R., Puryear S., Wall E., "Analyzing the Competitiveness of Inland Waterway Ports: An Application of Stochastic Analytical Hierarchy Process," *Proceedings of IISE Annual Conference and Expo 2018*, 2018, pp. 47–52.

[97] Nur F., Marufuzzaman M., Puryear S., Usher J.M., "Optimizing InlandWaterway Port operations for Mississippi River," *Proceedings of Transportation Research Board 98th Annual Meeting 2019*, 2019.

[98] Nur F., Marufuzzaman M., Puryear S.M., "Optimizing inland waterway port management decisions considering water level fluctuations," *Computers & Industrial Engineering*, vol. 140, 2020, p. 106210.

[99] Nur F., Marufuzzaman M., Puryear S.M., Wall E.S., Burch R., "Inland waterway ports selection and evaluation using stochastic analytical hierarchy process," *International Journal of Systems Science: Operations & Logistics*, 2020, pp. 1–21.

[100] Olsen J.R., Zepp L. J., Dager C.A., "Climate impacts on inland navigation," *Impacts of Global Climate Change*, 2005, pp. 1–8.

[101] Ozdamar L., Aksu D.T., Yasa E., Ergunes B., "Disaster relief routing in limited capacity road networks with heterogeneous flows," *Journal of Industrial & Management Optimization*, 2018, pp. 327–338.

[102] Oztanriseven F., Nachtmann H., "Economic impact analysis of inland waterway disruption response," *The Engineering Economist*, vol. 62, no. 1, 2017, pp. 73–89.

[103] Pant R., Barker K., Landers T.L., "Dynamic impacts of commodity flow disruptions in inland waterway networks," *Computers & Industrial Engineering*, vol. 89, 2015, pp. 137–149.

[104] Papadakos N., "Practical enhancements to the Magnanti-Wong method.," *Operations Research Letters*, vol. 36, 2008, pp. 444–449.

[105] Papadakos N., "Integrated airline scheduling," *Computers & Operations Research*, vol. 36, no. 1, 2009, pp. 176–195.

[106] S. R. Poudel, M. A. Quddus, M. Marufuzzaman, L. Bian, et al., "Managing congestion in a multi-modal transportation network under biomass supply uncertainty," *Annals of Operations Research*, 2017, pp. 1–43.

[107] Poudel S., Marufuzzaman M., Bian L., "A hybrid decomposition algorithm for designing a multi-modal transportation network under biomass supply uncertainty," *Transportation Research Part E*, vol. 94, 2016, pp. 1–25.

[108] Poudel S., Quddus M.A., Marufuzzaman M., Bian L., Burch R., "Managing Congestion in a Multi-Modal Transportation Network Under Biomass Supply Uncertainty," *Annals of Operations Research*, vol. doi:10.1007/s10479-017-2499-y, 2017.

[109] Poudel S.R., Marufuzzaman M., Bian L, "Designing a reliable bio-fuel supply chain network considering link failure probabilities," *Computers & Industrial Engineering*, vol. 91, 2016, pp. 85–99.

[110] Quddus M.A., Hossain N.U.I., Mohammad M., Jaradat R.M., Roni M.S., "Sustainable network design for multi-purpose pellet processing depots under biomass supply uncertainty," *Computers & Industrial Engineering*, vol. 110, 2017, pp. 462–483.

[111] Rahmaniani R., Crainic T.G., Gendreau M., Rei W., "The Benders decomposition algorithm: A literature review," *European Journal of Operational Research*, vol. 259, no. 3, 2017, pp. 801–817.

[112] Rahmaniani R, C.T., Gabriel G, Michel and Rei W, "Accelerating the Benders decomposition method: Application to stochastic network design problems," *SIAM Journal on Optimization*, vol. 28, no. 1, 2018, pp. 875–903.

[113] Rainwater C., Nachtmann H., Adbesh F., "Optimal dredge fleet scheduling within environmental work windows.," *MarTREC Report*, 2016.

[114] Rakke J., Christiansen M., Fagerholt K., Laporte G., "The traveling salesman problem with draft limits," *Computers & Operations Research*, vol. 39, no. 9, 2012, pp. 2161–2167.

[115] Rawls C.G., Turnquist M.A., "Pre-positioning of emergency supplies for disaster response," *Transportation research part B: Methodological*, vol. 44, no. 4, 2010, pp. 521–534.

[116] Rei W., Cordeau J.F., Gendreau M., Soriano P., "Accelerating Benders decomposition by local branching.," *INFORMS Journal on Computing*, vol. 21, no. 2, 2009, pp. 333–345.

[117] Rockafellar R.T., Wets R.J.-B., "Scenarios and policy aggregation in optimization under uncertainty," *Mathematics of operations research*, vol. 16, 1991, pp. 119–147.

[118] Roso V., "Evaluation of the dry port concept from an environmental perspective: A note.," *Transportation Research Part D*, vol. 12, no. 7, 2007, pp. 523–527.

[119] Santoso T., Ahmed S., Goetschalckx M., Shapiro A., "A stochastic programming approach for supply chain network design under uncertainty.," *European Journal of Operational Research*, vol. 167, 2005, pp. 96–115.

[120] Schutz P., Tomasgard A., Ahmed S., "Supply chain design under uncertainty using sample average approximation and dual decomposition.," *European Journal of Operational Research*, vol. 199, 2009, pp. 409–419.

[121] Shabayek A.A., Yeung W.W., "A simulation model for the Kwai Chung container terminals in Hong Kong," *European Journal of Operational Research*, vol. 140, no. 1, 2002, pp. 1–11.

[122] Sherali H.D., Smith J.C., "Improving discrete model representations via symmetry considerations.," *Management Science*, vol. 47, 2001, pp. 1396–1407.

[123] Shi H., Xu P., Yang Z., "Optimization of transport network in the Basin of Yangtze River with minimization of environmental emission and transport/investment costs," *Advances in Mechanical Engineering*, vol. 8, no. 8, 2016, p. 1687814016660923.

[124] Sierksma G., *Linear and integer programming: theory and practice*, CRC Press, 2001.

[125] Simões P., Marques R.C., "Seaport performance analysis using robust nonparametric efficiency estimators.," *Transportation Planning and Technology*, vol. 33, no. 5, 2010, pp. 435–451.

[126] Skjæveland G., Hilstad K.V., *Ship Traffic Scheduling and Disruption Management for the Kiel Canal-A Simulation-Optimization Approach*, master's thesis, NTNU, 2018.

[127] Tan Z., Wang Y., Meng Q., Liu Z., "Joint Ship Schedule Design and Sailing Speed Optimization for a Single Inland Shipping Service with Uncertain Dam Transit Time," *Transportation Science*, 2018.

[128] The American Waterways Operators., "Economic Contribution of the US Tugboat, Towboat, and Barge Industry.," Available from: `https://www.marad.dot.gov/wp-content/uploads/pdf/Econ-Impact-of-US-Tugboat-Towboat-and-Barge-Industry-lh-6-22-17.pdf`, 2017.

[129] Ting C., Schonfeld P., "Integrated control for series of waterway locks.," *Journal of Waterway, Port, Coastal, and Ocean Engineering*, vol. 124, no. 4, 1998, pp. 199–206.

[130] Ting C.J., Schonfeld P., "Optimization through simulation of waterway transportation investments.," *Transportation Research Record: Journal of the Transportation Research Board*, , no. 1620, 1998, pp. 11–16.

[131] Tockner K., Ward J.V., Arscott D.B., Edwards P.J., Kollmann J., Gurnell A.M., Petts G.E., Maiolini B., "The Tagliamento River: a model ecosystem of European importance ," *Aquatic Sciences*, vol. 65, no. 3, 2003, pp. 239–253.

[132] Trotter P.S., Johnson G.A., Ricks R., Smith D.R., "Floods on the lower Mississippi: An historical economic overview.," Available from: `http://www.srh.noaa.gov/topics/attach/html/ssd98-9.htm`, 2011.

[133] United States Department of Agriculture, "Usual Planting and Harvesting Dates for U.S. Field Crops.," Available from: `https://usda.mannlib.cornell.edu/usda/nass/planting/uph97.pdf`, 1997.

[134] United States Department of Agriculture., "Barge Transportation.," Available from: `https://www.ams.usda.gov/sites/default/files/media/RTIReportChapter12.pdf`, 2008.

[135] United States Department of Agriculture., "National Agricultural Statistics Service.," Available from: `https://quickstats.nass.usda.gov/`, 2014.

[136] United States Department of Agriculture., "Forests of Mississippi, 2014.," Available from: `https://www.srs.fs.usda.gov/pubs/ru/ru_srs049.pdf`, 2015.

[137] United States Department of Agriculture, "Fertilizer Use and Price.," Available from: `https://www.ers.usda.gov/data-products/fertilizer-use-and-price.aspx`, 2018.

[138] U.S. Army Corps of Engineers., "FY 2000 Planning Guidance Shallow Draft Vessel Costs.," Available from: `http://www.iwr.usace.army.mil/Portals/70/docs/iwrreports/00-05.pdf`, 2000.

[139] U.S. Army Corps of Engineers, "Water levels of Rivers and Lakes.," Available from: `http://rivergages.mvr.usace.army.mil/WaterControl/stationinfo2.cfm?dt=S\&sid=CE40F18A\&fid\=VCKM6`, 2018.

[140] U.S. Department of Transportation. Bureau of Transportation Statistics, "Transportation Statistics Annual Report 2015, Washington, DC.," 2015.

[141] Venturini G., Iris C., Kontovas C.A., Larsen A., "The multi-port berth allocation problem with speed optimization and emission considerations.," *Transportation Research Part D*, vol. 54, 2017, pp. 142–159.

[142] Verweij B., Ahmed S., Kleywegt A.J., Nemhauser G., Shapiro A., "The sample average approximation method applied to stochastic routing problems: A computational study.," *Computational Optimization and Applications*, vol. 24, 2003, pp. 289–333.

[143] Vidyarthi N., Jayaswal S., "Efficient solution of a class of location–allocation problems with stochastic demand and congestion," *Computers & Operations Research*, vol. 48, 2014, pp. 20–30.

[144] Wallace S.W., Helgason T., "Structural properties of the progressive hedging algorithm," *Annals of Operations Research*, vol. 31, 1991, pp. 445–456.

[145] Wang S., Meng Q., "Robust bunker management for liner shipping networks," *European Journal of Operational Research*, vol. 243, no. 3, 2015, pp. 789–797.

[146] Wang S., Meng Q., Sun Z., "Container routing in liner shipping.," *Transportation Research Part E*, vol. 49, no. 1, 2013, pp. 1–7.

[147] Wang S.L., Schonfeld P., "Scheduling interdependent waterway projects through simulation and genetic optimization.," *Journal of Waterway, Port, Coastal, and Ocean Engineering*, vol. 131, no. 3, 2005, pp. 89–97.

[148] Wang Z., Guo C., "Minimizing the risk of seaport operations efficiency reduction affected by vessel arrival delay," *Industrial Management & Data Systems*, vol. 118, no. 7, 2018, pp. 1498–1509.

[149] Watling D.P., Hazelton M.L., "Asymptotic approximations of transient behaviour for day-to-day traffic models," *Transportation Research Part B: Methodological*, vol. 118, 2018, pp. 90–105.

[150] Watson J.P., Woodruff D.L., "Progressive hedging innovations for a class of stochastic mixed-integer resource allocation problems," *Computational Management Science*, vol. 8, 2011, pp. 355–370.

[151] Wiegmans B., Konings R., "Intermodal inland waterway transport: Modelling conditions influencing its cost competitiveness.," *The Asian Journal of Shipping and Logistics*, vol. 31, no. 2, 2015, pp. 273–294.

[152] Wiegmans B., Witte P., "Efficiency of inland waterway container terminals: Stochastic frontier and data envelopment analysis to analyze the capacity design-and throughput efficiency," *Transportation Research Part A: Policy and Practice*, vol. 106, 2017, pp. 12–21.

[153] Williams J.L, "Information theoretic sensor management.," Available from: `http://hdl.handle.net/1721.1/38534`, 2007.

[154] Yan X.P., Wan C.P., Zhang D., Yang Z.L., "Safety management of waterway congestions under dynamic risk conditionsA case study of the Yangtze River," *Applied Soft Computing*, vol. 59, 2017, pp. 115–128.

[155] Zhang M., Janic M., Tavasszy L.A., "A freight transport optimization model for integrated network, service, and policy design.," *Transportation Research Part E*, vol. 77, 2015, pp. 61–76.

[156] Zhen L., "Modeling of yard congestion and optimization of yard template in container ports," *Transportation Research Part B: Methodological*, vol. 90, 2016, pp. 83–104.

[157] Zhen L., Wang K., Wang S., Qu X., "Tug scheduling for hinterland barge transport: A branch-and-price approach," *European Journal of Operational Research*, vol. 265, no. 1, 2018, pp. 119–132.

[158] Zou J., Ahmed S., Sun X.A., "Multistage stochastic unit commitment using stochastic dual dynamic integer programming," *IEEE Transactions on Power Systems*, 2018.